Université de Montréal

Novel Molecular Mechanisms of Neuronal and Vascular Protection in Experimental Glaucoma

Par

MOHAMMADALI ALMASIEH

Département de pathologie et biologie cellulaire
Faculté de Médecine

Thèse présentée à la Faculté des études supérieures
en vue de l'obtention du grade de Philosophiæ Doctor (Ph.D.)
en neurocytologie moléculaire

Avril 2012

Université de Montréal

Faculté des études supérieures et postdoctorales

Cette thèse de doctorat intitulée :

«Novel Molecular Mechanisms of Neuronal and Vascular Protection in Experimental Glaucoma»

Présentée par :

MOHAMMADALI ALMASIEH

a été évaluée par un jury composé des personnes suivantes :

Karl J.L. Fernandes, Ph.D.
président-rapporteur

Adriana Di Polo, Ph.D.
directeur de recherche

Christian Casanova, Ph.D.
co-directeur

Hélène Girouard, Ph.D.
membre du jury

William H. Baldridge, Ph.D.
examinateur externe

Laurent Descarries, Ph.D.
représentant du doyen de la FES

RÉSUMÉ

Le glaucome est la deuxième cause de cécité irréversible dans le monde. La perte de vision qui se produit lors du glaucome s'explique par une dégénérescence du nerf optique et une mort progressive et sélective des cellules ganglionnaires de la rétine (CRG). L'hypertension oculaire est un facteur de risque majeur dans le glaucome, mais des défauts du champ visuel continuent à se développer chez un contingent de patients malgré l'administration de médicaments qui abaissent la pression intraoculaire (PIO). Par conséquent, bien que la PIO représente le seul facteur de risque modifiable dans le développement du glaucome, son contrôle ne suffit pas à protéger les CRGs et préserver la fonction visuelle chez de nombreux patients. Dans ce contexte, j'ai avancé l'**hypothèse centrale** voulant que les stratégies de traitement du glaucome visant à promouvoir la protection structurale et fonctionnelle des CRGs doivent agir sur les mécanismes moléculaires qui conduisent à la mort des ces neurones.

Dans la première partie de ma thèse, j'ai caractérisé l'effet neuroprotecteur de la galantamine, un inhibiteur de l'acétylcholinestérase qui est utilisé cliniquement dans le traitement de la maladie d'Alzheimer. Cette étude s'est basée sur l'hypothèse que la galantamine, en modulant l'activité du récepteur de l'acétylcholine, puisse améliorer la survie des CRGs lors du glaucome. Nous avons utilisé un modèle expérimental bien caractérisé d'hypertension oculaire induite par l'administration d'une solution saline hypertonique dans une veine épisclérale de rats Brown Norway. Les résultats de cette étude (Almasieh et al. *Cell Death and Disease*, 2010) ont démontré que l'administration quotidienne de galantamine améliore de manière significative la survie des corps cellulaires et des axones CRGs. La protection structurelle des CRGs s'accompagne d'une préservation remarquable de la fonction visuelle, évaluée par l'enregistrement des potentiels évoqués visuels (PEV) dans le collicule supérieur, la cible principale des CRGs chez le rongeur. Une autre constatation intéressante de cette étude est la perte substantielle de capillaires rétiniens et la réduction du débit sanguin associé à la perte des CRGs dans le glaucome expérimental. Il est très intéressant que la galantamine ait également favorisé la protection de la microvascularisation et amélioré le débit sanguin rétinien des animaux glaucomateux (Almasieh et al. en préparation). J'ai notamment démontré que les neuro-et vasoprotections médiées par la galantamine se produisent par

l'activation des récepteurs muscariniques de l'acétylcholine.

Dans la deuxième partie de ma thèse, j'ai étudié le rôle du stress oxydatif ainsi que l'utilisation de composés réducteurs pour tester l'hypothèse que le blocage d'une augmentation de superoxyde puisse retarder la mort des CRG lors du glaucome expérimental. J'ai profité d'un composé novateur, un antioxydant à base de phosphine-borane (PB1), pour tester sur son effet neuroprotecteur et examiner son mécanisme d'action dans le glaucome expérimental. Les données démontrent que l'administration intraoculaire de PB1 entraîne une protection significative des corps cellulaire et axones des CRGs. Les voies moléculaires conduisant à la survie neuronale médiée par PB1 ont été explorées en déterminant la cascade de signalisation apoptotique en cause. Les résultats démontrent que la survie des CRGs médiée par PB1 ne dépend pas d'une inhibition de signalisation de protéines kinases activées par le stress, y compris ASK1, JNK ou p38. Par contre, PB1 induit une augmentation marquée des niveaux rétiniens de BDNF et une activation en aval de la voie de survie des ERK1 / 2 (Almasieh et al. *Journal of Neurochemistry*, 2011).

En conclusion, les résultats présentés dans cette thèse contribuent à une meilleure compréhension des mécanismes pathologiques qui conduisent à la perte de CRGs dans le glaucome et pourraient fournir des pistes pour la conception de nouvelles stratégies neuroprotectrices et vasoprotectrices pour le traitement et la gestion de cette maladie.

Mots-clés: glaucome, cellule ganglionnaire de la rétine, neuroprotection, inhibiteur de l'acétylcholinestérase, muscarinique, superoxyde, facteur neurotrophique dérivé du cerveau, *kinases 1 et 2* régulées par des signaux *extracellulaires,* microvascularisation rétinienne, débit sanguin rétinien.

SUMMARY

Glaucoma is the second cause of irreversible blindness worldwide. Loss of vision in glaucoma is accompanied by progressive optic nerve degeneration and selective loss of retinal ganglion cells (RGCs). Ocular hypertension is a major risk factor in glaucoma, but visual field defects continue to progress in a large group of patients despite the use of drugs that lower intraocular pressure (IOP). Therefore, although IOP is the sole modifiable risk factor in the development of glaucoma, its regulation is not sufficient to protect RGCs and preserve visual function in many affected patients. To address this issue, I put forward the **central hypothesis** that effective therapeutic strategies for glaucoma must interfere with molecular mechanisms that lead to RGC death to successfully promote structural and functional protection of these neurons.

In the first part of my thesis, I characterized the neuroprotective effect of galantamine, an acetylcholinesterase inhibitor that is clinically used for the treatment of Alzheimer's disease. The specific hypothesis of this study was that galantamine, by modulating acetylcholine receptor activity, can improve the survival of injured RGCs in glaucoma. A well characterized experimental model of ocular hypertension induced by administration of a hypertonic saline into an episcleral vein of Brown Norway rats was used. The results of this study (Almasieh et al. *Cell Death and Disease*, 2010) demonstrated that daily administration of galantamine significantly improved the survival of RGC soma and axons in this model. Structural protection of RGCs correlated with substantial preservation of visual function, assessed by recording visual evoked potentials (VEPs) from the superior colliculus, the primary target of RGCs in the rodent brain. An interesting finding during the course of my thesis was that there is a substantial loss of retinal capillaries and a reduction in retinal blood that correlates with RGC loss in experimental glaucoma. Interestingly, galantamine also promoted the protection of the microvasculature and improved retinal blood flow in ocular hypertensive animals (Almasieh et al. in preparation). Importantly, I demonstrated that galantamine-mediated neuro- and vasoprotection occur through activation of muscarinic acetylcholine receptors.

In the second part of my thesis, I investigated the role of oxidative stress and the use of reducing compounds to test the hypothesis that blockade of a superoxide burst may delay RGC death in experimental glaucoma. I took advantage of a novel phosphine-

borane based antioxidant compound available to us (PB1) to investigate its neuroprotective effect and mechanism of action in experimental glaucoma. The data demonstrate that intraocular administration of PB1 resulted in significant protection of RGC soma and axons. I also explored the molecular pathways leading to PB1-mediated neuronal survival by analyzing the components of survival and apoptotic signaling pathways involved in this response. My results show that PB1-mediated RGC survival did not correlate with inhibition of stress-activated protein kinase signaling, including ASK1, JNK or p38. Instead, PB1 led to a striking increase in retinal BDNF levels and downstream activation of the pro-survival ERK1/2 pathway (Almasieh et al. *Journal of Neurochemistry*, 2011).

In conclusion, the findings presented in this thesis contribute to a better understanding of the pathological mechanisms underlying RGC loss in glaucoma and might provide insights into the design of novel neuroprotective and vasoprotective strategies for the treatment and management of this disease.

Key words: glaucoma, retinal ganglion cell, neuroprotection, acetylcholinesterase inhibitor, muscarinic, superoxide, brain-derived neurotrophic factor, extracellular signal-regulated kinase 1/2, retinal microvasculature, retinal blood flow.

TABLE OF CONTENTS

LIST OF TABLES

LIST OF FIGURES

CHAPTER 1

CHAPTER 2

CHAPTER 3

CHAPTER 4

CHAPTER 5

LIST OF ABBREVIATIONS

AAV	adeno-associated virus
ACh	acetylcholine
AChE	acetylcholinesterase
AD	Alzheimer's disease
AGIS	advanced glaucoma intervention study
AMPA	α-amino-3-hydroxy-5-methyl-4-isoxazolepropionic acid
APL	allosteric potentiating ligand
APP	amyloid precursor protein
ARE	antioxidant response element
ARRIVE	animal research: reporting in vivo experiments
ASK1	apoptosis signal regulating kinase 1
Aß	amyloid beta
BDNF	brain-derived neurotrophic factor
cAMP	cyclic adenosine monophosphate
ChAT	choline acetyltransferase
CNS	central nervous system
CNTGSG	collaborative normal-tension glaucoma study group
CREB	cAMP response element binding protein
DHß-E	dihydro-ß-erythroidine hydrobromide
DMSO	dimethyl sulfoxide
DNA	deoxyribonucleic acid
EAAT	excitatory amino acid transporter
ERG	electroretinogram
ERK 1/2	extracellular signal-regulated kinases 1/2
ET-1	endothelin-1
GABA	gamma-aminobutyric acid
GAPDH	glyceraldehyde 3-phosphate dehydrogenase
GFAP	glial fibrillary acidic protein
GLAST	glutamate-aspartate transporter
GLT-1	glutamate transporter-1

GSH	glutathione
HIF-1α	hypoxia-inducible factor-1 alpha
Hsp	heat-shock protein
IOP	intraocular pressure
JNKs	c-Jun N-terminal kinases
LGN	lateral geniculate nucleus
L-NAME	N-nitro-L-arginine methyl ester
L-NMMA	N-monomethyl-L-arginine
mAChR	muscarinic acetylcholine receptor
MAPKKK	mitogen-activated protein kinase kinase kinase
MAPKs	mitogen-activated protein kinases
MEK1	mitogen-activated protein kinase kinase 1
MLA	methyllycaconitine citrate
mm	millimeters
MMA	mecamylamine hydrochloride
mRNA	messenger RNA
nAChR	nicotinic acetylcholine receptor
NADPH	nicotinamide adenine dinucleotide phosphate
NF-κB	nuclear factor kappa-light-chain-enhancer of activated B cells
NGF	nerve growth factor
NMDA	N-methyl-D-aspartic acid
NO	nitric oxide
NOLA	N-nitro-L-arginine
NOS	nitric oxide synthase
Nrf2	NF-E2-related factor-2
NT-3	neurotrophin-3
NT-4/5	neurotrophin-4/5
NTG	normal tension glaucoma
OHT	ocular hypertension
ONH	optic nerve head
PACG	primary angle-closure glaucoma

PB1	bis (3-propionic acid methyl ester) phenylphosphine borane complex 1
PBS	phosphate-buffered saline
PFA	paraformaldehyde
PI3K	phosphatidylinositol 3-kinase
PKC	protein kinase C
PLC	phospholipase C
POAG	primary open angle glaucoma
PRZ	pirenzepine dihydrochloride
Redox	reduction-oxidation reactions
RGCs	retinal ganglion cells
RNA	ribonucleic acid
RNFL	retinal nerve fiber layer
ROS	reactive oxygen species
SAP	standard achromatic automated perimetry
SAPKs	stress-activated protein kinases
SC	superior colliculus
SCO	scopolamine hydrobromide
SOD	superoxide dismutase
SWAP	short-wavelength automated perimetry
TM	trabecular meshwork
TNFα	tumor necrosis factor-alpha
Trk	tropomyosin related kinase
TRO	tropicamide
TRX	thioredoxin
TRXR	thioredoxin reductase
TXNIP	thioredoxin -interacting protein
VEP	visual evoked potential
XIAP	x-linked inhibitor of apoptosis protein
[^{14}C]-IMP	N-isopropyl-p-^{14}C-iodoamphetamine
μm	micrometers
4-DAMP	diphenylacetoxy-N-methylpiperidine methiodide

ACKNOWLEDGEMENTS

I am heartily thankful to my supervisor, Dr. Adriana Di Polo, for the opportunity to work in her lab and for providing the guidance and encouragement that enabled me to pursue the projects. I have benefited greatly from her scientific vision and thoughtful criticism throughout the years and I am grateful for her kind support.

I would also like to express my deep appreciation to my co-supervisor Dr. Christian Casanova for his support and trust on me and for helping to expand the prospects of this work.

I would like to thank all the co-authors and collaborators of my papers in particular Drs. Melanie Kelly, Leonard Levin and Elvire Vaucher and the members of their labs for their support and contribution.

I would furthermore like to thank the members of my thesis jury for accepting to evaluate my work. I would also like to express my appreciation to members of my advisory and pre-doctoral committees Drs. Nicole Leclerc, Guy Doucet and Jean-Francois Bouchard for their valuable advice and guidance.

Many thanks to the members of the Di Polo lab past and present. It was my pleasure to work with Mike, Vincent, Yu, Johanne, Fred, Annie, Stephan and Marius. Many thanks to Philippe for his kind support. I would like to express my gratitude to Marilyne, Barbara, Ariel, Mathieu, Dara, Jorge and Sri for being awesome and for their friendship and spirit throughout the years. I would also like to thank members of the Casanova lab, Brian, Martin, Matthieu and Reza and in particular to thank Geneviève, Karine, Marouane, Nawal and Marilyse for their help and support.

Many thanks to my friend in the department: Casimir, Moogeh, Li, Jie, Greg, David, Isabel, Sarah-Jane, Mylène and Bahram. Special thanks to my friend Hamid for insightful discussions.

I would further like to thank the professors and members of the Department of Pathology and Cell Biology specially Dr. Nicole Leclerc, Dr. Mark Pelletier, Monique, Marielle, Michel Lauzon and Christine for their support. I also thank Faculté des études supérieures et postdoctorales and Groupe de Recherche sur le Système Nerveux Central for providing financial support.

"A hair divides what is false and true"

- Omar Khayyám

To my father, Mahmood, for his dedication to the family and to science

To my mother, Ashraf, for her love for us and for her wisdom

To my brother, Reza, for his perseverance and support

To my sister, Neda, for her kindness and talent

CHAPTER 1

I. GENERAL INTRODUCTION

I.1. GLAUCOMA: DEFINITION, PREVALENCE AND RISK FACTORS

Glaucoma is a group of chronic optic neuropathies characterized by progressive visual field defects and optic disc damage which ultimately leads to irreversible blindness due to the loss of retinal ganglion cells (RGCs). It is estimated that more than 60 million people suffer from glaucoma worldwide (Quigley and Broman, 2006) and according to a report from the World Health Organization, glaucoma is the second cause of blindness globally accounting for 12.3% of total cases (Resnikoff et al., 2004).

There are a number of risk factors that increase the incidence of glaucoma. Demographic factors including age and ethnic background are among the most recognized risk factors for glaucoma. For example people over the age of 60 have a much higher risk of developing glaucoma (Coleman and Miglior, 2008). Also, the rate of glaucoma progression is faster in individuals diagnosed with glaucoma within certain population subgroups (Sommer et al., 1991; Varma et al., 2004). Moreover, belonging to a certain ethnic background significantly lowers the age at which those individuals are at risk of developing glaucoma. For instance, individuals of African-descent 40 years and older are at higher risk of developing glaucoma and have the highest rate of blindness due to glaucoma (Congdon et al., 2004; Leske, 2007). Family history is another recognized risk factor for developing glaucoma as individuals with a family member with glaucoma have a four times higher risk of developing this disease (Wiggs, 2007).

Elevated intraocular pressure (IOP) is an important risk factor for developing glaucoma. Considering that the normal value of IOP for adult individuals is usually around 15 mmHg, people with an IOP over 21 mmHg are known as ocular hypertensive (Quigley et al., 1994). Interestingly, there is a correlation between systemic blood pressure and IOP levels as an increase or a reduction of systemic blood pressure results in higher or lower IOP, respectively (Klein et al., 2005; McLeod et al., 1990). Indeed, high systemic blood pressure is considered a risk factor in glaucoma (Deokule and Weinreb, 2008). Although IOP is regarded as an important risk factor, it is not an accurate predictor of glaucoma since more than 30% of the glaucoma patients have an IOP in the normal range (Nemesure et al., 2007).

Corneal thickness is also considered another risk factor and thinner central corneas have been correlated with visual field loss in glaucoma (Medeiros et al., 2003).

High myopia is another risk factor correlating with glaucoma occurrence (Loyo-Berros and Blustein, 2007; Mastropasqua et al., 1992). An association between diabetes and glaucoma has also been suggested (Bonovas et al., 2004). Some cases of diabetes also have higher IOP levels compared to control individuals (Klein et al., 1984; Tielsch et al., 1995).

I.2. PATHOLOGICAL AND CLINICAL FEATURES OF GLAUCOMA

I.2.1. Loss of RGCs, optic disc cupping and axonal damage

Glaucoma is characterized by damage to the neural components of the visual pathway including the retina, the optic tract and the brain. The visual information in the retina travels vertically through photoreceptors, bipolar cells and finally RGCs. RGCs play an essential role in vision because they are the only neurons responsible for relaying the visual signal from the eye to the higher centers in the brain (Figure 1). One of the highlights of glaucoma pathology is the selective loss of RGCs, which is characteristic of all glaucoma patients (Kendell et al., 1995; Quigley, 1999).

RGCs axons extend from their cell bodies over the inner surface of retina to reach the optic disc. They join to form axon bundles at the retinal nerve fiber layer supported by both the processes of Müller cells and astrocytes (Radius and Anderson, 1979). The optic disc or optic nerve head (ONH) is the region where RGC axons exit the eye to form the optic nerve. The ONH includes a prelaminar area formed by loose trabecular glial tissue and bundles of unmyelinated nerve fibers. The laminar area of the ONH is called the lamina cribrosa; it is composed of parallel collagen laminas located in a canal in the posterior part of the sclera (Jonas et al., 1991). The lamina cribrosa forms a sieve-like network and axons of RGCs exit the retina through its pores; it also allows passage of the central retinal vessels (Hernandez et al., 1986).

The area of the ONH that contains the nerve fibers, called the neuroretinal rim, surrounds the central and slightly depressed part called the cup (Jonas et al., 1988). Increased depth of the optic cup is a well known clinical feature of glaucoma (Jonas et al., 1999). ONH cupping is one of the first detectable signs of glaucoma and often precedes the loss of visual field (Pederson and Anderson, 1980). The optic disc cupping

FIGURE 1.

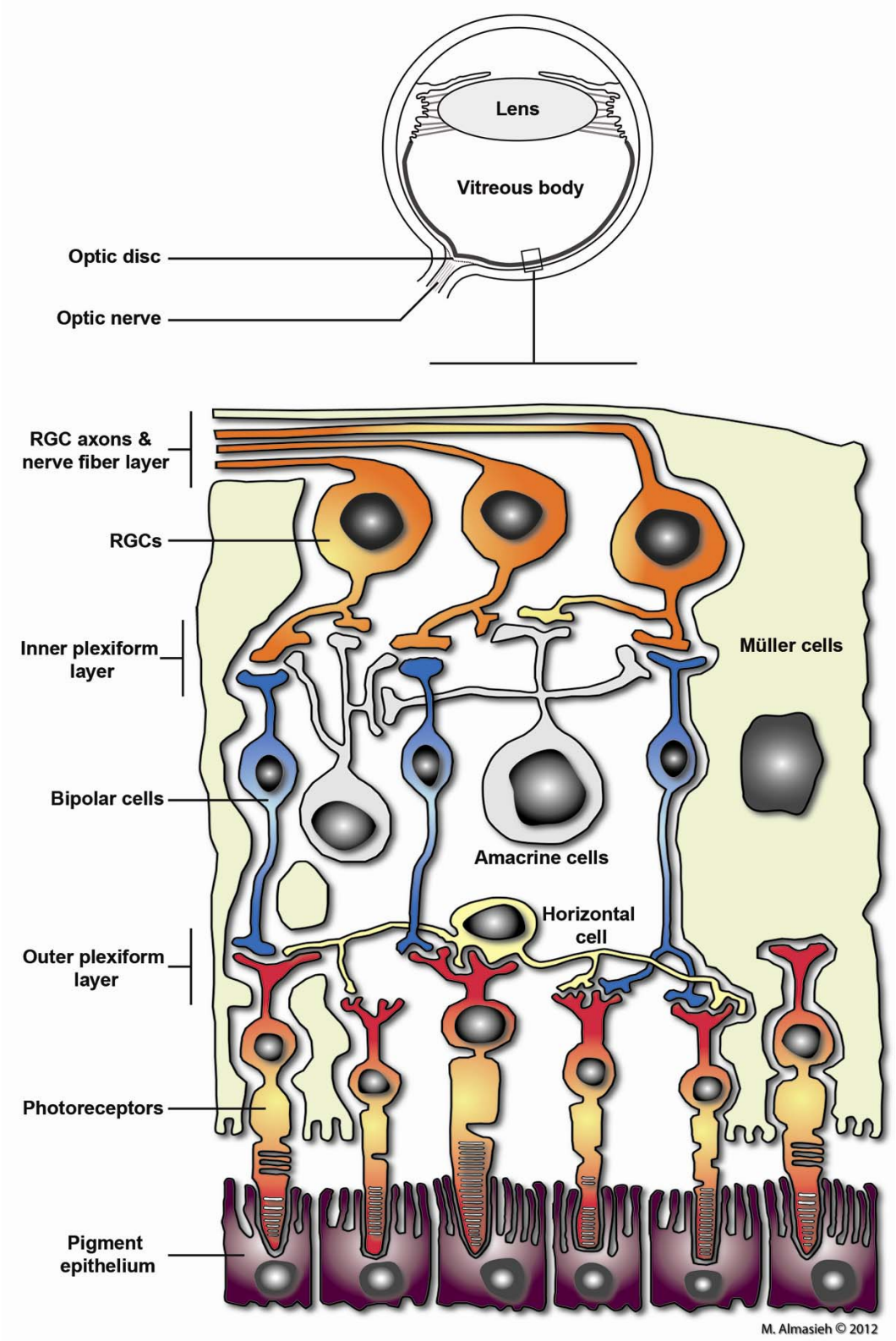
Lens
Vitreous body
Optic disc
Optic nerve
RGC axons & nerve fiber layer
RGCs
Inner plexiform layer
Bipolar cells
Outer plexiform layer
Photoreceptors
Pigment epithelium
Müller cells
Amacrine cells
Horizontal cell
M. Almasieh © 2012

Figure 1. A schematic diagram of the retina demonstrating the principal cell types involved in retinal signaling. The photoreceptor cells (rods and cones) are the outermost neuronal layer of the retina. Photoreceptors are light-sensitive and transduce light stimuli into electrical signals. The signal is subsequently transferred from the photoreceptors to bipolar cells. The outer plexiform layer (OPL) contains the synaptic connections between photoreceptors to bipolar cells and horizontal cells. Bipolar cells make synaptic connections with RGCs in the inner plexiform layer (IPL). RGC axons travel toward the optic disc in the nerve fiber layer and exit the eye forming the optic nerve. Cellular components of the retina are supported by Müller cells and the interconnections provided by horizontal cells and amacrine cells participate in retinal processing and modifications of visual signal. Source of image: Mohammadali Almasieh.

correlates with changes in the organization of connective tissue bundles and thinning of laminar beams in the lamina cribrosa in experimental and human glaucoma (Fukuchi et al., 1992; Miller and Quigley, 1987; Morrison et al., 1990). ONH changes also include abnormal deposition of extracellular matrix components such as collagen, laminin and elastin (Hernandez et al., 1990; Johnson et al., 1996; Morrison et al., 1990). ONH tissue remodeling occurs partly due to activation of resident glial cells since abnormal deposition of extracellular material correlates with increased expression of elastin mRNA in local astrocytes (Pena et al., 2001). Activated and proliferating astrocytes, characterized by hypertrophic soma and expression of glial fibrillary acidic protein (GFAP), are found in human and experimental glaucoma (Hernandez et al., 2008; Johnson et al., 2007a). Tissue remodeling can also result in biomechanical alterations at the ONH leading to stress-induced damage of RGC axons at this location (Burgoyne, 2010).

I.2.2. Loss of visual field

Glaucoma is not the only optic neuropathy accompanied by visual loss; however, based on the characteristic changes of the optic disc and the typical patterns of visual field loss, glaucomatous visual defects can be distinguished from other optic neuropathies. Because damage to RGC axons happens mostly at the superior and inferior parts of the ONH and considering that nerve fibers make a superior or inferior arc around the horizontal raphe before entering the optic disc, typical arcuate scotomas are the characteristic visual field loss pattern in the glaucoma (Figure 2) (Hood and Kardon, 2007; Spector, 1990). It is typical for glaucomatous vision loss to be peripherally located as occurrences of scotomas are usually paracentral; central vision will remain intact until very late in the course of the disease. Several methods are currently used for diagnosis of glaucomatous visual field abnormalities including standard achromatic automated perimetry (SAP) or selective perimetry (Sakata et al., 2007; Sample et al., 2000; Sharma et al., 2008). Due to considerable overlap in the receptive fields of different RGC types, SAP does not allow detection of visual defects unless 40-50% of RGCs are already lost. However, short-wavelength (blue-yellow color sensitive) automated perimetry (SWAP) that targets the small bistratified RGCs, enables physicians to detect functional loss years

FIGURE 2.

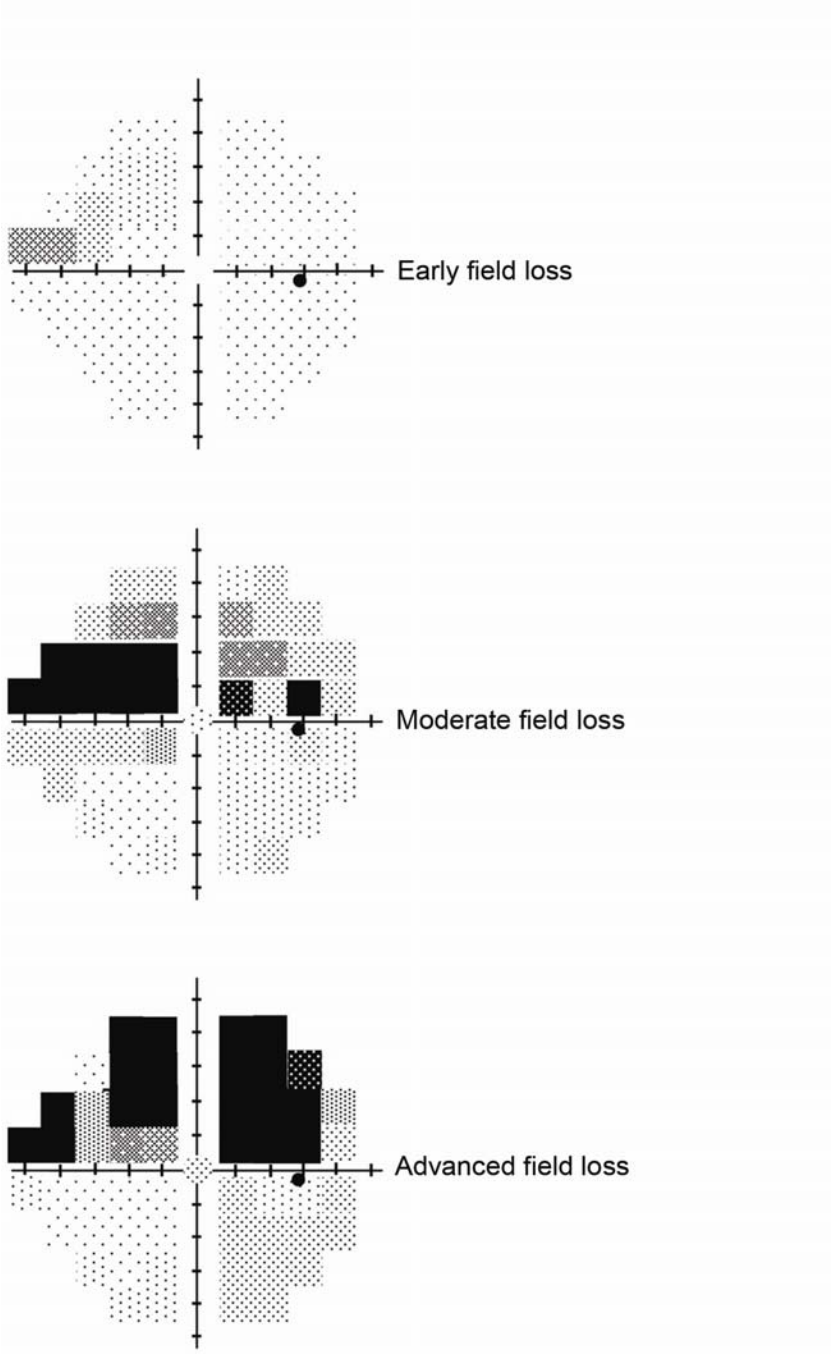

Figure 2. Grey scale plot of visual field derived from short-wavelength automated perimetry showing large arcuate scotoma in the superior visual field. Three panels indicate progressive loss of visual field. Different gray spectra show the level of visual loss and black indicates the blind spots. Source of image: adapted from Clement et, al., Br J Ophthalmol. 2009.

earlier because it is selective for a particular ganglion cell type (Johnson et al., 1993; Sit et al., 2004).

Pathological changes in glaucoma are also detected in visual centers in the brain and could account for visual defects. The lateral geniculate nucleus (LGN), a major central target of RGC axons in primates, shows significant atrophy and neuronal loss in primate experimental glaucoma (Ito et al., 2009; Yücel et al., 2001). Activated glial cells play important roles in the degenerative changes in the LGN as astrocytosis and microglial activation have been reported in the LGN and visual cortex in experimental glaucoma (Lam et al., 2009).

I.3. GLAUCOMA CLASSIFICATION AND EXPERIMENTAL MODELS

Glaucoma has been divided into two major categories: primary angle-closure glaucoma (PACG) and primary open-angle glaucoma (POAG). However, other sub-categories have been added to accommodate for the diversity of pathologies. The production, circulation and drainage of the aqueous humour (the clear fluid that fills the anterior and posterior chambers of the eye) are determining factors for the IOP level of the eye. Therefore, the anatomical structures of the eye involved in the production and circulation of the aqueous humour will be reviewed briefly.

The aqueous humour is produced by the ciliary epithelium of the ciliary body, provides nutrition for the lens and removes metabolic waste as it flows through the pupil into the anterior chamber of the eye (Krupin et al., 1986). The aqueous humour fills the anterior chamber providing nutrition to the cornea as well. There is an area in the anterior chamber where the cornea and iris join, the angle, where the drainage of aqueous humour takes place (Figure 3). Aqueous fluid flows toward the angle where it enters the trabecular meshwork (TM) (Tamm, 2009), a sieve-like structure that filters and directs the aqueous fluid into the Schlemm's canal (Johnstone, 2004). A portion of the aqueous humour leaves the anterior chamber through an alternative route called the uveo-scleral pathway (Gabelt and Kaufman, 2005; Goel et al., 2010). Several models of inducible and spontaneous glaucoma rely on blockade of the aqueous humour drainage and will be discussed in subsequent sections.

FIGURE 3.

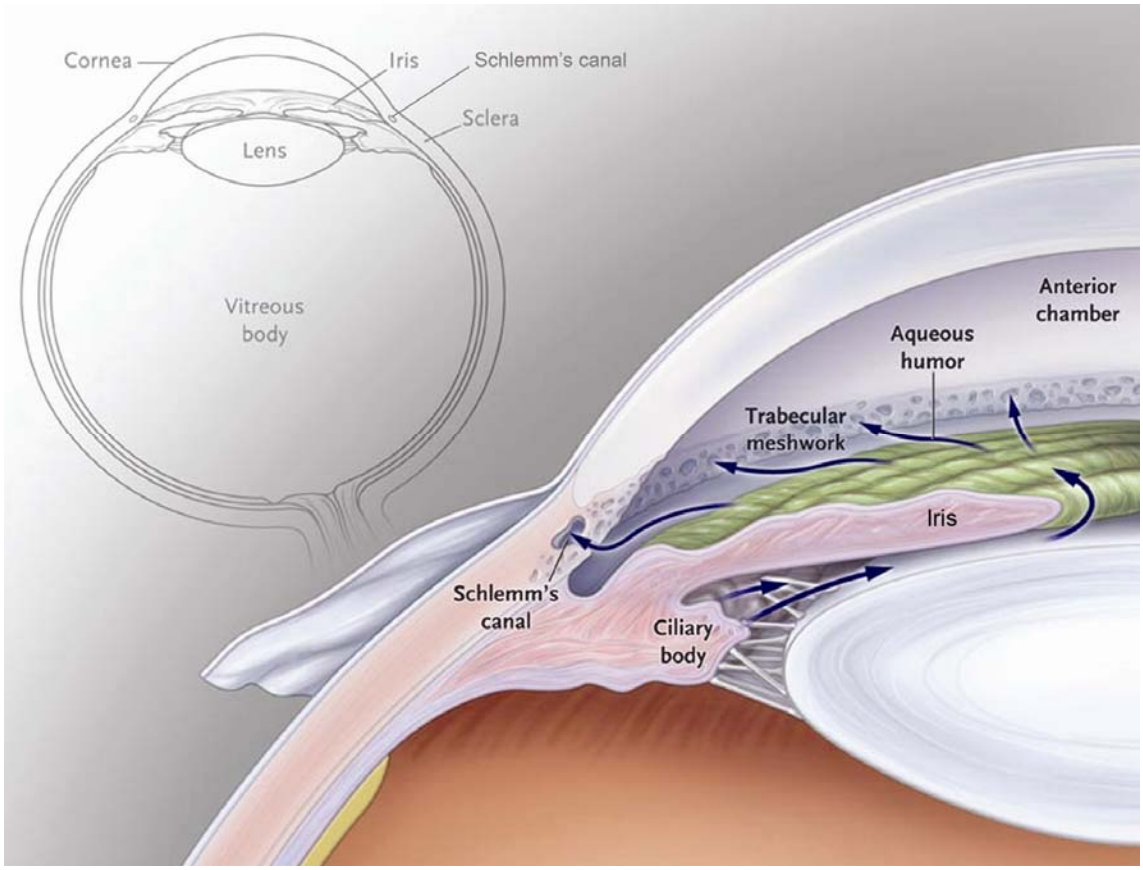

Figure 3. A schematic presentation of the structures in the angle of the eye and aqueous humour circulation. The aqueous humour is produced by the ciliary body and enters the anterior chamber via the pupil. The trabecular meshwork (TM) is located in the angle between the cornea and iris and provides a circumferential outlet for drainage of aqueous. In PACG, access to the TM is limited or severed due to physical closure of the anterior chamber angle; whereas in POAG, the TM is accessible, however ultrastructural changes in the TM itself result in reduction of outflow. Aqueous humour enters Schlemm's canal and after being collected in a circumferential venous plexus, joins the blood circulation via episcleral veins. Source of image: Kwon et. al., N. Engl. J. Med. 2009.

I.3.1. Primary angle-closure glaucoma

PACG is characterized by the blockade of the aqueous humour drainage and/or its circulation. This results in increased IOP and consequent damage to the retina and optic nerve. If the IOP increase is sudden and acute, it is often accompanied by pain and redness of the eye, blurry vision, headache and nausea (Sihota, 2011). The name "angle-closure" was originally used after the observation that the aqueous humour drainage is blocked in the angle of the eye resulting in IOP build up. PACG is primarily caused by an abnormal contact between anterior segment structures of the eye, including the cornea, iris, TM, ciliary body, and the lens. This could happen due to abnormal dilation of the pupil causing congestion of the iris in the angle of the eye. There is also a condition called plateau iris, characterized by an abnormal position of ciliary processes that push and hold the iris forward placing it too close to the TM (Kumar et al., 2008). Some PACG cases also involve pupillary blockade of the aqueous fluid. Pupillary blockade happens when the back of the iris adheres to the lens and blocks the passage of the aqueous humour to the anterior chamber. This not only increases the pressure in the posterior chamber but also pushes the periphery of the iris forward resulting in angle closure (Tarongoy et al., 2009). The extent of pupillary blockade and angle closure determines the magnitude and time-course of IOP increase, therefore PACG has been divided into acute (with sudden and severe IOP increase) and chronic (with a more gradual IOP increase) subcategories. When angle-closure happens as a result of other ocular diseases, it is referred to as secondary angle-closure glaucoma. For instance, secondary angle-closure glaucoma could happen due to an anterior-shift of the lens after ocular trauma (Sankar et al., 2001).

People of Asian descent and individuals with small axial eye length, have a greater risk of developing PACG. The common procedure for the treatment of acute PACG is to lower the IOP by medications (Hoh et al., 2002). Surgical techniques such as peripheral iridotomy, the generation of small holes in the peripheral iris using a laser, might also be required (Lam et al., 2007; Tarongoy et al., 2009). Analysis of the eyes with acute PACG revealed that although IOP was lowered immediately after diagnosis, there was still a significant reduction in the thickness of the retinal nerve fiber layer (RNFL) weeks after the acute episode (Aung et al., 2004).

I.3.1.1. Experimental models of primary angle-closure glaucoma

Several breeds of dogs are prone to develop glaucoma (Reinstein et al., 2009) and the high prevalence of glaucoma in some pure-bred dogs suggests a genetic basis for this disease (Gelatt and MacKay, 2004). For instance, a canine model (Basset Hounds) of hereditary PACG shows gradual narrowing and collapse of iridocorneal angles leading to complete angle-closure by 20 months of age; angle-closure in these dogs is accompanied by IOP build up, cupping of ONH and loss of RGCs (Grozdanic et al., 2010). However, the high cost of purchasing and housing dogs, their requirements for special care and the inherent problem of handling dogs in large experimental groups, results in limited use of this model.

Laser photocoagulation has been adapted for mice to induce the closure of the anterior chamber angle (Aihara et al., 2003). A diode laser is focused on the corneal limbus to create burn spots that directly attach the iris root to the peripheral cornea; consequently, obstruction of the aqueous outflow results in elevation of IOP (Aihara et al., 2003). Despite the differences in the structure of ONH between mice and humans, such as the lack of lamina cribrosa (May and Lütjen-Drecoll, 2002), the elevation of IOP in this model is accompanied by significant loss of RGC axons (Mabuchi et al., 2003). However, the small size of the mice eye demands a high level of expertise by the experimenter in using the laser as excessive or misplace laser burns could result in abrupt IOP increase, inflammatory response and retinal damage.

I.3.2. Primary open-angle glaucoma

Primary open-angle glaucoma (POAG) is the most common form of the glaucoma worldwide. POAG is characterized by changes in the optic disc, damage to RGC axons in the optic nerve, loss of RGCs in the retina and gradual visual field defects (Quigley, 2005). POAG is not necessarily associated with IOP elevation, however, high IOP is a major risk factor for developing POAG and a significant percentage of POAG cases show a gradual increase of IOP over the years (Leske et al., 2003). The increase in IOP is not necessarily accompanied with severe changes in anterior angle structures as previously described for PACG. Since resistance to the aqueous humour outflow is a major determinant of IOP levels, age-related or pathologic changes in the TM or Schlemm's

canal might lead to the gradual increase of the outflow resistance and IOP build up (Gabelt and Kaufman, 2005; Wordinger and Clark, 1999). Although morphological changes in optic disc vary little between PACG and POAG (Boland et al., 2008; Nouri Mahdavi et al., 2011), functional evaluation demonstrated that PACG patients have a more diffuse pattern of visual field loss compared to POAG patients (Boland et al., 2008; Rhee et al., 2001).

I.*3.2.1. Experimental models of primary open-angle glaucoma*

Our understanding about the mechanism of aqueous humour outflow and its importance in regulating IOP has been used to develop a number of experimental glaucoma models. Several animal species are suitable for induction of experimental ocular hypertension (OHT) and have provided useful functional and structural information about glaucoma onset and progression.

I.3.2.1.a. Primate model of POAG

In this model, Rhesus or Cynomolgus monkeys are subjected to laser photocoagulation, that by creating burn spots on the circumference of the TM, results in moderate IOP increase (Wang et al., 1998). A disadvantage is that multiple sessions of laser treatment are required to induce OHT. IOP elevation in this model is accompanied with ONH cupping and thinning of RNFL (Gaasterland and Kupfer, 1974). Loss of RGCs and functional defects are well documented in this model, indicating a close similarity to human POAG (Hare et al., 2001b; Hood et al., 1999; Morgan et al., 2000). Pathological changes in the visual centers in the brain such as loss of neurons in the magno and parvocellular layers of LGN are also detected (Yücel et al., 2003; Yücel et al., 2000). The high cost of monkeys, their limited availability and difficulty to work with are major disadvantages particularly for studies on neuroprotection since they require large number of animals.

I.3.2.1.b. Rodent models of POAG

The laser photocoagulation technique has also been used for induction of OHT in rodents (Levkovitch-Verbin et al., 2002b; Schori et al., 2001; Ueda et al., 1998; Wijono et al., 1999; WoldeMussie and Feldman, 1997). A beam of diode laser is concentrated on

the circumference of the TM to create burn spots; the peak IOP reaches 35-49 mmHg and it is sustained for at least 3 weeks (Levkovitch-Verbin et al., 2002b). A similar technique has been adapted for induction of OHT in mice (Gross et al., 2003; Ji et al., 2005).

The aqueous humour flows through the TM into the Schlemm's canal and then via collector channels into the limbal venous plexus and finally drains through the episcleral veins. This pathway has been used for retrograde transfusion of solutions towards the TM (Moore et al., 1993; Morrison et al., 1995). In the Morrison model of rat OHT, hypertonic saline solution is injected into an episcleral vein of Brown Norway rat eyes. Hypertonic saline causes sclerotic damage to the TM cells, disrupts the structure of the TM and gradually reduces the aqueous outflow, resulting in IOP elevation (Morrison et al., 1997). Another method of reducing the aqueous outflow is by cauterizing the episcleral veins (Shareef et al., 1995). In this model, two to three veins are isolated and blocked using an ophthalmic cautery (Shareef et al., 1995).

Obstruction of the TM and elevation of IOP can also be achieved by injection of sterile latex microspheres (Urcola et al., 2006; Weber and Zelenak, 2001) or microbeads into the anterior chamber of rodents (Chen et al., 2011; Sappington et al., 2010). Finally, a hereditary mutation in the DBA/2J mice leads to iris pigment dispersion and anterior synechia (adhesion of the iris to the cornea) that results in significant elevation of IOP by 6 months of age (John et al., 1998).

To select a suitable rodent glaucoma model for research, the objectives of the study and the advantages/disadvantages of each model should be considered carefully. For instance, rat models are generally more appropriate for ONH studies because unlike mouse, the rat ONH has a well-defined lamina cribrosa. The structure of the lamina is similar to that in primates regarding protein content, connective tissue components and blood vessels (Morrison et al., 1995). Elevation of IOP in rat models results in cupping of ONH, loss of axons in the optic nerve and RGCs death. Mouse glaucoma models in the other hand, confer the advantage of using transgenic animals to study the role of specific genes in the development of glaucoma (Whitehouse et al., 1982).

The major disadvantage of laser photocoagulation technique is the necessity of multiple treatments to achieve a steady IOP elevation. In addition, retinal oedema and haemorrhage often occur in this model. The cauterization model has a slow rate of

progress with considerable variability in the pattern and number of RGC death (Danias et al., 2006); there is also the possibility of necrosis of the eye if several episcleral trunks are blocked (Ahmed et al., 2001; Laquis et al., 1998). The DBA/2J mouse model shows great variability in the onset and progression of glaucoma between individual animals which dramatically increases the number of animals required for each experiment. The microbeads injection model is a relatively simple and promising model but there is high variability in the levels of IOP achieved following injection of microbeads (Chen et al., 2011; Sappington et al., 2010). The Morrison model is also a simple, reliable and reproducible model of experimental glaucoma in Brown Norway rats. IOP elevation in this model results in ONH cupping and gradual loss of axons in the optic nerve (Johnson et al., 1996; Morrison et al., 1997). Progressive loss of RGC in this model is also well documented (Guo et al., 2005; Johnson et al., 2007b). General anaesthetics are often used in rodents to allow IOP measurements, however, anaesthetics result in a substantial decrease of IOP (Jia et al., 2000). An advantage of the Morrison model is that Brown Norway rats are extremely docile allowing IOP measurements in unanaesthetized animals, thus providing the most accurate documentation of IOP history. Due to its advantages, particularly in regard to neuroprotection studies, the Morrison model was selected and used throughout this thesis.

I.3.3. Normal tension glaucoma

Many glaucoma patients display typical glaucomatous visual defects and RGC loss while their IOP is within the normal range (CNTGSG, 1998). These cases are classified as normal tension glaucoma (NTG). The visual field loss in NTG patient progresses with a similar rate as POAG patients, therefore diagnosis and treatment of NTG demands particular attention (Ahrlich et al., 2010). The exact cause of NTG is unknown; however, several mechanisms have been proposed. Among these are the association of visual field loss and decreased blood flow in the optic disc of NTG patients (Ciancaglini et al., 2001; Nicolela et al., 1996; Sato et al., 2006) and the higher rate of the hemorrhages in the fundus (Ishida et al., 2000; Tezel et al., 1996); suggesting a correlation between ocular blood flow and vascular dysfunction in NTG. There is also evidence of an autoimmune response, highlighted by elevated levels of antibodies against

heat shock proteins (HSPs) (Wax et al., 1998). Since glaucoma is now considered a neurodegenerative disease, oxidative damage and excitotoxicity may play a role in the pathology of NTG.

I.4. MECHANISMS OF NEURONAL DAMAGE IN GLAUCOMA

I.4.1. The role of vascular dysfunction in the pathology of glaucoma

An increasing body of evidence suggests that retinal and ONH blood flow are among the risk factors for the development of glaucoma (Flammer et al., 2002; Osborne et al., 2001). There is a significant reduction of blood flow in the ONH of PAOG patients (Piltz-seymour et al., 2001). Elevated IOP and compression of the vessels at the level of the lamina cribrosa has been proposed to be the cause of blood flow reduction (Downs et al., 2008; Feher et al., 2005). However, loss of visual field in NTG patients is also associated with decreased optic disc blood flow (Ciancaglini et al., 2001; Nicolela et al., 1996; Sato et al., 2006) and the severity of neuronal damage in NTG and POAG patients correlates with a reduction in retinal blood flow (Bjärnhall et al., 2007; Sato et al., 2006). When the IOP of healthy volunteers was temporarily increased, it resulted in a clear vasodilatory response. However, the same level of temporary IOP increase in POAG patients resulted in a much smaller vasodilatory response (Nagel et al., 2001). These observations suggest an underlying vascular deficiency contributing to the pathology of glaucoma.

I.4.1.1. The retinal circulation

In terms of blood supply, the retina is divided into two regions: *i*) the outer retina, including photoreceptors, outer nuclear and outer plexiform layers, is supplied by the choroid capillaries originating from the posterior ciliary arteries (Saint Geniez and D'Amore, 2004); *ii*) the inner retina, including the nerve fiber layer, RGC layer, inner plexiform and inner nuclear layer, is supplied by the central retinal artery (Figure 4). The branches of the central retinal artery expand to form two inner capillary networks, one superficial, at the level of nerve fiber layer and one deeper, between the inner nuclear and outer plexiform layers (Pournaras et al., 2008). The capillaries of the inner retinal

networks are in close interaction with RGCs and other neuronal-glial elements of the retina to meet the metabolic demands of this tissue.

Retinal capillaries are composed of a single layer of endothelial cells enclosed in a basement membrane shared with surrounding pericytes (Kniesel and Wolburg, 2000; Russ et al., 1998). Pericytes are specialized mural cells found in the CNS that play an integral role in vascular tone (Bandopadhyay et al., 2001). Retinal capillaries are smaller in diameter with thinner walls compare to non-neuronal capillaries and are morphologically very similar to cerebral capillaries; however, their endothelial cells have a higher density of vesicles and higher permeability compare to their counterparts in the brain (Stewart and Tuor, 1994). Retinal capillaries are also accompanied by a considerable higher number of pericytes (up to 4.5-fold) compared to cerebral capillaries and their pericyte processes cover more than 85% of the circumference of the retinal endothelial tube (Frank et al., 1987; Stewart and Tuor, 1994). Pericytes together with the glial cell's end-foot processes, strengthen the blood-retinal barrier and play important roles in compensating for more permeable endothelial cells compared to brain capillaries (Kim et al., 2006a; Stewart and Tuor, 1994).

I.4.1.2. Regulatory mechanisms of retinal circulation

The proper regulation of ocular blood flow is vital for normal retinal function. The ocular vessels respond to the increased neuronal activity by increasing the blood flow, a phenomena known as neurovascular coupling (Garhöfer et al., 2004; Riva et al., 2005). The choroidal vascular bed is innervated by autonomic vasoactive nerves that control the choroidal blood flow (Schrder et al., 1994). Unlike the choroid, the central retinal artery has limited sympathetic innervation that ends at the level of lamina cribrosa (Laties, 1967). Therefore, local vasodilatory and vasoconstrictor mediators play important roles in regulating the retinal blood flow (Metea and Newman, 2007). The production and release of vasoactive compounds by endothelial cells contribute to the regulation of retinal vascular tone. Nitric oxide (NO) and endothelins (ET) are among the most important endothelium-derived vasoactive factors (Chakravarthy et al., 1995; Loscalzo and Welch, 1995; Takagi et al., 1996).

FIGURE 4.

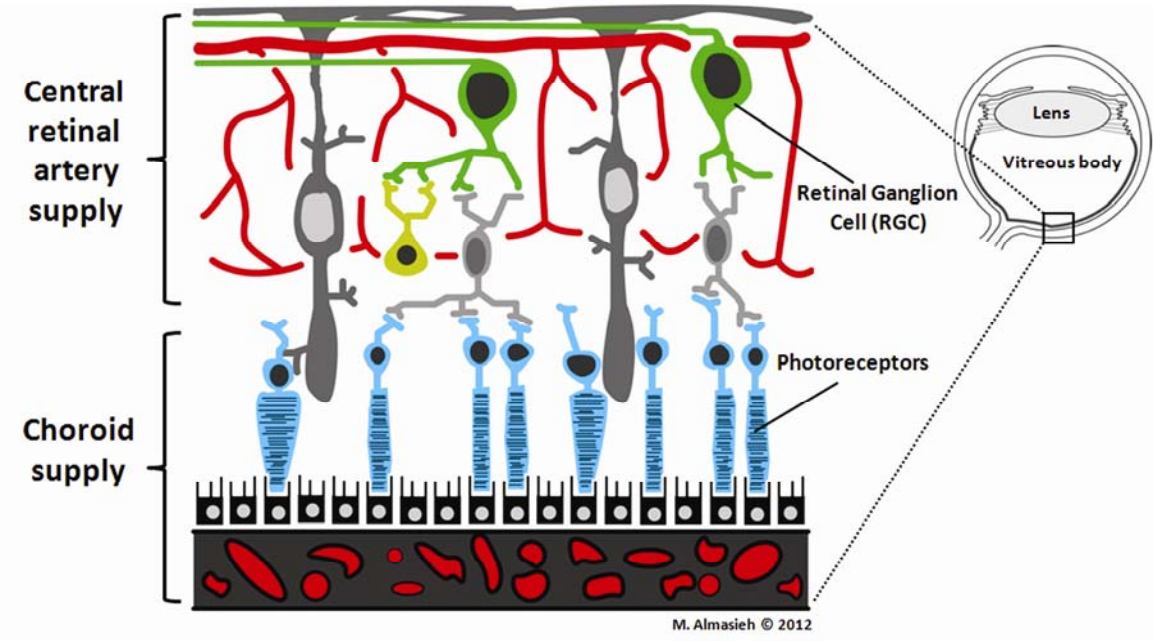

Figure 4. Sources of blood supply for the retina and optic nerve. The central retinal artery and the posterior ciliary arteries are branches of the ophthalmic artery. Branches of posterior ciliary arteries enter the eye to form the choroid. The central retinal artery enters the optic nerve at 8–12mm behind the globe and after supplying the optic nerve with a few small branches, it divides into two major trunks before leaving the optic disc. The branches of the central retinal artery expand to form two inner capillary networks, one superficial, at the level of nerve fiber layer and one deeper, between the inner nuclear and outer plexiform layers. Source of image: Mohammadali Almasieh.

I.4.1.2.a. Nitric oxide

NO is a potent neurotransmitter that regulates a wide variety of cellular functions. Three different isoforms of nitric oxide synthase (NOS) are involved in NO production: neuronal (nNOS or NOS1), inducible (iNOS or NOS2) and endothelial (eNOS or NOS3) (Alderton et al., 2001). In the retina, nNOS is expressed by RGCs, photoreceptors and amacrine cells; while eNOS is expressed by endothelial cells (Neufeld et al., 2000; Shareef et al., 1999). iNOS is activated in response to inflammation or tissue damage and is thought to contribute to cytotoxic NO signaling (Calabrese et al., 2007; Chiou, 2001). In physiological concentrations, NO signals through activation of guanylyl cyclase receptors and production of cGMP (Garthwaite, 2008). NO plays an important vasodilatory role in the retina. Experimental inhibition of retinal NOS by intravitreal injection of its inhibitors N-monomethyl-L-arginine (L-NMMA) or (L-NAME) resulted in significant vasoconstriction of retinal arterioles and venules indicating that NO production is necessary for maintaining a basal level of vascular relaxation (Donati et al., 1995; Dorner et al., 2003). Hyperemia is the activity-induced increase in blood flow in a tissue and can be easily induced in the retina by light flicker (Maelicke, 2000). Inhibition of NOS significantly reduces the retinal hyperemic response to light flicker, indicating that NO also participates in the activity dependent modulation of the retinal blood flow (Dorner et al., 2003). In normal subjects, systemic inhibition of NOS significantly reduces ONH blood flow (Luksch et al., 2000). Dysfunctional NO signaling in glaucomatous eyes became evident by a much smaller response of POAG patients to NOS inhibition (Polak et al., 2007). NO levels also effect production and drainage of the aqueous humour (Whitehouse et al., 1982). Reduction of NO levels and eNOS activity has been reported in ocular tissues of POAG patients including the TM (Nathanson and McKee, 1995).

I.4.1.2.b. Endothelins

Endothelins are a family of vasoconstrictor peptides. They are released by endothelial cells and interact with their G-protein-coupled, ET_A and ET_B receptors (Davenport, 2002; Yanagisawa et al., 1988). ET_A receptors are mainly expressed by the smooth muscle cells of blood vessels and mediate vasoconstriction upon binding of

endothelin-1 (ET-1) (Pierre and Davenport, 1998). ET_B receptors have a broader pattern of expression and can be found on neuronal and glial components of the retina (MacCumber and D'Anna, 1994; Stitt et al., 1996). It appears that ET_A and ET_B subtypes can mediate opposing actions in a complex manner. Blockade of the ET_B receptors significantly increases peripheral vasoconstriction (Strachan et al., 1999). Activation of ET_B receptors alone has a net constrictor effect but simultaneous activation of both subtypes is vasodilatory (Just et al., 2004; Mickley et al., 1997). Endothelial cells express ET_B and its activity results in the release of relaxing factors such as nitric oxide and prostanoids from endothelial cells (Hirata et al., 1993; Just et al., 2005).

The level of endothelins and the expression of their receptors change in experimental and human glaucoma. For instance, levels of ET-1 in serum and aqueous humour of POAG patients is higher than in control individuals (Emre et al., 2005; Nicolela et al., 2003; Noske et al., 1997; Sugiyama et al., 1995; Tezel et al., 1997). In addition, ET-1 levels in the ONH of animals subjected to experimental glaucoma increases significantly compare to control groups (Howell et al., 2011; Prasanna et al., 2005). Receptor dysfunction has been proposed to play central role in blood flow irregularities in glaucomatous eyes. While treatment of normal subjects with an antagonist of ET_A resulted in a significant vasodilatory response, a similar treatment had a lesser effect on the vascular tone of NTG patients (Henry et al., 2006; Henry et al., 1999). Recently, ET_A gene polymorphisms have been considered to be a potential risk factor for developing NTG (Ishikawa et al., 2005; Kim et al., 2006b). Endothelins might also be involved in the induction of a glial response in the glaucomatous ONH. Reactive astrocytes in the ONH of experimental and human glaucoma are characterized by the expression of ET_A and ET_B (Wang et al., 2006; Wang et al., 2009). Incubation of isolated ONH astrocytes with ET-1 results in their activation and induces marked proliferation (Murphy et al., 2010; Prasanna et al., 2002). ET_A is also expressed in structures of the anterior segment such as the iris, ciliary body, trabecular cells and endothelial lining of the Schlemm's canal (Fernández-Durango et al., 2003). Therefore endothelin signaling can also participate in the production of aqueous humour and the control of its outflow. A treatment strategy based on endothelin antagonism has been proposed to control IOP

increase and to improve retinal blood flow (Fernández-Durango et al., 2003; Rosenthal and Fromm, 2011).

I.4.1.3. Vascular degeneration

In addition to vasomodulatory abnormalities, there is also evidence of structural changes in the vasculature of glaucomatous eyes. In some POAG patients, the central retinal artery is characterized by arteriosclerotic changes such as the thickening of the basement membrane, proliferation of muscle cells into the intimae, fragmentation of the inner elastic membrane and arteriosclerotic plaques in the intimae (Gottanka et al., 2005). Narrowing of the lumen of smaller arterioles in the optic nerve and deposits of amorphous material in the basement membrane of endothelium are the other pathological findings in the POAG (Feher et al., 2005; Gottanka et al., 2005). A significant decrease in the density of capillaries has been observed in the optic nerve laminar region of POAG patients and in rat experimental glaucoma (Daz et al., 2010; Gottanka et al., 2005). These observation are in agreement with initial reports by Quigley and colleagues indicating a considerable loss of disc tissue and its capillaries (Quigley et al., 1984). Fluorescein angiograms show a high rate of capillary non-perfusion in the optic disc of NTG and POAG patients (Plange et al., 2006). Pathological changes in the vasculature also play important roles in the progression of other neurodegenerative diseases such as Alzheimer's disease (Budinger, 2003). In fact, pathological vascular changes like acellular capillaries have been found in both glaucomatous retinas and in the brains of Alzheimer's patients (Brown, 2010b).

I.4.1.4. Neurotrophic factors and vascular reactivity

In addition to neurons, neurotrophic factors also regulate survival and function of non-neuronal cells. In fact production of neurotrophic factors like BDNF and NGF is not limited to neuronal tissues as several non-neuronal tissues including the elements of cardiovascular system also express neurotrophins and their receptors (Scarisbrick et al., 1993; Yamamoto et al., 1996). Interaction of neurons and vasculature through neurotrophic factors is in particular complex and plays important role in development and physiological functions of both systems.

Neurotrophins are involved in regulation of angiogenesis, for instance, activation of neurons by BDNF and NGF increases production and secretion of VEGF by neurons which in turn results in endothelial cells proliferation (Nakamura et al., 2011). Brain-derived endothelial cells themselves shown to synthesis BDNF and express TrkB and $p75^{NTR}$ receptors (Kim et al., 2004b). They also produce NGF and express its receptor TrkA (Moser et al., 2004). Direct activation of TrkA receptors of endothelial cells by exogenous NGF results in proliferation of these cells and also increases the secretion of NGF by endothelial cells (Moser et al., 2004). In addition, NGF improves survival of endothelial cells under oxygen-glucose deprivation conditions (Lecht et al., 2010). Local production and release of major neurotrophin family members like BDNF and NGF by endothelial cells and the interaction of these trophic factors with TrkA, TrkB and $p75^{NTR}$ receptors provides an autocrine/paracrine regulatory system for cell proliferation in the vasculature (Kim et al., 2004b; Tanaka et al., 2004).

Recent studies show that neurotrophic factors produced by brain endothelial cells could be important for survival of neurons as they significantly extend the survival of isolated cortical neurons (Dugas et al., 2008). Endothelial source of BDNF also provides significant support for neurons in a number of situations like oxidative stress-hypoxia and neurotoxicity (Guo et al., 2008). In addition, secration of BDNF by endothelial cells provides important support for migrating neuroblasts that originate from sub-ventricular zone or sub-ependymal zone and helps to guide them towards their targets in the brain (Leventhal et al., 1999; Snapyan et al., 2009).

Currently, our knowledge about the effects of neurotrophins on retinal blood flow is limited; however, neurotrophins like BDNF stimulate the endothelial cells to generate more NO and shown to have vasodilatory effects in other systems (Meuchel et al., 2011). It has also been shown that using the viral vectors to overexpress BDNF in cerebral vessels results in upregulation of prostacyclin (PGl2) that leads to vascular relaxation (Santhanam et al., 2010); however, no significant change in the expression or activity of the eNOS has been detected in these experiments (Santhanam et al., 2010). It is important to mention that early in the development of brain, PGI2 is the primary mediator of endothelium-dependent relaxations in cerebral circulation; however, in the adult and aging brain, nitric oxide takes over as the primary vascular vasodilator (Charpie et al.,

1994; Willis and Leffler, 2001). Interestingly, intraocular application of BDNF results in a higher expression of vasoactive intestinal polypeptide by amacrine cells that by relaxing smooth muscle cells leads to vasodilation (Cellerino et al., 2003).

Intraocular application of BDNF significantly increases survival of RGCs in the traumatic optic nerve damage models and also increases NOS activity as it has been evaluated by NADPH-diaphorase reactivity (Klcker et al., 1998). However, it is suspected that BDNF also results in activation of iNOS that considered to be a limiting factor for the survival of RGCs due to promotion of nitrosative stress through formation of peroxynitrite (Klcker et al., 1998; Klcker et al., 1999). Further studies in line with development of new experimental protocols are needed to evaluate the role of neurotrophic factors in the improvement of retinal blood flow and protection of RGCs in pathological conditions.

I.4.2. Oxidative stress

Oxidative stress, caused by the imbalance between the production of reactive oxygen species (ROS) and their elimination by antioxidants, has been recognized as a central contributor to neuronal injury and death. ROS are continuously produced by mitochondria through the electron transport chain, but can also be generated by enzymatic degradation of neurotransmitters, neuroinflammatory mediators, and redox reactions (Halliwell, 2006). Increased levels of ROS like superoxide anion ($O^{2\bullet}$) and hydroxyl radical ($OH^{\bullet}$), a common feature of neurodegenerative diseases, can originate from mitochondrial dysfunction, abnormal protein folding, and defective ubiquitination and proteasome degradation systems (Andersen, 2004).

There is evidence that oxidative damage occurs in experimental models of optic nerve injury and in human glaucoma. For example, the presence of DNA damage and accumulation of protein and lipid peroxidation products have been documented in the TM and retinas from experimental ocular hypertension models and POAG patients (Babizhayev and Bunin, 1989; Izzotti et al., 2003; Ko et al., 2005; Moreno et al., 2004; Sacc et al., 2005; Tezel et al., 2005). Furthermore, an intracellular ROS superoxide burst has been proposed to be a critical death signal triggered by axonal injury leading to RGC apoptosis (Geiger et al., 2002; Kanamori et al., 2010; Lieven et al., 2006; Nguyen et al.,

2003; Swanson et al., 2005). During hypoxia, the generation of mitochondrial ROS is necessary for activation of the hypoxia-inducible factor-1 alpha (HIF-1α), a transcriptional regulator required for the induction of a variety of genes (Chandel et al., 2000; Duranteau et al., 1998). Expression of HIF-1α and HIF-1α target genes, including erythropoietin, heat-shock protein 27 (Hsp-27) and vascular endothelial growth factor, increase in experimental rat glaucoma (Ergorul et al., 2010), and high levels of HIF-1α are found in the retina and optic nerve head of glaucoma patients (Tezel and Wax, 2004).

I.4.2.1. Neuronal antioxidant systems

Cells are naturally equipped with an arsenal of protective antioxidant systems such as superoxide dismutase (SOD), catalase, and glutathione peroxidase and glutathione reductase (Vendemiale et al., 1999). The SOD family of enzymes catalyze the dismutation of superoxide into molecular oxygen (O_2) and H_2O_2, decreasing the chance of $OH^{\bullet}$ formation (Fridovich, 1995). The byproduct of this process, H_2O_2, is toxic and therefore is converted to water by catalases and glutathione peroxidases. Logic follows that an insufficiency in ROS neutralizing mechanisms in RGCs might play a role in the progression of glaucoma and, in fact, circumstantial evidence exists in favor of this idea. SOD activity decreases in the trabecular meshwork of patients with glaucoma (Behndig et al., 1998; De La Paz and Epstein, 1996) and in the retina in experimental ocular hypertension (Moreno et al., 2004). RGCs are particularly vulnerable to the lack of the copper- and zinc-containing cytoplasmic form of SOD (SOD-1), as SOD1 knock-out mice are characterized by loss of RGC function, accumulation of superoxide in RGC soma and age-dependent RGC loss (Hashizume et al., 2008; Yuki et al., 2011). Exogenous supplementation or overexpression of SOD-1, however, have yielded conflicting results: while some studies showed neuroprotection of axotomized RGCs following SOD-1 administration (Kanamori et al., 2010; Schlieve et al., 2006), others reported accelerated RGC death in transgenic mice overexpressing SOD-1 (Levkovitch-Verbin et al., 2000).

The regulation of cellular redox status is provided by the glutathione and the thioredoxin (TRX) systems. Glutathione is a tripeptide molecule composed of glutamate, cysteine and glycine; in its reduced form, reduced glutathione (GSH) is a necessary

cofactor for the glutathione peroxidase family of enzymes (Sarma and Mugesh, 2008). In the retina, glutathione is produced mainly by Müller cells but also in smaller quantities by horizontal cells (Pow and Crook, 1995). Glutathione is then transferred from Müller cells to RGCs and other neurons in the retina (Schtte and Werner, 1998). The TRX system is a key endogenous defense mechanism against oxidative damage that includes TRX proteins, TRX-interacting protein (TXNIP), TRX reductase (TRXR) and NADPH (Lillig and Holmgren, 2007). The major TRX protein isoforms, the cytoplasmic TRX1 and the mitochondrial TRX2, act as antioxidants by maintaining a reduced environment within cells through their dithiol/disulphide reducing activity and by inhibiting the oxidative aggregation of toxic proteins (Collet and Messens, 2010). TRX2 plays an important antioxidant role against mitochondrial oxidative stress (Yoshida et al., 2003): heterozygous ($Trx2^{+/-}$) transgenic mice display reduced mitochondrial function and ATP production as well as increased oxidative damage (Pérez et al., 2008).

Neurons also respond to redox imbalance by upregulating endogenous antioxidant machinery. Upon oxidative insult, expression of several antioxidant enzymes, controlled by the antioxidant response element (ARE) promoter, are upregulated. (Dringen et al., 2005; Hayes and McLellan, 1999; Nguyen et al., 2009). NF-E2-related factor-2 (Nrf2) transcription factor plays a major role in activation of ARE-controlled genes in response to oxidative stress (de Vries et al., 2008; Kensler et al., 2007; Kobayashi and Yamamoto, 2006). Activation and nuclear translocation of Nrf2 itself is controlled by cellular redox state; under normal conditions Nrf2 is bound to an inhibitor protein, Keap1, which retains Nrf2 in the cytoplasm and targets it for ubiquitination (Furukawa and Xiong, 2005; Sun et al., 2007). However Keap1 is a redox sensitive protein and its oxidation results in Nrf2 and Keap1 dissociation, leading to nuclear translocation of Nrf2, where it promotes transcription of ARE-controlled genes (Kensler et al., 2007).

I.4.2.2. Oxidative stress and activation of apoptotic pathways

TRX proteins also regulate cell death by redox modification of pro-apoptotic kinases. The mitogen-activated protein kinases (MAPKs) are a large family of protein Ser/Thr kinases with central regulatory role in many cellular functions (Cargnello and Roux, 2011). Activation of pro-survival MAPKs like extracellular signal-regulated

kinases 1/2 (Erk1/2) promote RGCs survival (Zhou et al., 2005). In contrast, pro-apoptotic MAPKs like p38 mitogen activated protein kinases and c-Jun N-terminal kinases (JNKs), also known as stress-activated protein kinases (SAPKs), are typically activated by a variety of stress signals and contribute to RGC death (Brecht et al., 2005; Cuadrado and Nebreda, 2010; Curran and Franza, 1988).

Apoptosis signal regulating kinase 1 (ASK1), is a SAPK belonging to the mitogen-activated protein kinase kinase kinase (MAPKKK) family and plays key roles in human neurodegenerative diseases (Hattori et al., 2009); ASK1 activates JNK and p38 in response to diverse stress stimuli, particularly inflammatory cytokines and oxidative stress (Hatai et al., 2000; Ichijo et al., 1997; Min et al., 2008; Zhang et al., 2007a). Reduced TRX is normally bound to ASK1 thus preventing ASK1 autophosphorylation. Oxidation of cysteine thiols in TRX results in its dissociation from ASK1, triggering ASK1 autophosphorylation and downstream stimulation of JNK and p38 death signaling (Hatai et al., 2000; Ichijo et al., 1997; Saitoh et al., 1998). A significant decrease in TRX1 and TRX2 was reported in acute and chronic models of optic nerve damage, including ocular hypertension (Munemasa et al., 2008; Munemasa Y, 2009) while the levels of TXNIP, a negative regulator of TRX, increased (Caprioli et al., 2009). Furthermore, over-expression of TRX1 and TRX2 protected RGCs from pharmacologically-induced oxidative stress, optic nerve axotomy and ocular hypertension (Caprioli et al., 2009).

A recent *in vivo* study using live imaging demonstrated that superoxide increases sharply in RGCs at the single-cell level, soon after optic nerve axotomy, and precedes RGC apoptosis (Kanamori et al., 2010). ROS can modulate protein function by altering redox states leading to cysteine sulfhydryl oxidation. Oxidative cross-linking creates new disulfide bonds causing protein conformational changes and subsequent activation of cell death signals (Carugo et al., 2003; Park and Raines, 2001). Consistent with this, RGC viability depends on the intracellular sulfhydryl redox state, with survival observed under mildly reducing conditions and increased death rates induced by sulfhydryl oxidation (Castagne and Clarke, 1996; Castagne et al., 1999; Geiger et al., 2002; Swanson et al., 2005). An attractive hypothesis is that reduction of oxidized sulfhydryls on critical proteins might attenuate the activation of death pathways that influence the fate of RGCs

after injury. In this thesis, we will explore this hypothesis by using a reducing agent based on a borane-protected phosphine backbone.

I.4.2.3. ROS and retinal vasculature

Oxidative stress and ischemic retinopathies are often followed by activation of angiogenic cytokines leading to vascular inflammatory reactions and ocular neovascularization (Dong et al., 2009). It has been shown that exogenous ROS, in particular peroxynitrite, by nitrating the tyrosine residues of phosphatidylinositol 3-kinase results in inhibition of the Akt activity that blocks the pro-survival effect of VEGF on vasculature (El-Remessy et al., 2005). However, hypoxic conditions significantly increase the VEGF mRNA half-life; this post-transcriptional regulation is via modification of a 3′- region of the VEGF mRNA by ROS that results in the improved stability of the VEGF mRNA (Levy et al., 1996). Hypoxia also effects transcriptional regulation of an important gene encoding the VEGF receptor (Flt-1), resulting in upregulation in the expression of this receptor (Gerber et al., 1997). In addition, ROS like peroxynitrite, via activation of STAT3 pathway, increase expression of VEGF itself (Platt et al., 2005). Peroxynitrite also through a nitration-independent mechanism promotes angiogenesis as exogenous peroxynitrite was able to phosphorylate the VEGFR2 leading to endothelial cell growth and capillary formation (El Remessy et al., 2007). VEGF receptor activation is followed by intracellular generation of hydrogen peroxide that leads to activation of phosphatidylinositol 3-kinase and the small GTPase Rac-1and facilitates the angiogenesis, therefore, ROS could act as intracellular angiogenic mediators. (Colavitti et al., 2002). It is interesting to know that in the mice deficient for superoxide dismutase 1 (Sod1($^{-/-}$)), signs of oxidative stress are accompanied by severe ocular neovascularization, that is improved by antioxidants treatment (Dong et al., 2011).

I.4.2.3.1. ROS and vascular tone

ROS play important role in both physiologic and pathologic regulation of vascular tone. For instance, endothelium-dependent relaxation produced by vasodilator bradykinin, is mediated through hydroxyl radical (Rosenblum, 1987). Further studies showed that vasodilatory effects of bradykinin and arachidonic acid is mediated via SOD activity and is result of H_2O_2 production (Sobey et al., 1997). In the brain, exposure to

superoxide, hydrogen peroxide and peroxynitrite results in cerebral vasodilation (Wei et al., 1996). There are evidence that vascular regulatory systems are also under redox regulation, in particular, production of prostanoids is regulated by a nitric oxide-superoxide system (Bachschmid et al., 2005; Schildknecht and Ullrich, 2009). Activity of vasoactive agent, ET-1, also has been linked to intracellular production of ROS as activation of ET(A) receptors in the retinal microvessles is followed by increased formation of superoxides anions (Matsuo et al., 2009).

Hypoxic and ischemic conditions also result in release of ATP into the extracellular space that activates ATP-sensitive potassium channels of pericytes and leads to retinal vasodilation (Li and Puro, 2001). These ATP-sensitive potassium channels are predominantly located on capillaries of the retina (compare to arterioles) which boosts response of microvessels to hypoxic conditions (Jiang et al., 1998). ATP-sensitive potassium channels located on retinal microvasculature are redox sensitive and presence of ROS increases their activity (Ishizaki et al., 2009). Endothelial cells in this microvessels are also rich in polyamine-dependent potassium channels and their activation in hypoxic conditions is followed by endothelial cell death (Nakaizumi and Puro, 2011).

I.4.3. Nitrosative stress

NO participates in the post-translational modification of proteins by nitrating specific cysteine amino acids, a process known as S-nitrosylation, which has a significant impact on the regulation of protein function (Choi et al., 2000; Jaffrey et al., 2001b). NO can also interact with other free radicals as it does with superoxide to form peroxynitrite, a potent oxidant and nitrating agent (Beckman and Koppenol, 1996). Unlike NO, which favors nitration of cysteine residues in proteins, peroxynitrite results in the nitration of tyrosine residues leading to the formation of nitrotyrosine which has been associated with neuronal damage (Beckman, 1996; Pacher et al., 2007). NO entry to the mitochondria can also increase superoxide production, therefore the risk of peroxynitrite formation increases in such cases (Brown, 1999). Several important cellular processes are regulated by S-nitrosylation including the transcriptional activity of NF-κB, CREB and HIF. S-nitrosylation also modulates the Ca^{2+} influx through NMDAR and other Ca^{2+} channels

and nitrosylation of substrates such as caspase-3, TRX, Glyceraldehyde 3-phosphate dehydrogenase (GAPDH) and X-linked inhibitor of apoptosis protein (XIAP) critically effect the balance of cell survival and death (Chung, 2010). The wide range of roles and interactions attributed to NO might explain its contribution to both pro-survival and pro-apoptotic pathways in neurons (Brown, 2010a; Fiscus, 2002; Kim et al., 1999; Nicotera et al., 1997).

The initial evidence for the involvement of NO in the pathophysiology of glaucoma came from studies showing increased iNOS expression in the astrocytes isolated from the ONH of glaucoma patients (Liu and Neufeld, 2000; Neufeld et al., 1997). Although increased expression of iNOS has also been reported in the retina and ONH astrocytes from rats with ocular hypertension (Shareef et al., 1999; Vidal et al., 2006), other groups failed to detect changes in iNOS levels in both inducible and genetic models of glaucoma or ocular tissues from POAG patients (Libby et al., 2007; Pang et al., 2005). The non-specific NOS inhibitors N-nitro-L-arginine (NOLA) N-nitro-l-arginine methyl ester (l-NAME) delayed RGC death after optic nerve axotomy (Koeberle and Ball, 1999). The iNOS inhibitor aminoguanidine was neuroprotective in an episcleral vein cauterization rat glaucoma model (Neufeld, 2004), but the same compound did not promote RGC survival in rats with ocular hypertension induced by episcleral injection of hypertonic saline (Pang et al., 2005). Furthermore, genetic deficiency of iNOS or aminoguanidine treatment did not attenuate optic nerve damage in DBA/2J mice (Libby et al., 2007).

An alternative approach to evaluate the potential role of NO in glaucoma is to examine the generation of nitrotyrosine in target proteins, a hallmark of peroxynitrite production. The retinal expression of nitrotyrosine has been recently shown to increase in models of optic nerve crush injury (Thaler et al., 2010) and excitotoxic damage (Al-Gayyar et al., 2010). In POAG patients, nitrotyrosine formation was detected in astrocytes, endothelial cells and smooth muscle cells located in the pre-laminar area of the ONH (Feilchenfeld et al., 2008). Nitrotyrosine expression was also detected in the TM of POAG subjects with a noticeable increase in iNOS and reduction of eNOS in this tissue (Fernndez-Durango et al., 2008). Of interest, increased nitrotyrosine immunoreactivity was detected in the LGN of primates with experimental glaucoma

(Luthra et al., 2005). Though circumstantial, these studies point to an abnormal accumulation of nitrosylation products that extends from the TM to the brain suggesting a possible role of NO pathology, acting in separate visual system compartments in glaucoma. The use of techniques with higher sensitivity and specificity, including proteomics, might improve the detection of nitrotyrosine-modified proteins in glaucoma as well as provide information about the identity of the target proteins involved (Bigelow and Qian, 2008).

I.4.4. The role of neurotrophic factors

I.4.4.1. The neurotrophin family and their receptors

Neurotrophins are diffusible trophic molecules that exert a potent survival effect on adult CNS neurons. They are a family of small, secreted peptides that include nerve growth factor (NGF), brain-derived neurotrophic factor (BDNF), neurotrophin-3 (NT-3) and neurotrophin-4/5 (NT-4/5) in mammals (Huang and Reichardt, 2001; Segal and Greenberg, 1996). In addition to cell survival, neurotrophins mediate several key cellular responses in the developing and mature CNS including proliferation, differentiation, axon growth, as well as dendrite and synapse formation. Among neurotrophins, BDNF has received particular attention because of its potent role on the survival of RGCs. The first evidence of the neuroprotective effect of BDNF emerged from studies showing that BDNF promoted the survival of developing, axotomized RGCs in culture (Johnson et al., 1986). Since then, it has become clear that BDNF is a powerful neurotrophin for developing and adult RGCs following optic nerve injury (Ma et al., 1998; Mansour-Robaey et al., 1994; Takano et al., 2002; Watanabe and Fukuda, 2002; Weibel et al., 1995). Consistent with this, BDNF is strongly expressed in the superior colliculus (Hofer et al., 1990; Wetmore et al., 1990), the main target of RGCs in the rodent brain, and it is retrogradely transported by RGC axons to the retina (Herzog and von Bartheld, 1998; Ma et al., 1998). Within the retina, BDNF is produced by cells in the ganglion cell layer and inner nuclear layer (Cohen-Cory and Fraser, 1994; Pérez and Caminos, 1995; Vecino et al., 1998).

The biological effects of neurotrophins are mediated by two classes of cell surface receptors: i) the tropomyosin related kinase (Trk) family of receptor tyrosine kinases

comprising TrkA, the receptor for NGF; TrkB, the receptor for BDNF and NT-4/5; and TrkC, the receptor for NT-3 (Kaplan et al., 1991; Klein et al., 1991; Lamballe et al., 1991); and ii) the p75 receptor ($p75^{NTR}$) which binds all neurotrophins with similar affinity (Huang and Reichardt, 2003; Teng and Hempstead, 2004). The Trk receptors share in common a large extracellular ligand binding domain, a single trans-membrane domain, and a cytoplasmic tyrosine kinase catalytic domain. Neurotrophins are homodimers, associated in a non-covalent fashion, that bind and dimerize Trk receptors thus triggering activation of the tyrosine kinase domain and intracellular signaling. Both Trk and $p75^{NTR}$ receptors can be present on the same cell population, however, activation of Trk receptors has been typically associated with cell survival, while $p75^{NTR}$ can stimulate both survival and apoptotic pathways (Chao, 1994; Miller and Kaplan, 2001).

In the naïve retina, developing and adult RGCs have been shown to express high levels of TrkB (Jelsma et al., 1993; Pérez and Caminos, 1995; Rickman and Brecha, 1995). The NGF receptor TrkA is also expressed by developing RGCs (Cui et al., 2002; Rickman and Brecha, 1995), but TrkA levels in adult RGCs are low (Lebrun-Julien et al., 2009b; Rudzinski et al., 2004). The NT-3 receptor TrkC is expressed by RGCs during retinal development (Bovolenta et al., 1996; Das et al., 1997; Hallbook et al., 1996), and by a small population of adult RGCs (Cui et al., 2002; Lindqvist et al., 2002). Interestingly, although developing RGCs express $p75^{NTR}$ (Frade et al., 1999; Frade et al., 1996; Gonzalez-Hoyuela et al., 2001; Harada et al., 2006), this receptor is not expressed by adult RGCs (Hu et al., 1998; Hu et al., 1999; Lebrun-Julien et al., 2009b), and a structurally related receptor named TROY has been proposed to mediate some of the functions originally attributed to $p75^{NTR}$ (Park et al., 2005; Shao et al., 2005). Therefore, RGCs are endowed with the molecular machinery to differentially respond to neurotrophins depending on their developmental stage and on the injury modality as will be discussed in subsequent sections.

I.4.4.2. The neurotrophic factor deprivation hypothesis

The primary mechanism of RGC damage in glaucoma is not well understood, but there is evidence that neuronal loss in this disease occurs largely by apoptosis (Nickells, 1999; Quigley, 1999). This self-destructive, genetically driven, death program can be

activated in all neurons. It is now widely accepted that neurotrophic factors promote neuronal survival by inhibiting default apoptotic pathways (Raff et al., 1993). During development of the nervous system, young neurons require trophic factors for their survival, differentiation and the establishment of synaptic connections. Neurotrophic factors are produced in limited amounts; therefore only neurons exposed to optimal levels of these molecules survive, whereas less fortunate neurons are eliminated by apoptosis (Lewin et al., 1998). In rodents, ~65% of RGCs die during retinal development (Crespo et al., 1985; Sefton and Lam, 1984; Tay et al., 1986). Excess RGCs are eliminated in two successive phases of cell death in the chick retina: the first phase peaks at embryonic day 6 (E6), when RGCs differentiate; and the second phase coincides with the arrival of RGC axons to the brain, when these neurons become dependent on target-derived trophic support (Frade et al., 1997; Rager, 1980). RGC axon terminals uptake and retrogradely transport BDNF applied to the superior colliculus (Fournier et al., 1997; Herzog and von Bartheld, 1998). Moreover, intracollicular injection of BDNF in newborn hamsters reduces the rate of developmental RGC death (Ma et al., 1998) suggesting that target-derived BDNF regulates the survival of developing RGCs (Figure 5A).

The role of endogenous target-derived factors in the maintenance of adult RGCs is considerably less clear. Studies in which RGC target tissue was ablated in adult cats showed that RGC loss was not detected until six months after the lesion (Pearson and Stoffler, 1992; Pearson and Thompson, 1993). The observation that loss of target-derived neurotrophic factors does not affect RGC survival for several months is consistent with the protracted RGC death characteristic of glaucoma, which often occurs over several decades. It has been proposed that the retrograde transport of neurotrophins to the retina might initially be a redundant mechanism and that retina-derived neurotrophic factors may temporarily support the survival of RGCs that have been disconnected from their targets (Murphy and Clarke, 2006). Conversely, target-derived factors may act to compensate for deficits in local trophic support. Given that neurotrophic factors are produced locally in the retina and distally by target cells, it is logical to think that both sources are important for the survival and function of adult RGCs. At present, a full understanding of the contribution of target-derived neurotrophic factors for RGC survival in glaucoma is lacking. Target ablation experiments may result in terminal damage which

can potentially confound the interpretation of the results. Thus, experiments that selectively disrupt the production of neurotrophic factors by the target neurons using function blocking antibodies or genetic approaches that involve conditional deletion of neurotrophin genes might be useful in assessing the contribution of trophic factors derived from the target tissue in adult organisms.

I.4.4.3. Axonal transport failure

Although the requirement of target-derived neurotrophic factors in the survival of adult RGCs has been elusive, a current hypothesis is that blockade of axonal transport in glaucoma leads to deficits in the levels and availability of these factors and subsequent RGC death (Figure 5B). Evidence for this idea is provided by early observations that both anterograde and retrograde axonal transport in the optic nerve is blocked in experimental glaucoma in primates (Anderson and Hendrickson, 1974; Gaasterland et al., 1978; Hayreh et al., 1979; Minckler et al., 1977; Quigley and Anderson, 1976; Quigley and Addicks, 1980; Quigley and Anderson, 1977). More recently, deficits in retrograde axonal transport have been reported in rat and mouse glaucoma models (Kim et al., 2004a; Salinas-Navarro et al., 2009; Salinas-Navarro et al., 2010) and in human high-pressure secondary glaucoma (Knox et al., 2007). Moreover, retrograde transport of radiolabeled BDNF was impaired following intraocular pressure increase in rats, and accumulation of TrkB immunolabeling was found in the ONH in this model (Pease et al., 2000; Quigley et al., 2000). Elevated intraocular pressure has also been shown to correlate with the ONH and retinal accumulation of dynein, a motor protein required for axonal transport (Martin et al., 2006). A recent study in DBA/2J mice, a strain that spontaneously develops glaucoma, demonstrated that axonal transport failure occurs early and progresses in a distal-to-proximal pattern (Crish et al., 2010). Of interest, RGC axons and pre-synaptic terminals persisted in the superior colliculus well after axonal transport failed (Crish et al., 2010) suggesting that restoration of transport along RGC axons might be an early therapeutic target for glaucoma. Therefore, axonal transport blockade, whether it involves neurotrophic factor deprivation or insufficient levels of other essential molecules, continues to be an attractive posit for the loss of RGCs in glaucoma.

FIGURE 5.

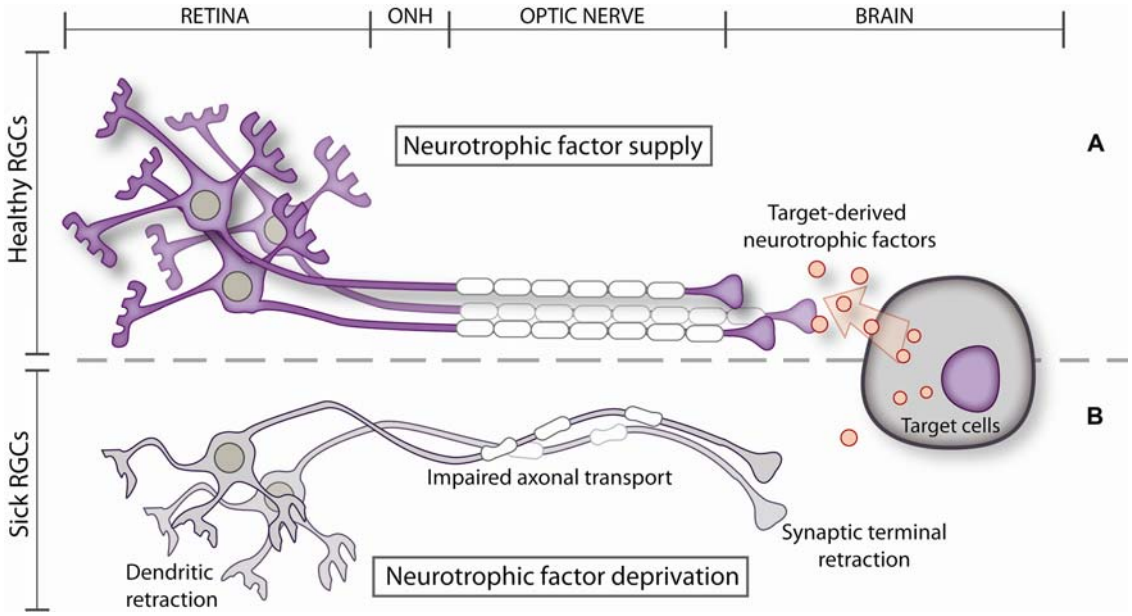

Figure 5. The neurotrophic factor deprivation hypothesis. Axonal transport failure leading to deficits in neurotrophic factor supply has been proposed to contribute to RGC death in glaucoma. (A) Neurons that successfully obtain optimal amounts of essential neurotrophic factors will survive. (B) Damaged RGCs that are disconnected from their targets and undergo obstruction of axonal transport will experience neurotrophic deprivation and die. Source of image: Almasieh et. al., Prog. Retin. Eye. Res., March 2012.

I.4.4.4. Neurotrophin supplementation therapies

Supplementation of neurotrophic factors has been extensively studied as a potential strategy to prevent the death of injured RGCs. Among neurotrophic factors, BDNF stands out because of its potent neuroprotective effect. Intraocular injection of exogenous BDNF protein or viral-mediated BDNF gene transfer using adenovirus or adeno-associated virus (AAV) promote robust RGC survival after optic nerve transection or crush (Chen and Weber, 2001; Di Polo et al., 1998; Klöcker et al., 2000; Leaver et al., 2006; Mansour-Robaey et al., 1994; Mey and Thanos, 1993; Parrilla-Reverter et al., 2009; Peinado-Ramon et al., 1996). For example, a single intraocular injection of recombinant BDNF confers 100% survival of axotomized RGCs at one week after lesion (compared to 50% in control eyes), and an average of 48% survival at two weeks post-injury (compared to ~10% in control eyes), based on quantification of retrogradely labeled RGC soma (Berkelaar et al., 1994; Cheng et al., 2002; Mansour-Robaey et al., 1994; Peinado-Ramon et al., 1996). The combination of BDNF gene transfer with additional therapies including free radical scavengers and cell-permeable cAMP further increase RGC neuroprotection (Hellström and Harvey, 2011; Isenmann et al., 1998). In experimental glaucoma induced by chronic eye pressure elevation, intraocular delivery of BDNF protein (Ko et al., 2001) or gene transfer using an AAV vector led to marked RGC neuroprotection (Martin et al., 2003). For example, at four weeks of ocular hypertension, 68% of RGC survival was reported in eyes treated with AAV.BDNF compared to only 48% in control eyes (20% protection) as assessed by quantification of RGC axons (Martin et al., 2003). Therefore, exogenous BDNF confers RGC soma and axon protection in acute models of optic nerve injury and in experimental glaucoma.

I.4.4.5. BDNF/TrkB signaling

Several lines of evidence support a key role for BDNF/TrkB signaling on the survival of adult RGCs. Both exogenous BDNF administration and strategies that result in TrkB activation lead to enhanced RGC survival in acute and chronic models of optic nerve damage (Chen and Weber, 2001; Cheng et al., 2002; Di Polo et al., 1998; Hu et al., 2010; Klöcker et al., 2000; Leaver et al., 2006; Mey and Thanos, 1993; Parrilla-Reverter et al., 2009). Paradoxically, the number of RGCs in BDNF or TrkB knockout mice have

been shown to be similar to those found in wild-type animals (Cellerino et al., 1997; Pollock et al., 2003; Rohrer et al., 2001), suggesting that other neurotrophic factors compensate for the lack of BDNF or that BDNF signaling through TrkB is not required for RGC survival during development. Of interest, however, RGCs from BDNF null mice displayed hypomyelinated axons (Cellerino et al., 1997) which correlated with marked functional deficits (Rothe et al., 1999), a phenotype that might increase the vulnerability of these neurons to die following glaucomatous optic nerve damage.

Upon binding to the TrkB receptor, BDNF stimulates multiple signaling pathways in the retina, including the extracellular signal-regulated kinases 1/2 (Erk1/2) (Figure 6) and the phosphatidylinositol-3 kinase (PI3K)/Akt pathways. Erk1/2 and (PI3K)/Akt by activating transcription factors like cAMP response element binding protein (CREB) stimulate the transcription of pro-survival molecules such as Bcl-2 and Bcl-xL (Bonni et al., 1995; Du and Montminy, 1998; Finkbeiner et al., 1997; Wilson et al., 1996). Both the Erk1/2 and the PI3K pathways are stimulated in adult RGCs following TrkB activation *in vivo* (Cheng et al., 2002; Hu et al., 2010; Nakazawa et al., 2002). Furthermore, pharmacological inhibition of the obligate upstream activator of Erk1/2, the mitogen activated protein (MAP) kinase kinase 1 (MEK1), blocked the survival effect produced by AAV-mediated TrkB overexpression, while PI3K inhibition did not alter this neuroprotective effect (Cheng et al., 2002). These results support the hypothesis that activation of the Erk1/2 pathway, but not the PI3K pathway, mediates TrkB-induced RGC survival. Furthermore, *in vivo* stimulation of Erk1/2 by overexpression of a constitutively active MEK1 mutant potentiated RGC survival after optic nerve axotomy (Pernet et al., 2005) and in a rat model of ocular hypertension (Zhou et al., 2005). These data indicate that the Erk1/2 pathway plays a key role in the regulation of adult RGC survival after traumatic injury and in experimental glaucoma.

I.4.4.6. Neurotrophins and neuronal redox homeostasis

Under oxidative stress conditions, treatment with neurotrophins like NGF results in a rapid improvement in cell survival and reduction of ROS levels (Dugan et al., 1997). In the retina, BDNF application significantly increases survival of RGC in chemically induced hypoxia (Ikeda et al., 1999). Both BDNF and CNTF also demonstrat significant RGC protection in a model of NO-induced neuronal cell death in the retina (Takahata et al., 2003). Further study has shown that neurotrophins can alter the process of ROS synthesis towards a less harmful end-product, for instance by facilitating production of

FIGURE 6.

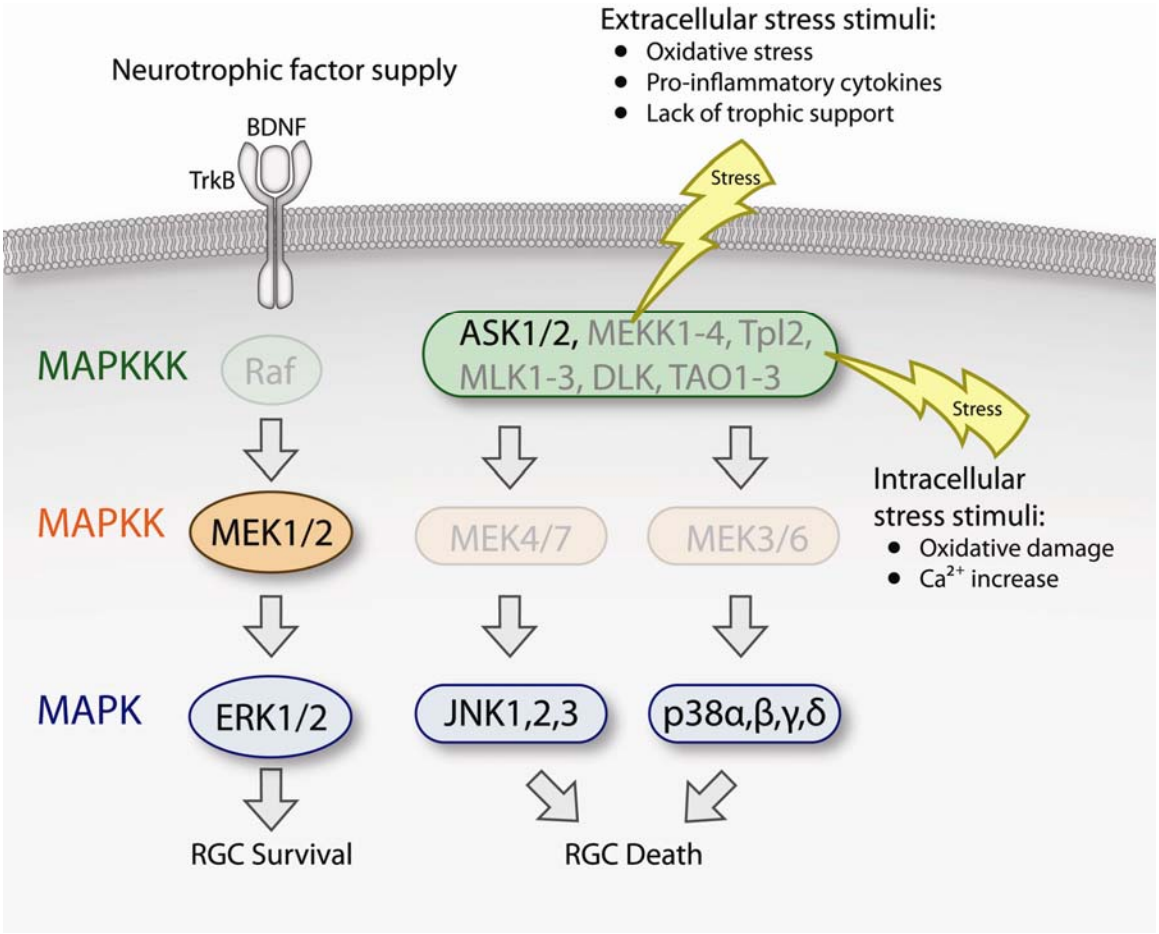

Figure 6. Activation of ERK1/2 survival pathway via BDNF and TrkB signaling. MAPK family members regulate the fate of injured RGCs and play anti- and pro-apoptotic roles**.** BDNF-mediated activation of TrkB receptors stimulates the MEK1/2 and results in ERK1/2 activation leading to robust RGC survival after axotomy and in experimental glaucoma. Stress stimuli activate ASK1, and its downstream effectors JNK and p38, a pathway that contributes to RGC death and optic nerve degeneration. Source of image: Almasieh et. al., Prog. Retin. Eye. Res., March 2012.

H_2O_2 instead of superoxide anion (Satoh et al., 1999). Modulation in free radical formation mediated by neurotrophins has been linked to activation of MAPK pathway as application of PD98059, specific inhibitors of MEK, increases the ROS production (Dugan et al., 1997). However, in some conditions like mixed neuronal-glial culture, treatment with BDNF induces ROS production that is thought to be result of NADPH oxidase activation and leads to oxidative neuronal death (Kim et al., 2002). Other studies have suggested this ROS production could be result of increased activity of NADPH oxidase in glial cells (Abramov et al., 2005).

Neurotrophins through activation of pathways like Ras/ERK, PI3K/Akt are involved in several important neuronal process like survival, growth and plasticity (Mayr and Montminy, 2001; Shaywitz and Greenberg, 1999). Many of downstream signaling pathways of neurotrophins lead to activation of CREB kinases that phosphorylate CREB. Interestingly, nNOS activity by regulating the redox homeostasis and protein S-nitrosylation is also involved in neurotrophin control of transcriptional activity (Jaffrey et al., 2001a). It has been suggested that nuclear proteins that associate with CREB target genes are redox sensitive, BDNF by activation of nNOS initiates a NO-dependent signaling pathway that leads to S-nitrosylation of these proteins and therefore controls CREB-DNA binding and gene expression (Riccio et al., 2006). A recent study has shown that activity of nNOS is necessary for BDNF induced proteins synthesis and neuronal plasticity (Gallo and Iadecola, 2011). Similarly, inhibition of NOS by L-NAME abolishes S-nitrosylation of proteins associated with CRE sequences and although it does not affect BDNF stimulated CREB phosphorylation, however it blocks CREB-DNA binding and gene expression (Riccio et al., 2006).

I.4.5. Excitotoxic Damage

Glutamate is the predominant excitatory amino acid in many regions of the CNS, including the retina. Glutamate-mediated neurotransmission plays a major role in the relay of visual information from photoreceptors to bipolar cells, then to RGCs and onto brain centers (Lukasiewicz, 2005). Retinal glutamate receptors are located in the outer plexiform layer where glutamatergic synapses connect photoreceptors to bipolar and horizontal cells; and also in the inner plexiform layer which contains the bulk of

glutamatergic synapses from bipolar cells to RGCs and amacrine cells (Gründer et al., 2000; Lagrèze et al., 2000; Lukasiewicz, 2005; Peng et al., 1995). The central hypothesis of excitotoxic injury is that excess glutamate binds to cell surface ionotropic glutamate receptors, primarily N-Methyl-D-aspartic acid (NMDA) receptors (NMDAR), triggering massive Ca^{2+} influx and activation of pro-apoptotic signaling cascades in neurons. Elevation of endogenous glutamate and activation of glutamate receptors have been shown to contribute to a variety of acute and chronic neurological disorders, including stroke, trauma, seizures, and various forms of dementia and neurodegeneration (Kalia et al., 2008). In the retina, excess glutamate has been proposed to underlie common neurodegenerative disorders such as retinal artery occlusion and glaucoma (Casson, 2006; Seki and Lipton, 2008). A number of studies have now demonstrated that adult RGCs are exquisitely sensitive to exogenously applied NMDA, which triggers rapid death of these neurons, and that inhibitors of NMDAR and/or downstream pathways are neuroprotective in experimental models of retinal ischemia and glaucoma (Hare et al., 2004; Kido et al., 2000; Lam et al., 1999; Manabe and Lipton, 2003).

I.4.5.1. Glutamate levels in glaucomatous retinas

Early reports indicated an increase in glutamate levels in the vitreous of dogs and monkeys with ocular hypertension and in glaucoma patients (Brooks et al., 1997; Dreyer et al., 1996). However, several studies thereafter were unable to reproduce these findings in vitreous humor samples from experimental animals with retinal ischemia or ocular hypertension, and in human glaucoma (Carter-Dawson et al., 2002; Honkanen et al., 2003; Kwon et al., 2004; Levkovitch-Verbin et al., 2002a; Wamsley et al., 2005). Therefore, experimental data on this topic has been controversial and progress stalled after the field was marred by a major scientific fraud (Dalton, 2001). As a consequence, our understanding of the actual contribution of excitotoxic damage in glaucoma has advanced slowly. A misconception has been that, for excitotoxicity to occur, elevated glutamate levels must be detected in the retina/ocular fluids of experimental animals or humans with glaucoma (Lotery, 2005; Osborne et al., 2006). Massive glutamate release is a hallmark of acute brain injuries with fast and severe neural tissue damage (Choi and Rothman, 1990), but this is not necessarily characteristic of a slow, progressing

neurodegenerative disease like glaucoma. For instance, in retinal diseases with a clear ischemic component, such as retinal detachment, there is a detectable glutamate elevation in the vitreous and the subretinal space (Bertram et al., 2008; Diederen et al., 2006). However, the chronic, gradual nature of glaucoma defies any drastic elevation or accumulation of glutamate throughout the course of the disease. Glutamate increase is likely to occur only in localized areas of the retina or optic nerve at any one time during glaucomatous neurodegeneration and, together with glutamate clearance and diffusion mechanisms, is unlikely to result in a detectable increase in retinal or vitreal glutamate. On the other hand, small and consistent fluctuations in extracellular glutamate levels could play a role in glaucoma progression. For instance, the voltage-dependent activation of NMDAR is normally blocked by Mg^{2+} ions under resting membrane potential conditions (Mayer et al., 1984; Nowak et al., 1984). Glutamate-induced Ca^{2+} influx occurs through NMDAR activation in isolated post-natal RGCs, and extracellular Mg^{2+} inhibits the response of these neurons to glutamate (Hartwick et al., 2008). In principle, voltage-dependent Mg^{2+} blockade can be overcome when the neuronal membrane potential becomes more positive (depolarized) than the resting potential. This scenario may lead to NMDAR channel opening and excitotoxic damage even at physiological levels of glutamate. Of interest, motoneurons subjected to axonal injury displayed reduced voltage-dependent Mg^{2+} block of NMDAR currents *in vivo* which may increase neuronal susceptibility to excitotoxic damage (Furukawa et al., 2000). In summary, to rule out an excitotoxic component in RGC death in glaucoma based on the absence of glutamate accumulation in ocular tissues is far too simplistic.

I.4.5.2. The role of glial cells: glutamate transporters

A major limitation of the central tenet of excitotoxic injury is that it focuses only on the neuronal response, but growing evidence indicates that glial cells play critical roles in the regulation and response to glutamate. For example, Müller cells are responsible for the uptake of excess glutamate via glutamate/aspartate transporters (GLAST) or excitatory amino acid transporter 1 (EAAT1) (Derouiche and Rauen, 1995; Otori et al., 1994), which is essential to maintain physiological concentrations of glutamate. Even normal levels of glutamate in the retina can be potentially neurotoxic if this amino acid is not

removed in a timely manner. A number of other glutamate transporters are also expressed by both retinal glia and neurons including the glutamate transporter-1 (GLT-1 or EAAT2), the excitatory amino acid carrier 1 (EAAC1 in rats or EAAT3 in humans), EAAT4 and EAAT5 in rats (Danbolt, 2001; Kugler and Beyer, 2003). Most neuronal glutamate transporters in the retina are positioned at the synapse to rapidly remove the released glutamate and limit its spillover from the synaptic cleft (Diamond, 2001; Hasegawa et al., 2006; Scimemi et al., 2009). In contrast, glial glutamate transporters appear to remove the extrasynaptic portion of glutamate from the retina (Figure 7) (Rauen et al., 1998). Since most NMDAR on RGCs are believed to be distributed extrasynaptically (Chen and Diamond, 2002; Zhang and Diamond, 2006), the susceptibility of RGCs to glial glutamate transporter dysfunction is likely to contribute to excitotoxic damage. Consistent with this, decreased retinal GLAST and GLT-1 expression has been correlated with optic nerve damage in experimental rat glaucoma (Martin et al., 2002) and in DBA/2J mice (Schuettauf et al., 2007). Importantly, mice lacking the gene encoding GLAST displayed exacerbated loss of RGC soma and axons (Harada et al., 2007). However, the precise role of glutamate transporters in glaucomatous pathophysiology requires further evaluation. For instance, chronic and moderate elevation of intraocular pressure in rats did not disrupt retinal glutamate clearance mechanisms as shown by Ca^{2+} imaging experiments (Hartwick et al., 2005). Marked increase in the GLAST (Woldemussie et al., 2004) and GLT-1c levels are also reported in experimental models and glaucoma patients (Sullivan et al., 2006). Since GLT-1c is not normally expressed by adult RGCs (Rauen et al., 2004), this finding suggests a compensatory response in neurons possibly triggered by dysregulation of glutamate clearance. Finally, single-nucleotide polymorphisms in the GLAST gene were not associated with the manifestation of normal tension glaucoma patients (Yasumura et al., 2011). Future work to establish the functional role of different subtypes of glutamate transporters after glaucomatous injury is warranted.

I.4.5.3. The role of glial cells: cytokines

Another mechanism by which glial cells may contribute to excitotoxic damage is the production of neurotoxic factors in response to excess glutamate. Along these lines, a

FIGURE 7.

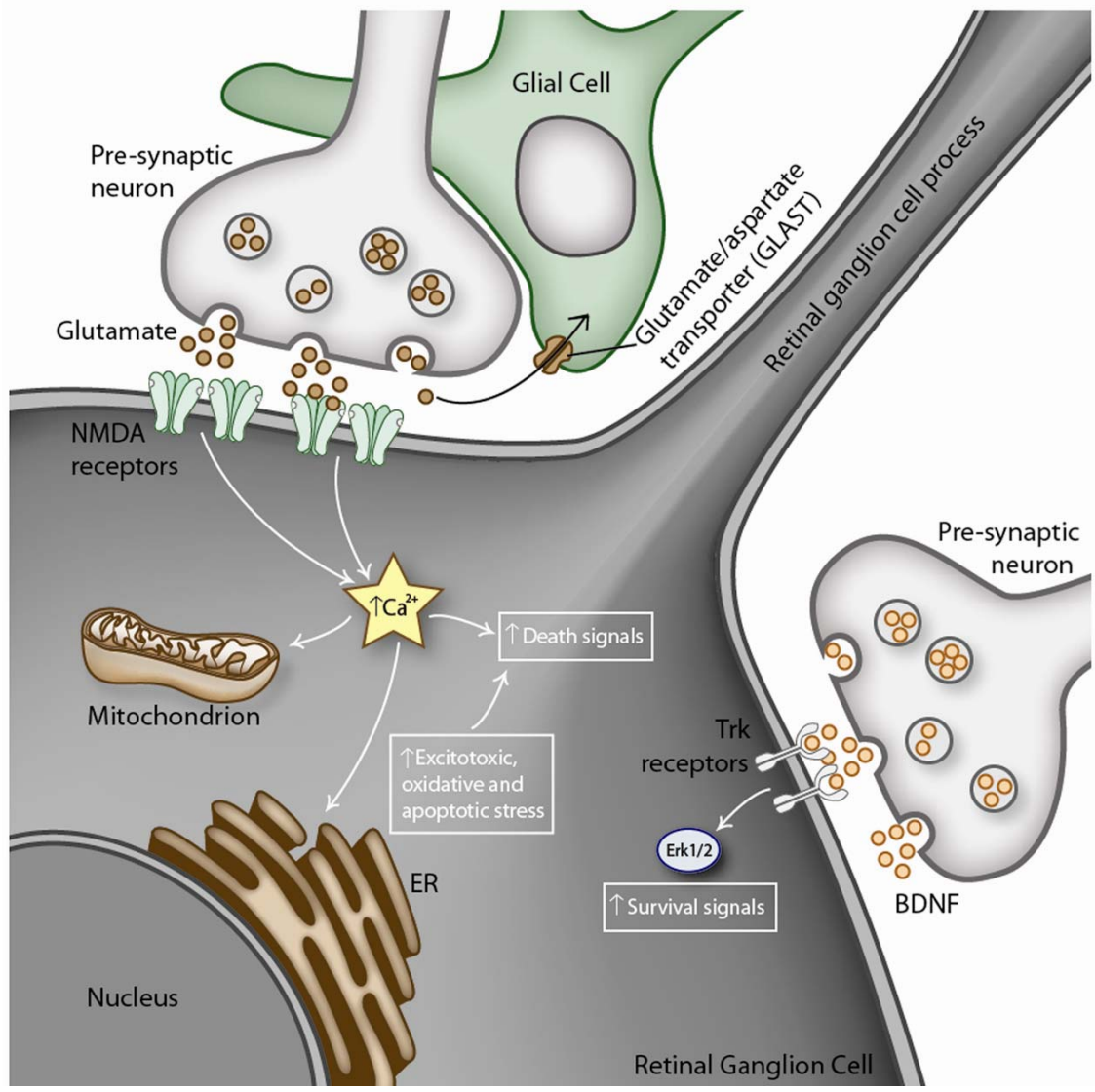

Figure 7. Neuronal and glial component of retina in the excitotoxicity. The classical model of excitotoxic damage is based on the premise that excess glutamate binds to ionotropic glutamate receptors (e.g. NMDA receptor) triggering calcium influx, organelle stress and activation of pro-apoptotic pathways. Excitotoxic damage overrides the pro-survival effect of endogenous and exogenous neurotrophic factor supply. Glial cells are responsible for the uptake of excess glutamate via glutamate/aspartate transporters (GLAST) and deficits in transporter function have been shown to contribute to RGC damage. Source of image: Almasieh et. al., Prog. Retin. Eye. Res., March 2012.

recent study demonstrated that Müller cells are extraordinarily sensitive to NMDA and respond rapidly by upregulating NF-κB activity (Lebrun-Julien et al., 2009a). In this study, NF-κB activation induced by NMDA was detected in Müller cells, but not in retinal neurons. Furthermore, NMDA-dependent activation of NF-κB in Müller cells led to production of endogenous glia-derived TNFα which in turn rendered RGCs highly sensitive to excitotoxicity by increasing their surface levels of Ca^{2+}-permeable type of AMPAR (Lebrun-Julien et al., 2009a). The observation that molecular events in Müller glia play a decisive role in RGC death shifts our understanding of excitotoxic damage and supports a novel model in which glial cells exacerbate RGC loss. A controversial study published in 2004 questioned the vulnerability of RGCs to excitotoxic damage because saturating concentrations of glutamate or NMDA did not promote RGC death in dissociated cultures or *ex-vivo* (Ullian et al., 2004). A simple explanation for this finding is that retinas were exposed to NMDA for 1 hr, which is a short time based on well-controlled studies showing that RGC death only starts at 3-6 hrs after NMDA administration (Lebrun-Julien et al., 2009a; Manabe and Lipton, 2003; Pernet et al., 2007). The slow onset of RGC death following excitotoxic damage was proposed to result from a loss of trophic support provided by amacrine cells which die rapidly in the presence of NMDA (Ullian et al., 2004). An alternative explanation is that NMDA affects Müller cells early, by a mechanism yet to be identified, and these glial cells then secrete neurotoxic TNFα that promotes RGC death (Lebrun-Julien et al., 2009a). In the case of chronic, neurodegenerative diseases where an excitotoxic component is thought to be involved, such as in glaucoma, blockade of glutamate receptors may not ameliorate disease progression unless other damaging factors (e.g. glia-derived TNFα) are also inhibited.

I.4.5.4. AMPAR mediated excitotoxicity

Another shortcoming of the traditional excitotoxicity model is that it focuses almost exclusively on the NMDAR. Antagonists of NMDAR have been intensely investigated as `agents that may confer neuroprotection, but these compounds have consistently failed to show neuroprotection in human clinical trials (Lipton, 2004; Osborne, 2008). Accumulating evidence supports that AMPA type of glutamate receptor,

are key contributors to neuronal injury. AMPAR mediate fast synaptic transmission and play crucial roles during development and synaptic plasticity (Dingledine et al., 1999). AMPAR channels are tetrameric complexes composed of various combinations of four subunits (GluR1-R4), each encoded by a different gene. The conductance of AMPAR varies depending on whether the GluR2 subunit is present and, if so, whether it has undergone mRNA editing. Editing of GluR2 mRNA changes the uncharged amino acid glutamine (Q) to positively-charged arginine (R) and, as a result, Ca^{2+} cannot be transported due to electrostatic repulsion by the arginine residues that line the AMPAR pore. Since most GluR2 subunits in the CNS are fully edited (e.g. GluR2(R) isoforms) it has been proposed that a role for this editing mechanism is to guard against excitotoxicity (Kim et al., 2001). Despite this, some cells express GluR2-lacking AMPARs and as a result are permeable to divalent ions in the external milieu such as Ca^{2+} and Zn^{2+} (Geiger et al., 1995; Hollmann et al., 1991; Verdoorn et al., 1991). Interestingly, the proportion of cells expressing Ca^{2+}-permeable-AMPAR increases acutely during ischemia, excitotoxicity, epileptic seizures (Gorter et al., 1997; Grooms et al., 2000; Pellegrini-Giampietro et al., 1992), and in neurodegenerative diseases such as Alzheimer's disease and amyotrophic lateral sclerosis (Ikonomovic et al., 1997; Kawahara et al., 2004). Recent studies have demonstrated increased cell surface expression of Ca^{2+}-permeable-AMPAR in RGCs after excitotoxic damage (Lebrun-Julien et al., 2009a) and in experimental glaucoma (Cueva Vargas et al., 2011). An in-depth examination of non-NMDA glutamate receptors is required to establish their role as mediators of RGC death in glaucoma.

I.4.6. Common neurodegenerative pathways: glaucoma and Alzheimer's disease

It is increasingly being recognized that glaucoma shares a number of pathological features with other neurodegenerative diseases, most notably with Alzheimer's disease (AD) (Jackson and Owsley, 2003; Kirby et al., 2010; McKinnon, 2003; Parisi, 2003). AD is the most common cognitive disorder worldwide (Sloane et al., 2002) and its progress is characterized by appearance of senile plaques and neurofibrillary tangles in brain tissues. Senile plaques are composed of amyloid beta (Aß) peptides whereas neurofibrillary tangles are composed of insoluble aggregated tau, a microtubule-associated protein

normally enriched in the axon (Lee et al., 2001; Mandell and Banker, 1996). AD patients are affected by visual deficits including difficulty reading, abnormal depth perception, color recognition and spatial contrast sensitivity (Cronin Golomb, 1995; Cronin Golomb et al., 1991; Gilmore and Whitehouse, 1995; Guo et al., 2010; Hinton et al., 1986; Jackson and Owsley, 2003; Katz and Rimmer, 1989; Lee and Martin, 2004; Mendez et al., 1996). A preferential loss of large diameter RGCs and axons has been documented in AD (Hinton et al., 1986), which may account for the impaired contrast sensitivity and motion perception in AD patients (Hinton et al., 1986; Jackson and Owsley, 2003; Katz and Rimmer, 1989; Lee and Martin, 2004). Likewise, there is a high occurrence of glaucoma amongst AD patients, and glaucoma shares a number of pathological and clinical features with AD such as the presence of retinal Aß and hyperphosphorylated tau (Guo et al., 2010; Gupta et al., 2008; Yoneda et al., 2005). Cognitive impairment, depression and anxiety have also been reported among glaucoma patients (Yochim et al., 2011). AD and glaucoma are both age-related diseases, characterized by the loss of selective neuronal populations, mitochondrial dysfunction, and dendritic changes leading to loss of synaptic connectivity (Kong et al., 2009; Liu et al., 2011).

Although several studies have suggested a clinical correlation between glaucoma and AD (Sugiyama et al., 2006; Tamura et al., 2006; Wostyn, 2006; Wostyn et al., 2009), a clear causal link between these two diseases has not been unequivocally established. Nonetheless, compelling evidence from laboratory work supports the idea that neuronal loss in AD and glaucoma share common neurodegenerative mechanisms. For example, abnormal processing of amyloid precursor protein (APP), a hallmark of AD, has been documented in an ocular hypertension rat glaucoma model (McKinnon et al., 2002). In this model, caspase-3 was activated in RGCs leading to cleavage of APP and neurotoxic accumulation of Aß (McKinnon, 2003). Intraocular injection of Aß, a major culprit in AD, has been shown to induce RGC apoptosis (Cordeiro et al., 2006). Furthermore, Aß deposition was associated with RGC apoptosis in experimental glaucoma, and blockade of the Aß pathway reduced glaucomatous RGC loss (Guo et al., 2007). A recent study demonstrated that curcumin, a biologically safe fluorochrome, can be used to visualize Aß plaques in the retina of a transgenic AD mouse model (Koronyo-Hamaoui et al., 2011). These lesions appeared first in the retina and later in the brain, indicating that

early pathological changes in the retina could be used to predict onset and monitor progression of AD.

I.4.6.1. Drug based neuroprotective strategies for treatment of glaucoma

The observation that AD and glaucoma share common neurodegenerative pathways have raised the provocative idea that drugs currently used for the treatment of AD may also be used to treat glaucoma. An example of this is memantine, an NMDAR channel blocker (Parsons et al., 1999) approved by regulatory agencies for the treatment of AD (Reisberg et al., 2003). Several studies in rat and monkey OHT models demonstrated the efficacy of memantine to block RGC death (Hare et al., 2001a; Hare et al., 2004; Lagrèze et al., 1998). Subsequently, memantine was advanced for clinical testing in glaucoma but failed to meet its primary endpoint in Phase III trials (http://agn.client.shareholder.com/releasedetail.cfm?ReleaseID=290764). Although a neuroprotective strategy based entirely on the principle of blocking NMDAR function has intrinsic limitations (Danesh-Meyer and Levin, 2009; Osborne, 2008), nevertheless, the information stemming from this trial should serve as a baseline for the effective study design of future clinical testing for neuroprotection in glaucoma (Danesh-Meyer and Levin, 2009).

Other drugs currently approved for the treatment of AD are acetylcholinesterase AChE inhibitors. AChE is the enzyme responsible for ACh breakdown, and its inhibition was introduced for AD treatment following the cholinergic hypothesis of AD. The cholinergic hypothesis argues that cognitive deficits in AD are partly due to the loss of cholinergic neurons and reduction of cholinergic transmission in the areas of the brain associated with learning, memory, and higher cognitive functions (Razay and Wilcock, 2008; Whitehouse et al., 1982). Consequently, AChE inhibitors such as galantamine, donepezil and rivastigmine have been prescribed to boost the cholinergic signaling and provided modest cognitive improvements for the AD patients (Birks, 2006; Jann et al., 2002).

Among the AChE inhibitors, galantamine conveys unique effects beyond those of AChE inhibition alone, since it is also an allosteric modulator of nicotinic ACh receptors (nAChRs) enhancing their sensitivity to ACh (Schrattenholz et al., 1996). An allosteric

potentiating ligand (APL) of nAChRs binds to a site on the receptor that differs from the agonist binding site (Schrder et al., 1994). APL binding to the postsynaptic nAChR results in conformational changes that amplifies the action of ACh, thereby increasing ionic conductance and neurotransmission (Maelicke, 2000). Binding of galantamine to nAChR also directly activates the PI3K and leads to phosphorylation of Akt; application of a specific antibody against the allosteric binding site on nAChR blocks the galantamine mediated PI3K activation (Kihara et al., 2004). *In vitro,* galantamine protects the cortical neurons from ß-amyloid toxicity and improves survival of the motoneurons in glutamate excitotoxicity (Kihara et al., 2004; Melo et al., 2009; Shimohama and Kihara, 2001). In vivo, galantamine significantly improves the survival of hippocampal neurons in an ischemic model and also protects dopaminergic neurons against the neurotoxins (Lorrio et al., 2007; Yanagida et al., 2008). Pharmacological antagonists of nAChR have been shown to partially reduce the neuroprotective effect of galantamine against ß-amyloid toxicity in culture (Arias et al., 2004; Kihara et al., 2004). These observations suggest that galantamine is a promising drug with potential for treatment of other neurodegenerative diseases.

I.4.6.2. Retinal cholinergic system and glaucoma

In the immature vertebrate retinas, cholinergic transmission is essential for the early development of retina. Inputs from the cholinergic amacrine cells produce synchronized bursts of action potentials in RGCs, known as retinal waves (Feller et al., 1996). These propagating waves driven by cholinergic transmission, together with other inputs to RGCs, define the pattern of connections between axonal terminals of RGCs and their central visual targets (Hahm et al., 1999; Wong, 1999). In the adult retina, inputs from the AChRs located on the RGCs no longer generate action potentials because glutamate-mediated signaling pathway forms the major excitatory input for activation of RGCs (Lukasiewicz, 2005; Wong et al., 2000). However, RGCs continue to express both nicotinic and muscarinic AChRs and inputs from these receptors play important modulatory role on functional properties of the adult RGCs and the processing of the visual information (Baldridge, 1996; Beelke and Sannita, 2002; Fischer et al., 1998; Sastry, 1985a; Schmidt et al., 1987). Recent studies suggested a cholinergic dysfunction

might also contribute in the pathology of glaucoma. In DBA/2J mice, progression of glaucoma is accompanied by a significant reduction in the immunoreactivity of amacrine cells for choline acetyltransferase (ChAT), gamma-aminobutyric acid (GABA) and Protein kinase C (PKC) (Gunn et al., 2011; Hernandez et al., 2009; Moon et al., 2005). ChAT is the enzyme involved in the synthesis of ACh and it is mostly localized in the processes of the cholinergic amacrine cells in the inner plexiform layer (Ross et al., 1985). These observations support the idea of a reduced cholinergic transmission in the glaucomatous retinas.

I.4.6.3. AChRs and neuroprotection

Nicotinic AChRs are a family of ligand-gated Na^{+} and Ca^{2+} permeable cation channels (Sargent, 1993). Nicotinic nAChRs receptors are pentameric and in the nervous system they are composed of different combinations of alpha (α2- α10) and beta (β2- β4) subunits (Gotti et al., 1997). Among the nAChRs subunits, the neuroprotective properties of the α4, α7 and β2 subunits have been well studied (Jonnala and Buccafusco, 2001; Thompson et al., 2006). Adult RGCs express several nAChRs subunits including the α7 (Cox et al., 2008; Gilbert et al., 2009). The binding site for the APLs thought to be located on the α7 subunit (Schrattenholz et al., 1993). Activation of nAChRs promotes neuronal survival via stimulation of different pro-survival pathways (Figure 8) (Arias et al., 2004; Kihara et al., 2004). Signaling through nAChRs also modulates the activity of the pro-apoptotic pathways, as seen in a glutamate excitotoxicity model where nicotinic signaling protected neurons by reducing phospho-p38 MAPK levels (Asomugha et al., 2010). p38 MAPK belongs to a major pro-apoptotic pathway and its activation leads to RGC death (Cuadrado and Nebreda, 2010; Kikuchi et al., 2000). Recently, it has been suggested that heteromeric nAChRs, such as α4 β2, have an anti-inflammatory effect. Non-receptor tyrosine kinases like janus kinase 2 (JAK2) suppress inflammation via down regulation of $NF\text{-}_{k}B$ at transcriptional level (Hosur and Loring, 2011). This anti-inflammatory signaling pathway appears to be activated independently of calcium or cAMP (Hosur and Loring, 2011).

Muscarinic AChRs (m AChRs) are G-protein coupled receptors consisting of five (M1-M5) subtypes (Caulfield and Birdsall, 1998). Signaling through mAChRs has been

FIGURE 8.

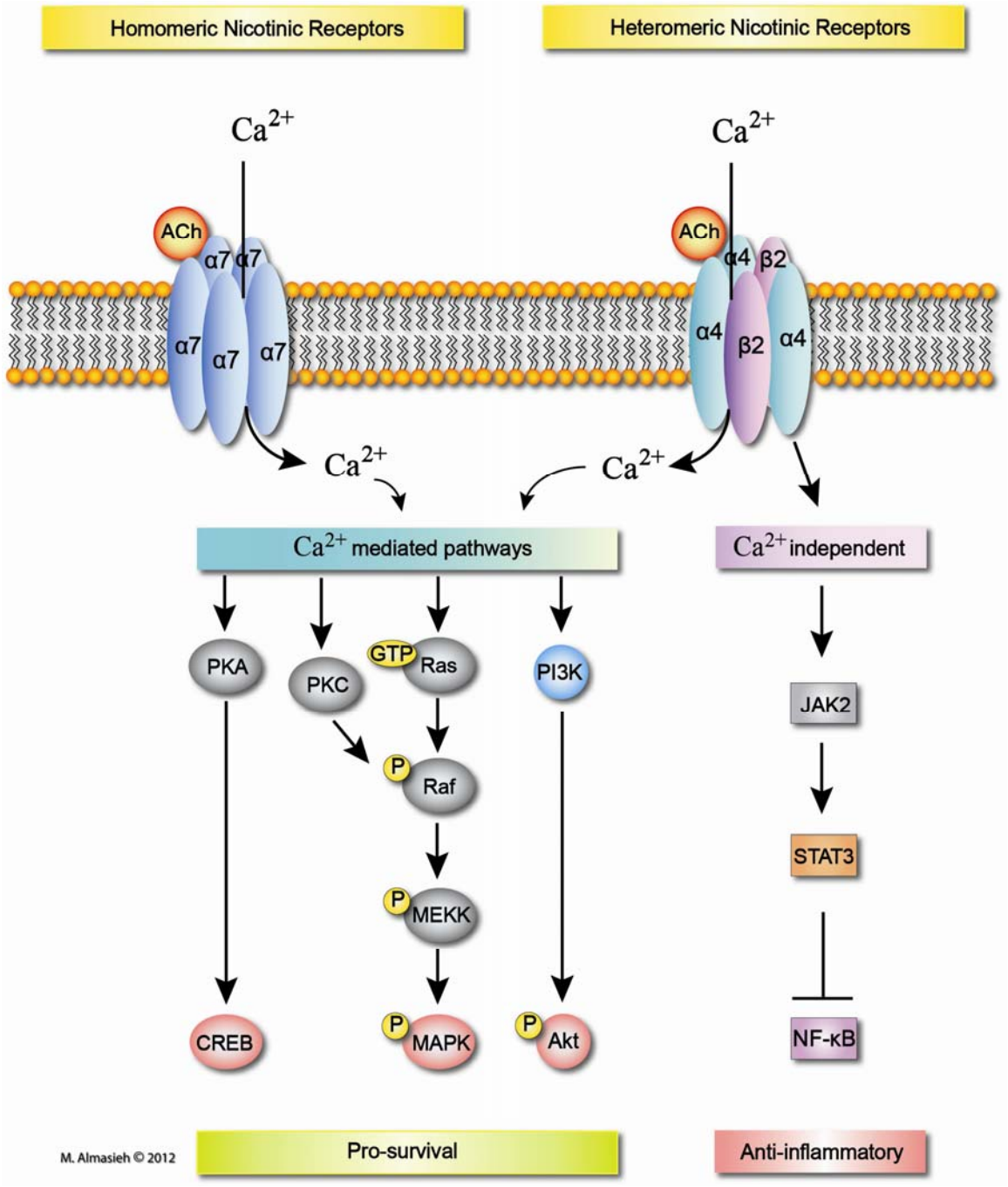
Homomeric Nicotinic Receptors
Heteromeric Nicotinic Receptors
Ca2+
Ca2+
ACh
α7 α7
α7 α7 α7
ACh
α4 β2
α4 β2 α4
Ca2+
Ca2+
Ca2+ mediated pathways
Ca2+ independent
PKA
PKC
GTP Ras
PI3K
JAK2
P Raf
STAT3
P MEKK
NF-κB
CREB
P MAPK
P Akt
M. Almasieh © 2012
Pro-survival
Anti-inflammatory

Figure 8. Activation of survival pathways via nAChRs signaling. Upon binding of ligands to the homomeric α7 and heteromeric nAChRs their channels are opened and allow Ca^{2+} entry. An increase in the intracellular concentration of Ca^{2+} promotes activation of protein kinase C (PKC) and Ras that in turn lead to phosphorylation of Raf and activation of MAPKs family. PI3K also is activated by increased Ca^{2+} levels and promotes phosphorylation of Akt and cell survival. cAMP-dependent activation of protein kinase A (PKA) results in activation of the transcription factor CREB and promotes cell survival. Activity of the low Ca^{2+} permeable heteromeric nAChRs also by inhibiting activation of NF-$_k$B has an anti-inflammatory effect. Source of image: Mohammadali Almasieh.

linked to key transduction pathways including cell survival (Felder, 1995; Migeon and Nathanson, 1994). For example, M1/M3 subtypes mediate activation of the pro-survival ERK pathway (Berkeley et al., 2001) whereas M2/M4 subtypes via Gβγ enhance the activity of the PI3K/Akt pathway and neuronal viability (Wu and Wong, 2006). Intracellular Ca^{+2} homeostasis is another important example of the modulatory role of mAChRs. The interaction of M1/M3/M5 mAChRs with G_q/G_{11} complex stimulates phospholipase C (PLC) leading to the release of Ca^{+2} from intracellular stores (Felder, 1995). Adenylate cyclase activity and intracellular levels of cAMP are also regulated by M2/M4 mAChRs through their interaction with $G_{i/o}$ proteins (Felder, 1995; Migeon and Nathanson, 1994). The correlation of nicotinic and muscarinic AChRs activity with neuronal survival pathways provides a promising insight into novel neuroprotective strategies based on the modulation of these receptors for rescuing RGCs in glaucoma.

I.5. OBJECTIVES OF THE THESIS, HYPOTHESES AND EXPERIMENTAL APPROACHES

Problem and objectives: Glaucoma, a group of diseases characterized by progressive optic nerve degeneration, is the leading cause of irreversible blindness worldwide. Several risk factors have been proposed to contribute to glaucoma progression including elevated intraocular pressure, genetic background and age. The existence of any of these factors might determine an individual's risk to develop glaucoma, but they are not necessarily the cause of this condition. For example, although high intraocular pressure is common among open-angle glaucoma patients, only a limited subset of individuals with ocular hypertension will develop this disease. Moreover, a significant number of patients presenting with glaucoma continue to lose vision despite responding well to therapies that lower eye pressure. Therefore, strategies that delay or halt RGC loss have been recognized as potentially beneficial to preserve vision in glaucoma. The success of these approaches, however, depends on an in-depth understanding of the mechanisms that lead to RGC dysfunction and death. The primary objectives of this thesis were: i) to test novel neuroprotective strategies for injured RGCs,

and ii) to elucidate the molecular pathways leading to neuronal survival using *in vivo* models of optic nerve injury.

Hypotheses: The central hypothesis of this thesis is that effective therapeutic strategies for glaucoma must take into account mechanisms that lead to RGC death to successfully promote structural and functional protection of these neurons. To test this, I used two different approaches that target distinct molecular pathways proposed to contribute to RGC death. First, I took advantage of an existing drug currently approved for the treatment of Alzheimer's disease, the acetylcholinesterase inhibitor galantamine, to assess its neuro- and vasoprotective effects in experimental glaucoma and to elucidate its mechanism of action. The specific hypothesis for this project was that galantamine, by modulating acetylcholine receptor activity, can provide RGC and vascular protection in glaucoma. Second, I used a novel cell-permeable phosphine-borane compound (PB1) to investigate its effect on the survival of injured RGCs and to assess the role of reactive oxygen species superoxide in experimental glaucoma. The specific hypothesis for this project was that PB1 can promote RGC survival via inhibition of the negative effects of oxidative damage caused by axonal injury.

Experimental Approaches: I used a variety of experimental approaches to achieve our research objectives during my Ph.D. work including: 1) a rat model of experimental glaucoma in Brown Norway rats in which ocular hypertension is induced by injection of a hypertonic saline solution into an episcleral vein (Morrison model), 2) an acute paradigm of optic nerve injury in Sprague-Dawley rats based on complete transection (axotomy) of the optic nerve, 3) retrograde labeling of RGCs by application of fluorescent tracers to the superior colliculus, the main target region of these neurons in the brain, 4) intraocular and/or intraperitoneal administration of drugs, 5) quantification of RGC survival by counting fluorescently-labeled neurons in flat-mounted retinas, 6) western blot analysis of signaling components of survival and apoptotic intracellular pathways, 7) visual evoked potentials recorded from the superficial layers of the superior colliculus to assess the functional status of RGCs, and 8) quantification of retinal capillary density using isolectin staining and measurements of regional ocular blood flow assessed by quantitative autoradiography.

CHAPTER 2

II. FIRST ARTICLE: "STRUCTURAL AND FUNCTIONAL NEUROPROTECTION IN GLAUCOMA: ROLE OF GALANTAMINE-MEDIATED ACTIVATION OF MUSCARINIC ACETYLCHOLINE RECEPTORS".

Cell Death and Disease (2010) 1, e27.

STRUCTURAL AND FUNCTIONAL NEUROPROTECTION IN GLAUCOMA: ROLE OF GALANTAMINE-MEDIATED ACTIVATION OF MUSCARINIC ACETYLCHOLINE RECEPTORS.

Mohammadali Almasieh[1], Yu Zhou[1], Melanie E.M. Kelly[2], Christian Casanova[3] and Adriana Di Polo[1,*]

[1]Department of Pathology and Cell Biology and Groupe de Recherche sur le Système Nerveux Central (GRSNC), [2]Department of Pharmacology, Dalhousie University, Halifax, Nova Scotia, [3]School of Optometry, Université de Montréal, Montreal, Quebec, Canada.

Running title: Galantamine protects neurons in glaucoma.

***Correspondence to:** **Adriana Di Polo**
Department of Pathology and Cell Biology
University of Montréal
2900, Boulevard Edouard-Montpetit
Pavillon Roger Gaudry, Room S-520
Montreal, Quebec H3T 1J4, Canada.
Phone: (514) 343-6109, Fax: (514) 343-5755

II.1. ABSTRACT

Glaucoma is the leading cause of irreversible blindness worldwide. Loss of vision in glaucoma is caused by the selective death of retinal ganglion cells. Treatments for glaucoma, limited to drugs or surgery to lower intraocular pressure, are insufficient. Therefore, a pressing medical need exists for more effective therapies to prevent vision loss in glaucoma. In this *in vivo* study, we demonstrate that systemic administration of galantamine, an acetylcholinesterase inhibitor, promotes protection of retinal ganglion cell somata and axons in a rat glaucoma model. Functional deficits caused by high intraocular pressure, assessed by recording visual evoked potentials from the superior colliculus, were improved by galantamine. These effects were not related to a reduction in ocular pressure because galantamine did not change the pressure in glaucomatous eyes and it promoted neuronal survival after optic nerve axotomy, a pressure-independent model of retinal ganglion cell death. Importantly, we demonstrate that galantamine-induced ganglion cell survival occurred via activation of types M1 and M4 muscarinic acetylcholine receptors, while nicotinic receptors were not involved. These data provide the first evidence of the clinical potential of galantamine as neuroprotectant for glaucoma and other optic neuropathies, and identify muscarinic receptors as potential therapeutic targets for preventing vision loss in these blinding diseases.

Keywords: retinal ganglion cell, glaucoma, acetylcholinesterase, muscarinic.

II.2. INTRODUCTION

Glaucoma is the leading cause of irreversible blindness worldwide. It has been estimated that >50 million people around the world are affected by this disease, with >7 million presenting bilateral blindness (Quigley, 2005). Loss of vision in glaucoma is caused by the selective death of retinal ganglion cells (RGCs), the output neurons that relay visual information from the retina to the brain via their axons in the optic nerve. Although the precise cause of RGC death in glaucoma is unknown, high intraocular pressure (IOP) is a major risk factor for developing this disease. Current treatments for glaucoma are limited to lowering IOP by medication or surgery, but a significant number of patients continue to experience visual loss despite responding well to pressure lowering therapies (Georgopoulos et al., 1997). Moreover, >50% of patients have normal tension glaucoma characterized by optic nerve degeneration in the absence of high IOP (Anderson, 2003; Shields, 2008). Therefore, current therapies for glaucoma are insufficient and novel strategies to save RGCs and prevent vision loss would be valuable.

Galantamine is a small molecule acetylcholinesterase (AChE) inhibitor and allosteric ligand of nicotinic ACh receptors (nAChR) currently used for the symptomatic treatment of Alzheimer's disease (Razay and Wilcock, 2008). Galantamine was initially thought to ameliorate cognitive deficits in Alzheimer's disease patients only due to its cholinergic boosting activity, but recent studies have demonstrated that it also has neuroprotective effects. In vitro, galantamine protects cortical neurons from ß-amyloid toxicity and motor neurons from excess glutamate (Kihara et al., 2004; Melo et al., 2009; Shimohama and Kihara, 2001). In vivo, galantamine improves the survival of hippocampal neurons following transient global ischemia and of dopamine neurons damaged by 6-OHDA (Lorrio et al., 2007; Yanagida et al., 2008). Pharmacological antagonists of nAChR have been shown to partially reduce the neuroprotective effect of galantamine against ß-amyloid toxicity in culture (Arias et al., 2004; Kihara et al., 2004), suggesting that nAChR may be involved in galantamine-induced cell survival. However, the precise mechanisms underlying neuroprotection mediated by galantamine in vivo remain poorly defined.

In this study, we examined the role of galantamine in the visual system and asked whether it stimulates RGC survival in a rat glaucoma model. Our data demonstrate that

galantamine leads to structural protection of RGCs from ocular hypertension damage. We show that the profound functional impairments caused by high IOP are markedly attenuated in galantamine-treated eyes. Intriguingly, galantamine-induced RGC neuroprotection is mediated through activation of muscarinic ACh receptors (mAChR), and is independent of nAChR. Our study provides the first evidence of the therapeutic potential of galantamine in glaucoma and reveals mAChR as a potential clinical target for this neurodegenerative disease.

II.3. MATERIALS AND METHODS

II.3.1. Experimental animals

All procedures were carried out in accordance with the guidelines of the Society for Neuroscience, the Association for Research in Vision and Ophthalmology, and the Canadian Council on Animal Care for the use of experimental animals. Ocular hypertension (OHT) surgery was performed in aging, male Brown Norway rats (Charles River Canada), retired breeders between 10-12 months of age (300-400 g). Brown Norway rats were used because they have a larger eye suitable for the OHT surgical procedure, and this glaucoma model has been well characterized in these animals (Morrison et al., 1997). The optic nerve axotomy model, which is independent of OHT damage, was used as an acute paradigm of RGC death and was carried out in adult Sprague-Dawley rats (Charles River, 180-200 g). The number of animals used in each experiment is indicated above the bar in the corresponding graph.

II.3.2. Retrograde labeling of RGCs

For quantification of neuronal survival, RGCs were retrogradely labeled with DiI (1,1'-dioctadecyl-3,3,3’,3’-tetramethyl-indocarbocyanine perchlorate; Molecular Probes, Junction City, OR) for the glaucoma model, or with Fluorogold (2%, Fluorochrome, Englewood, CO) for the axotomy model. DiI crystals (3%) or Fluorogold (2%) were dissolved in 0.9% NaCl containing 10% dimethyl sulfoxide (DMSO) and 0.5% Triton X-100. The superior colliculus was exposed and a small piece of gelfoam (Pharmacia and Upjohn Inc., Mississauga, ON) soaked in tracer was applied to the surface. Seven days

after tracer application, the time required for labeling the entire RGC population, animals were subjected to ocular hypertension surgery or axotomy.

II.3.3. Ocular hypertension surgery and optic nerve axotomy

Surgical procedures were performed under general anesthesia by intraperitoneal (i.p.) injection of 1 ml/kg standard rat cocktail consisting of ketamine (100 mg/ml, Bimeda-MTC Animal Health Inc., Cambridge, ON), xylazine (20 mg/ml, Bimeda-MTC Animal Health Inc., Cambridge, ON), and acepromazine (10 mg/ml, Ayerst Veterinary Laboratories, Guelph, ON). Unilateral elevation of IOP was induced as previously described (Morrison et al., 1997) by a single injection of a hypertonic saline solution into an episcleral vein. A plastic ring was applied to the ocular equator to confine the injection to the limbal plexus and a microneedle was then used to inject 50 µl of sterile 1.85 M NaCl solution through an episcleral vein. The plastic ring temporarily blocks off other episcleral veins forcing the saline solution into the Schlemm's canal to create isolated scarring. Following injection, the plastic ring was removed and the eyes were examined to assess the extent to which the saline solution traversed the limbal vasculature. Polysporin ophthalmic ointment (Pfizer Canada Inc., Kirkland QC) was applied to the operated eye and the animal was allowed to recover from the surgery. Animals were kept in a room with constant low fluorescent light (40-100 lux) to stabilize circadian IOP variations. For optic nerve axotomies, animals were deeply anesthetized (2% Isoflurane, 0.8 liter/min), the left optic nerve was exposed and carefully transected at 0.5-1 mm from the optic nerve head avoiding injury to the ophthalmic artery. Fundus examination was routinely performed immediately after axotomy and 3-5 days later to check the integrity of the retinal circulation after surgery. Animals showing signs of compromised blood supply were excluded from the study.

II.3.4. Measurement of intraocular pressure (IOP)

IOP from glaucomatous and normal eyes was measured in awake animals because general anesthetics cause a marked IOP reduction (Jia et al., 2000). A calibrated tonometer (TonoPen XL, Medtronic Solan, Jacksonville, FL) was used to measure IOP after application of one drop of proparacaine hydrochloride (0.5%, Alcon Laboratories, Inc., Fort Worth, TX) per eye. The tonometer was held exactly perpendicular to the

corneal surface and ~10 consecutive readings per eye were taken and averaged to obtain an accurate IOP measurement. IOP was measured daily for two weeks after ocular hypertension surgery, then every other day for the entire duration of the experiment. The mean and peak (maximum) IOP for each eye were calculated and these values were used to estimate the mean and peak IOP for experimental and control groups.

II.3.5. Drug delivery

Drug delivery in the glaucoma model was carried out by daily intraperitoneal (i.p.) injection to avoid multiple intraocular injections, which lead to IOP reduction in glaucomatous eyes. For this purpose, the following compounds that cross the blood-brain/retinal barrier were administered alone or in combination: galantamine hydrobromide (3.5 mg/kg, Tocris Bioscience, Ellisville, MO), memantine hydrochloride (4 mg/kg, Sigma-Aldrich, St. Louis, MO), donepezil hydrochloride (4 mg/kg, Jubilant Organosys Inc., Stamford, CT), or scopolamine hydrobromide (1 mg/kg, Tocris Bioscience). Control animals received daily i.p. injections of sterile vehicle (phosphate-buffered saline: PBS). In some experiments, animals were treated with the ß-adrenergic receptor blocker timolol maleate (0.5%, Sabex Inc., Boucherville, QC) applied daily on the cornea of the glaucomatous eye to control IOP increase.

In the axotomy model, drug delivery was carried out by intravitreal injection of the following compounds in a total volume of 5 µl: galantamine hydrobromide (100 mM), methyllycaconitine citrate (MLA, 10 µM, Sigma-Aldrich), dihydro-ß-erythroidine hydrobromide (DHß-E, 100 µM, Sigma-Aldrich), mecamylamine hydrochloride (MMA, 10 mM, Sigma-Aldrich), scopolamine hydrobromide (10 mM, Tocris Bioscience), pirenzepine dihydrochloride (1 mM, Tocris Bioscience), 11-[[2-[(Diethylamino)methyl]-1-piperidinyl]acetyl]-5,11-dihydro-6H-pyrido[2,3-b][1,4]benzodiazepin-6-one (DX116, 1 mM, Tocris Bioscience), Diphenylacetoxy-N-methylpiperidine methiodide (4-DAMP, 1 mM, Tocris Bioscience), or tropicamide (1 mM, Tocris Bioscience). Control eyes received an intravitreal injection of sterile vehicle (PBS). Drugs were injected into the vitreous chamber using a 10-µl Hamilton syringe adapted with a 32-gauge glass microneedle, the tip of which was inserted into the superior hemisphere of the eye, at a ~45° angle, through the sclera into the vitreous body. This route of administration

avoided retinal detachment or injury to eye structures, including the iris and lens that release factors that may induce RGC survival. Surgical glue (Indermill, Tyco Health Care, Mansfield, MA) was used to seal the injection site.

II.3.5. Quantification of RGC soma and axons

Quantification of RGC bodies and axons was performed in duplicate by an observer masked to the treatment assignments. For RGC density counts, rats were deeply anesthetized and perfused transcardially with 4% paraformaldehyde (PFA) in 0.1 M phosphate buffer following which both eyes were immediately enucleated. Retinas were dissected and flat-mounted on a glass slide with the ganglion cell layer side up. RGCs were counted within three square areas at distances of 1, 2 and 3 mm from the optic disc in each of the four retinal quadrants (superior, inferior, nasal and temporal) for a total of 12 retinal areas. Macrophages and microglia that may have incorporated fluorescent tracer after phagocytosis of dying RGCs were excluded from our quantitative analysis based on cell-specific markers and morphology (Lebrun-Julien et al., 2009). For axon counts, animals received a transcardial injection of heparin (1,000 u/kg) and sodium nitroprusside (10 mg/kg) followed by perfusion with 2% PFA and 2.5% glutaraldehyde in 0.1 M phosphate buffer. Optic nerves were dissected, fixed in 2% osmium tetroxide, and embedded in epon resin. Semi-thin sections (0.7-µm-thick) were cut on a microtome (Reichert, Vienna, Austria) and stained with 1% toluidine blue. RGC axons were counted at 1 mm from the optic nerve head in five non-overlapping areas of each optic nerve section, encompassing a total area of 5,500 µm2 per nerve. The five optic nerve areas analyzed included: one in the center of the nerve, two peripheral dorsal and two peripheral ventral regions. The total area per optic nerve cross-section was measured using Northern Eclipse image analysis software (Empix Imaging, Toronto, ON), and this value was used to estimate the total number of axons per optic nerve.

II.3.6. Visual evoked potential (VEP) and electroretinogram (ERG) recordings

For VEP recordings, animals were anesthetized with isoflurane (3% for induction and 1.5% for maintenance) and placed in a stereotaxic head holder. The electrocardiogram was continuously monitored and the core body temperature was maintained at 37°C using a feedback controlled heating pad. Atropine sulfate eye drops

(1%, Allergan Canada, Markham, ON) were used to dilate the pupils and the corneas were protected by application of artificial tears (Allergan Canada). A bilateral craniotomy was performed anterior to the lambda, at bregma coordinates -6.8 and 1.5 mm lateral to the sagittal suture, to expose the cerebral cortex overlying the superior colliculus of each hemisphere. The dura was then incised and a tungsten multiunit recording microelectrode (impedance 0.8Ω Microprobe, Gaithersburg, MD, USA) was lowered under microscopic view until the tip touched the surface of the cortex. The skull opening was then filled with agar to protect the tissue from desiccation and, using a micromanipulator (Motorized Microdrive, FHC Inc., Bowdoinham ME), the microelectrode was advanced vertically to 300 μm from the superficial layer of the superior colliculus into the stratum griseum superficiale. Visual stimulation was provided by a diffuse flash (f = 1 Hz, Grass photostimulator, Astro-Med Inc, Brossard, QC) placed 30 cm away from the contralateral eye. Triggered evoked potentials were averaged over 40 successive presentations. VEP signals were amplified and bandpass filtered between 10 and 1,000 Hz and acquired via an analogue/digital interface (CED 1401 plus) to a PC running acquisition software (Signal 2, CED, Cambridge, UK). At the end of the experiment, the final electrode location was marked by passing a direct current (D.C.) of 10 mA for 5 sec through the recording electrode. The animals were then perfused with 4% PFA, the brains were removed and processed for serial sectioning. Sections (50 μm) were stained with cresyl violet and the electrode location mark was visualized as an iron precipitate following incubation in a 2% $K_4Fe(CN)_6$ solution. The depth of recording was confirmed by the position of the mark and the depth reading of the micromanipulator.

For ERG recordings, animals were dark adapted for a 12-hour period. Under dim red light illumination, the animals were anesthetized with a mixture of ketamine hydrochloride (80 mg/kg) and xylazine (6 mg/kg) and the pupils were dilated with cyclopentolate hydrochloride 1%. ERGs were recorded with a Dawson, Trick and Litzkow (DTL) fibre electrode (27/7X-Static, silver coated conductive nylon yarn, Sauquoit Industries, Scranton, PA) that was positioned and maintained on the cornea using a drop of 1% methylcellulose. The ERG (bandwidth: 1-1,000 Hz; x 10,000; Grass, P511 amplifier) and oscillatory potentials (bandwidth: 100-1000 Hz; x 50,000) were

recorded simultaneously with the Acknowledge data acquisition system (Biopac MP 100 WS, BIOPAC System Inc., Goleta, CA, USA).

II.3.7. Statistical analysis

Data analysis and statistics were performed using the GraphPad Instat software (GraphPad Software Inc., San Diego, CA) by a one-way (two-way for IOP measurments) analysis of variance (ANOVA) test followed by Bonferroni's multiple comparison post-test.

II.4. RESULTS

II.4.1. Galantamine protects RGC soma and axons from hypertension-induced death

We tested the neuroprotective effect of galantamine in vivo in a rat ocular hypertension (OHT) model of glaucoma. Unilateral elevation of IOP was induced after a single injection of hypertonic solution into an episcleral vein, a procedure named OHT surgery. Gradual increase of eye pressure and progressive death of RGCs are observed in this model, with an excellent linear correlation between IOP increase and degree of RGC loss and optic nerve damage (Morrison et al., 1997). Inner retinal atrophy, optic nerve degeneration, and optic nerve head remodeling in this model are similar to those seen in human glaucoma, making this model one of the best experimental in vivo paradigms to study glaucoma.

RGCs were visualized with the fluorescent tracer DiI, which was applied to the superior colliculus at least 1 week before OHT surgery to ensure retrograde labeling prior to any changes in optic nerve function caused by experimental glaucoma (Figure 1a). Unlike other retrograde markers that leak from the cell body after several weeks, DiI has been shown to persist in RGCs in vivo for periods of up to 9 months without fading or leakage (Vidal-Sanz et al., 1988). Consistent with previous studies, the average total RGC population detected by DiI in intact, non-injured Brown-Norway rat retinas was 1841 ± 15 RGCs/mm^2 (mean ± S.E.M., n = 9) (Figure 1b). Galantamine is a small molecule capable of crossing the blood-brain and blood-retinal barriers; therefore its neuroprotective effect was evaluated following daily intraperitoneal (i.p.) injection of 3.5

mg per kg of body weight (mg/kg), a dose selected based on previous studies showing efficacy in vivo (Lorrio et al., 2007; Yanagida et al., 2008). Galantamine treatment was initiated once IOP elevation was detected (~1 week after OHT surgery, Figure 1a) and continued thereafter for the entire duration of the experiment.

Analysis of DiI-positive RGCs in retinal whole mounts showed that galantamine led to higher neuronal densities in glaucomatous eyes compared to control eyes treated with vehicle (PBS) (Figure 1b-d). Quantitative analysis confirmed that daily galantamine treatment led to a robust increase in survival of injured RGCs at 3 weeks after OHT surgery (90%: 1,627 ± 29 RGCs/mm^2, mean ± S.E.M., n=11) compared to vehicle (55%: 1,025 ± 22 RGCs/mm^2, n=9) (ANOVA, $p < 0.001$). Although neuronal damage was more severe at 5 weeks after OHT surgery, galantamine still protected 70% of RGC soma (1,270 ± 74 RGCs/mm^2, n=10) compared to only 37% with PBS (657 ± 52 RGCs/mm^2, n=9) (ANOVA, $p < 0.001$) (Figure 1e). We carried out a comparative study on the neuroprotective effect of galantamine with respect to memantine, an N-Methyl-D-Aspartic acid (NMDA) channel blocker, and donepezil, another acetylcholinesterase inhibitor, both currently used in Alzheimer's disease. Our results show that galantamine was more effective than memantine or donepezil at preventing RGC loss in experimental glaucoma (Figure 2).

Glaucoma is characterized by the degeneration of RGC axons in the optic nerve posterior to the lamina cribrosa; hence we also investigated the effect of galantamine on RGC axon protection. Analysis of optic nerve cross-sections demonstrated a larger number of RGC axon fibers with normal morphology in galantamine-treated eyes compared to PBS-treated control eyes (Figure 3a-c), the latter showing extensive axon degeneration including disarray of fascicular organization and degradation of myelin sheaths. Quantitative analysis confirmed that galantamine promoted substantial protection of RGC axons from glaucomatous damage (Figure 3d). Collectively, these results indicate that galantamine effectively protects both RGC soma and axons in experimental glaucoma.

II.4.2. Galantamine-mediated neuroprotection is not due to decreased IOP

To investigate if daily treatment with galantamine led to IOP reduction, which could account for the observed neuroprotective effect, we measured eye pressure daily for two weeks after ocular hypertension surgery and then every other day for the entire duration of the experiment. Our results demonstrate that daily i.p. administration of galantamine did not reduce IOP over a period of several weeks (Figure 4a). The mean sustained pressure elevation among galantamine-treated and PBS-treated groups was similar: ~34 mm Hg at 3 weeks after OHT surgery and ~40 mm Hg at 5 weeks after OHT surgery (Table 1), well within the range of IOP increases observed in this model (Morrison et al., 1997). Given that the rate of RGC death is proportional to IOP, the similar elevation in IOP among groups allowed for reliable comparison of the neuroprotective effect of galantamine versus vehicle.

To further test whether galantamine-mediated neuroprotection was independent of IOP-induced damage, we examined the effect of galantamine after axotomy of the optic nerve (Figure 4b-e), an acute insult that leads to rapid apoptotic death of RGCs (Berkelaar et al., 1994). RGCs were retrogradely labeled with Fluorogold and subjected to optic nerve transection with concomitant intraocular injection of galantamine. The average total RGC population detected with Fluorogold in intact, non-injured Sprague-Dawley rat retinas was 2,223 ± 24 RGCs/mm^2 (mean ± S.E.M., n=5), a slightly higher density than in Brown-Norway rats, consistent with previous studies (Mansour-Robaey et al., 1994; Pernet and Di Polo, 2006). After axotomy, all RGCs survive for 5 days and then die abruptly: the population of RGCs is reduced to approximately 50% by 1 week and to ~10% at 2 weeks post-axotomy. In galantamine-treated eyes, 75% of RGCs survived at 1 week after axotomy compared to 50% that survived in the PBS-treated group (1,611 ± 47 RGCs/mm^2, n=6, and 920 ± 32 RGCs/mm^2, n=5, respectively, ANOVA, $P < 0.001$). The effect of galantamine was still marked at 2 weeks after axotomy: 30% of all RGCs remained alive compared to only 10% survival in PBS-treated eyes (616 ± 30 RGCs/mm^2, n=5, and 216 ± 15 RGCs/mm^2, n=5, respectively, ANOVA, $P < 0.01$) (Figure 4E). Collectively, these results demonstrate that galantamine can delay RGC loss following chronic (glaucoma) or acute (axotomy) optic nerve injury.

II.4.3. RGC functional deficits in glaucoma are improved by galantamine

Our results show structural protection of RGCs, both at the level of the cell bodies and axons, but are these neurons functional? To investigate whether galantamine preserved RGC function in glaucoma, we measured visual evoked potentials (VEPs) following flash stimulation. The main target of RGCs in the rat brain is the superior colliculus, thus VEPs recorded from this region provide a faithful representation of surviving RGC function and were used as the primary outcome to assess functional neuroprotection. The flash electroretinogram (ERG) provides information about the outer retina and was not used to assess RGC function. ERGs were routinely performed prior to VEPs to ensure that the outer retina was functioning properly and that RGCs received adequate input following visual stimulation. All the animals in this study had normal ERGs.

First, we investigated whether galantamine daily treatment had any effect on the VEP response to flash stimulation in normal, non-glaucomatous eyes. Our data demonstrate that VEPs recorded from galantamine-treated normal brains were indistinguishable from those treated with PBS or without treatment (Figure 5a), indicating that galantamine by itself does not alter the response of normal RGCs or target neurons in the superior colliculus. At 3 weeks after OHT surgery, examination of VEP responses to flash stimulation showed substantial reduction in evoked currents recorded from PBS-treated eyes compared to intact, non-glaucomatous controls (Figure 5b). In contrast, galantamine administration led to marked preservation of the VEP. Quantification of peak-to-peak VEP amplitudes demonstrated that galantamine preserved 66% of the intact VEP response compared to only 30% in PBS-treated controls (ANOVA, $p < 0.001$).

At 5 weeks after OHT surgery, both PBS-treated and galantamine-treated glaucomatous eyes showed complete obliteration of the VEP (Figure 5c). This lack of response could not be solely attributed to RGC degeneration because galantamine protected almost 70% of RGC soma and axons at 5 weeks after OHT (Figures 1and 3). We then hypothesized that sustained high IOP impairs the visual function of the surviving RGCs. To test this idea, we evaluated the effect of galantamine on the VEP response using a protocol in which IOP in the glaucomatous eye was controlled by

topical (corneal) application of timolol, a commonly used ß-adrenergic receptor blocker. Treatment with timolol began at 3 weeks after OHT and continued for the entire duration of the experiment. Timolol limited the IOP increase in galantamine-treated glaucomatous eyes to a mean IOP of 35.6 mm Hg compared to 42.7 mm Hg in eyes without timolol (Table 1). Interestingly, this difference in IOP (7 mm Hg) was sufficient to restore 47% of the VEP response in galantamine-treated eyes, but not in PBS-treated eyes (Figure 5c), indicating that IOP reduction only rescued RGC function when combined with galantamine. The recovery of VEP was not due to a neuroprotective effect of timolol because animals treated with PBS and timolol did not show any functional improvement. Furthermore, VEP recovery was not due to increased survival because RGC densities in the presence of timolol and galantamine (1,387 ± 50 RGCs/mm^2, mean ± S.E.M., n=8) were not statistically different from those in eyes treated with galantamine alone (1,270 ± 85 RGCs/mm^2, n=10, $p > 0.05$). The absence of VEP responses in eyes treated with PBS also confirmed that topical application of timolol, by itself, was not neuroprotective. Taken together, these results indicate that high IOP leads to dramatic deficits in retinal function that can be markedly attenuated by galantamine, and highlight the importance of combining galantamine with IOP lowering drugs to achieve long-term functional RGC protection.

II.4.4. ACh muscarinic, but not nicotinic, receptors mediate the neuroprotective effect of galantamine in experimental glaucoma

In the nervous system, there are two major types of ACh receptors: i) nicotinic receptors (nAChR) including the α7 and the α4ß2 nAChR, which are the most abundant subtypes in the brain, and metabotropic muscarinic receptors (mAChR), which are selectively activated by muscarine-like ligands and include five distinct isoforms (M1-M5) corresponding to the products of five separate genes (Bonner et al., 1987). To gain mechanistic insight into how galantamine promotes RGC neuroprotection in vivo, we asked whether blockade of nAChR or mAChR would compromise galantamine-induced RGC survival. For this purpose, we first assessed the survival of axotomized RGCs following intraocular injection of galantamine in combination with selective pharmacological blockers of nAChR or mAChR. Co-injection of galantamine with

scopolamine, an inhibitor of all mAChR types, abrogated the pro-survival effect of galantamine. In contrast, co-administration of galantamine with either methyllycaconitine (MLA), a specific antagonist of α7 nAChR, dihydro-ß-erythroidine (DHß-E), a specific antagonist of α4ß2 nAChR, or mecamylamine (MMA), a blocker of all neuronal nAChR, did not reduce galantamine-induced RGC survival (Figure 6a). A range of concentrations of these nAChR inhibitors was tested (10 μM to 10 mM) with similar outcome, indicating that their lack of effect was not the result of suboptimal doses of these drugs. Consistent with these findings, daily i.p. injection of galantamine and scopolamine, which readily cross the blood-brain/retinal barrier, completely inhibited RGC neuroprotection in glaucomatous eyes at 5 weeks after OHT (Figure 6b). Administration of MLA, DHß-E, MMA or scopolamine, by themselves, did not cause RGC death or adverse effects in non-injured retinas, nor did they promote survival in injured rat retinas at the doses used here (Figure 6c and d).

To establish which mAChR were involved in RGC survival, the following selective antagonists of mAChR subtypes were co-administered with galantamine: pirenzepine (M1), DX116 (M2), 4-DAMP (M3) or tropicamide (M4). These mAChR antagonists do not cross the blood-brain/retinal barrier or exhibit extremely low barrier permeability (Mickala et al., 1996; Stein et al., 1995; van Waarde et al., 1994), thus their effect was tested on galantamine-induced protection of axotomized RGCs after intraocular injection. Figure 6e shows that while blockade of M2 by DX116 or M3 by 4-DAMP did not have any effect on RGC survival mediated by galantamine, blockade of M1 with pirenzepine completely abrogated RGC neuroprotection. The M4 antagonist tropicamide also reduced RGC survival, albeit to a lesser extent than pirenzepine. Collectively, these data strongly suggest that M1 and M4 mAChR are mediators of galantamine-induced RGC neuroprotection.

II.5. DISCUSSION

This study supports four major findings. First, galantamine treatment leads to survival of RGC somata and axons in experimental glaucoma. Second, RGC structural protection is independent of IOP-induced damage, as evidenced by the neuroprotective action of this drug after optic nerve axotomy. Third, functional deficits caused by high

IOP are markedly improved by galantamine. Fourth, galantamine-mediated neuroprotection occurs primarily through activation of retinal mAChR M1, and is independent of nAChR.

Several recent clinical studies have suggested a correlation between glaucoma and Alzheimer's disease (Wostyn et al., 2009), but the most compelling evidence supporting such link stems from laboratory work. For example, neuronal loss in both glaucoma and Alzheimer's disease occurs by apoptosis (Tatton et al., 2003), caspases are activated both in Alzheimer's disease and in injured RGCs (McKinnon, 2003), and intraocular injection of ß-amyloid has been shown to induce RGC degeneration (Cordeiro et al., 2006). More recently, ß-amyloid deposition was associated with RGC death in experimental glaucoma and blockade of the ß-amyloid pathway reduced glaucomatous damage (Guo et al., 2007). Although the etiology of glaucoma and Alzheimer's disease may differ, their common features raise the provocative idea that drugs currently used to treat Alzheimer's disease may also have utility in glaucoma. Here, we show that one such drug, galantamine, is a powerful neuroprotectant for injured RGCs. Daily galantamine treatment promoted the survival of RGC somata and axons in glaucoma. Importantly, administration of galantamine by intravitreal injection also led to robust RGC protection after axotomy of the optic nerve. These data highlight several important properties of galantamine: it is effective when administered systemically or by intraocular injection, it promotes structural protection of RGCs in an IOP-independent manner, and it delays RGC loss in different models, both acute and chronic, of optic nerve damage.

The neuroprotective effect of galantamine was superior to that conferred by memantine or donepezil. Galantamine has been shown to be a weaker AChE inhibitor than donepezil (Geerts et al., 2005), therefore other factors likely account for this difference in neuroprotective efficacy. First, donepezil is a non-competitive inhibitor of AChE, which may result in the development of tolerance to donepezil and consequent downregulation of ACh receptors (Wilkinson, 1999). In contrast, galantamine is a competitive AChE inhibitor and the galantamine-AChE complex follows the typical kinetics of reversible inhibitors, dissociating readily in the presence of excess ACh, with a reduced potential for tolerance (Farlow, 2003). Second, galantamine acts more broadly on other neurotransmitter systems and has been shown to regulate the release of

glutamate, serotonin and α-aminobutyric acid (Albuquerque et al., 2000; Alkondon et al., 2000), thus potentially modulating neural activity and delaying neurodegeneration. Third, mAChR are amenable to modulation at allosteric sites (Gregory et al., 2007) hence it is possible that galantamine may activate mAChR directly, although this possibility presently remains unknown.

Patients with glaucoma experience diminished visual function and poor quality of life; therefore an ideal neuroprotective drug should preserve the structural viability of RGCs while retaining their ability to respond to visual stimulation. In this study, we aimed to provide a structure-function link based on the neuroprotective effect of galantamine. Our results demonstrate that there are major visual deficits in glaucomatous eyes treated with PBS, while galantamine treatment led to substantial preservation of the VEP amplitude at 3 weeks after OHT. Of interest, following longer periods of OHT (5 weeks) galantamine-protected RGCs (70%) did not respond to light stimulation unless IOP was also reduced. An IOP decrease of just a few mm Hg was sufficient to restore almost 50% of the VEP response in galantamine-treated eyes, but not in PBS-treated controls. The observation that the majority of RGCs exposed to galantamine remained alive at 5 weeks of OHT but did not respond to light stimulation suggests that sustained high IOP has additional deleterious effects on RGC function. We conclude that, in the long-term, structural protection alone is not sufficient to restore visual function unless IOP is also controlled.

Galantamine increases the availability of ACh through its inhibitory action on AChE, the enzyme responsible for ACh breakdown, and it is also an allosteric modulator of nAChR enhancing their sensitivity to ACh (Albuquerque et al., 1997; Schrattenholz et al., 1996). ACh in the retina is released by starburst cholinergic amacrine cells onto RGC dendrites and plays a crucial role in visual information processing (Beelke and Sannita, 2002). Therefore, we postulated that galantamine-induced neuroprotection might result from stimulation of ACh receptors. Since galantamine is an allosteric modulator of nAChR, its neuroprotective effect has been compared to that of nicotine. In fact, nicotine has been shown to promote neuronal survival in different models of neurodegeneration via nAChR and downstream activation of survival pathways (Picciotto and Zoli, 2008; Shimohama, 2009). Previous in vitro studies showed that galantamine promoted the

survival of cortical neurons or neuroblastoma cells via α7nAChR and stimulation of phosphatidylinositol-3-kinase (Arias et al., 2004; Kihara et al., 2004). As RGCs express several nAChR subtypes including α7nAChR (Cox et al., 2008; Gilbert et al., 2009), we initially postulated that nAChR activation would contribute to galantamine-mediated neuroprotection. Surprisingly, our data show that blockade of nAChR had no effect whereas inhibition of mAChR completely curtailed the neuroprotective effect of galantamine in vivo. The total blockade of galantamine-induced neuroprotection in the presence of mAChR inhibitors indicates that these receptors are the primary locus of the specific action of galantamine in the retina.

Immunocytochemical studies on the localization of mAChR subtypes in primate, rat and chick retinas showed that M2 and M4 are expressed by amacrine cells, and M3 is expressed primarily by bipolar cells (Fischer et al., 1998; Wassélius et al., 1998; Yamada et al., 2003). In addition, Müller cells, the most abundant glial cell type in the mammalian retina, express M1 and M4 mAChR types (Da Silva et al., 2008). Muscarine was shown to increase intracellular Ca^{+2} in rabbit RGCs (Baldridge, 1996), however, this effect was thought to be indirect because expression of mAChR has not been detected in isolated rat or cat RGCs, and muscarine did not elicit membrane currents measured in whole-cell patch clamp preparations (Kaneda et al., 1995; Lipton et al., 1987). Our results indicate that galantamine-mediated RGC neuroprotection in vivo occurs primarily via activation of M1, a mAChR subtype expressed by Müller cells. The M4 mAChR subtype, expressed by both Müller glia and amacrine cells, also contributes to this effect but to a lesser extent than M1 mAChR. Collectively, these data support a model in which non-cell-autonomous signaling events downstream of mAChR play a major role in galantamine-induced RGC neuroprotection. Activation of M1/M4 mAChR on neighboring Müller glia and amacrine cells may lead to stimulation of signaling pathways and production of pro-survival factors that protect injured RGCs. Other retinal cell types that express these mAChR subtypes, including endothelial cells (Sastry, 1985; Wu et al., 2003), may also participate in galantamine-mediated RGC survival.

M1 and M4 mAChR are G-protein-coupled receptors linked to different signal transduction pathways. M1 mAChR are preferentially coupled to pertussis toxin (PTX)-insensitive Gq/G11 proteins that stimulate phospholipase C (PLC) and

phosphatidylinositol hydrolysis with subsequent Ca^{+2} mobilization from intracellular stores (Felder, 1995). M4 mAChR, on the other hand, are preferentially coupled to PTX-sensitive Gi/o proteins that inhibit adenylate cyclase and regulate intracellular cAMP levels (Felder, 1995; Migeon and Nathanson, 1994). It has become increasingly clear that mAChR downstream signaling pathways converge or intersect with mediators of cell survival. For example, M4 mAChR interacts with the nerve growth factor receptor, via Gβγ complexes, to enhance phosphatidylinositol 3-kinase (PI3K)/Akt activation and neuronal survival (Wu and Wong, 2006). Of interest, M1 mAChR via Gαq and PLC leads to activation of Nrf2, a transcription factor involved in redox homeostasis, which may increase the cellular anti-oxidant defenses and confer neuroprotection against oxidative stress (Espada et al., 2009). Moreover, M1 mAChR activation also regulates the activity of the hypoxia-inducible factor-1 (HIF-1), a transcription factor involved in the cellular response to hypoxia (Hirota et al., 2004). Oxidative stress and ischemia/hypoxia have been proposed to be major contributors to glaucomatous neurodegeneration. An important priority in future studies will be to determine the M1- and M4-coupled signaling pathways underlying galantamine-induced RGC neuroprotection. The precise delineation of these molecular events should be useful for the design of novel therapeutic interventions applicable to glaucoma.

In summary, our study reveals the potent role of galantamine in the protection of RGC structure and function in glaucoma, which could be used in conjunction with standard pressure controlling drugs. Our data also identifies retinal mAChR as a novel therapeutic target for prevention of neuronal death and vision loss in optic neuropathies.

CONFLICT OF INTEREST: The authors declare no conflict of interest.

ACKNOWLEDGEMENTS: We thank Drs. Timothy Kennedy, Leonard Levin and William Baldridge for helpful discussions on the manuscript; and Philippe Bourgeois, Annie Douillette, Nawal Zabouri and Geneviève Cyr for technical assistance. This work was supported by grants from the Canadian Institutes of Health Research to (A.D.P. and C.C., Grant # PPP-79112) and the American Health Assistance Foundation/National Glaucoma Research (A.D.P. and C.C., Grant # G2008-027). A.D.P. holds a Fonds de recherche en santé du Québec (FRSQ) Chercheur Senior Scholarship.

II.6. REFERENCES

Albuquerque, E.X., Pereira, E.F., Alkondon, M., Schrattenholz, A., Maelicke, A., 1997. Nicotinic acetylcholine receptors on hippocampal neurons: distribution on the neuronal surface and modulation of receptor activity. J. Recept. Signal Transduct. Res. 17, 243-266.

Albuquerque, E.X., Pereira, E.F.R., Mike, A., Eisenberg, H.M., Maelicke, A., Alkondon, M., 2000. Neuronal nicotinic receptors in synaptic functions in humans and rats: physiological and clinical relevance. Behav. Brain Res. 113, 131-141.

Alkondon, M., Pereira, E.F.R., Eisenberg, H.M., Albuquerque, E.X., 2000. Nicotinic Receptor Activation in Human Cerebral Cortical Interneurons: a Mechanism for Inhibition and Disinhibition of Neuronal Networks. J. Neurosci. 20, 66-75.

Anderson, D.R., 2003. Collaborative Normal Tension Glaucoma Study. Curr. Opin. Ophthalmol. 14, 86-90.

Arias, E., Alés, E., Gabilan, N.H., Cano-Abad, M.F., Villarroya, M., García, A.G., López, M.G., 2004. Galantamine prevents apoptosis induced by [beta]-amyloid and thapsigargin: involvement of nicotinic acetylcholine receptors. Neuropharmacol. 46, 103-114.

Baldridge, W.H., 1996. Optical Recordings of the Effects of Cholinergic Ligands on Neurons in the Ganglion Cell Layer of Mammalian Retina. J. Neurosci. 16, 5060-5072.

Beelke, M., Sannita, W.G., 2002. Cholinergic function and dysfunction in the visual system. Meth. Find. Exp. Clin. Pharmacol. 24, Suppl D:113-117.

Berkelaar, M., Clarke, D.B., Wang, Y.-C., Bray, G.M., Aguayo, A.J., 1994. Axotomy results in delayed death and apoptosis of retinal ganglion cells in adult rats. J. Neurosci. 14, 4368-4374.

Bonner, T.I., Buckley, N.J., Young, A.C., Brann, M.R., 1987. Identification of a family of muscarinic acetylcholine receptor genes. Science 237, 527-532.

Clements, C., McNally, R., Conti, B., Mak, T., Ting, J.P.Y., 2006. DJ-1, a cancer- and Parkinson's disease-associated protein, stabilizes the antioxidant transcriptional master regulator Nrf2. Proceedings of the National Academy of Sciences of the United States of America 103, 15091-15096.

Cordeiro, M., Guo, L., Maass, A., Luong, V., Moss, S.E., Fitzke, F.W., Salt, T.E., 2006. Beta amyloid and retinal ganglion cell apoptosis: implications and applications to glaucoma. Invest. Ophthalmol. Vis. Sci. 47, S2698.

Cox, B.C., Marritt, A.M., Perry, D.C., Kellar, K.J., 2008. Transport of multiple nicotinic acetylcholine receptors in the rat optic nerve: high densities of receptors containing alpha6 and beta3 subunits. J. Neurochem. 105, 1924-1938.

Da Silva, N., Herron, C.E., Stevens, K., Jollimore, C.A.B., Barnes, S., Kelly, M.E., 2008. Metabotropic Receptor-Activated Calcium Increases and Store-Operated Calcium Influx in Mouse Muller Cells. Invest. Ophthalmol. Vis. Sci. 49, 3065-3073.

Espada, S., Rojo, A.I., Salinas, M., Cuadrado, A., 2009. The muscarinic M1 receptor activates Nrf2 through a signaling cascade that involves protein kinase C and inhibition of GSK-3beta: connecting neurotransmission with neuroprotection. J. Neurochem. 110, 1107-1119.

Farlow, M.R., 2003. Clinical pharmacokinetics of galantamine. Clin. Pharmacokinet. 42, 1383-1392.

Felder, C.C., 1995. Muscarinic acetylcholine receptors: signal transduction through multiple effectors. FASEB J. 9, 619-625.

Fischer, A.J., McKinnon, L.A., Nathanson, N.M., Stell, W.K., 1998. Identification and localization of muscarinic acetylcholine receptors in the ocular tissues of the chick. J. Comp. Neurol. 392, 273-284.

Geerts, H., Guillaumat, P.-O., Grantham, C., Bode, W., Anciaux, K., Sachak, S., 2005. Brain levels and acetylcholinesterase inhibition with galantamine and donepezil in rats, mice, and rabbits. Brain Res. 1033, 186-193.

Georgopoulos, G., Andreanos, D., Liokis, N., Papakonstantinou, D., Vergados, J., Theodossiadis, G., 1997. Risk factors in ocular hypertension. Eur. J. Ophthalmol. 7, 357-363.

Gilbert, D., Lecchi, M., Arnaudeau, S., Bertrand, D., Demaurex, N., 2009. Local and global calcium signals associated with the opening of neuronal [alpha]7 nicotinic acetylcholine receptors. Cell calcium 45, 198-207.

Gregory, K.J., Sexton, P.M., Christopoulos, A., 2007. Allosteric modulation of muscarinic acetylcholine receptors. Curr. Neuropharmacol. 5, 157-167.

Guo, L., Salt, T.E., Luong, V., Wood, N., Cheung, W., Maass, A., Ferrari, G., Russo-Marie, F., Sillito, A.M., Cheetham, M.E., Moss, S.E., Fitzke, F.W., Cordeiro, M.F., 2007. Targeting amyloid-beta in glaucoma treatment. Proc. Natl. Acad. Sci. U S A 104, 13444-13449.

Hirota, K., Fukuda, R., Takabuchi, S., Kizaka-Kondoh, S., Adachi, T., Fukuda, K., Semenza, G.L., 2004. Induction of hypoxia-inducible factor 1 activity by muscarinic acetylcholine receptor signaling. J. Biol. Chem. 279, 41521-41528.

Jia, L., Cepurna, W.O., Johnson, E.C., Morrison, J.C., 2000. Effect of general anesthetics on IOP in rats with experimental aqueous outflow obstruction. Invest. Ophthalmol. Vis. Sci. 41, 3415-3419.

Kaneda, M., Hashimoto, M., Kaneko, A., 1995. Neuronal nicotinic acetylcholine receptors of ganglion cells in the cat retina. Jpn. J. Physiol. 45, 491-508.

Kihara, T., Sawada, H., Nakamizo, T., Kanki, R., Yamashita, H., Maelicke, A., Shimohama, S., 2004. Galantamine modulates nicotinic receptor and blocks A[beta]-enhanced glutamate toxicity. Biochem. Biophys. Res. Comm. 325, 976-982.

Lebrun-Julien, F., Duplan, L., Pernet, V., Osswald, I.K., Sapieha, P., Bourgeois, P., Dickson, K., Bowie, D., Barker, P.A., Di Polo, A., 2009. Excitotoxic death of retinal neurons in vivo occurs via a non-cell-autonomous mechanism. J. Neurosci. 29, 5536-5545.

Lipton, S.A., Aizenman, E., Loring, R.H., 1987 Neural nicotinic acetylcholine responses in solitary mammalian retinal ganglion cells. Pflugers Arch. 410, 37-43.

Lorrio, S., Sobrado, M., Arias, E., Roda, J.M., Garcia, A.G., Lopez, M.G., 2007. Galantamine Postischemia Provides Neuroprotection and Memory Recovery against Transient Global Cerebral Ischemia in Gerbils. J. Pharmacol. Exp. Ther. 322, 591-599.

Mansour-Robaey, S., Clarke, D.B., Wang, Y.-C., Bray, G.M., Aguayo, A.J., 1994. Effects of ocular injury and administration of brain-derived neurotrophic factor on

survival and regrowth of axotomized retinal ganglion cells. Proc. Natl. Acad. Sci. USA 91, 1632-1636.

McKinnon, S.J., 2003. Glaucoma: ocular Alzheimer's disease? Front. Biosci. 8, 1140-1156.

Melo, J.B., Sousa, C., Garção, P., Oliveira, C.R., Agostinho, P., 2009. Galantamine protects against oxidative stress induced by amyloid-beta peptide in cortical neurons. Eur. J. Neurosci. 29, 455-464.

Mickala, P., Boutin, H., Bellanger, C., Chevalier, C., MacKenzie, E.T., Dauphin, F., 1996. In vivo binding, pharmacokinetics and metabolism of the selective M2 muscarinic antagonist Nucl. Med. Biol. 23, 173-179.

Migeon, J.C., Nathanson, N.M., 1994. Differential regulation of cAMP-mediated gene transcription by m1 and m4 muscarinic acetylcholine receptors. Preferential coupling of m4 receptors to Gi alpha-2. J. Biol. Chem. 269, 9767-9773.

Morrison, J.C., Moore, C.G., Deppmeier, L.M.H., Gold, B.G., Meshul, C.K., Johnson, E.C., 1997. A rat model of chronic pressure-induced optic nerve damage. Exp. Eye Res. 64, 85-96.

Pernet, V., Di Polo, A., 2006. Synergistic action of brain-derived neurotrophic factor and lens injury promotes retinal ganglion cell survival, but leads to optic nerve dystrophy in vivo. Brain 129, 1014-1026.

Picciotto, M.R., Zoli, M., 2008. Neuroprotection via nAChRs: the role of nAChRs in neurodegenerative disorders such as Alzheimer's and Parkinson's disease. Front. Biosci. 13, 492-504.

Quigley, H.A., 2005. Glaucoma: Macrocosm to Microcosm The Friedenwald Lecture. Invest. Ophthalmol. Vis. Sci. 46, 2663-2670.

Razay, G., Wilcock, G.K., 2008. Galantamine in Alzheimer's disease. Exp. Rev. Neurother. 8, 9-17.

Sastry, B.V., 1985 Cholinergic systems and multiple cholinergic receptors in ocular tissues. J. Ocul. Pharmacol. 1, 201-226.

Schrattenholz, A., Pereira, E.F., Roth, U., Weber, K.H., Albuquerque, E.X., Maelicke, A., 1996. Agonist responses of neuronal nicotinic acetylcholine receptors are potentiated by a novel class of allosterically acting ligands. Mol. Pharmacol. 49, 1-6.

Shields, M.B., 2008. Normal-tension glaucoma: is it different from primary open-angle glaucoma? Curr. Opin. Ophthalmol. 19, 85-88

Shimohama, S., 2009 Nicotinic receptor-mediated neuroprotection in neurodegenerative disease models. Biol. Pharm. Bull. 32, 332-336. .

Shimohama, S., Kihara, T., 2001. Nicotinic receptor-mediated protection against [beta]-amyloid neurotoxicity. Biol. Psych. 49, 233-239.

Stein, R., Bachoo, M., Polosa, C., 1995. Pirenzepine-sensitive component of forelimb vascular resistance and heart rate in cats. J. Autonom. Nerv. Syst. 54, 49-58.

Tatton, W., Chen, D., Chalmers-Redman, R., Wheeler, L., Nixon, R., Tatton, N., 2003. Hypothesis for a Common Basis for Neuroprotection in Glaucoma and Alzheimer's Disease: Anti-Apoptosis by Alpha-2-Adrenergic Receptor Activation. Survey of Ophthalmology 48, S25-S37.

van Waarde, A., Visser, G.M., Visser, T.J., Bouwer, J., Paans, A.M., Vaalburg, W., 1994. Rodent biodistribution and metabolism of tritiated 4-DAMP, a M3 subtype-selective cholinoceptor ligand. Nucl. Med. Biol. 21, 41-47.

Vidal-Sanz, M., Villegas-Perez, M.P., Bray, G.M., Aguayo, A.J., 1988. Persistent retrograde labeling of adult rat retinal ganglion cells with the carbocyanine dye diI. Exp. Neurol. 102, 92-101.

Wassélius, J., Johansson, K., Bruun, A., Zucker, C., Ehinger, B., 1998. Correlations between cholinergic neurons and muscarinic m2 receptors in the rat retina. Neuroreport. 9, 1799-1802.

Wilkinson, D.G., 1999. The pharmacology of donepezil: a new treatment of Alzheimer's disease. Expert Opin. Pharmacother. 1, 121-135.

Wostyn, P., Audenaert, K., De Deyn, P.P., 2009. Alzheimer's disease and glaucoma: Is there a causal relationship? Br. J. Ophthalmol., [Epub ahead of print].

Wu, D.M., Kawamura, H., Sakagami, K., Kobayashi, M., Puro, D.G., 2003. Cholinergic regulation of pericyte-containing retinal microvessels. Am. J. Physiol. Heart Circ. Physiol. 284, H2083-2090.

Wu, E.H., Wong, Y.H., 2006. Activation of muscarinic M4 receptor augments NGF-induced pro-survival Akt signaling in PC12 cells. Cell Signal 18, 285-293.

Yamada, E.S., Dmitrieva, N., Keyser, K.T., Lindstrom, J.M., Hersh, L.B., Marshak, D.W., 2003. Synaptic connections of starburst amacrine cells and localization of acetylcholine receptors in primate retinas. J. Comp. Neurol. 461, 76-90.

Yanagida, T., Takeuchi, H., Kitamura, Y., Takata, K., Minamino, H., Shibaike, T., Tsushima, J., Kishimoto, K., Yasui, H., Taniguchi, T., Shimohama, S., 2008. Synergistic effect of galantamine on nicotine-induced neuroprotection in hemiparkinsonian rat model. Neurosci. Res. 62, 254-261.

Figure 1. Galantamine protects RGC somata in glaucoma.

(A) Outline of the experimental protocol used to test the effect of galantamine on RGC survival in experimental glaucoma. RGCs were retrogradely labeled with the fluorescent tracer DiI and ocular hypertension (OHT) surgery was performed a week later. Galantamine treatment (3.5 mg/kg, i.p.) was initiated at ~1 week after OHT surgery, and continued thereafter for the entire duration of the experiment. Retinas and optic nerves were examined at 3 and 5 weeks following OHT surgery. (B) DiI-labeled RGCs in a flat mount preparation from intact, uninjured Brown Norway rat retina. At 5 weeks after OHT surgery galantamine treatment (C) led to higher neuronal densities compared to eyes treated with PBS (D). (E) Quantitative analysis of RGC survival in experimental glaucoma following treatment with galantamine (solid bars) or vehicle (PBS, hatched bars) (n = 8-11 rats per group). The density of RGCs in intact, untreated Brown Norway rat retinas (open bars) is shown as reference. Galantamine markedly increased the number of RGCs that survived at 3 and 5 weeks after OHT surgery (ANOVA, ***: $P<0.001$). Data are expressed as the mean ± S.E.M. Scale bars (B-D): 100 μm.

Figure 2. Comparative analysis of RGC survival in experimental glaucoma.

Mediated by galantamine (solid bars), memantine (crossed hatched bars), donepezil (vertical lines) or vehicle (PBS, hatched bars) at 3 and 5 weeks after OHT (n=7–11 rats per group) (ANOVA, ***P<0.001). Data are expressed as the mean±S.E.M.

Figure 3. Galantamine protects RGC axons in glaucoma.

Cross-sections of optic nerve segments from intact (A) and glaucomatous eyes treated with galantamine (B) or PBS (C) at 5 weeks after ocular hypertension (OHT) surgery. Galantamine-treated eyes displayed a larger number of axonal fibers with normal morphology compared to PBS-treated control eyes, which showed extensive axon degeneration. Panel D shows the quantitative analysis of RGC axons in the optic nerve following daily i.p. injection of galantamine (solid bar), or PBS (hatched bar) (n = 8-9 rats per group) (ANOVA, ***: $P<0.001$). The number of axons in the intact, uninjured Brown Norway rat optic nerve is shown as reference (open bar). Data are expressed as the mean ± S.E.M. Scale bars (A-C): 20 μm.

Figure 4. Galantamine-mediated neuroprotection is not due to decreased intraocular pressure.

(A) Daily i.p. administration of galantamine did not reduce intraocular pressure (IOP) over a period of several weeks. (B) Fluorogold-labeled RGCs in a flat mount preparation from intact, uninjured Sprague-Dawley rat retina. (C) Galantamine treatment led to marked survival of axotomized RGCs with respect to PBS-treated eyes (D). (E) Quantitative analysis of RGC survival following intraocular injection of galantamine (solid bars) or PBS (hatched bars) (n = 8-11 rats per group) (ANOVA, ***: $P<0.001$). The density of RGCs in intact, uninjured Sprague-Dawley rat retinas is shown as reference (open bar). Data are expressed as the mean ± S.E.M. Scale bars (A-C): 100 μm.

Figure 5. RGC functional deficits in glaucoma are improved by galantamine.

(A) Visual evoked potentials (VEP) recorded from galantamine-treated normal brains were indistinguishable from those treated with PBS or without treatment. (B) At 3 weeks after OHT surgery, galantamine administration led to marked preservation of the VEP responses (ANOVA, *: $p < 0.001$). (C) At 5 weeks after OHT surgery, both PBS-treated and galantamine-treated glaucomatous eyes showed complete obliteration of the VEP response. Daily application of timolol drops on the cornea was sufficient to restore the VEP response in galantamine-treated eyes but not in PBS-treated eyes (ANOVA, *: $p < 0.001$).

Figure 6. The neuroprotective effect of galantamine in glaucoma is mediated by activation of muscarinic ACh receptors.

(a) Intraocular co-injection of galantamine with scopolamine, an inhibitor of all mAChR types, abrogated the prosurvival effect of galantamine. In contrast, the α7nAChR antagonist methyllycaconitine (MLA), the α4β2 nAChR antagonist dihydro-b-erythroidine (DHβ-E) or the antagonist of all nAChR mecamylamine (MMA) did not reduce galantamine-induced survival of axotomized RGCs (ANOVA, *P<0.001). (b) Intraperitoneal co-administration of galantamine and scopolamine (SCO) completely inhibited galantamine-induced RGC neuroprotection in glaucomatous eyes at 5 weeks after OHT (ANOVA, *P<0.001). Intraocular administration of MLA, DHβ-E, MMA or SCO, by themselves, did not cause RGC death or adverse effects in non-injured retinas (c), nor did they promote survival in injured rat retinas (d) (n=3-6). (e) Intraocular injection of galantamine in combination with the M1 mAChR blocker pirenzepine (PRZ), the M2 mAChR antagonist DX116, the M3 mAChR blocker 4-DAMP or the M4 mAChR antagonist tropicamide (TRO), showed that galantamine-induced neuroprotection is mediated through activation of M1 and M4 mAChR (ANOVA, *P<0.001).

II.7. TABLES

Table 1. Intraocular pressure (IOP) elevation in glaucomatous eyes.

Time after OHT surgery	Group	N	Mean IOP (mm Hg)			Peak IOP (mm Hg)	
			Glaucoma	Control	Difference	Glaucoma	Control
3 weeks	Galantamine	27	34.71 ± 1.8	22.41 ± 0.2	11.09 ± 2.4	39.45 ± 1.4	26.81 ± 1.3
	Vehicle	23	33.11 ± 1.6	22.59 ± 0.3	11.73 ± 0.3	38.23 ± 1.2	25.67 ± 1.6
	No treatment	7	34.11 ± 0.6	23.09 ± 0.2	11.02 ± 0.4	38.41 ± 0.9	26.25 ± 1.2
	P value (ANOVA)		0.6	0.12	-	0.41	0.85
5 weeks	Galantamine	23	42.71 ± 0.2	23.63 ± 1.5	17.08 ± 0.8	49.11 ± 4.2	25.11 ± 0.5
	Vehicle	22	39.11 ± 1.0	23.4 ± 2.0	16.73 ± 1.0	48.17 ± 1.0	26.55 ± 0.7
	Ga l+ Timolol	6	35.64 ± 0.8	22.11 ± 2.2	13.53 ± 1.4	41.80 ± 0.8	26.05 ± 2
	Vehicle + Timolol	6	34.54 ± 1.6	22.23 ± 1.3	12.31 ± 0.5	42.36 ± 0.5	26.28 ± 4.2
	No treatment	10	41.35 ± 0.8	22.80 ± 1.7	17.55 ± 1.7	49.65 ± 0.9	25.08 ± 0.9
	P value (ANOVA)		0.45	0.12	-	0.32	0.71

II.8. FIGURES

FIGURE 1

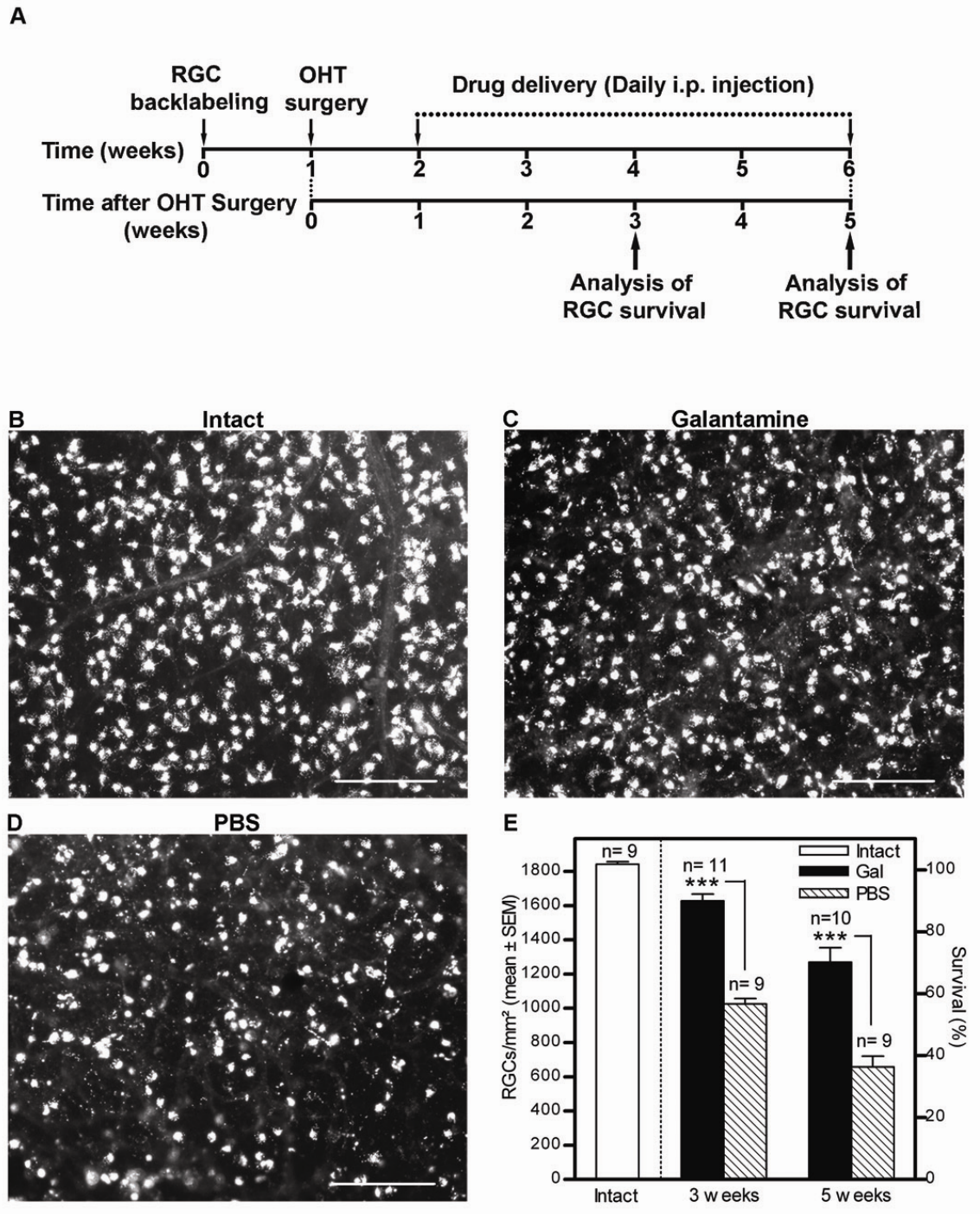

FIGURE 2

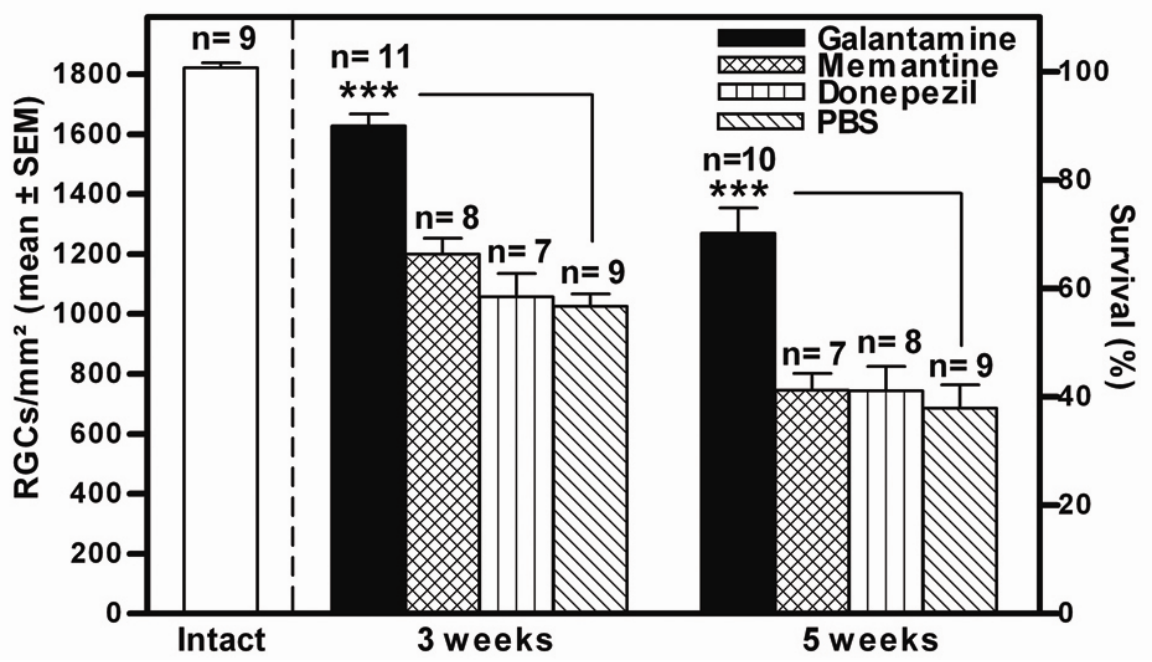
n= 9
n= 11
***
n= 8
n= 7
n= 9
n=10
***
n= 7
n= 8
n= 9
Galantamine
Memantine
Donepezil
PBS
RGCs/mm² (mean ± SEM)
Survival (%)
0
200
400
600
800
1000
1200
1400
1600
1800
0
20
40
60
80
100
Intact
3 weeks
5 weeks

FIGURE 3

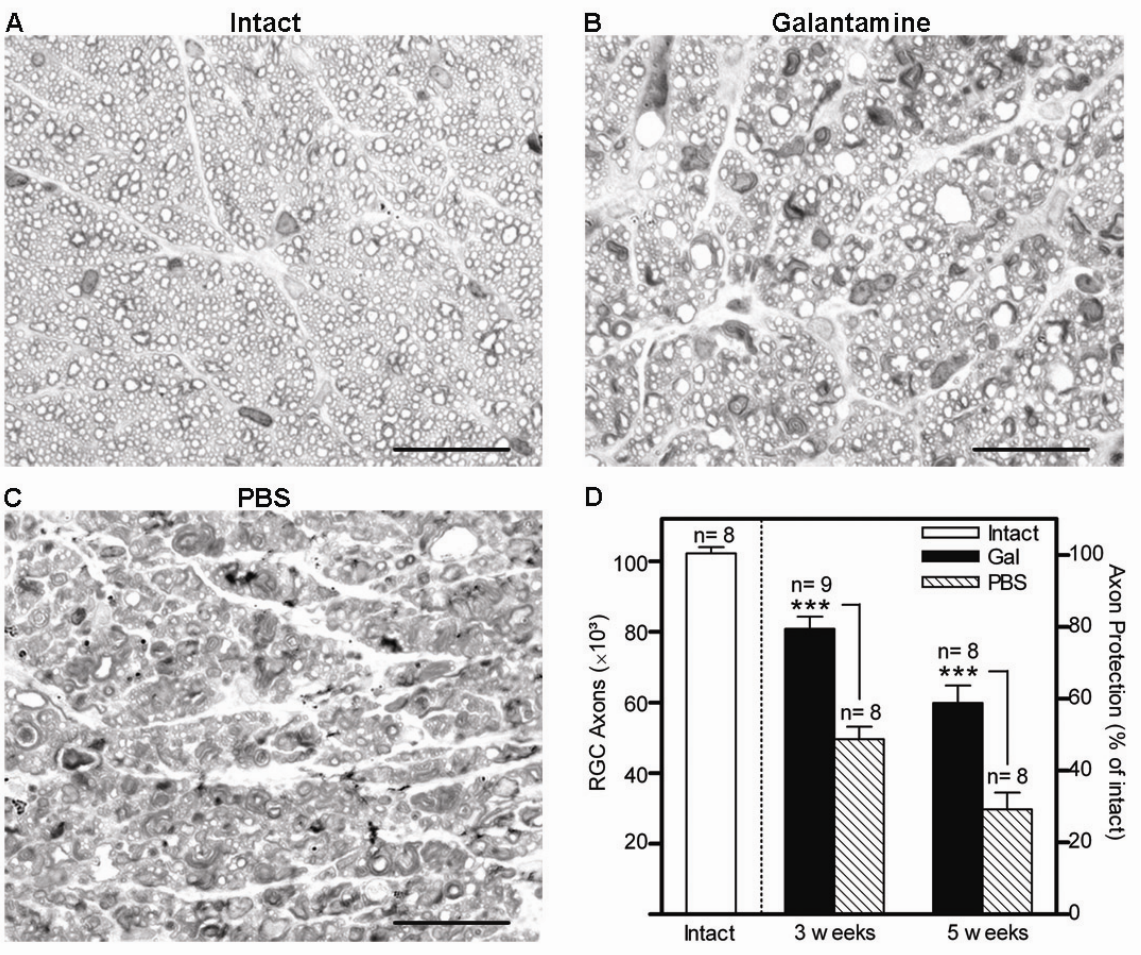
A
Intact
B
Galantamine
C
PBS
D
n= 8
n= 9
***
n= 8
n= 8
***
n= 8
Intact
Gal
PBS
RGC Axons (×10³)
Axon Protection (% of intact)
100
80
60
40
20
0
Intact
3 weeks
5 weeks

FIGURE 4

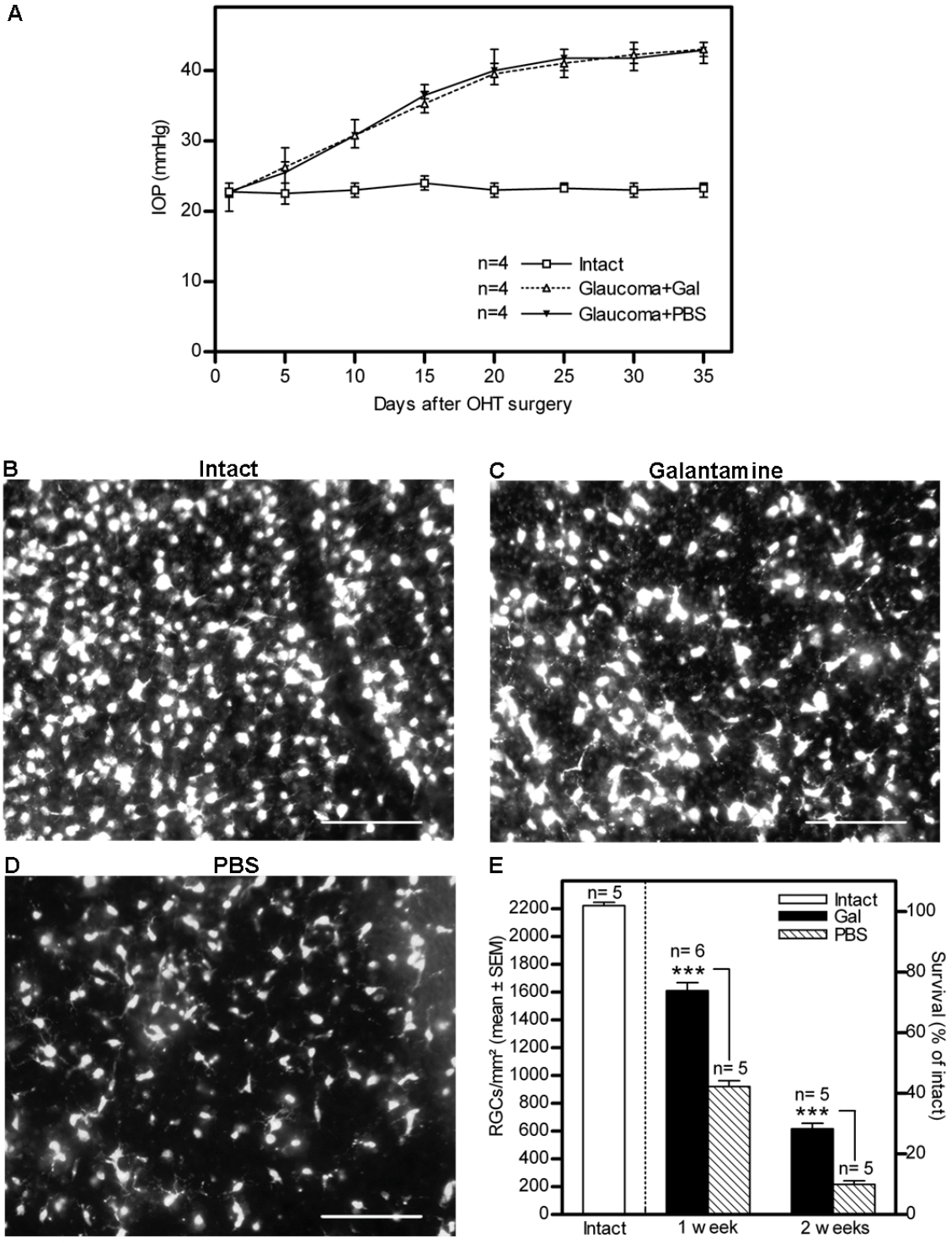
A
IOP (mmHg)
Days after OHT surgery
n=4 Intact
n=4 Glaucoma+Gal
n=4 Glaucoma+PBS
B Intact
C Galantamine
D PBS
E
RGCs/mm² (mean ± SEM)
Survival (% of intact)
Intact
Gal
PBS
n= 5
n= 6
***
n= 5
n= 5
***
n= 5
Intact
1 week
2 weeks

FIGURE 5

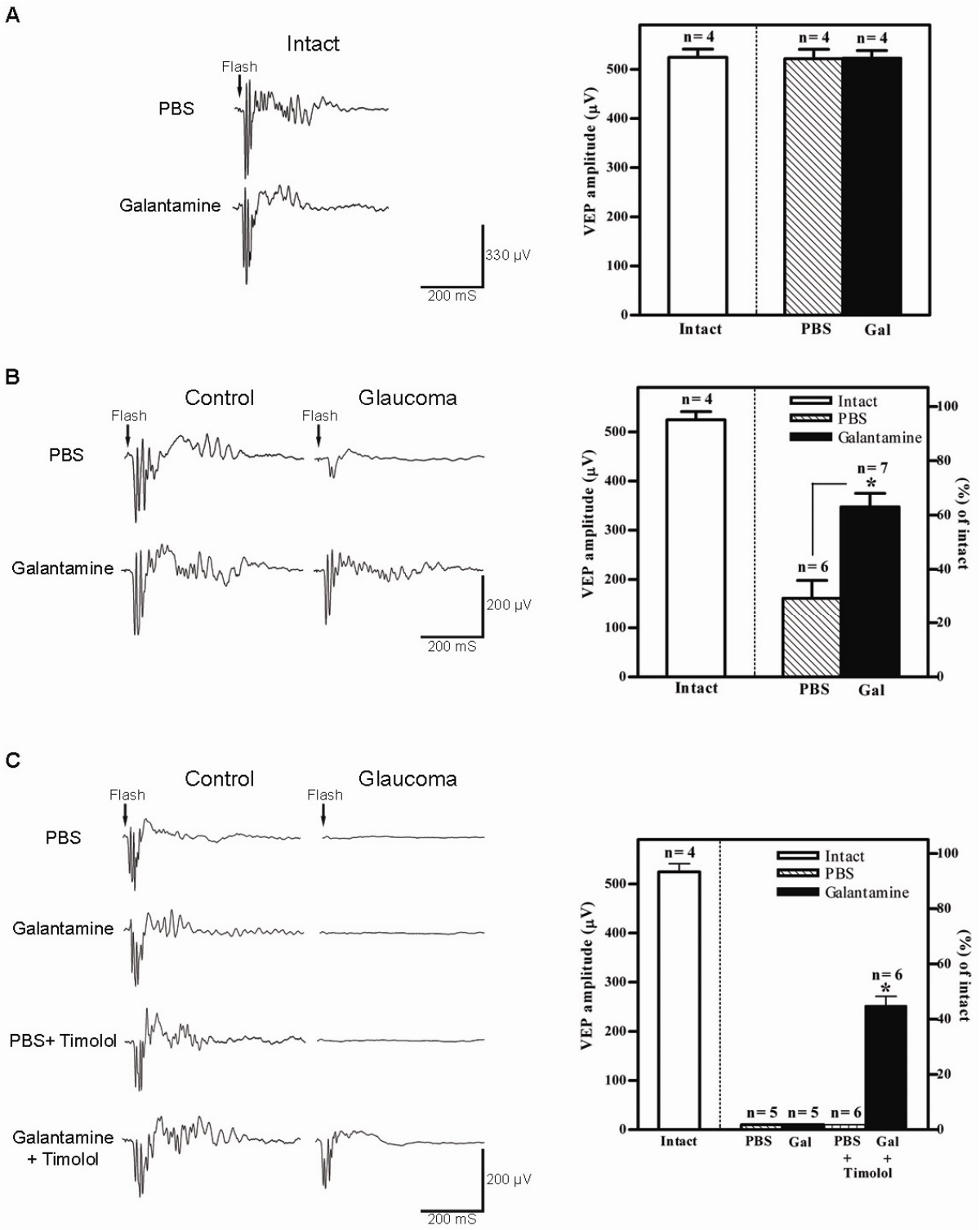
A
Intact
Flash
PBS
Galantamine
330 µV
200 mS
VEP amplitude (µV)
n=4
n=4
n=4
Intact
PBS
Gal
B
Control
Glaucoma
Flash
Flash
PBS
Galantamine
200 µV
200 mS
Intact
PBS
Galantamine
n=4
n=7
n=6
(%) of intact
C
Control
Glaucoma
Flash
Flash
PBS
Galantamine
PBS+ Timolol
Galantamine
+ Timolol
200 µV
200 mS
n=5
n=5
n=6
PBS
+
Timolol
Gal
+

FIGURE 6

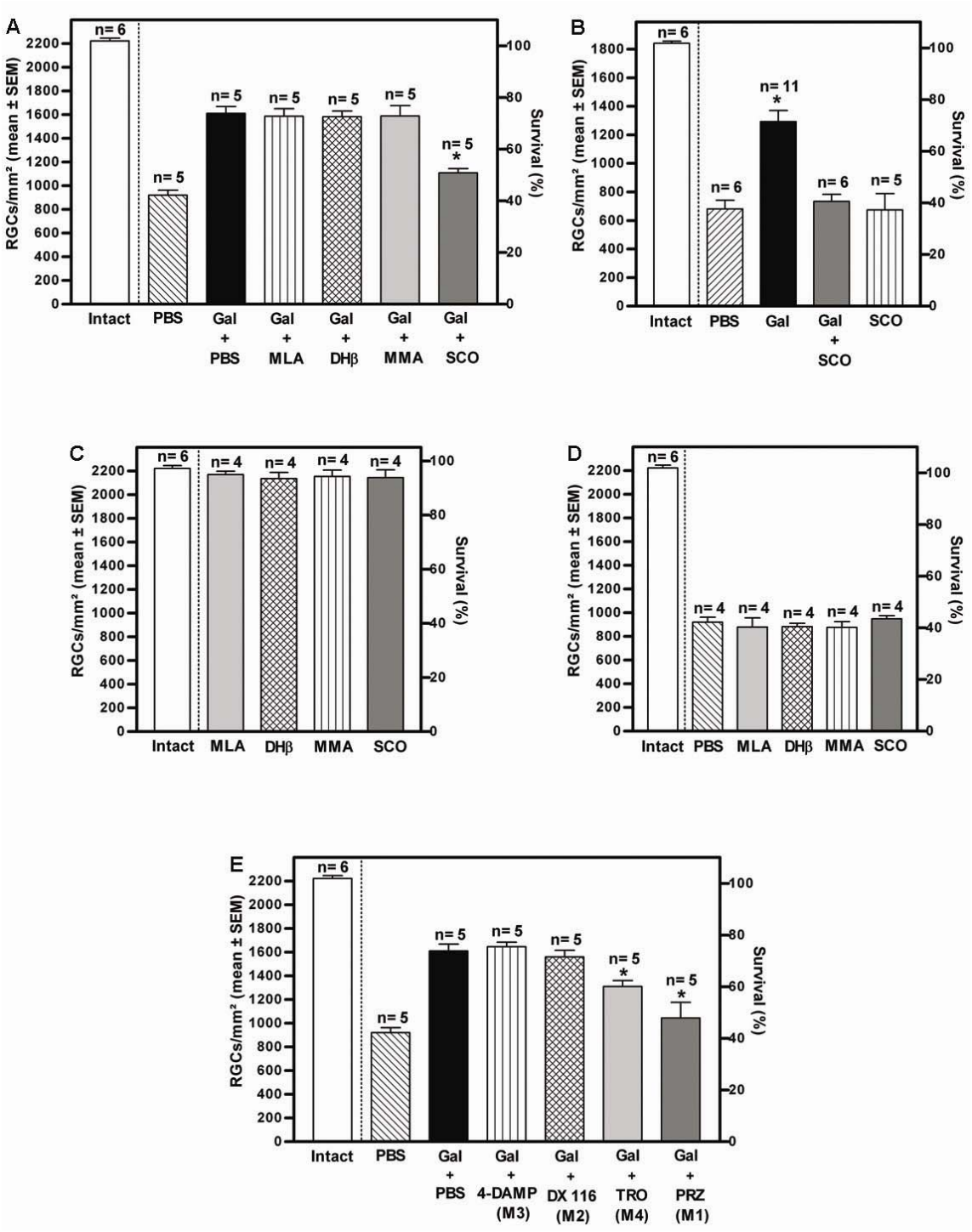
A
RGCs/mm² (mean ± SEM)
Survival (%)
n= 6
n= 5
n= 5
n= 5
n= 5
n= 5
*
Intact
PBS
Gal + PBS
Gal + MLA
Gal + DHβ
Gal + MMA
Gal + SCO
B
n= 6
n= 6
n= 11
*
n= 6
n= 5
Intact
PBS
Gal
Gal + SCO
SCO
C
n= 6
n= 4
n= 4
n= 4
n= 4
Intact
MLA
DHβ
MMA
SCO
D
n= 6
n= 4
n= 4
n= 4
n= 4
n= 4
Intact
PBS
MLA
DHβ
MMA
SCO
E
n= 6
n= 5
n= 5
n= 5
n= 5
*
n= 5
*
Intact
PBS
Gal + PBS
Gal + 4-DAMP (M3)
Gal + DX 116 (M2)
Gal + TRO (M4)
Gal + PRZ (M1)

CHAPTER 3

III. SECOND ARTICLE: "RETINAL MICROVASCULATURE PROTECTION CORRELATES WITH RETINAL GANGLION CELL SURVIVAL AND BLOOD FLOW RESTORATION IN EXPERIMENTAL GLAUCOMA".

In preparation

RETINAL MICROVASCULATURE PROTECTION CORRELATES WITH RETINAL GANGLION CELL SURVIVAL AND BLOOD FLOW RESTORATION IN EXPERIMENTAL GLAUCOMA

Mohammadali Almasieh[1], Alex Dong[2], Mylène Pouliot[3], Christian Casanova[3], Elvire Vaucher[3], Melanie Kelly[2] and Adriana Di Polo[1,*]

[1]Department of Pathology and Cell Biology and Groupe de Recherche sur le Système Nerveux Central (GRSNC), Université de Montréal, Montreal, Quebec, Canada; [2]Department of Pharmacology, Dalhousie University, Halifax, Nova Scotia, Canada; [3]School of Optometry, Université de Montréal, Montreal, Quebec, Canada.

***Corresponding Author:** **Adriana Di Polo, Ph.D.**

Department of Pathology and Cell Biology
Université de Montréal
2900, Boulevard Edouard-Montpetit
Pavillon Roger-Gaudry, Room N-535
Montreal, Quebec H3T 1J4, Canada
Phone: (514) 343-6109
Fax: (514) 343-5755

III.1. ABSTRACT

The relationship between neuronal and vasculature degeneration in glaucoma is not well understood. We previously demonstrated that the acetylcholinesterase inhibitor galantamine protects retinal ganglion cells (RGCs) in experimental glaucoma. Here, we asked whether galantamine-induced neuroprotection correlates with changes in the retinal microvasculature and blood flow. The retinal microvasculature density was quantified using isolectin, and the regional ocular blood flow was assessed by quantitative autoradiography using N-isopropyl-p-^{14}C-iodoamphetamine ([^{14}C]-IMP). *Ex vivo* experiments were carried out on isolated retinal arterioles. RGC death was accompanied by a dramatic reduction in the density of the retinal microvasculature and blood flow. Galantamine-mediated protection of RGCs correlated with the preservation of retinal capillaries at 5 weeks of OHT. Furthermore, vasculature protection correlated with marked restoration of blood flow in glaucomatous eyes compared to control eyes. Consistent with an increase in blood flow, galantamine induced vasodilation in isolated retinal arterioles pre-constricted with endothelin-1 in an endothelial cells dependent manner. Blockers of muscarinic ACh receptors (mAChRs) inhibited the neuro- and vaso-protective effects of galantamine. Our study supports a tight relationship between neuronal and vascular preservation in experimental glaucoma. We also demonstrate a role for galantamine in RGC and vascular protection mediated by mAChRs activation.

Keywords: glaucoma, retinal microvasculature, inner retinal capillaries, retinal blood flow, retinal ganglion cells, isolated retinal vessels, acetylcholinesterase, muscarinic.

III.2. INTRODUCTION

Glaucoma is the second cause of irreversible blindness worldwide (Resnikoff et al. 2004) and its incidence increases dramatically with age (Coleman & Miglior 2008). Loss of vision in glaucoma is caused by the selective death of retinal ganglion cells (RGCs) (Quigley 1999). The only modifiable risk factor in the development of glaucoma is high intraocular pressure (IOP), thus current standard therapies rely solely on lowering IOP by medication or surgery. A significant proportion of patients, however, continue to experience visual loss despite responding well to treatments that lower eye pressure. In addition, >30% of glaucoma patients show optic nerve degeneration in the absence of high intraocular pressure, also known as normal (or low) tension glaucoma (NTG) (Nemesure et al. 2007). Therefore, a pressing medical need exists to identify underlying molecular mechanisms contributing to RGC death and to develop effective neuroprotective therapies to prevent vision loss in glaucoma.

It has been proposed that deregulations of the vascular system may contribute to glaucoma onset and progression (Tielsch et al. 1995). Insufficient retinal blood flow in NTG patients has been correlated with visual field loss suggesting a role for vascular dysfunction in glaucoma (Chung et al. 1999, Harris et al. 1994). Capillary deficits have been observed in glaucoma patients including slower arteriovenous passage time within the retinal vasculature (Kaiser et al. 1997, Duijm et al. 1997, Wolf et al. 1993). Both NTG and primary open angle glaucoma (POAG) individuals have high rates of capillary non-perfusion in the optic disc (Plange et al. 2006) suggesting that the microvasculature undergoes pathological changes during glaucomatous damage. RGCs are in close contact with capillaries and depend on the retinal microvasculature for metabolic support and nutrition. Conversely, RGCs provide growth factors including angiopoietins and vascular endothelial growth factor (VEGF) that stimulate vessel growth and endothelial cell survival (Sapieha et al. 2008, Hata et al. 1995). In spite of this, a clear correlation between vascular deficiency and RGC death in glaucoma has not been established.

In this study, we asked whether there is a loss of retinal capillaries in experimental glaucoma and, if so, whether it occurs early in the disease. We also sought to determine whether capillary loss occurred prior, concomitantly or after RGC death.

Finally, we asked if neuroprotective strategies that promote RGC survival would also lead to vascular protection.

III.3. MATERIAL AND METHODS

III.3.1. Experimental animals

Male Brown Norway rats, 10-12 months old (Charles River Canada, 300-400 g) were used for ocular hypertension (OHT) surgery, retinal microvasculature isolation and blood flow experiments. All procedures were performed in compliance with the Canadian Council on Animal Care for the use of experimental animals and the guidelines of the Association for Research in Vision and Ophthalmology. The number of animals used in each experiment is indicated above the bar in the corresponding graph.

III.3.2. Retrograde labeling of RGCs

RGCs were retrogradely labeled with DiI (1,1'-dioctadecyl-3,3,3',3'-tetramethyl-indocarbocyanine perchlorate; Molecular Probes, Junction City, OR) or with Fluorogold (2%, Fluorochrome, Englewood, CO). DiI crystals (3%) or Fluorogold (2%) were dissolved in 0.9% NaCl containing 10% dimethyl sulfoxide (DMSO) and 0.5% Triton X-100. The superior colliculus was exposed and a small piece of gelfoam (Pharmacia and Upjohn Inc., Mississauga, ON) soaked in tracer was applied to the surface as previously described (Almasieh et al. 2010). Seven days after tracer application, the time required for labeling the entire RGC population, animals were subjected to ocular hypertension surgery.

III.3.3. Ocular hypertension surgery and measurement of intraocular pressure

Unilateral elevation of IOP was induced as previously described (Morrison et al. 1997) by a single injection of a hypertonic saline solution (1.85 M NaCl) into an episcleral vein. Animals were kept in a room with constant low fluorescent light (40-100 lux) to stabilize circadian IOP variations. IOP from glaucomatous and normal eyes was measured in awake animals because general anesthetics lower IOP (Jia et al. 2000). A calibrated tonometer (TonoPen XL, Medtronic Solan, Jacksonville, FL) was used to measure IOP after application of one drop of proparacaine hydrochloride (0.5%, Alcon

Laboratories, Inc., Fort Worth, TX) per eye. The tonometer was held exactly perpendicular to the corneal surface and ~10 consecutive readings per eye were taken and averaged to obtain an accurate IOP measurement. IOP was measured daily for two weeks after ocular hypertension surgery, then every other day for the entire duration of the experiment. The mean and peak (maximum) IOP for each eye were calculated and these values were used to estimate the mean and peak IOP for experimental and control groups.

III.3.4. *In vivo* drug delivery

Galantamine hydrobromide (3.5 mg/kg, Tocris Bioscience, Ellisville, MO) and scopolamine hydrobromide (1 mg/kg, Tocris Bioscience, Ellisville, MO), both of which readily cross the blood-brain barrier, were delivered by daily intraperitoneal (i.p.) injection. Drug delivery started immediately after IOP stabilization following ocular hypertension surgery and continued for the entire duration of the experiment. Control animals received daily i.p. injections of vehicle (PBS). In some experiments, galantamine (100 mM), mecamylamine (10 mM, Sigma-Aldrich, St. Louis, MO) or scopolamine (10 mM, Tocris Bioscience, Ellisville, MO) were injected intraocularly in a total volume of 5 µl. For intraocular delivery, drugs were injected into the vitreous chamber using a 10-µl Hamilton syringe adapted with a 32-gauge glass microneedle, the tip of which was inserted into the superior hemisphere of the eye at a ~45° angle through the sclera into the vitreous body. This route of administration avoided retinal detachment or injury to eye structures, including the iris and lens. Surgical glue (Indermill, Tyco Health Care, Mansfield, MA) was used to seal the injection site.

III.3.5. Quantification of RGC soma

For RGC density counts, rats were deeply anesthetized and perfused transcardially with 4% paraformaldehyde (PFA) in 0.1 M phosphate buffer. Eyes were quickly enucleated and retinas were dissected out and flat-mounted on a glass slide with the ganglion cell layer side up. RGCs were counted in three square areas at distances of 1, 2 and 3 mm from the optic disc in each of the four retinal quadrants (superior, inferior, nasal and temporal) for a total of 12 retinal areas encompassing a total area of 1 mm^2. Macrophages and microglia that may have incorporated fluorescent tracer after phagocytosis of dying RGCs were excluded from our quantitative analysis based on cell-

specific markers and morphology (Lebrun-Julien et al. 2009). Data analysis and statistics were performed using the GraphPad Instat software (GraphPad Software Inc., San Diego, CA) by a one-way analysis of variance (ANOVA) test followed by Bonferroni's multiple comparison post-test.

III.3.6. Isolectin staining

Dissected retinas were placed in a 24-well plate, washed twice with PBS and then permeabilized with 100% ice cold methanol for 10 minutes. TRITC-labeled isolectin antibody (4µg/ml Sigma-Aldrich, St. Louis, MO) was prepared in PBS containing 1% Triton X-100 and incubated at room temperature overnight. Retinas were flat-mounted on a glass slide with the ganglion cell layer side up and visualized using a Zeiss Axiovert fluorescent microscope. The total length of the retinal microvasculature was measured per mm^2 of retinal surface using Northern Eclipse image analysis software (Empix Imaging, Toronto, ON).

III.3.7. Quantitative autoradiography

Retinal blood flow measurements were performed by quantitative autoradiography using the diffusible blood flow tracer N-isopropyl-p-[^{14}C]-iodoamphetamine ([^{14}C]-IMP) as previously described (Pouliot et al. 2009). Briefly, [^{14}C]-IMP (100 µCi/kg; PerkinElmer, Boston, MA,) was dissolved in saline solution and infused through a femoral vein catheter over a 30 sec period at a constant rate of 1.2 ml/min. Arterial blood samples were collected from the femoral artery catheter at a continuous rate until animal was sacrificed (2 min after [^{14}C]-IMP infusion onset). The eyes were quickly removed and post-fixed in 4% PFA for 1 hr. The retinas were dissected out, flat-mounted on a glass slide with the ganglion cell layer side up and exposed to X-ray film for 4 days alongside [^{14}C] standards (ARC, St. Louis, MO). Retinal blood flow was calculated by implementing the principle of indicator-fractionation technique using the equations $F= [C_{IMP} (T) \times 10^{-1} / \int_0^T Ca\ (t)\ ]$ for autoradiographic analysis of flat-mount retinas as previously described (Pouliot et al. 2011, Pouliot et al. 2009, Lear et al. 1982). F represents the blood flow (ml/100 g/min), C_{IMP} (T) is the radioactivity measured from the autoradiogram (µCi/g) at the time T (min) after sampling and Ca (t) is arterial blood sample radioactivity (µCi/ml). To obtain C_{IMP}(T) values, a computerized image analysis

system (MCID Basic Software, v7.0, Interfocus Imaging, Linton, England) was used to collect readings from a 0.8 mm^2 circular area acquired at 1, 2 and 3 mm (isopters) from the optic nerve in each eye quadrant (Pouliot et al. 2009). The Ca (t) value was obtained by measuring radioactivity in the collected blood samples using a scintillation counter (LS6500, Beckman Coulter, Mississauga, ON).

III.3.8. Retinal arteriole isolation and vessel diameter measurements

Following transcardial perfusion with heparin (16 u/ml, Sigma-Aldrich, St. Louis, MO), the retinas were dissected out and placed in a low Mg^{2+}/low Ca^{2+} dissociation buffer. Each retina was cut into small pieces with surgical scissors and triturated gently with a fire-polished pipette. Dissociated retinal tissue containing retinal vessel segments were plated onto laminin-coated dishes and allowed to adhere for 15 min before superfusion with bath solution (145 NaCl, 5 KCl, 10 HEPES, 5 D-Glucose, 2 mM $CaCl_2$, 1 mM $MgCl_2$, pH 7.3). Isolated retinal arterioles were identified under an inverted light microscope and vessel diameter was recorded at 120 Hz with a video edge detector (Crescent Electronics, Sandy, UT). Human endothelin-1 (ET-1, 10 nM, Peptide Institute Inc., OSAKA, Japan), galantamine hydrobromide (Gal, 50 μM, Tocris Bioscience, Ellisville, MO), scopolamine hydrobromide (SCO, 10 μM, Tocris Bioscience, Ellisville, MO), mecamylamine hydrochloride (MMA, 10 μM, Sigma-Aldrich, St. Louis, MO), pirenzepine dihydrochloride (PRZ, 1 μM, Tocris Bioscience, Ellisville, MO), diphenylacetoxy-N-methylpiperidine methiodide (4-DAMP, 1 μM, Tocris Bioscience, Ellisville, MO), tropicamide (1-10 μM, Tocris Bioscience, Ellisville, MO) or 11-[[2-[(Diethylamino)methyl]-1-piperidinyl]acetyl]-5,11-dihydro-6H-pyrido [2,3-b] [1,4] benzo-diazepin-6-one (DX116, 1-10 μM, Tocris Bioscience, Ellisville, MO) were applied to isolated retinal vessels using a rapid solution switcher device that allowed the application of drugs at 37^{o}C. Vessels were superfused with bath solution for 10 min followed by application of 10 nM ET-1 until a stable contraction was obtained (1- 2 min) after which vessel diameter was recorded for an additional 10 min. Some experiments were conducted on vessels denuded of endothelium by application of CHAPS (0.3%, Sigma-Aldrich St. Louis, MO) at the time of perfusion Digital photomicrographs of vessels were captured with an Infinity 3-1C digital camera (Lumenera Corp.) mounted on

a Nikon Eclipse E800 microscope, and analyzed with Infinity Analyze (Lumenera Corp.) and Adobe Photoshop CS3 (Adobe Systems, Inc., San Jose, CA). Data were analyzed using two-tailed unpaired t-tests and one-way analyses of variance (ANOVA) with a Newman-Keuls *post hoc* test.

III.4. RESULTS

III.4.1. Loss of the retinal microvasculature occurs concomitantly with RGC death in experimental glaucoma

Nerve fiber layer capillaries play crucial physiological roles by supplying oxygen and nutrients to RGCs and their axons. We sought to determine whether there is loss of inner retinal capillaries in experimental glaucoma and, if so, whether this damage occurs prior, concurrently or after RGC death. To achieve this, we carried out a detailed temporal analysis of glaucomatous retinas in which we simultaneously visualized retinal capillaries using TRITC-labeled isolectin, a marker of functional endothelial cells (Laitinen 1987; Goldstein et al., 1981), while identifying RGCs with the fluorescent retrograde tracer DiI (Figure 1).

Quantification of the retinal microvascular density at three days after OHT surgery, a time when there is no detectable increase in IOP, revealed a small (~10%) but significant reduction in capillary density (17,837 ± 410 $\mu m/mm^2$, n=6) compared to non-injured retinas (19,710 ± 594 $\mu m/mm^2$, n=6) (Figure 1A, 1B, 1M). In these same retinas, a significant reduction in the density of RGC soma (1,646 ± 31 RGCs/mm^2, n=6) compared to control retinas (1,803 ± 24 RGCs/mm^2, n=6) was also found, confirming that degenerative changes occur in both neuronal and vascular compartments early after glaucomatous damage and prior to a detectable increase in IOP (Fig 1G, 1H, 1M). Weekly analysis of retinal capillary density throughout the entire duration of the study (up to 5 weeks after OHT) demonstrated a steady loss of the microvasculature that occurred concomitantly with RGC death (Fig. 1C-F, 1I-L, 1M). These data indicate a tight neurovascular relationship between RGCs and retinal capillaries, and demonstrate that both neurons and the microvasculature are similarly affected in experimental glaucoma.

III.4.2. Galantamine mediates vasoprotection in experimental glaucoma

The observation that RGC death occurs concomitantly with microvasculature loss puts forward the idea that protective therapies for glaucoma should ideally target both the neuronal and the vascular compartments. We previously demonstrated that galantamine, a small molecule acetylcholinesterase (AChE) inhibitor, promotes robust structural and functional protection of RGC soma and axons (Almasieh et al., 2010). To establish whether galantamine had a vasoprotective effect, we examined capillary density in experimental animals subjected to OHT surgery followed by daily intraperitoneal injection of galantamine (treatment onset: ~1 week after OHT) (Fig. 2). Galantamine treatment resulted in robust preservation of capillary density at three weeks (~80%: 15,423 ± 290 μm/mm^2, n=4) and five weeks (~40%: 13,986 ± 602 μm/mm^2, n=5) after OHT, compared to PBS-treated control groups (3 weeks: 13,421 ± 685 μm/mm^2, n=5; 5 weeks: 7,901 ± 618 μm/mm^2, n=5). The vasoprotective effect of galantamine was most apparent at five weeks of OHT when considerable loss of retinal capillaries has already occurred in non-treated eyes. Importantly, galantamine treatment virtually prevented further retinal capillary degeneration between three and five weeks after OHT (Fig. 2E). These data demonstrate that in addition to neuroprotection, galantamine also confers robust vascular protection in experimental glaucoma.

III.4.3. Retinal blood flow impairment in experimental glaucoma is partially restored by galantamine

To assess the functional status of the microvascular network in glaucomatous versus control eyes and in the presence or absence of galantamine, we investigated regional blood flow using [^{14}C]-IMP as previously described by us (Pouliot et al., 2009) (Fig. 3). A significant reduction of retinal blood flow was observed in glaucomatous eyes, visualized in pseudo-colored autoradiograms, at five weeks after OHT compared to non-injured eyes (Figs. 3B, 3D). Galantamine treatment markedly restored retinal blood flow in experimental glaucoma (82% of intact) compared to PBS-treated control animals (50% of intact) (Figs 3C, 3D, 3E). To establish whether restoration of blood flow occurred locally or throughout the retina, regional blood flow was quantified in three consecutive isopters at 1, 2 and 3 mm from the optic nerve head (Fig. 3A, 3F, Table 1). In non-injured

retinas, higher blood perfusion was measured in central regions compared to the periphery (Fig. 3B, 3F). In experimental glaucoma, the central retina underwent the most dramatic reduction in blood flow at five week after OHT (Fig. 3D, 3F). Nonetheless, the galantamine-mediated restoration of blood flow was proportional in central and peripheral retinal regions (Fig. 3F, Table 1). Our data indicate that retinal blood flow is markedly reduced in experimental glaucoma, a response that is most prominent in the central retina. Treatment with galantamine not only significantly increased global retinal blood flow in hypertensive eyes, but it was particularly beneficial in central regions of the retina which undergo marked hypoperfusion during glaucomatous damage.

III.4.4. Galantamine stimulates retinal arteriole relaxation

To evaluate the mechanisms of galantamine-mediated vascular protection, we carried out studies on isolated retinal vessels pre-contracted with endothelin (ET-1). ET-1 treatment alone led to a stable reduction in vessel diameter (32% contraction), while application of galantamine promoted significant relaxation of pre-contracted vessels (Figure 4A-C). A concentration of galantamine as low as 5 μM was sufficient to promote vessel relaxation, however, the optimal relaxation-promoting dose of galantamine was 50 μM leading to maximum relaxation and increased the diameter of vessels by 50% (17% contraction). In a second group of experiments, we used isolated retinal arterioles in which endothelial cells were removed by application of CHAPS at the time of perfusion. Application of ET-1 resulted in a higher pre-contraction level (45% contraction) compared to vessel preparations with intact endothelial cells (Fig. 4C). Furthermore, addition of galantamine (50 μM) to pre-contracted vessels devoid of endothelium failed to undergo relaxation (Fig. 4C). Collectively, these data demonstrate that a moderate dose of galantamine effectively leads to vasodilation of pre-contracted retinal vessels *ex vivo*, and that galantamine-mediated relaxation requires the presence of endothelial cells.

III.4.5. Muscarinic acetylcholine receptors mediate the vasodilator and vasoprotective effects of galantamine in experimental glaucoma

We previously demonstrated that galantamine-mediated RGC protection in experimental glaucoma requires activation of muscarinic acetylcholine receptors (mAChRs) (Almasieh et al., 2010). To establish whether this mechanism played a role in

vasoprotection, we carried out experiments using isolated pre-contracted vessels exposed to galantamine alone or in combination with pharmacological inhibitors of mAchR. Combined application of galantamine and scopolamine (SCO), a pan-inhibitor of all mAChR sub-types, arrested its vasodilator effect on pre-contracted vessels (Fig. 4D). In contrast, combined application of galantamine with mecamylamine (MMA), a blocker of all neuronal nicotinic acetylcholine receptors (nAChRs), did not significantly alter galantamine-induced vasodilation (Fig. 4D). These results indicate that galantamine mediates retinal arteriole relaxation through mAChRs activation. To further establish which mAChR sub-type was involved in this response; we used selective mAChR antagonists co-administered with galantamine. Application of pirenzepine, a selective blocker of the M1 mAChR subtype, or 4-DAMP, an inhibitor of the M3 mAChR subtype, abolished galantamine-mediated relaxation of pre-contracted vessels (Fig. 4E). In contrast, tropicamide or DX116, blockers of M4 or M2 mAChRs respectively, did not have a significant effect on galantamine-induced vasodilation (not shown). These data indicate that M1 and M3 mAChRs are molecular mediators of the relaxation effect of galantamine on retinal vessels.

To assess whether mAChRs played a role in the microvasculature protection conferred by galantamine in experimental glaucoma *in vivo*, we tested the effect of galantamine in combination with MMA or SCO. Since these AChR antagonists do not cross the blood-brain/retinal barrier or exhibit extremely low barrier permeability (Mickala et al., 1996; Stein et al., 1995), they were administered by intravitreal injection at one week after OHT as previously described by us (Almasieh et al., 2010) and analysis of microvasculature density was performed two weeks later. Co-administration of galantamine and SCO completely inhibited the vasoprotective effect of galantamine. Although combination of galantamine and MMA led to a slight reduction in capillary density, this effect was not significantly different from that of galantamine alone (Fig. 4F). Thus, we conclude that the vasoprotective effect of galantamine *in vivo* is mediated primarily through activation of mAChRs in experimental glaucoma.

III.5. DISCUSSION

This study reports a number of important findings. First, we detected substantial loss of small capillaries in the inner retina early during glaucomatous degeneration. Second, we found that loss of retinal capillaries occurred concomitantly with the death of RGCs following OHT. The onset of microvasculature and RGC loss occurred at the same time and proceeded at the same rate for at least three weeks after the initial insult. Lastly, systemic administration of the neuroprotective drug galantamine increased microvasculature density and improved blood flow in experimental glaucoma. Galantamine-mediated protection of the retinal microvasculature occurred through activation of M1 and M3 mAChR subtypes.

Although retinal and ONH blood flow defects have been suggested to play a role in glaucoma (Flammer et al., 2002; Osborne et al., 2001), a clear correlation between neuronal and vascular compartments in this disease has not been established. Quantification of retinal capillary density demonstrated that retinal microvasculature loss occurs as early as three days after OHT surgery and continues to progress thereafter. Intriguingly, we did not detect a significant increase in IOP at this early time point as measured using a calibrated TonoPen, consistent with the gradual increase in IOP that occurs over 7-10 days reported in this rat glaucoma model (Morrison et al., 1997). A likely explanation is that a subtle increase in IOP, not detectable using conventional tonometry, is sufficient to trigger a cascade of events leading to capillary and RGC loss. Furthermore, an IOP increase below a detectable threshold can lead to small but significant changes in endogenous factors that threaten the integrity of the retinal vasculature including reactive oxygen species, tumor necrosis factor alpha (TNFα) and glutamate, triggering endothelial cell apoptosis. The identification of the endogenous signals leading to loss of retinal capillaries early after glaucomatous damage should be a priority of future studies.

Importantly, our data also demonstrate that the time-course of retinal capillary loss is indistinguishable from that of RGC death. Given the tight functional relationship between RGCs and the retinal microvasculature during disease onset and progression, we asked whether strategies that promote RGC neuroprotection can be used to sustain the retinal capillary bed and enhance blood flow. We previously demonstrated that

galantamine, an acetylcholinesterase inhibitor, promotes robust structural and functional RGC protection of RGCs in experimental glaucoma (Almasieh et al., 2010). In the present study, we show that galantamine treatment resulted in a substantial preservation of capillary density that correlated with increased retinal blood flow in the central and peripheral retina. Therefore, in addition to neuronal protection, galantamine has marked vasoprotective properties.

Due to the tight relationship between RGC and capillary loss in glaucoma, it is not clear whether galantamine first promotes the neuroprotection which then leads to vasoprotection or vice versa. To address the mechanism of action of galantamine-induced vasoprotection, we first used an ex vivo preparation of isolated retinal vessels. Our data show that galantamine superfusion led to marked relaxation of pre-contracted vessels, a response that was lost after removal of their endothelium with CHAPS. This finding suggests a direct effect of galantamine on retinal arteries that is dependent on the presence of healthy endothelial cells. Moreover, our results demonstrate that galantamine-mediated vessel relaxation in vitro and vasoprotection in experimental glaucoma in vivo occur primarily through mAChRs activation. We previously demonstrated that galantamine-induced RGC protection in experimental glaucoma also occurs via mAChRs, primarily the M1 and M4 subtypes (Almasieh et al. 2010). Here, we show that vasoprotection following galantamine administration involves M1 and M3 mAChR subtypes. Intriguingly, RGCs do not express mAChRs (Da Silva et al., 2008), whereas retinal and brain endothelial cells abundantly express M1 and M3 mAChR subtypes (Elhusseiny et al., 1999; Sastry, 1985). Both M1 and M3 mAChRs have been implicated in cholinergic mediated vasomodulation in the brain (Dauphin et al., 1994) and ACh-dependent vascular relaxation is lost in M3 mAChR knockout mice (Bény et al., 2008), thus supporting our finding that galantamine relaxes pre-contracted isolated retinal arterioles via M1 and M3 mAChRs. Since RGCs lack mAChR while endothelial cells can directly respond to galantamine, it is tempting to speculate that vasoprotection is a pre-requisite for galantamine-mediated neuroprotection in experimental glaucoma. However, we cannot rule out the contribution of other retinal cells expressing M1, M3 or M4 mAChRs, including Müller glia, bipolar and horizontal cells (Da Silva et al., 2008; Fischer et al., 1998; Yamada et al., 2003). Indeed, activation of retinal M1 and M3

mAChRs subtypes stimulates nNOS levels and activity leading to vasodilation (Borda et al., 2005), thus activation of mAChRs in retinal cells other than endothelial might help restore retinal blood flow in experimental glaucoma.

In summary, in this study we demonstrate an early and significant loss of the retinal microvasculature intimately associated with RGC death in experimental glaucoma. We demonstrated that a clinically approved drug, galantamine, promotes effective vasoprotection and restores retinal blood flow following ocular hypertension damage. These findings are particularly important for the treatment of glaucomatous neuropathies because while RGC death is irreversible, the retinal microvasculature retains the capacity to regenerate. Therefore, therapeutic strategies based on vascular protection and vessel regeneration may provide essential, long-term support to neurons and improve visual outcome in glaucoma.

Acknowledgements: We thank Jessica McIntyre and Dara O'connor for their collaboration and technical assistance.

III.6. REFERENCES

Almasieh, M., Zhou, Y., Kelly, M.E., Casanova, C., Di Polo, A., 2010. Structural and functional neuroprotection in glaucoma: role of galantamine-mediated activation of muscarinic acetylcholine receptors. Cell Death Dis 1, e27-e27.

Bény, J.-L., Nguyen, M., Marino, M., Matsui, M., 2008. Muscarinic receptor knockout mice confirm involvement of M3 receptor in endothelium-dependent vasodilatation in mouse arteries. J Cardiovasc Pharmacol 51, 505-512.

Borda, E., Berra, A., Saravia, M., Ganzinelli, S., Sterin Borda, L., 2005. Correlations between neuronal nitric oxide synthase and muscarinic M3/M1 receptors in the rat retina. Exp Eye Res 80, 391-399.

Chung, H.S., Harris, A., Kagemann, L., Martin, B., 1999. Peripapillary retinal blood flow in normal tension glaucoma. Br J Ophthalmol 83, 466-469.

Coleman, A.L., Miglior, S., 2008. Risk Factors for Glaucoma Onset and Progression. Surv Ophthalmol 53, S3-S10.

Da Silva, N., Herron, C., Stevens, K., Jollimore, C.A.B., Barnes, S., Kelly, M.E.M., 2008. Metabotropic receptor-activated calcium increases and store-operated calcium influx in mouse Müller cells. Invest Ophthalmol Vis Sci 49, 3065-3073.

Dauphin, F., Linville, D.G., Hamel, E., 1994. Cholinergic dilatation and constriction of feline cerebral blood vessels are mediated by stimulation of phosphoinositide

metabolism via two different muscarinic receptor subtypes. J Neurochem 63, 544-551.

Duijm, H.F., van den Berg, T.J., Greve, E.L., 1997. A comparison of retinal and choroidal hemodynamics in patients with primary open-angle glaucoma and normal-pressure glaucoma. Am J Ophthalmol 123, 644-656.

Elhusseiny, A., Cohen, Z., Olivier, A., Stanimirović, D.B., Hamel, E., 1999. Functional acetylcholine muscarinic receptor subtypes in human brain microcirculation: identification and cellular localization. J Cereb Blood Flow Metab 19, 794-802.

Fischer, A.J., McKinnon, L.A., Nathanson, N.M., Stell, W.K., 1998. Identification and localization of muscarinic acetylcholine receptors in the ocular tissues of the chick. J Comp Neurol 392, 273-284.

Flammer, J., Orgül, S., Costa, V.P., Orzalesi, N., Krieglstein, G.K., Serra, L.M., Renard, J.-P., Stefánsson, E., 2002. The impact of ocular blood flow in glaucoma. Prog Retin Eye Res 21, 359-393.

Goldstein, I.J., Blake, D.A., Ebisu, S., Williams, T.J., Murphy, L.A., 1981. Carbohydrate binding studies on the Bandeiraea simplicifolia I isolectins. Lectins which are mono-, di-, tri-, and tetravalent for N-acetyl-D-galactosamine. J Biol Chem 256, 3890-3893.

Harris, A., Sergott, R.C., Spaeth, G.L., Katz, J.L., Shoemaker, J.A., Martin, B.J., 1994. Color Doppler analysis of ocular vessel blood velocity in normal-tension glaucoma. Am J Ophthalmol 118, 642-649.

Hata, Y., Nakagawa, K., Ishibashi, T., Inomata, H., Ueno, H., Sueishi, K., 1995. Hypoxia-induced expression of vascular endothelial growth factor by retinal glial cells promotes in vitro angiogenesis. Virchows Archiv 426, 479-486.

Jia, L., Cepurna, W.O., Johnson, E.C., Morrison, J.C., 2000. Effect of general anesthetics on IOP in rats with experimental aqueous outflow obstruction. Invest. Ophthalmol. Vis. Sci. 41, 3415-3419.

Kaiser, H.J., Schoetzau, A., Stmpfig, D., Flammer, J., 1997. Blood-flow velocities of the extraocular vessels in patients with high-tension and normal-tension primary open-angle glaucoma. Am J Ophthalmol 123, 320-327.

Laitinen, L., 1987. Griffonia simplicifolia lectins bind specifically to endothelial cells and some epithelial cells in mouse tissues. Histochem J 19, 225-234.

Lear, J.L., Ackermann, R.F., Kameyama, M., Kuhl, D.E., 1982. Evaluation of [123I] isopropyliodoamphetamine as a tracer for local cerebral blood flow using direct autoradiographic comparison. J Cereb Blood Flow Metab 2, 179-185.

Lebrun-Julien, F., Duplan, L., Pernet, V., Osswald, I.K., Sapieha, P., Bourgeois, P., Dickson, K., Bowie, D., Barker, P.A., Di Polo, A., 2009. Excitotoxic death of retinal neurons in vivo occurs via a non-cell-autonomous mechanism. J. Neurosci. 29, 5536-5545.

Mickala, P., Boutin, H., Bellanger, C., Chevalier, C., MacKenzie, E.T., Dauphin, F., 1996. In vivo binding, pharmacokinetics and metabolism of the selective M2 muscarinic antagonist Nucl. Med. Biol. 23, 173-179.

Morrison, J.C., Moore, C.G., Deppmeier, L.M.H., Gold, B.G., Meshul, C.K., Johnson, E.C., 1997. A rat model of chronic pressure-induced optic nerve damage. Exp. Eye Res. 64, 85-96.

Nemesure, B., Honkanen, R., Hennis, A., Wu, S.Y., Leske, M.C., 2007. Incident open-angle glaucoma and intraocular pressure. Ophthalmology 114, 1810-1815.

Osborne, N.N., Melena, J., Chidlow, G., Wood, J.P., 2001. A hypothesis to explain ganglion cell death caused by vascular insults at the optic nerve head: possible implication for the treatment of glaucoma. Br J Ophthalmol 85, 1252-1259.

Plange, N., Kaup, M., Huber, K., Remky, A., Arend, O., 2006. Fluorescein filling defects of the optic nerve head in normal tension glaucoma, primary open-angle glaucoma, ocular hypertension and healthy controls. Ophthalmic Physiol Opt 26, 26-32.

Pouliot, M., Deschênes, M.C., Hétu, S., Chemtob, S., Lesk, M.R., Couture, R., Vaucher, E., 2009. Quantitative and regional measurement of retinal blood flow in rats using N-isopropyl-p-[14C]-iodoamphetamine ([14C]-IMP). Exp Eye Res 89, 960-966.

Pouliot, M., Hétu, S., Lahjouji, K., Couture, R., Vaucher, E., 2011. Modulation of retinal blood flow by kinin B1 receptor in Streptozotocin-diabetic rats. Exp Eye Res 92, 482-489.

Quigley, H.A., 1999. Neuronal death in glaucoma. Prog Retin Eye Res18, 39-57.

Resnikoff, S., Pascolini, D., Etya'ale, D., Kocur, I., Pararajasegaram, R., Pokharel, G., Mariotti, S., 2004. Global data on visual impairment in the year 2002. Bull World Health Organ 82, 844-851.

Sapieha, P., Sirinyan, M., Hamel, D., Zaniolo, K., Joyal, J.-S., Cho, J.-H., Honor, J.-C., Kermorvant Duchemin, E., Varma, D., Tremblay, S., Leduc, M., Rihakova, L., Hardy, P., Klein, W., Mu, X., Mamer, O., Lachapelle, P., Di Polo, A., Beausjour, C., Andelfinger, G., Mitchell, G., Sennlaub, F., Chemtob, S., 2008. The succinate receptor GPR91 in neurons has a major role in retinal angiogenesis. Nat Med 14, 1067-1076.

Sastry, B.V., 1985. Cholinergic systems and multiple cholinergic receptors in ocular tissues. J Ocul Pharmacol. 1, 201-226.

Stein, R., Bachoo, M., Polosa, C., 1995. Pirenzepine-sensitive component of forelimb vascular resistance and heart rate in cats. J. Autonom. Nerv. Syst. 54, 49-58.

Tielsch, J.M., Katz, J., Sommer, A., Quigley, H.A., Javitt, J.C., 1995. Hypertension, perfusion pressure, and primary open-angle glaucoma. A population-based assessment. Arch Ophthalmol 113, 216-221.

Wolf, S., Arend, O., Sponsel, W.E., Schulte, K., Cantor, L.B., Reim, M., 1993. Retinal hemodynamics using scanning laser ophthalmoscopy and hemorheology in chronic open-angle glaucoma. Ophthalmology 100, 1561-1566.

Yamada, E., Dmitrieva, N., Keyser, K., Lindstrom, J., Hersh, L., Marshak, D., 2003. Synaptic connections of starburst amacrine cells and localization of acetylcholine receptors in primate retinas. J Comp Neurol 461, 76-90.

Figure 1. Loss of inner retinal capillaries along with RGCs in experimental glaucoma.

Retinal flat-mounts show isolectin-labeled retinal capillaries from non-injured, non-treated eye (A, Intact) and glaucomatous non-treated eyes (B-F) and DiI-labeled retinal ganglion cells from non-injured, non-treated eyes (G, Intact) and glaucomatous non-treated eyes (H-L); Scale bars: 100 μm. (M) Quantitative analysis of capillary length in the nerve fiber layer of retinas from glaucomatous eyes; retinas were examined at 3 days, 1, 2, 3, and 5 weeks after OHT surgery, the average total values for each group (hatched bars) is presented as percentage of capillary density value for non-injured, non-treated retinas from Brown-Norway rat retinas (19710 ± 594 $\mu m/mm^2$, mean ± S.E.M., n = 6). Quantitative analysis of RGC survival also was examined in the same retinas (solid bars) and results are presented as percentage of the average total RGC population in non-injured, non-treated retinas from Brown-Norway rat retinas (1830 ± 24 $RGCs/mm^2$, mean ± S.E.M., n = 6) (M). Number of animals in each group is indicated above the related bar.

Figure 2. Galantamine protects inner retinal capillaries in experimental glaucoma. Isolectin-labeled retinal vasculatures in flat-mount preparation of glaucomatous retinas demonstrating galantamine treated (3.5 mg/kg, i.p.) (A, 3 weeks and C, 5 weeks) and vehicle (PBS) treated groups (B, 3 weeks and D, 5 weeks). (E) Quantitative analysis of capillary length after OHT indicates significant preservation of inner retinal capillaries in galantamine treated groups (solid bars) compare to vehicle treated (hatched bars). Data are expressed as $\mu m/mm^2 \pm$ S.E.M and number of animals in each group is indicated above the related bar (ANOVA, $^{**}p < 0.01$). Scale bars (A-D): 100 μm.

Figure 3. Galantamine-mediated improvement of the retinal blood flow in glaucomatous retinas.

(A) Schematic of a flat-mounted retina representing method of sampling; filled circles indicate standard sampling probe and light circular lines show same isopters of different retinal quadrants. (B) Pseudo-colored autoradiogram of a flat-mounted intact retina, (C) galantamine treated and (D) vehicle treated retinas 5 weeks after OHT surgery. (E) Measurements of blood flow values indicated a significant decline of global retinal blood flow in glaucomatous retinas 5 weeks after OHT (hatched bar), galantamine significantly improved global retinal blood flow in glaucomatous retinas (solid bar). (F) Reduction in the blood flow was also reflected in each isopter (hatched bars) and was significantly improved by galantamine treatment (solid bars) compare to vehicle treated. Data are expressed as ml/100 g/min ± S.E.M and number of animals in each group is indicated above the related bar (ANOVA, $*p < 0.05$).

Figure 4. Galantamine mediates vasodilation and vasoprotection via signaling through muscarinic acetylcholine receptors.

(A) Contraction of isolated retinal vessels in response to incubation with Endothelin-1. (B) Application of galantamine to pre-contracted vessels resulted in relaxation and increase of their diameter. (C) Quantitative analysis indicated that presence of endothelial cells is necessary for vasodilatory effect of galantamine; as denudation of endothelium by CHAPS eliminates the galantamine-mediated relaxation. (D) Muscarinic ACh receptors blocker, scopolamine (SCO), abolished vasodilatory effect of galantamine whereas nicotinic blocker, Mecamylamine (MMA) did not have significant effect on inhibition of galantamine mediated relaxation. (E) Galantamine-mediated vasorelaxation was selectively inhibited by blockers of M1 (Pirenzepine, PRZ) and M3 (4-DAMP) subtypes of muscarinic receptors. (A-E) Data is presented as percentage of vessels diameter before application of Endothelin-1. (F) Intraocular application of muscarinic receptor inhibitor (SCO) abolished galantamine-mediated protection of inner retinal capillaries; data are expressed as $\mu m/mm^2 \pm$ S.E.M and number of animals in each group is indicated above the related bar (ANOVA, $*p < 0.05$).

III.7. TABLES

Table 1. Autoradiography values of the blood flow for each retinal isopter.

	Control	Galantamine	Vehicle
Nasal			
1 mm	**129 ± 17**	**109 ± 10**	**67 ± 23**
2 mm	**111 ± 16**	**100 ± 18**	**64 ± 22**
3 mm	**97 ± 6**	**86 ± 11**	**54 ± 20**
Temporal			
1 mm	**132 ± 13**	**116 ± 15**	**67 ± 16**
2 mm	**110 ± 15**	**97 ± 9**	**59 ± 21**
3 mm	**94 ± 11**	**86 ± 13**	**49 ± 11**
Superior			
1 mm	**121 ± 20**	**108 ± 7**	**58 ± 9**
2 mm	**114 ± 18**	**89 ± 12**	**55 ± 11**
3 mm	**90 ± 15**	**81 ± 9**	**47 ± 6**
Inferior			
1 mm	**119 ± 9**	**106 ± 11**	**68 ± 8**
2 mm	**113 ± 13**	**99 ± 12**	**53 ± 6**
3 mm	**93 ± 20**	**86 ± 15**	**44 ± 7**

Values are means ± SD and are expressed in ml/100 g/min. All the groups including control, galantamine and vehicle treated consisted of n=4 animals.

III.8. FIGURES

FIGURE 1

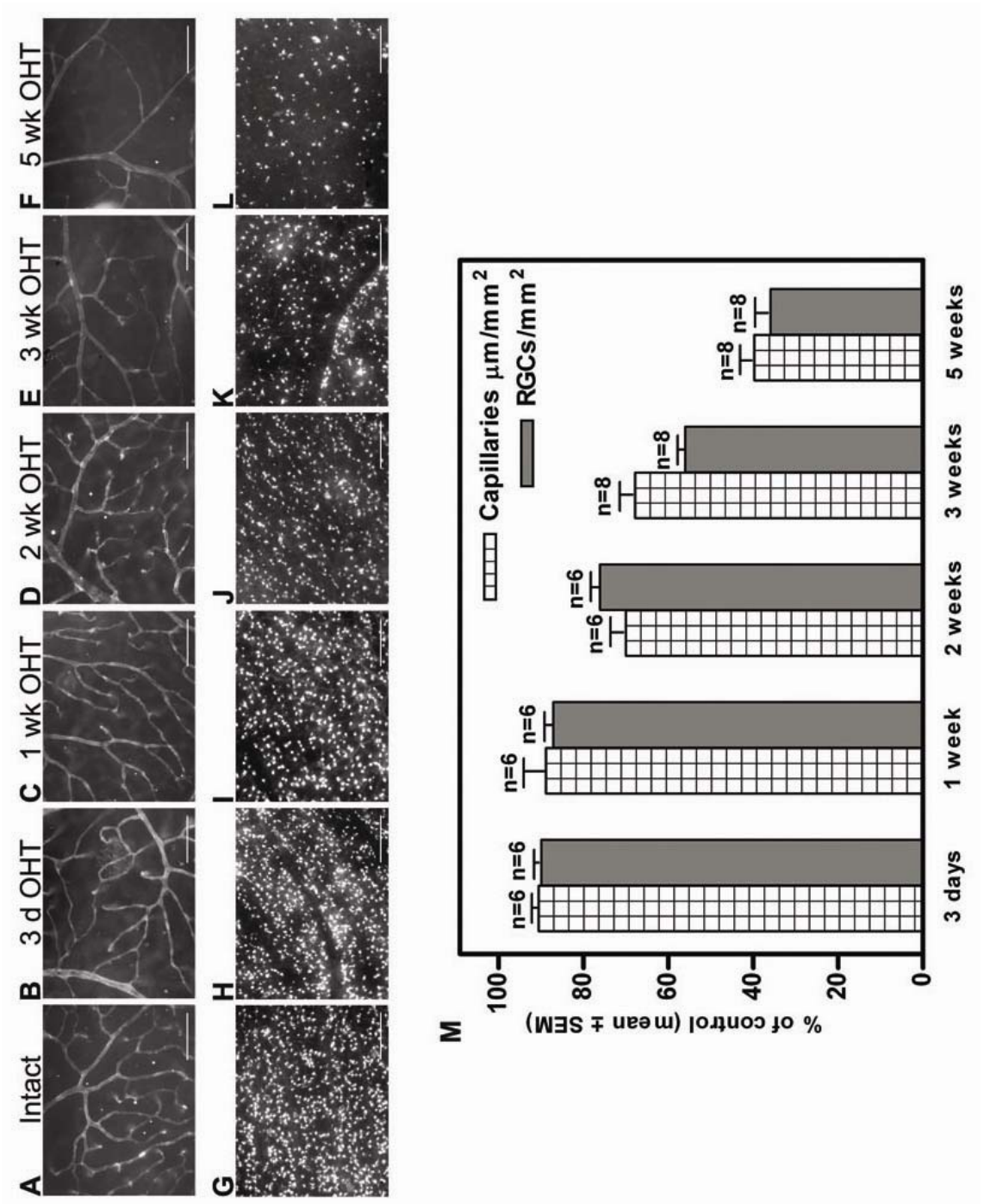

FIGURE 2

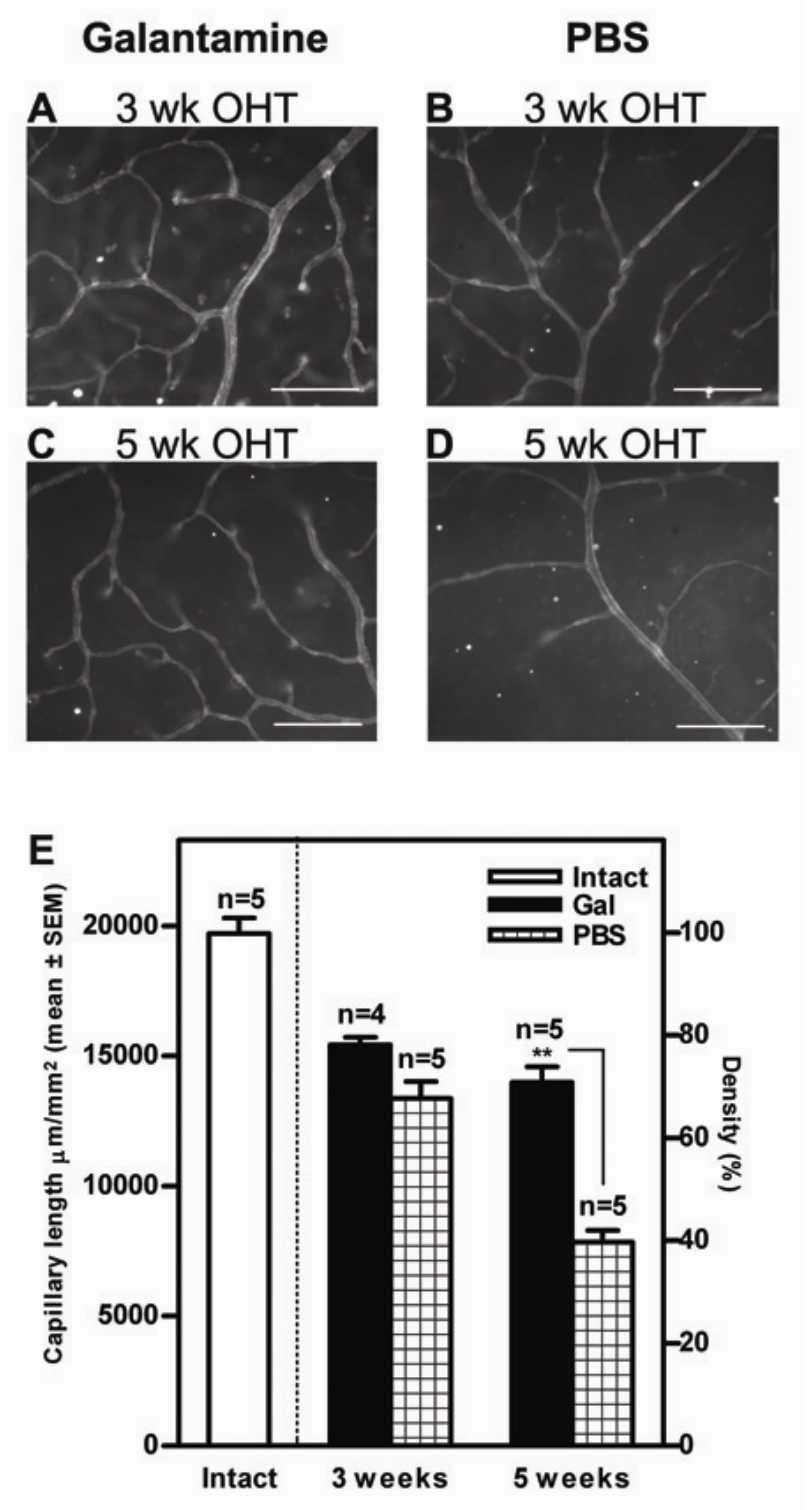
Galantamine
PBS
A 3 wk OHT
B 3 wk OHT
C 5 wk OHT
D 5 wk OHT
E
Capillary length µm/mm² (mean ± SEM)
Density (%)
Intact
Gal
PBS
n=5
n=4
n=5
n=5
**
n=5
20000
15000
10000
5000
0
100
80
60
40
20
0
Intact
3 weeks
5 weeks

FIGURE 3

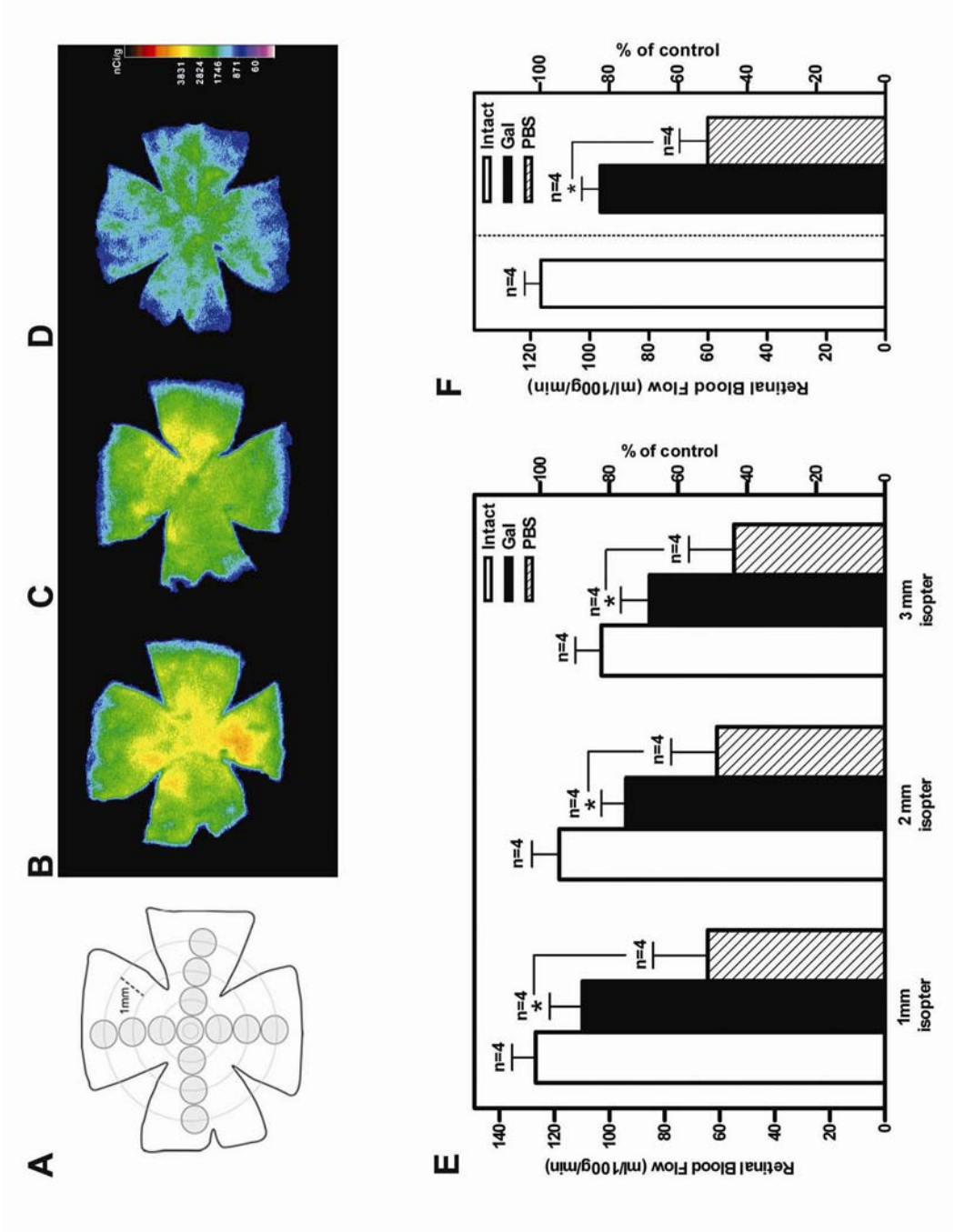
A
B
C
D
nCi/g
3831
2824
1746
871
60
1mm
E
Retinal Blood Flow (ml/100g/min)
% of control
Intact
Gal
PBS
n=4
*
1mm isopter
2 mm isopter
3 mm isopter
F
Retinal Blood Flow (ml/100g/min)
% of control

FIGURE 4

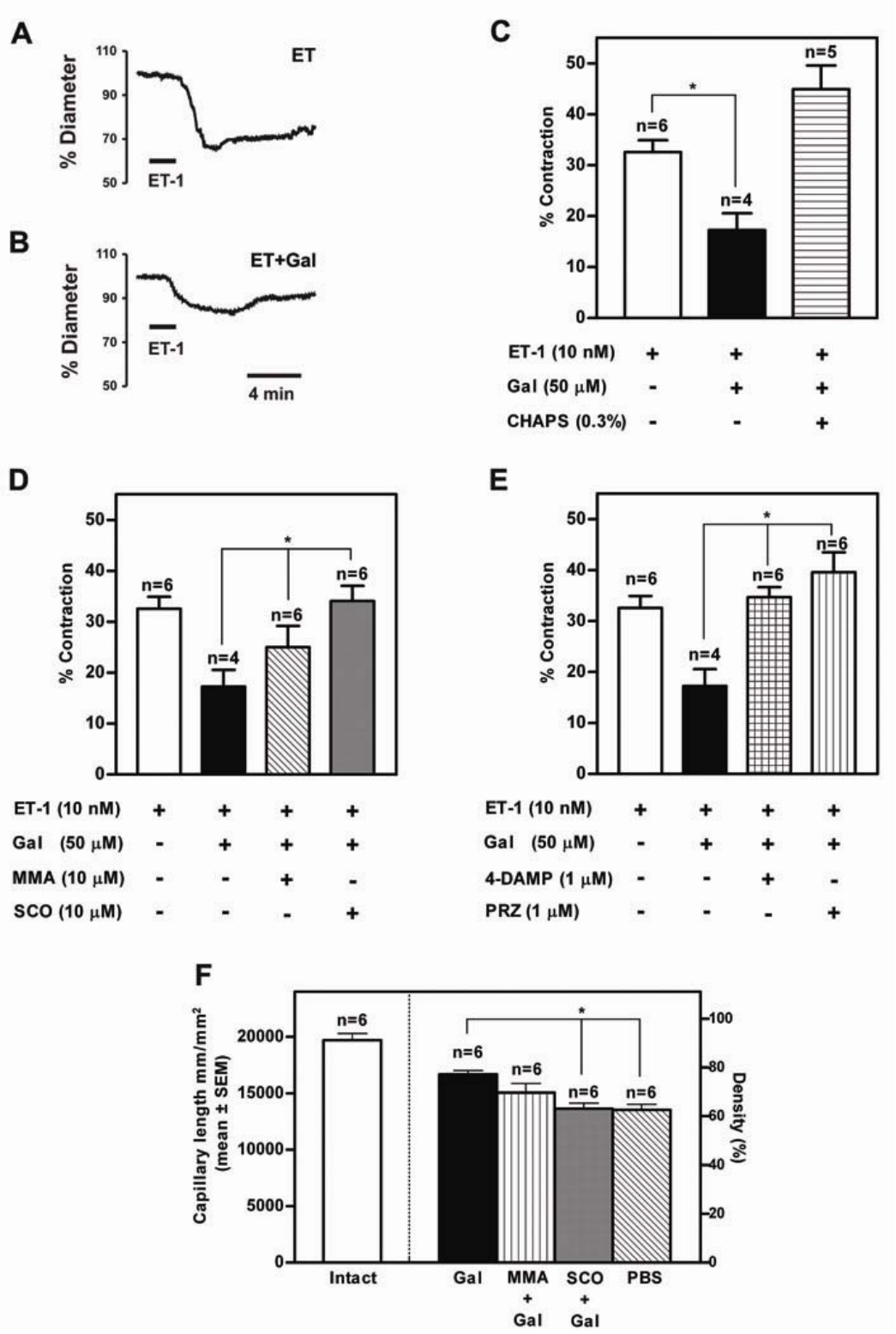
A
ET
% Diameter
110
90
70
50
ET-1
B
ET+Gal
% Diameter
ET-1
4 min
C
% Contraction
n=6
n=4
n=5
*
ET-1 (10 nM) + + +
Gal (50 μM) - + +
CHAPS (0.3%) - - +
D
% Contraction
n=6
n=4
n=6
n=6
*
ET-1 (10 nM) + + + +
Gal (50 μM) - + + +
MMA (10 μM) - - + -
SCO (10 μM) - - - +
E
% Contraction
n=6
n=4
n=6
n=6
*
ET-1 (10 nM) + + + +
Gal (50 μM) - + + +
4-DAMP (1 μM) - - + -
PRZ (1 μM) - - - +
F
Capillary length mm/mm² (mean ± SEM)
Density (%)
n=6
n=6
n=6
n=6
n=6
*
Intact
Gal
MMA + Gal
SCO + Gal
PBS

CHAPTER 4

IV. THIRD ARTICLE: "A CELL-PERMEABLE PHOSPHINE-BORANE COMPLEX DELAYS RETINAL GANGLION CELL DEATH AFTER AXONAL INJURY THROUGH ACTIVATION OF THE PRO-SURVIVAL EXTRACELLULAR SIGNAL-REGULATED KINASES 1/2 PATHWAY".

Journal of Neurochemistry, 2011, 118 (6): 1075-86.

A CELL-PERMEABLE PHOSPHINE-BORANE COMPLEX DELAYS RETINAL GANGLION CELL DEATH AFTER AXONAL INJURY THROUGH ACTIVATION OF THE PRO-SURVIVAL EXTRACELLULAR SIGNAL-REGULATED KINASES 1/2 PATHWAY.

Mohammadali Almasieh[1], Christopher J. Lieven[2], Leonard A. Levin[2, 3, *], and Adriana Di Polo[1, 3, *]

[1]Department of Pathology and Cell Biology and Groupe de Recherche sur le Système Nerveux Central (GRSNC), University of Montreal; [2]Department of Ophthalmology and Visual Sciences, University of Wisconsin School of Medicine and Public Health, Madison, Wisconsin, USA; and [3]Maisonneuve-Rosemont Research Center and Department of Ophthalmology, University of Montreal, Montreal, Quebec, Canada.

***Correspondence to:** **Adriana Di Polo**
Department of Pathology and Cell Biology
University of Montréal
2900, Boulevard Edouard-Montpetit
Pavillon Roger Gaudry, Room N-535
Montreal, Quebec H3T 1J4, Canada.
Phone: (514) 343-6109, Fax: (514) 343-5755

Leonard A. Levin
Department of Ophthalmology and Visual Sciences,
600 Highland Ave,
Madison, WI, 53792, USA.

IV.1. ABSTRACT

The reactive oxygen species superoxide has been recognized as a critical signal triggering retinal ganglion cell (RGC) death after axonal injury. Although the downstream targets of superoxide are unknown, chemical reduction of oxidized sulfhydryls has been shown to be neuroprotective for injured RGCs. Based on this; we developed novel phosphine-borane complex compounds that are cell permeable and highly stable. Here, we report that our lead compound, bis (3-propionic acid methyl ester) phenylphosphine borane complex 1 (PB1), promotes RGC survival in rat models of optic nerve axotomy and in experimental glaucoma. PB1-mediated RGC neuroprotection did not correlate with inhibition of stress-activated protein kinase signaling, including ASK1, JNK or p38. Instead, PB1 led to a striking increase in retinal BDNF levels and downstream activation of the ERK1/2 pathway. Pharmacological inhibition of ERK1/2 entirely blocked RGC neuroprotection induced by PB1. We conclude that PB1 protects damaged RGCs through activation of pro-survival signals. These data support a potential cross-talk between redox homeostasis and neurotrophin-related pathways leading to RGC survival after axonal injury.

Keywords: Superoxide, Redox Signaling, Retinal Ganglion Cell, Neuroprotection, Brain-Derived Neurotrophic Factor, Extracellular Signal-Regulated Kinase 1/2.

Running title: Phosphine-Borane Complex-Induced Neuroprotection of Retinal Neurons.

IV.2. INTRODUCTION

Axonal injury is a common cause of neuronal death in the central nervous system (CNS) of adult mammals and is the primary damaging event in most optic nerve diseases, including glaucoma. A crucial element in the pathophysiology of optic neuropathies is the death of retinal ganglion cells (RGCs), the neurons that convey visual information from the retina to the brain. The signals leading to RGC loss in glaucoma are not well understood (Nickells, 2007; Wax and Tezel, 2002), but several mechanisms have been proposed, including neurotrophic factor deprivation, mechanical compression, excitotoxicity, reactive astrocytosis and induction of pro-apoptotic pathways (Carpenter et al., 1986; Cui and Harvey, 1995; Kikuchi et al., 2000; Kiryu-Seo et al., 2000; Mansour-Robaey et al., 1994; Pearson and Thompson, 1993; Shen et al., 1999; Stys et al., 1990; Yoles et al., 1997). The relationship between these processes is complex and it is likely that more than one signal leads to RGC death induced by axonal damage.

The hypothesis that neurotrophin deprivation contributes to RGC death after axonal injury has received considerable attention because a lack of target-derived brain-derived neurotrophic factor (BDNF) or nerve growth factor (NGF) leads to apoptotic death of developing RGCs (Chau et al., 1992; Nurcombe and Bennett, 1981; Rabacchi et al., 1994; Thoenen et al., 1987). Although the role of neurotrophins in the maintenance of adult RGCs is less clear, there is substantial evidence showing that administration of exogenous BDNF promotes robust RGC survival in a variety of optic nerve injury paradigms (Chen and Weber, 2001; Di Polo et al., 1998; Klöcker et al., 2000; Mansour-Robaey et al., 1994; Mey and Thanos, 1993; Peinado-Ramon et al., 1996). Upon binding of BDNF to its cognate receptor TrkB, multiple signaling pathways are activated including the extracellular signal-regulated kinases 1/2 (ERK1/2) and the phosphatidylinositol-3 kinase (PI3K)/Akt pathways (Kaplan and Miller, 2000). Endogenous activation of ERK1/2 and PI3K has been reported in RGCs in response to BDNF and other protective agents, and pharmacological inhibition of these molecules effectively blocks their survival effect (Cheng et al., 2002; Diem et al., 2001; Kermer et al., 2000; Schallenberg et al., 2009). Furthermore, we previously showed that viral vector-mediated stimulation of ERK1/2 was sufficient to protect RGCs from death induced by axotomy or ocular hypertension (Pernet et al., 2005; Zhou et al., 2005).

Oxidative signaling, caused by the imbalance between the production of reactive oxygen species (ROS) and their elimination by antioxidants, has been recognized as another central contributor to neuronal injury and death. ROS can modulate protein function by altering redox states leading to cysteine sulfhydryl oxidation. Oxidative cross-linking creates new disulfide bonds causing protein conformational changes and subsequent activation of cell death signals (Carugo et al., 2003; Park and Raines, 2001). Consistent with this, RGC viability has been shown to depend on the intracellular sulfhydryl redox state, with survival observed under mildly reducing conditions and increased death rates induced by sulfhydryl oxidation (Castagne and Clarke, 1996; Castagne et al., 1999; Geiger et al., 2002; Swanson et al., 2005).

We recently demonstrated that ROS superoxide is a key signal triggered by axonal injury leading to RGC apoptosis. Using live imaging, we showed that there is a marked elevation of superoxide in RGCs soon after optic nerve axotomy, and that a decrease in intracellular superoxide levels delays RGC death in vivo (Kanamori et al., 2010). Based on this, we hypothesized that reduction of oxidized sulfhydryls on critical proteins might attenuate the activation of death pathways that influence the fate of RGCs after injury. To test this, we developed reducing agents using a borane-protected phosphine backbone (Schlieve et al., 2006). Here we characterize a leading compound, bis (3-propionic acid methyl ester) phenylphosphine borane reducing complex 1 (PB1), and show that PB1 promotes RGC protection in rat paradigms of optic nerve injury. We demonstrate that, rather than inhibiting cell death pathways, PB1 leads to increased retinal levels of BDNF and that PB1-mediated RGC neuroprotection requires activation of ERK 1/2 in vivo. Our data support the conclusion that the reducing agent PB1 protects injured RGCs through activation of pro-survival pathways, and suggest a potential cross-talk between intracellular redox regulation and activation of neurotrophin-related neuroprotective signals in retinal neurons.

IV.3. MATERIALS AND METHODS

IV.3.1. Experimental animals

All procedures were carried out in accordance with the Animal Research: Reporting In Vivo Experiments (ARRIVE) and the Canadian Council on Animal Care guidelines. The optic nerve axotomy model, a paradigm of acute axonal damage and RGC death, was carried out in adult Sprague-Dawley rats (Charles River, 180-200 g). The experimental glaucoma model, induced by ocular hypertension (OHT) surgery, was performed in retired breeder Brown Norway rats (Charles River, Canada; 300-400 g). Brown Norway rats were used for the experimental glaucoma model because they have a larger eye suitable for the OHT surgical procedure (Johnson et al., 1996; Morrison et al., 1997). The number of animals used in each experiment (n) is indicated above the bar in the corresponding graph.

IV.3.2. RGC retrograde labeling

For quantification of neuronal survival, RGCs were retrogradely labeled with Fluorogold (2%, Fluorochrome, Englewood, CO) or DiI (3%, 1,1'-dioctadecyl-3,3,3',3'-tetramethyl-indocarbocyanine perchlorate; Molecular Probes, Junction City, OR). Tracers were dissolved in 0.9% NaCl containing 10% dimethyl sulfoxide (DMSO) and 0.5% Triton X-100. The superior colliculus was exposed bilaterally and a small piece of gelfoam (Pharmacia and Upjohn Inc., Mississauga, ON) soaked in tracer was applied to the surface. Seven days is the earliest time for detection of the entire RGC population after application of retrograde tracers to the rat superior colliculus (Vidal-Sanz et al., 1988). Thus, to ensure that all RGCs were fully labeled prior to axonal injury, axotomy or OHT surgery were performed at 7 days after tracer application.

IV.3.3. Optic nerve injury paradigms

IV.3.3.1. Optic nerve axotomy

Animals were deeply anesthetized (2% isoflurane, 0.8 liter/min) and the left optic nerve was carefully exposed within the dura and transected ~1 mm posterior to the globe. This procedure avoided injury to the ophthalmic artery and its branches. Fundus

examination was performed immediately after axotomy and 3-5 days later to check the integrity of the retinal circulation after surgery. Animals showing signs of compromised blood supply were excluded from the study.

IV.3.3.2 Ocular hypertension (morrison model)

Animals were anesthetized by intraperitoneal injection of 1 ml/kg of standard rat cocktail (100 mg/ml ketamine, 20 mg/ml xylazine, 10 mg/ml acepromazine). Unilateral elevation of intraocular pressure (IOP) was induced by a single injection of hypertonic saline solution (1.85 M NaCl) into an episcleral vein as previously described (Morrison et al., 1997), a procedure called OHT surgery. A plastic ring was applied to the ocular equator to confine the injection to the limbal plexus. Animals were kept in a room with constant low fluorescent light (40-100 lux) to stabilize circadian IOP variations (Jia et al., 2000b; Moore et al., 1996). IOP was measured using a calibrated tonometer (TonoPen XL, Medtronic Solan, Jacksonville, FL) in awake animals to avoid the anesthetic-induced reduction of IOP (Jia et al., 2000a).

IV.3.4. Phosphine-borane complex synthesis

Phosphine-borane complex 1 (PB1) was synthesized according to previously published methods (Schlieve et al., 2006). Briefly, the intermediate bis (3-propionic acid methyl ester) phenylphosphine (Phosphine 1) was produced by adding potassium hydroxide to phenylphosphine dissolved in acetonitrile, cooling to 0ºC, and then slowly adding methyl acrylate, maintaining the temperature below 35ºC. The reaction product was heated at 50ºC for 8 h, washed and dried over MgSO4, then concentrated and purified by distillation as a clear liquid. Phosphine 1 was dissolved in tetrahydrofuran (THF) and cooled to 0ºC. Borane-THF was slowly added and allowed to react. The solvent was then removed under reduced pressure and the residue purified by flash chromatography producing PB1.

IV.3.5. In vivo drug delivery

PB1 (150 μM) or the mitogen activated protein (MAP) kinase kinase 1 (MEK1) inhibitor PD98059 (200 μM, Sigma, Oakville, ON) were dissolved in phosphate buffered saline (PBS) containing 0.1% DMSO (vehicle). PB1, PD98059 or vehicle were injected

into the vitreous chamber of the injured eye using a Hamilton syringe fitted with a 32-gauge glass microneedle. We selected a PB1 concentration of 150 µM administered in a 4 µl volume, which yields an estimated final intravitreal concentration of 10 µM (approximate vitreous volume in rats: 60 µl), based on our previous in vitro study showing that this amount is an effective neuroprotective dose (Schlieve et al., 2006). The sclera was exposed and the tip of the needle was inserted at a 45° angle through the sclera and retina into the vitreous space using a posterior approach. This route of administration avoided injury to the iris or lens, which can promote RGC survival (Leon et al., 2000; Mansour-Robaey et al., 1994). The injection was performed within ~30 sec, after which the needle was gently removed. Some animals received two consecutive injections of PB1 and PD98059 or vehicle, through the same injection site, with a delay of 20 min between each injection. Surgical glue (Indermill, Tyco Health Care, Mansfield, MA) was used to seal the injection site.

IV.3.6. Quantification of RGC soma and axons

Quantification of RGC bodies or axons was performed in duplicate by an observer masked to the treatment assignments. For RGC density counts, rats were deeply anesthetized and perfused transcardially with 4% paraformaldehyde (PFA) and both eyes were immediately enucleated. Retinas were dissected and flat-mounted on a glass slide with the ganglion cell layer side up. RGCs were counted in three square areas at distances of 1, 2 and 3 mm from the optic disc in each of the four retinal quadrants (superior, inferior, nasal and temporal) for a total of 12 retinal areas encompassing a total area of 1 mm2. For axon counts, animals received a transcardial injection of heparin (1000 U/kg) and sodium nitroprusside (10 mg/kg), followed by perfusion with 2% PFA and 2.5% glutaraldehyde. Optic nerves were dissected, fixed in 2% osmium tetroxide, and embedded in Epon resin. Semi-thin sections (0.7-µm thick) were cut on a microtome (Reichert, Vienna, Austria) and stained with 1% toluidine blue. RGC axons were counted at 1 mm from the optic nerve head in five non-overlapping areas (center, peripheral dorsal and peripheral ventral) encompassing a total area of 5.5 mm^2 per nerve. The total area per optic nerve cross-section was measured using Northern Eclipse image analysis

software (Empix Imaging, Toronto, ON), and this value was used to estimate the total number of axons per optic nerve.

IV.3.7. Western blot analysis

Whole fresh retinas (n=4 per condition) were rapidly dissected and homogenized with an electric pestle (Kontes, Vineland, NJ) in ice-cold lysis buffer: 50 mM Tris (pH 7.4), 1 mM EDTA, 150 mM NaCl, 1% NP-40, 5 mM Na fluoride, 0.25% Na deoxycholate and 2 mM NaVO3 supplemented with protease and phosphatase inhibitors. Retinal extracts (60–150 µg) were resolved on 10-15% SDS polyacrylamide gels and transferred to nitrocellulose membranes (Bio-Rad Life Science, Hercules, CA, USA). Non-specific binding was blocked by incubation in 10 mM Tris (pH 8.0), 150 mM NaCl, 0.2% Tween 20 (TBST), and 5% bovine serum albumin (Fisher Scientific, Fair Lawn, NJ) for 1 h at room temperature (20ºC). Membranes were then incubated with the following primary antibodies: BDNF (1 µg/ml, Promega, Madison, WI), phospho-ERK1/2 (Thr185/Tyr187, 1 µg/ml, Invitrogen-BioSource, Carlsbad, CA), ERK1/2 (1 µg/ml, Invitrogen-BioSource), phospho-Akt (Thr308, 0.14 µg/ml, Cell Signaling, Danvers, MA), Akt (0.2 µg/ml, Cell Signaling), phospho-ASK1 (Thr838, 0.5 µg/ml, Cell Signaling), ASK1 (0.5 µg/ml, Cell Signaling), phospho-JNK (Thr183/Tyr185, 0.8 µg/ml, Cell Signaling), JNK (0.4 µg/ml, Cell Signaling), phospho-p38 (Thr180/Tyr182, 0.3 µg/ml, Cell Signaling), p38 (0.2 µg/ml, Cell Signaling), or ß-actin (0.5 µg/ml, Sigma). Blots were washed in TBST and incubated in the following peroxidase-linked secondary antibodies: anti-mouse or anti-rabbit (0.5 µg/ml, GE Healthcare, Little Chalfont Bucks, UK) or anti-chicken (0.5 µg/ml, Promega). Blots were developed using chemiluminescence reagents (ECL or Plus-ECL, Perkin Elmer Life and Analytical Sciences, Woodbridge, ON) and exposed to autoradiographic film (X-OMAT; Eastman Kodak, Rochester, NY). Densitometric analysis was performed using Scion Image software (Scion Corporation, Frederick, MD) on scanned autoradiographic films obtained from a series of 3 independent western blots each carried out using retinal samples from distinct experimental groups. The densitometric values obtained for BDNF were normalized with respect to their ß-actin loading controls in the same blot to obtain the final ratios. The densitometric values for phosphorylated (active) proteins were

normalized with respect to their loading (non-phosphorylated) controls in the same blot to obtain the final phosphorylated/total protein ratios.

IV.3.8. Statistical analysis

Data analysis and statistics were carried out using GraphPad InStat software (GraphPad Software Inc., San Diego, CA) by performing one-way analyses of variance (ANOVA) followed by Bonferroni multiple comparison post-hoc testing.

IV.4. RESULTS

IV.4.1. Intraocular delivery of the phosphine-borane compound PB1 protects RGCs from axotomy-induced death

PB1, an analogue of tris (2-carboxyethyl) phosphine (TCEP), was designed to contain a borane-protected phosphine group to prevent oxidation, thus enhancing the stability of the molecule (Schlieve et al., 2006). The phenyl group in PB1 is non-polar and increases the cell permeability of this compound. Once inside the cell, the methyl esters are cleaved by intracellular esterases resulting in an anionic molecule that is less likely to exit the cytosol (Fig.1). We previously demonstrated that PB1-mediated inhibition of sulfhydryl oxidation protects early postnatal, acutely axotomized RGCs in vitro (Schlieve et al., 2006), but the role of PB1 on the survival of adult RGCs in vivo was not established.

To investigate this, we first examined PB1-induced RGC survival following axotomy of the optic nerve, an injury modality that leads to rapid apoptotic RGC death (Berkelaar et al., 1994). Eyes that received an intraocular injection of PB1 showed robust RGC neuroprotection compared to control eyes injected with vehicle (Fig. 2A-C). Previous studies, including ours, have demonstrated that virtually all RGCs survive for 4 to 5 days after axotomy and then die rapidly: the RGC population is reduced to ~50% by day 7 and to ~10% by day 14 post-lesion (Berkelaar et al., 1994; Cheng et al., 2002; Mansour-Robaey et al., 1994). Figure 2D shows that in PB1-treated eyes, 66% of RGCs survived at one week after axotomy (1,434 ± 37 RGCs/mm^2, mean ± S.E.M., n=6) compared to only 47% remaining in vehicle-treated eyes (1,011 ± 37 RGCs/mm^2, n=4)

(ANOVA, $P < 0.001$). This neuroprotective effect was still substantial at 2 weeks after axotomy following PB1 treatment at the time of axotomy and one week later, accounting for 25% of RGC survival (533 ± 90 RGCs/mm^2, n=4) compared to 11% survival afforded by vehicle (239 ± 25 RGCs/mm^2, n=4) (ANOVA, $P < 0.01$). These data indicate that the reducing agent PB1 promotes adult RGC neuroprotection following acute optic nerve injury. Microglia and macrophages, which may have incorporated Fluorogold after phagocytosis of dying retinal ganglion cells, were excluded from our analysis based on well-established morphological criteria (Kacza and Seeger, 1997; Thanos, 1991). Microglia were identified by their invariably smaller cell size, visible process ramifications, and lack of axons (Figs. 2E, 2F) as previously described by us (Lebrun-Julien et al., 2009).

IV.4.2. PB1 protects RGC soma and axons in experimental glaucoma

To determine if PB1 was able to promote RGC survival in a paradigm of optic nerve injury resembling glaucomatous pathophysiology, we tested its neuroprotective effect in a rat ocular hypertension (OHT) model. Gradual increase of eye pressure and progressive death of RGCs are observed in this model, with an excellent linear correlation between IOP increase and RGC loss (Chauhan et al., 2002; Johnson et al., 1996; Morrison et al., 1997). Inner retinal atrophy, optic nerve degeneration, and optic nerve head remodeling in this model are similar to those seen in human glaucoma, therefore this model is considered a premier in vivo paradigm of this optic neuropathy. PB1 was injected intravitreally two weeks after OHT surgery to allow for IOP stabilization and RGC survival was examined at 3 or 5 weeks after OHT. Analysis of DiI-positive RGCs in retinal whole mounts showed that PB1 led to higher neuronal densities in glaucomatous eyes compared to control eyes at 3 weeks after OHT (Figure 3A-C). Quantitative analysis of RGC neuroprotection demonstrated that 82% of RGCs survived in the presence of PB1 (1,484 ± 36 RGCs/mm^2, mean ± S.E.M., n=6) compared to 59% in control eyes treated with vehicle (1,072 ± 64 RGCs/mm^2, n=6) (Fig. 3D, ANOVA, $p < 0.001$). The mean sustained IOP elevation in PB1- and vehicle-treated eyes was similar, allowing for a reliable comparison between these groups.

Glaucoma is characterized by the degeneration of RGC axons in the optic nerve followed by the progressive loss of cell bodies (Quigley, 1999; Schwartz et al., 1999), hence we also investigated the effect of PB1 on RGC axonal protection following ocular hypertensive damage. Analysis of axons in optic nerves treated with PB1 at 3 weeks after OHT demonstrated a higher number of RGC axons with normal morphology compared to vehicle-treated optic nerves, which featured extensive disarray of fascicular organization and degradation of myelin sheaths (Figure 4A-C). Axonal quantification in optic nerve cross sections showed that PB1 protected a significant number of RGC axons from glaucomatous damage (69% = 70,058 ± 4,547 axons, n=10) compared to vehicle-treated controls (55%= 55,997 ± 4,531 axons, n=6) (Fig. 4D, ANOVA, $p < 0.001$). Although a slight trend in RGC soma and axon protection was observed at 5 weeks after OHT (Table 1), this effect was not statistically significant suggesting that the biological activity of a single dose of PB1 has a limited duration in vivo. Collectively, these results indicate that PB1 attenuates the loss of both RGC soma and axons in experimental glaucoma.

IV.4.3. PB1-mediated RGC neuroprotection requires activation of the extracellular signal-regulated kinases 1/2 pathway

Oxidative stress has been linked to the activation of stress-activated protein kinase (SAPK) signaling and subsequent cell death (Cross and Templeton, 2004; Sumbayev and Yasinska, 2005). To gain mechanistic insight into how PB1 promoted RGC neuroprotection in vivo, we asked whether PB1 leads to inhibition of pro-apoptotic pathways. We chose the axotomy model for these experiments because the onset of RGC death in this injury paradigm is extremely consistent, starting at 4-5 days after optic nerve lesion (Berkelaar et al., 1994). This predictable time-course of RGC loss allowed us to examine protein changes prior to neuronal death (24 hrs), which are more likely to influence RGC fate. Furthermore, a well-defined burst of superoxide occurs within 24 hrs of optic nerve axotomy (Kanamori et al., 2010).

We first examined the activation of retinal Apoptosis Stimulating Kinase 1 (ASK1), a SAPK and mitogen-activated protein kinase kinase kinase (MAPKKK) family member, which is activated by ROS and has been shown to mediate RGC death (Harada et al., 2006; Harada et al., 2010). ASK1 is normally bound to reduced thioredoxin, a

protein disulfide oxidoreductase that prevents ASK1 autophosphorylation. Oxidation of cysteine thiols in thioredoxin results in its dissociation from ASK1, triggering ASK1 autophosphorylation and downstream stimulation of c-Jun NH2-terminal kinase (JNK) and p38 death signaling (Hatai et al., 2000; Ichijo et al., 1997; Saitoh et al., 1998). If PB1 exerted RGC neuroprotection via the regulation of ASK1, a decrease in phosphorylated ASK1 (P-ASK1) following PB1 treatment would be expected. Western blot analysis demonstrated low but detectable levels of phosphorylated ASK1 in intact (non-injured, non-treated) retinas (Fig. 5A). An increase in phospho-ASK1 was observed in control, axotomized eyes treated with vehicle, however, PB1 failed to significantly reduce the levels of activated ASK1. Consistent with this, the levels of ASK1 downstream effectors JNK (P-JNK, Fig. 5B) or p38 (P-p38, Fig. 5C) were not affected by PB1. These results suggest that PB1-mediated RGC neuroprotection does not involve the ASK1 pathway.

An alternative possibility is that PB1 results in the stimulation of pro-survival signals required for RGC viability after injury. To test this hypothesis, we investigated the levels of BDNF and its downstream effectors ERK1/2, Akt and CREB in axotomized retinas exposed to PB1 or vehicle. In control axotomized eyes treated with vehicle there was a slight, but significant, increase in BDNF compared to intact eyes (Fig. 6A), which is consistent with previous reports showing a ~50% increase in retinal BDNF mRNA after axotomy (Gao et al., 1997; Hirsch et al., 2000). Surprisingly, PB1 led to a 4-fold increase (200%) in BDNF protein levels after axotomy compared to intact retinas. Consistent with this, PB1 produced a robust activation of the BDNF effector ERK1/2 (P-ERK1/2, Fig. 6B) while Akt and the transcription factor CREB remained unchanged (P-Akt and P-CREB, Figs. 6C, D). Intraocular administration of PB1 at 2 weeks after OHT also resulted in enhanced ERK1/2 activation (Fig. 6E) suggesting that PB1 promotes RGC survival through activation of this pathway after acute and chronic optic nerve injury.

To establish whether ERK1/2 signaling was involved in PB1-mediated survival of axotomized RGCs, we co-injected PB1 with PD98059, a pharmacological inhibitor of MEK1, the obligate upstream activator of ERK1/2 (Dudley et al., 1995). We previously established that the optimal dose of PD98059 to selectively inhibit retinal Erk1/2 in vivo without affecting other pathways, including Akt, is 200 μM (16.7 μM intravitreal

concentration) (Cheng et al., 2002). Figure 7 shows that co-administration of PB1 and PD98059 resulted in complete inhibition of the survival effect produced by PB1, characterized by low RGC densities similar to those found in vehicle-treated retinas, at 1 week after optic nerve transection. Together, these findings demonstrate that the ERK1/2 pathway is essential for PB1-mediated survival of injured adult RGCs in vivo.

IV.5. DISCUSSION

The generation of an intracellular superoxide burst is a critical molecular event underlying RGC death after axonal injury (Geiger et al., 2002; Kanamori et al., 2010; Lieven et al., 2006; Nguyen et al., 2003; Swanson et al., 2005). Superoxide increases dramatically in RGCs at the single-cell level, soon after optic nerve axotomy, and precedes RGC apoptosis (Kanamori et al., 2010). Human glaucomatous retinas contain high levels of the lipid peroxidation indicator 4-hydroxy-2-nonenal (HNE), which leads to protein modification induced by superoxide (Tezel et al., 2010). Administration of pegylated superoxide dismutase-1 (SOD), which catalyzes the dismutation of superoxide into oxygen and hydrogen peroxide (H_2O_2), attenuates RGC death (Kanamori et al., 2010; Schlieve et al., 2006) supporting the idea that interfering with superoxide generation might be beneficial. However, the translation of a protein-based therapy that requires intracellular delivery is considerably more challenging than a small molecule approach. In this study, we characterized the neuroprotective role and mechanism of action of PB1, a small reducing compound with several advantages including good cell permeability, the ability to form a high intracellular concentration gradient, and stability.

Our data demonstrate that intraocular delivery of PB1 promotes RGC survival in vivo following traumatic optic nerve injury (axotomy) and ocular hypertension damage (experimental glaucoma). The finding that PB1-mediated neuroprotection was observed in these distinct injury paradigms, despite the fact that the RGC response to different types of lesion may vary widely, suggests that PB1 regulates a conserved pathway and underlines its translational potential to human disease. Glaucoma has been defined as an axogenic disease, characterized first by the degeneration of RGC axons in the optic nerve followed by the progressive loss of cell bodies (Schwartz et al., 1999). In the experimental glaucoma model, we performed quantitative analysis of the neuroprotective

effect of PB1 on two major RGC compartments: soma and axons. Consistent with the idea that the primary site of degeneration in glaucoma is at the level of the axon, we found that all eyes had more pronounced axonal loss than cell body loss. However, intraocular injection of PB1 protected a similar proportion of RGC soma and axons within the optic nerve at 3 weeks after OHT. The ability to protect all RGC compartments following hypertension damage is paramount for the preservation of neuronal function and vision; hence it is an important attribute of PB1. Interestingly, functional studies in macaque monkeys subjected to experimental glaucoma demonstrated that only subtle visual field defects are detected despite massive loss (>50%) of RGCs, whereas vision loss increases dramatically with more advanced glaucoma (Harwerth et al., 1999). Therefore, structural protection of a proportion of RGC soma and axons, as afforded by PB1, might be sufficient to preserve functional vision. The lack of significant soma or axon protection at 5 weeks after OHT suggests that a single dose of PB1 confers limited biological activity in vivo. A priority of future studies will be to devise sustained delivery strategies, such as PB1 coupled to nanoparticles, to achieve long-term neuroprotection.

What are the molecular mechanisms underlying PB1-mediated RGC survival? Evidence from studies on cell death inhibition induced by manipulation of the mitochondrial electron transport chain is consistent with PB1 acting externally to the mitochondrial matrix (Seidler et al., 2010). Phosphines might scavenge superoxide directly, but our studies with both borane-protected phosphines and deprotected PB1 have ruled out significant superoxide scavenging (Niemuth N.J., Lieven C.J., Thompson A.F., Levin L.A., unpublished data). The redox system can regulate the function of proteins involved in cell death and survival by modifying gene expression, posttranslational modifications (e.g. phosphorylation) and stability. In most cases, superoxide stimulates stress-activated protein kinase (SAPK) signaling and cell apoptosis (Sumbayev and Yasinska, 2005). Therefore, we hypothesized that PB1 might promote survival through inhibition of pro-apoptotic pathways. ASK1, a crucial redox sensor for initiation of the SAPK signaling cascade, leads to JNK and p38 stimulation and subsequent cell death (Kyriakis and Avruch, 2001). Contrary to our expectations, PB1 did not reduce the levels of phosphorylated (active) ASK1, JNK or p38 in axotomized retinas. Thus, we conclude

that the regulation of the SAPK cell death signaling pathway is not a target for PB1-induced neuroprotection.

We then considered an alternative scenario involving PB1-induced modification of RGC survival pathways. PB1 stimulated a robust increase of retinal BDNF levels that was several-fold higher than that observed in control axotomized eyes. Emerging data supports a tight redox regulation of transcription factors that encode cell survival proteins (Trachootham et al., 2008). The transcriptional regulation of BDNF is complex and often depends on activity-driven events that involve Ca^{+2}-responsive elements and cAMP-responsive elements (CRE) required for promoter transactivation (Shieh et al., 1998; Tao et al., 1998). CREB is an important transcription factor because it regulates BDNF gene expression, it also responds to BDNF by stimulating the transcription of pro-survival molecules such as Bcl-2 (Bonni et al., 1995; Finkbeiner et al., 1997; Wilson et al., 1996). Moreover, CREB plays a role in the regulation of ROS detoxification (Herzig et al., 2001; Krönke et al., 2003; Lee et al., 2009) and it is susceptible to redox regulation (Bedogni et al., 2003). PB1 failed to increase CREB activation, suggesting that other mechanisms including CREB-independent transcription, stability, subcellular localization, and translational events may underlie PB1-induced BDNF upregulation.

BDNF binds to its signaling receptor TrkB, which is abundantly expressed by adult RGCs (Jelsma et al., 1993; Pérez and Caminos, 1995; Rickman and Brecha, 1995), and activates the pro-survival ERK1/2 and Akt pathways. Our data demonstrate that ERK1/2, but not Akt, was activated following PB1 administration. This finding is consistent with our previous observation that combined BDNF and TrkB upregulation promoted RGC survival exclusively via ERK1/2, while Akt was not involved (Cheng et al., 2002). It is possible that endogenous BDNF leads to differential activation of downstream pathways depending on the redox status of the cell. In PB1-treated retinas, BDNF might selectively use the ERK1/2 pathway to promote RGC neuroprotection. In addition, PB1 might directly activate upstream molecules that converge on ERK1/2. This latter possibility is supported by the fact that autophosphorylation and activation of tyrosine kinase receptors, such as TrkB, can occur by direct thiol modification of the receptor (Chen et al., 1998). Similarly, the activity of Ras, an upstream activator of ERK1/2, is modulated by redox regulation (Lander et al., 1996; Mallis et al., 2001).

Nonetheless, the complete inhibition of RGC survival exerted by PB1 in the presence of PD98059 strongly supports our hypothesis that ERK1/2 activity is essential for PB1-mediated RGC neuroprotection in vivo.

In summary, we demonstrate that PB1, a novel phosphine-borane complex, promotes RGC neuroprotection in vivo through activation of the ERK1/2 pathway. BDNF is a potent anti-apoptotic factor for RGCs, but its clinical application has been hampered due to pleiotropic effects leading to non-specific signaling, potential toxicity and low diffusion rates (Barinaga, 1994; Verrall, 1994). The identification of small molecule compounds that mimic some of the beneficial effects of BDNF, such as PB1, is of clinical interest. Our study offers the interesting and unexpected possibility that redox homeostasis in RGCs can converge on neurotrophin-related pathways to promote survival after axonal injury.

ACKNOWLEDGEMENTS: The authors declare no conflict of interest. A patent on phosphine-borane complexes (US 7,932,239) has been assigned to the Wisconsin Alumni Research Foundation. This work was supported by grants from the Canadian Institutes of Health Research MOP-82786 (ADP) and the National Institutes of Health R21 EY017970 (LAL), P30 EY016665 (LAL). ADP is a FRSQ Chercheur Senior Scholar, and LAL is a Canada Research Chair of Ophthalmology and Visual Sciences.

IV.6. REFERENCES

Barinaga, M., 1994. Neurotrophic factors enter the clinic. Science 264, 772-774.

Bedogni, B., Pani, G., Colavitti, R., Riccio, A., Borrello, S., Murphy, M., Smith, R., Eboli, M.L., Galeotti, T., 2003. Redox Regulation of cAMP-responsive Element-binding Protein and Induction of Manganous Superoxide Dismutase in Nerve Growth Factor-dependent Cell Survival. J. Biol. Chem. 278, 16510-16519.

Berkelaar, M., Clarke, D.B., Wang, Y.-C., Bray, G.M., Aguayo, A.J., 1994. Axotomy results in delayed death and apoptosis of retinal ganglion cells in adult rats. J. Neurosci. 14, 4368-4374.

Bonni, A., Ginty, D.D., Dudek, H., Greenberg, M.E., 1995. Serine 133-Phosphorylated CREB Induces Transcription via a Cooperative Mechanism That May Confer Specificity to Neurotrophin Signals. Mol. Cell. Neurosci. 6, 168-183.

Carpenter, P., Sefton, A.J., Dreher, B., Lim, W.-L., 1986. Role of target tissue in regulating the development of retinal ganglion cells in the albino rat: Effects of kainate lesions in the superior colliculus. J. Comp. Neurol. 251, 240-259.

Carugo, O., Cemazar, M., Zahariev, S., Hudaky, I., Gaspari, Z., Perczel, A., Pongor, S., 2003. Vicinal disulfide turns. Protein Eng 16, 637-639.

Castagne, V., Clarke, P.G., 1996. Axotomy-induced retinal ganglion cell death in development: its time- course and its diminution by antioxidants. Proc. Royal Soc. London B Biol. Sci. 263, 1193-1197.

Castagne, V., Lefevre, K., Natero, R., Clarke, P.G., Bedker, D.A., 1999. An optimal redox status for the survival of axotomized ganglion cells in the developing retina. Neurosci. 93, 313-320.

Chau, R.M., Ren, F., Huang, W.Q., 1992. Programmed cell death of neonatal rat retinal ganglion cells due to turn-off expression of a novel 30-kD trophic factor and/or the lack of this factor supplied from the superior colliculus. Ann. N.Y. Acad. Sci. 21, 466-470.

Chauhan, B.C., Pan, J., Archibald, M.L., LeVatte, T.L., Kelly, M.E.M., Tremblay, F., 2002. Effect of Intraocular Pressure on Optic Disc Topography, Electroretinography, and Axonal Loss in a Chronic Pressure-Induced Rat Model of Optic Nerve Damage. Invest. Ophthalmol. Vis. Sci. 43, 2969-2976.

Chen, H., Weber, A.J., 2001. BDNF enhances retinal ganglion cell survival in cats with optic nerve damage. Invest. Opthalmol. Vis. Sci. 42, 966-974.

Chen, W., Martindale, J.L., Holbrook, N.J., Liu, Y., 1998 Tumor promoter arsenite activates extracellular signal-regulated kinase through a signaling pathway mediated by epidermal growth factor receptor and Shc. Mol. Cell. Biol. 18, 5178-5188.

Cheng, L., Sapieha, P., Kittlerová, P., Hauswirth, W.W., Di Polo, A., 2002. TrkB gene transfer protects retinal ganglion cells from axotomy-induced death in vivo. J. Neurosci. 22, 3977-3986.

Cross, J.V., Templeton, D.J., 2004. Thiol oxidation of cell signaling proteins: Controlling an apoptotic equilibrium. J. Cell. Biochem. 93, 104-111.

Cui, Q., Harvey, A.R., 1995. At least two mechanisms are involved in the death of retinal ganglion cells following target ablation in neonatal rats. J. Neurosci. 15, 8143-8155.

Di Polo, A., Aigner, L.J., Dunn, R.J., Bray, G.M., Aguayo, A.J., 1998. Prolonged delivery of brain-derived neurotrophic factor by adenovirus-infected Müller cells temporarily rescues injured retinal ganglion cells. Proc. Natl. Acad. Sci. USA 95, 3978-3983.

Diem, R., Meyer, R., Weishaupt, J.H., Bähr, M., 2001. Reduction of potassium currents and phosphatidylinositol 3-kinase-dependent Akt phosphorylation by tumor necrosis factor-alpha rescues axotomized retinal ganglion cells from retrograde cell death in vivo. J. Neurosci. 21, 2058-2066.

Dudley, D.T., Pang, L., Decker, S.J., Bridges, A.J., Saltiel, A.R., 1995. A synthetic inhibitor of the mitogen-activated protein kinase cascade. Proceedings of the National Academy of Sciences of the United States of America 92, 7686-7689.

Finkbeiner, S., Tavazoie, S.F., Maloratsky, A., Jacobs, K.M., Harris, K.M., Greenberg, M.E., 1997. CREB: A Major Mediator of Neuronal Neurotrophin Responses. Neuron 19, 1031-1047.

Gao, H., Qiao, X., Hefti, F., Hollyfield, J.G., Knüsel, B., 1997. Elevated mRNA expression of brain-derived neurotrophic factor in retinal ganglion cell layer after optic nerve injury. Invest. Ophthalmol. Vis. Sci. 38, 1840-1847.

Geiger, L.K., Kortuem, K.R., Alexejun, C., Levin, L.A., 2002. Reduced redox state allows prolonged survival of axotomized neonatal retinal ganglion cells. Neurosci. 109, 635-642.

Harada, C., Nakamura, K., Namekata, K., Okumura, A., Mitamura, Y., Iizuka, Y., Kashiwagi, K., Yoshida, K., Ohno, S., Matsuzawa, A., Tanaka, K., Ichijo, H., Harada, T., 2006. Role of apoptosis signal-regulating kinase 1 in stress-induced neural cell apoptosis in vivo. Am. J. Pathol. 168, 261-269.

Harada, C., Namekata, K., Guo, X., Yoshida, H., Mitamura, Y., Matsumoto, Y., Tanaka, K., Ichijo, H., Harada, T., 2010. ASK1 deficiency attenuates neural cell death in GLAST-deficient mice, a model of normal tension glaucoma. Cell Death Differ. 17, 1751-1759.

Harwerth, R.S., Carter-Dawson, L., Shen, F., Smith, E.L.r., Crawford, M.L., 1999. Ganglion cell losses underlying visual field defects from experimental glaucoma. Invest. Ophthalmol. Vis. Sci. 40, 2242-2250.

Hatai, T., Matsuzawa, A., Inoshita, S., Mochida, Y., Kuroda, T., Sakamaki, K., Kuida, K., Yonehara, S., Ichijo, H., Takeda, K., 2000. Execution of Apoptosis Signal-regulating Kinase 1 (ASK1)-induced Apoptosis by the Mitochondria-dependent Caspase Activation. J. Biol. Chem. 275, 26576-26581.

Herzig, S., Long, F., Jhala, U.S., Hedrick, S., Quinn, R., Bauer, A., Rudolph, D., Schutz, G., Yoon, C., Puigserver, P., Spiegelman, B., Montminy, M., 2001. CREB regulates hepatic gluconeogenesis through the coactivator PGC-1. Nature 413, 179-183.

Hirsch, S., Labes, M., Bahr, M., 2000. Changes in BDNF and neurotrophin receptor expression in degenerating and regenerating rat retinal ganglion cells. Restor. Neurol. Neurosci. 17, 125-134.

Ichijo, H., Nishida, E., Irie, K., Dijke, P.t., Saitoh, M., Moriguchi, T., Takagi, M., Matsumoto, K., Miyazono, K., Gotoh, Y., 1997. Induction of Apoptosis by ASK1, a Mammalian MAPKKK That Activates SAPK/JNK and p38 Signaling Pathways. Science 275, 90-94.

Jelsma, T.N., Friedman, H.H., Berkelaar, M., Bray, G.M., Aguayo, A.J., 1993. Different forms of the neurotrophin receptor trkB mRNA predominate in rat retina and optic nerve. J Neurobiol 24, 1207-1214.

Jia, L., Cepurna, W.O., Johnson, E.C., Morrison, J.C., 2000a. Effect of general anesthetics on IOP in rats with experimental aqueous outflow obstruction. Invest. Ophthalmol. Vis. Sci. 41, 3415-3419.

Jia, L., Cepurna, W.O., Johnson, E.C., Morrison, J.C., 2000b. Patterns of intraocular pressure elevation after aqueous humor outflow obstruction in rats. Invest. Ophthalmol. Vis. Sci. 41, 1380-1385.

Johnson, E.C., Morrison, J.C., Farrell, S., Deppmeier, L., Moore, C.G., McGinty, M.R., 1996. The effect of chronically elevated intraocular pressure on the rat optic nerve head extracellular matrix. Exp. Eye Res. 62, 663-674.

Kacza, J., Seeger, J., 1997. Transcellular labelling of activated retinal microglia following transection of the optic nerve. Inflammation Res. 46, 430-433.

Kanamori, A., Catrinescu, M.-M., Kanamori, N., Mears, K.A., Beaubien, R., Levin, L.A., 2010. Superoxide is an associated signal for apoptosis in axonal injury. Brain 133, 2612-2625.

Kaplan, D.R., Miller, F.D., 2000. Neurotrophin signal transduction in the nervous system. Curr. Opin. Neurobiol. 10, 381-391.

Kermer, P., Klöcker, N., Labes, M., Bähr, M., 2000. Insulin-like growth factor-1 protects axotomized rat retinal ganglion cells from secondary death via PI3-K-dependent Akt phosphorylation and inhibition of caspase-3 in vivo. J. Neurosci. 20, 722-728.

Kikuchi, M., Tenneti, L., Lipton, S.A., 2000. Role of p38 mitogen-activated protein kinase in axotomy-induced apoptosis of rat retinal ganglion cells. J Neurosci 20, 5037-5044.

Kiryu-Seo, S., Sasaki, M., Yokohama, H., Nakagomi, S., Hirayama, T., Aoki, S., Wada, K., Kiyama, H., 2000. Damage-induced neuronal endopeptidase (DINE) is a unique metallopeptidase expressed in response to neuronal damage and activates superoxide scavengers. Proc. Natl. Acad. Sci. USA 97, 4345-4350.

Klöcker, N., Kermer, P., Weishaupt, J.H., Labes, M., Ankerhold, R., Bähr, M., 2000. Brain-derived neurotrophic factor-mediated neuroprotection of adult rat retinal ganglion cells in vivo does not exclusively depend on phosphatidyl-inositol-3'-kinase/protein kinase B signaling. J. Neurosci. 20, 6962-6967.

Krönke, G., Bochkov, V.N., Huber, J., Gruber, F., BlÃ¼ml, S., FÃ¼rnkranz, A., Kadl, A., Binder, B.R., Leitinger, N., 2003. Oxidized Phospholipids Induce Expression of Human Heme Oxygenase-1 Involving Activation of cAMP-responsive Element-binding Protein. J. Biol. Chem. 278, 51006-51014.

Kyriakis, J.M., Avruch, J., 2001. Mammalian Mitogen-Activated Protein Kinase Signal Transduction Pathways Activated by Stress and Inflammation. Physiol. Rev. 81, 807-869.

Lander, H.M., Milbank, A.J., Tauras, J.M., Hajjar, D.P., Hempstead, B.L., Schwartz, G.D., Kraemer, R.T., Mirza, U.A., Chait, B.T., Burk, S.C., Quilliam, L.A., 1996. Redox regulation of cell signalling. Nature 381, 380-381.

Lebrun-Julien, F., Duplan, L., Pernet, V., Osswald, I.K., Sapieha, P., Bourgeois, P., Dickson, K., Bowie, D., Barker, P.A., Di Polo, A., 2009. Excitotoxic death of retinal neurons in vivo occurs via a non-cell-autonomous mechanism. J. Neurosci. 29, 5536-5545.

Lee, B., Cao, R., Choi, Y.-S., Cho, H.-Y., Rhee, A.D., Hah, C.K., Hoyt, K.R., Obrietan, K., 2009. The CREB/CRE transcriptional pathway: protection against oxidative stress-mediated neuronal cell death. J. Neurochem. 108, 1251-1265.

Leon, S., Yin, Y., Nguyen, J., Irwin, N., Benowitz, L.I., 2000. Lens injury stimulates axon regeneration in the mature rat optic nerve. J. Neurosci. 20, 4615-4626.

Lieven, C.J., Schlieve, C.R., Hoegger, M.J., Levin, L.A., 2006. Retinal ganglion cell axotomy induces an increase in intracellular superoxide anion. Invest. Ophthalmol. Vis. Sci. 47, 1477-1485.

Mallis, R.J., Buss, J.E., Thomas, J.A., 2001. Oxidative modification of H-ras: S-thiolation and S-nitrosylation of reactive cysteines. Biochem. J. 355, 145-153.

Mansour-Robaey, S., Clarke, D.B., Wang, Y.-C., Bray, G.M., Aguayo, A.J., 1994. Effects of ocular injury and administration of brain-derived neurotrophic factor on

survival and regrowth of axotomized retinal ganglion cells. Proc. Natl. Acad. Sci. USA 91, 1632-1636.

Mey, J., Thanos, S., 1993. Intravitreal injections of neurotrophic factors support the survival of axotomized retinal ganglion cells in adult rats in vivo. Brain Res. 602, 304-317.

Moore, C.G., Johnson, E.C., Morrison, J.C., 1996. Circadian rhythm of intraocular pressure in the rat. Curr. Eye Res. 15, 185-191.

Morrison, J.C., Moore, C.G., Deppmeier, L.M.H., Gold, B.G., Meshul, C.K., Johnson, E.C., 1997. A rat model of chronic pressure-induced optic nerve damage. Exp. Eye Res. 64, 85-96.

Nguyen, S.M., Alexejun, C.N., Levin, L.A., 2003. Amplification of a Reactive Oxygen Species Signal in Axotomized Retinal Ganglion Cells. Antioxid. Redox. Sign. 5, 629-634.

Nickells, R.W., 2007. From ocular hypertension to ganglion cell death: a theoretical sequence of events leading to glaucoma. Can. J. Ophthalmol. 42, 278-287.

Nurcombe, V., Bennett, M.R., 1981. Embryonic chick retinal ganglion cells identified "in vitro". Their survival is dependent on a factor from the optic tectum. Exp. Brain Res. 44, 249-258.

Park, C., Raines, R.T., 2001. Adjacent cysteine residues as a redox switch. Protein Eng 14, 939-942.

Pearson, H.E., Thompson, T.P., 1993. Atrophy and degeneration of ganglion cells in central retina following loss of postsynaptic target neurons in the dorsal lateral geniculate nucleus of the adult cat. Exp Neurol 119, 113-119.

Peinado-Ramon, P., Salvador, M., Villegas-Perez, M.P., Vidal-Sanz, M., 1996. Effects of axotomy and intraocular administration of NT-4, NT-3 and brain-derived neurotrophic factor on the survival of adult rat retinal ganglion cells. A quantitative in vivo study. Invest. Ophthalmol. Vis. Sci. 37, 489-500.

Pérez, M.T.R., Caminos, E., 1995. Expression of brain-derived neurotrophic factor and its functional receptor in neonatal and adult rat retina. Neurosci. Lett. 183, 96-99.

Pernet, V., Hauswirth, W.W., Di Polo, A., 2005. Extracellular signal-regulated kinase 1/2 mediates survival, but not axon regeneration, of adult injured central nervous system neurons in vivo. J. Neurochem. 93, 72-83.

Quigley, H.A., 1999. Neuronal death in glaucoma. Prog. Retin. Eye Res. 18, 39-57.

Rabacchi, S.A., Ensini, M., Bonfanti, L., Gravina, A., Maffei, L., 1994. Nerve growth factor reduces apoptosis of axotomized retinal ganglion cells in the neonatal rat. Neurosci. 63, 969-973.

Rickman, D.W., Brecha, N.C., 1995. Expression of the proto-oncogene, trk, receptors in the developing rat retina. Vis. Neurosci. 12, 215-222.

Saitoh, M., Nishitoh, H., Fujii, M., Takeda, K., Tobiume, K., Sawada, Y., Kawabata, M., Miyazono, K., Ichijo, H., 1998. Mammalian thioredoxin is a direct inhibitor of apoptosis signal-regulating kinase (ASK) 1. EMBO J 17, 2596-2606.

Schallenberg, M., Charalambous, P., Thanos, S., 2009. GM-CSF regulates the ERK1/2 pathways and protects injured retinal ganglion cells from induced death. Exp Eye Res 89, 665-677.

Schlieve, C.R., Tam, A., Nilsson, B.L., Lieven, C.J., Raines, R.T., Levin, L.A., 2006. Synthesis and characterization of a novel class of reducing agents that are highly neuroprotective for retinal ganglion cells. Exp. Eye Res. 83, 1252-1259.

Schwartz, M., Yoles, E., Levin, L.A., 1999. 'Axogenic' and 'somagenic' neurodegenerative diseases: definitions and therapeutic implications. Mol. Med. Today 5, 470-473.

Seidler, E.A., Lieven, C.J., Thompson, A.F., Levin, L.A., 2010. Effectiveness of novel borane-phosphine complexes in inhibiting cell death depends on the source of superoxide production induced by blockade of mitochondrial electron transport. ACS Chem. Neurosci. 1, 95-103.

Shen, S., Wiemelt, A.P., McMorris, F.A., Barres, B.A., 1999. Retinal ganglion cells lose trophic responsiveness after axotomy. Neuron 23, 285-295.

Shieh, P.B., Hu, S.-C., Bobb, K., Timmusk, T., Ghosh, A., 1998. Identification of a Signaling Pathway Involved in Calcium Regulation of BDNF Expression. Neuron 20, 727-740.

Stys, P.K., Ransom, B.R., Waxman, S.G., Davis, P.K., 1990. Role of extracellular calcium in anoxic injury of mammalian central white matter. Proc. Natl. Acad. Sci. U.S.A. 87, 4212-4216.

Sumbayev, V.V., Yasinska, I.M., 2005. Regulation of MAP kinase-dependent apoptotic pathway: implication of reactive oxygen and nitrogen species. Arch. Biochem. Biophys. 436, 406-412.

Swanson, K.I., Schlieve, C.R., Lieven, C.J., Levin, L.A., 2005. Neuroprotective effect of sulfhydryl reduction in a rat optic nerve crush model. Invest. Ophthalmol. Vis. Sci. 46, 3737-3741.

Tao, X., Finkbeiner, S., Arnold, D.B., Shaywitz, A.J., Greenberg, M.E., 1998. Ca2+ Influx Regulates BDNF Transcription by a CREB Family Transcription Factor-Dependent Mechanism. Neuron 20, 709-726.

Tezel, G., Yang, X., Luo, C., Kain, A.D., Powell, D.W., Kuehn, M.H., Kaplan, H.J., 2010. Oxidative stress and the regulation of complement activation in human glaucoma. Invest. Ophthalmol. Vis. Sci. 51 5071-5082.

Thanos, S., 1991. The Relationship of Microglial Cells to Dying Neurons During Natural Neuronal Cell Death and Axotomy-induced Degeneration of the Rat Retina. Eur. J. Neurosci. 3, 1189-1207.

Thoenen, H., Barde, Y.A., Davies, A.M., Johnson, J.E., 1987. Neurotrophic factors and neuronal death. Ciba Foundation Symposium 126, 82-95.

Trachootham, D., Lu, W., Ogasawara, M.A., Valle, N.R.-D., Huang, P., 2008. Redox Regulation of Cell Survival. Antioxid. Redox Sign. 10, 1343-1374.

Verrall, M., 1994. Lay-offs follow suspension of clinical trials of protein. Nature 370, 6.

Vidal-Sanz, M., Villegas-Perez, M.P., Bray, G.M., Aguayo, A.J., 1988. Persistent retrograde labeling of adult rat retinal ganglion cells with the carbocyanine dye diI. Exp. Neurol. 102, 92-101.

Wax, M.B., Tezel, G., 2002. Neurobiology of glaucomatous optic neuropathy: diverse cellular events in neurodegeneration and neuroprotection. Mol. Neurobiol. 26, 45-55.

Wilson, B.E., Mochon, E., Boxer, L.M., 1996. Induction of bcl-2 expression by phosphorylated CREB proteins during B- cell activation and rescue from apoptosis. Mol. Cell. Biol. 16, 5546-5556.

Yoles, E., Muller, S., Schwartz, M., 1997. NMDA-receptor antagonist protects neurons from secondary degeneration after partial optic nerve crush. J Neurotrauma 14, 665-675.

Zhou, Y., Pernet, V., Hauswirth, W.W., Di Polo, A., 2005. Activation of the extracellular signal-regulated kinase 1/2 pathway by AAV gene transfer protects retinal ganglion cells in glaucoma. Mol. Ther. 12, 402-412.

Figure 1. Chemical structure of bis (3-propionic acid methyl ester) phenylphosphine borane reducing complex 1 (PB1).

The borane group protects the phosphine from oxidation increasing chemical stability during storage and before administration. The non-polarity of the phosphine-borane and the phenyl group contribute to the ability of PB1 to readily cross cell membranes. The methyl esters are cleaved by extracellular amines and/or intracellular esterases, resulting in an anionic molecule that is unlikely to exit the cytosol and thus forms a strong intracellular concentration gradient.

Figure 2. The phosphine-borane compound PB1 protects RGCs from axotomy-induced death.

Retinal flat mounts show Fluorogold-labeled RGCs from non-injured, non-treated eyes (A, Intact) and axotomized PB1-treated (B) or vehicle-treated (C) eyes. Scale bars: 100 μm. (D) Quantitative analysis of RGC survival following injection of PB1 (solid bars) or vehicle (hatched bars) at the time of axotomy (n=4-6 rats/group) (ANOVA, ***: $P<0.001$). Animals examined at two weeks received an injection at the time of axotomy and a week later. The density of RGCs in intact, non-injured Sprague-Dawley rat retinas is shown as reference (open bar, 100%, n=8). Data are expressed as RGCs/mm^2 (mean ± S.E.M). (E, F) Microglia and macrophages (arrowheads) that may have incorporated Fluorogold after phagocytosis of dying retinal ganglion cells (arrows) were excluded from our analysis based on their distinct morphology. Scale bars: e, f = 10 μm.

Figure 3. PB1 protects RGC soma in experimental glaucoma.

Retinal flat mounts show DiI-labeled RGCs from non-injured, non-treated eyes (A, Intact) and glaucomatous PB1-treated (B) or vehicle-treated (C) eyes. Scale bars: 100 µm. (D) Quantitative analysis of RGC survival following injection of PB1 (solid bars) or vehicle (hatched bars) at three weeks after ocular hypertension surgery (OHT) (n=6 rats/group) (ANOVA, ***: $P<0.001$). The density of RGCs in intact, non-injured Brown Norway rat retinas is shown as reference (open bar, 100%, n=6). Data are expressed as RGC densities (RGCs/mm^2, mean ± S.E.M).

Figure 4. PB1 attenuates axonal loss in experimental glaucoma.

Cross-sections of optic nerve segments from non-injured eyes (A, Intact) and glaucomatous eyes treated with PB1 (B) or vehicle (C) at 3 weeks after ocular hypertension surgery (OHT). PB1-treated eyes displayed a larger number of axonal fibers with normal morphology compared to vehicle-treated control eyes, which showed extensive axon degeneration. Scale bars: 20 μm. (D) Quantitative analysis of RGC axons in optic nerves after treatment with PB1 (solid bar), or vehicle (hatched bar) (n=6-10 rats/group) (ANOVA, ***: $P<0.001$). The number of axons in the non-injured Brown Norway rat optic nerve is shown as reference (open bar, 100%, n=9). Data are expressed as the total number of RGC axons per optic nerve (mean ± S.E.M.).

Figure 5. The pro-apoptotic ASK1 signaling pathway is not regulated by PB1.
Western blots of total retinal extracts probed with antibodies that selectively recognize phosphorylated (active) ASK1, JNK or p38. Protein samples were collected from non-injured, non-treated eyes (Intact) or axotomized eyes treated with PB1 or vehicle and collected at 24 hrs post-lesion. (A) An injury-induced increase in phospho-ASK1 (P-ASK1) was observed in control, axotomized eyes treated with vehicle. PB1 failed to significantly reduce the levels of active ASK1 after axotomy. The levels of ASK1 downstream effectors P-JNK (B) or P-p38 (C) were not affected by PB1. The densitometric values are the ratio of phospho-proteins normalized to their loading (non-phosphorylated) controls in the same blot for intact (open bars), PB1-treated (solid bars) or vehicle-treated (hatched bars) eyes (n=4/group) (ANOVA, ***: $P<0.001$).

Figure 6. PB1 increases retinal BDNF and activates ERK1/2.

(A) PB1 led to a 4-fold increase in BDNF protein levels after axotomy compared to intact retinas. (B) Robust activation of the BDNF effector ERK1/2 was observed in PB1-treated axotomized eyes (P-ERK1/2), while Akt (P-Akt, C) and CREB (P-CREB, D) remained unchanged. The densitometric values are the ratio of phospho-proteins normalized to their loading (non-phosphorylated) controls in the same blot, or ß-action in the case of BDNF, for intact (open bars), PB1-treated (solid bars) or vehicle-treated (hatched bars) eyes (n=4/group) (ANOVA, ***: $P<0.001$, *: $p < 0.05$).

Figure 7. PB1-mediated RGC neuroprotection requires activation of ERK1/2.

(A-C) Retinal flat mounts show that co-administration of PB1 and the MEK1 inhibitor PD98059, injected intravitreally at the time of optic nerve transection, resulted in inhibition of the survival effect produced by PB1 at 1 week after optic nerve transection. (D) Quantitative analysis of Fluorogold-labeled neurons in eyes treated with PB1 and PD98059 (gray bar) showed that RGC density at 1 week post-lesion was similar to that found in control retinas treated with vehicle (hatched bar) (n=4-6/group) (ANOVA, ***: $P<0.001$). Data are expressed as RGCs/mm^2 (mean ± S.E.M).

IV.7. TABLES

Table 1. PB1-induced RGC soma and axonal survival in axotomy and ocular hypertension models

Modality of optic nerve damage	Time after injury	Treatment	RGCs/mm^2 (Mean ± S.E.M.)	RGC axons (Mean ± S.E.M.)
Axotomy	1 week	PB1	1434 ± 37 (n=6)	-
		Vehicle	1011 ± 37 (n=4)	-
	2 weeks	PB1	533 ± 90 (n=4)	-
		Vehicle	239 ± 25 (n=4)	-
Ocular hypertension	3 weeks	PB1	1484 ± 36 (n=6)	70058 ± 4547 (n=9)
		Vehicle	1072 ± 64 (n=6)	55997 ± 4531 (n=6)
	5 weeks	PB1	687 ± 35 (n=6)	311136 ± 5132 (n=7)
		Vehicle	598 ± 77 (n=6)	304158 ± 4673 (n=6)

IV.8. FIGURES

FIGURE 1

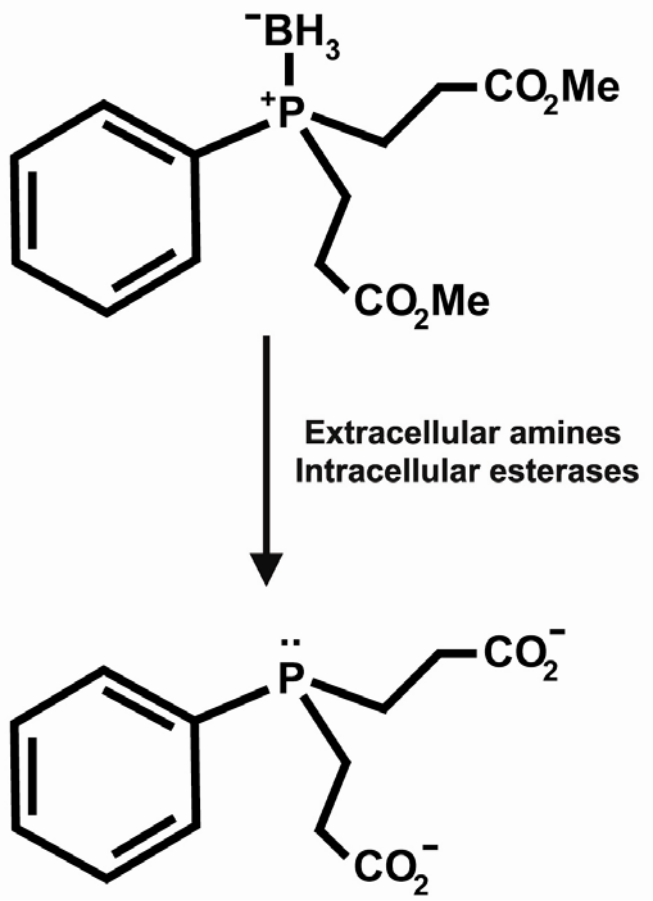

FIGURE 2

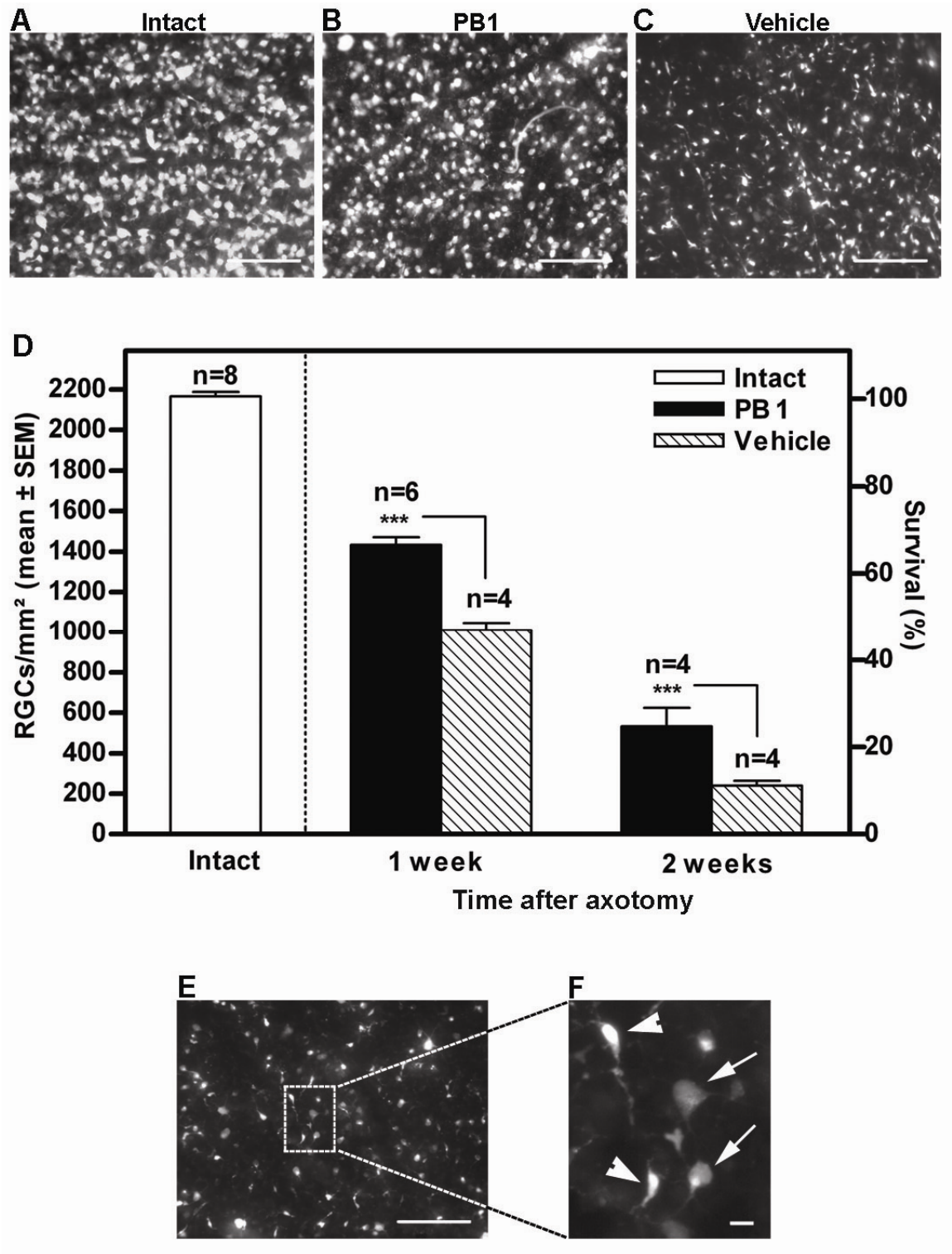
A
Intact
B
PB1
C
Vehicle
D
RGCs/mm² (mean ± SEM)
2200
2000
1800
1600
1400
1200
1000
800
600
400
200
0
n=8
n=6
***
n=4
n=4
***
n=4
Intact
PB 1
Vehicle
100
80
60
40
20
0
Survival (%)
Intact
1 week
2 weeks
Time after axotomy
E
F

FIGURE 3

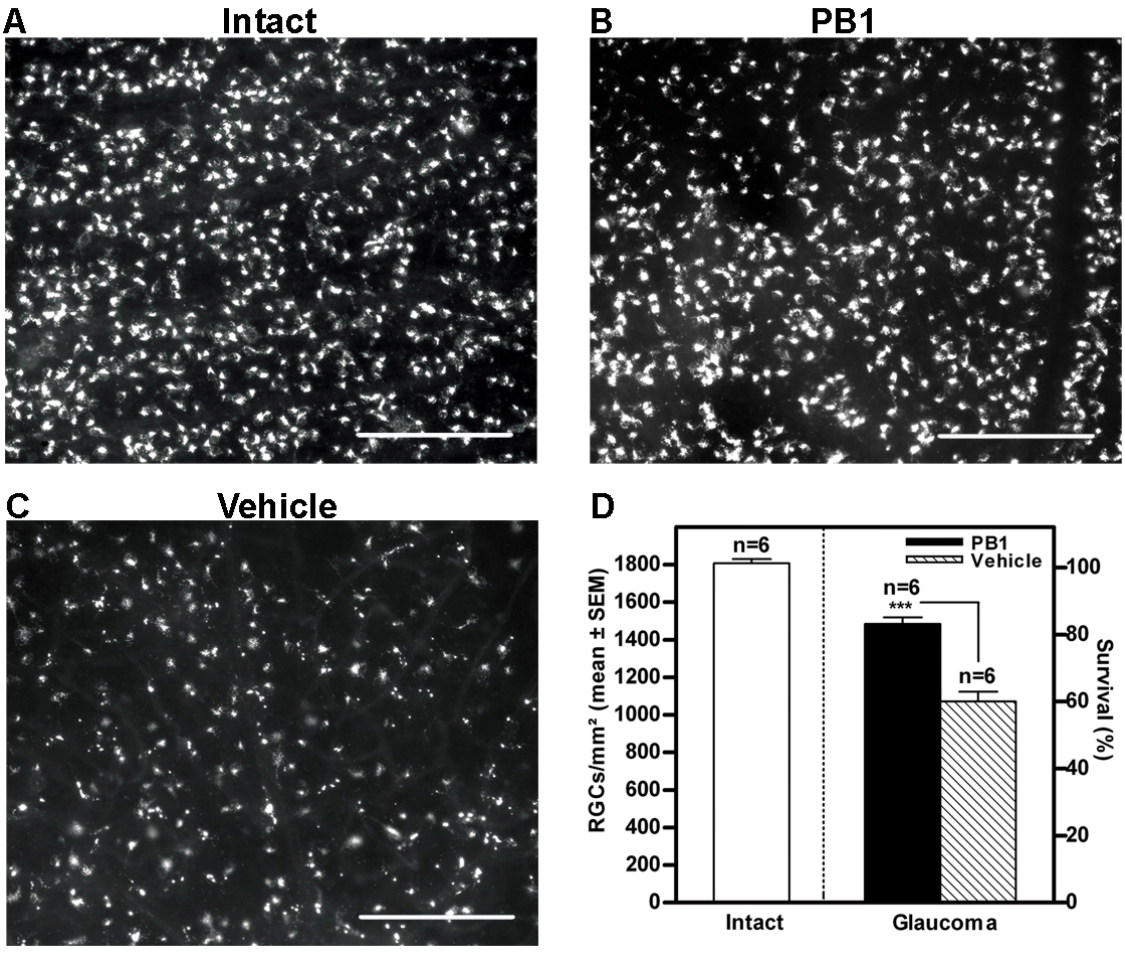
A
Intact
B
PB1
C
Vehicle
D
n=6
PB1
Vehicle
n=6
***
n=6
RGCs/mm² (mean ± SEM)
Survival (%)
1800
1600
1400
1200
1000
800
600
400
200
0
100
80
60
40
20
0
Intact
Glaucoma

FIGURE 4

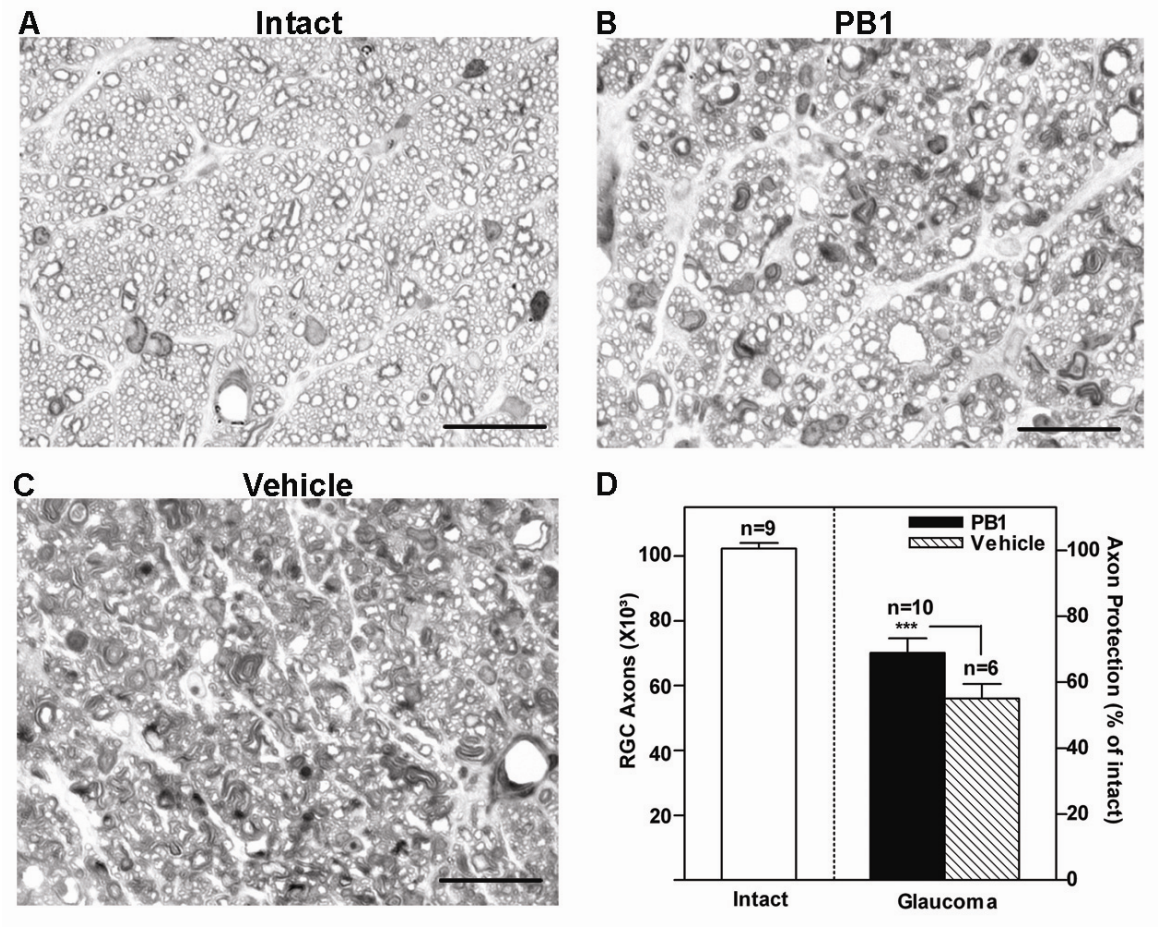
A
Intact
B
PB1
C
Vehicle
D
n=9
PB1
Vehicle
n=10
***
n=6
RGC Axons (X10³)
Axon Protection (% of intact)
100
80
60
40
20
0
Intact
Glaucoma

FIGURE 5

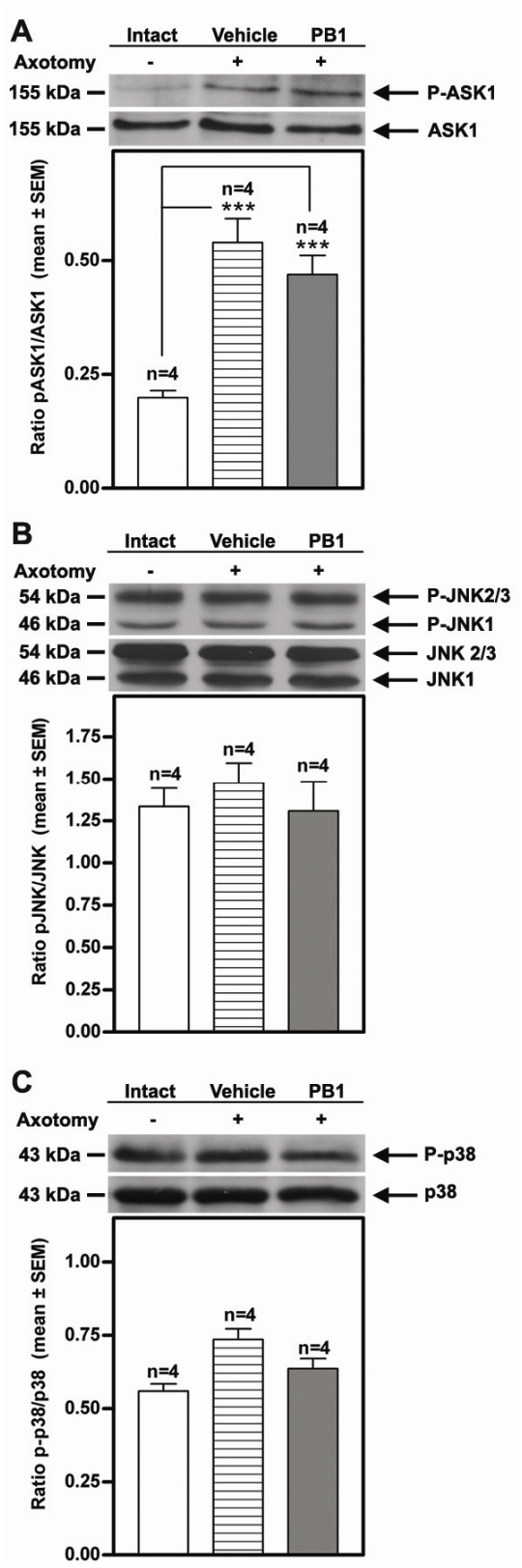
A
Intact
Vehicle
PB1
Axotomy
-
+
+
155 kDa
P-ASK1
155 kDa
ASK1
Ratio pASK1/ASK1 (mean ± SEM)
n=4
***
n=4
***
n=4
0.50
0.25
0.00
B
Intact
Vehicle
PB1
Axotomy
-
+
+
54 kDa
P-JNK2/3
46 kDa
P-JNK1
54 kDa
JNK 2/3
46 kDa
JNK1
Ratio pJNK/JNK (mean ± SEM)
1.75
1.50
1.25
1.00
0.75
0.50
0.25
0.00
n=4
n=4
n=4
C
Intact
Vehicle
PB1
Axotomy
-
+
+
43 kDa
P-p38
43 kDa
p38
Ratio p-p38/p38 (mean ± SEM)
1.00
0.75
0.50
0.25
0.00
n=4
n=4
n=4

FIGURE 6

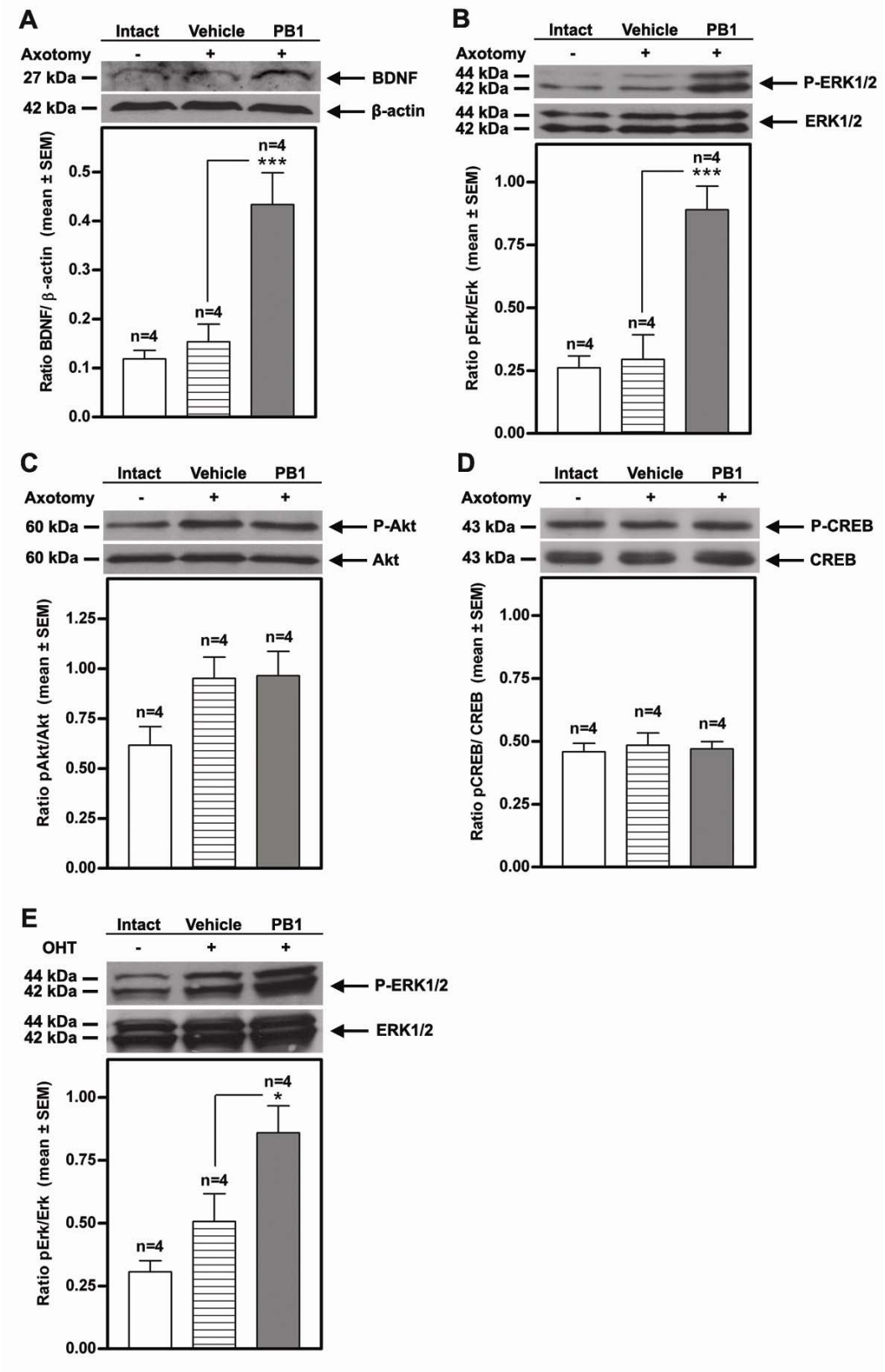
A
Intact
Vehicle
PB1
Axotomy
-
+
+
27 kDa
BDNF
42 kDa
β-actin
Ratio BDNF/ β-actin (mean ± SEM)
n=4
n=4
n=4
***
B
Intact
Vehicle
PB1
Axotomy
-
+
+
44 kDa
42 kDa
P-ERK1/2
44 kDa
42 kDa
ERK1/2
Ratio pErk/Erk (mean ± SEM)
n=4
n=4
n=4
***
C
Intact
Vehicle
PB1
Axotomy
-
+
+
60 kDa
P-Akt
60 kDa
Akt
Ratio pAkt/Akt (mean ± SEM)
n=4
n=4
n=4
D
Intact
Vehicle
PB1
Axotomy
-
+
+
43 kDa
P-CREB
43 kDa
CREB
Ratio pCREB/ CREB (mean ± SEM)
n=4
n=4
n=4
E
Intact
Vehicle
PB1
OHT
-
+
+
44 kDa
42 kDa
P-ERK1/2
44 kDa
42 kDa
ERK1/2
Ratio pErk/Erk (mean ± SEM)
n=4
n=4
n=4
*

FIGURE 7

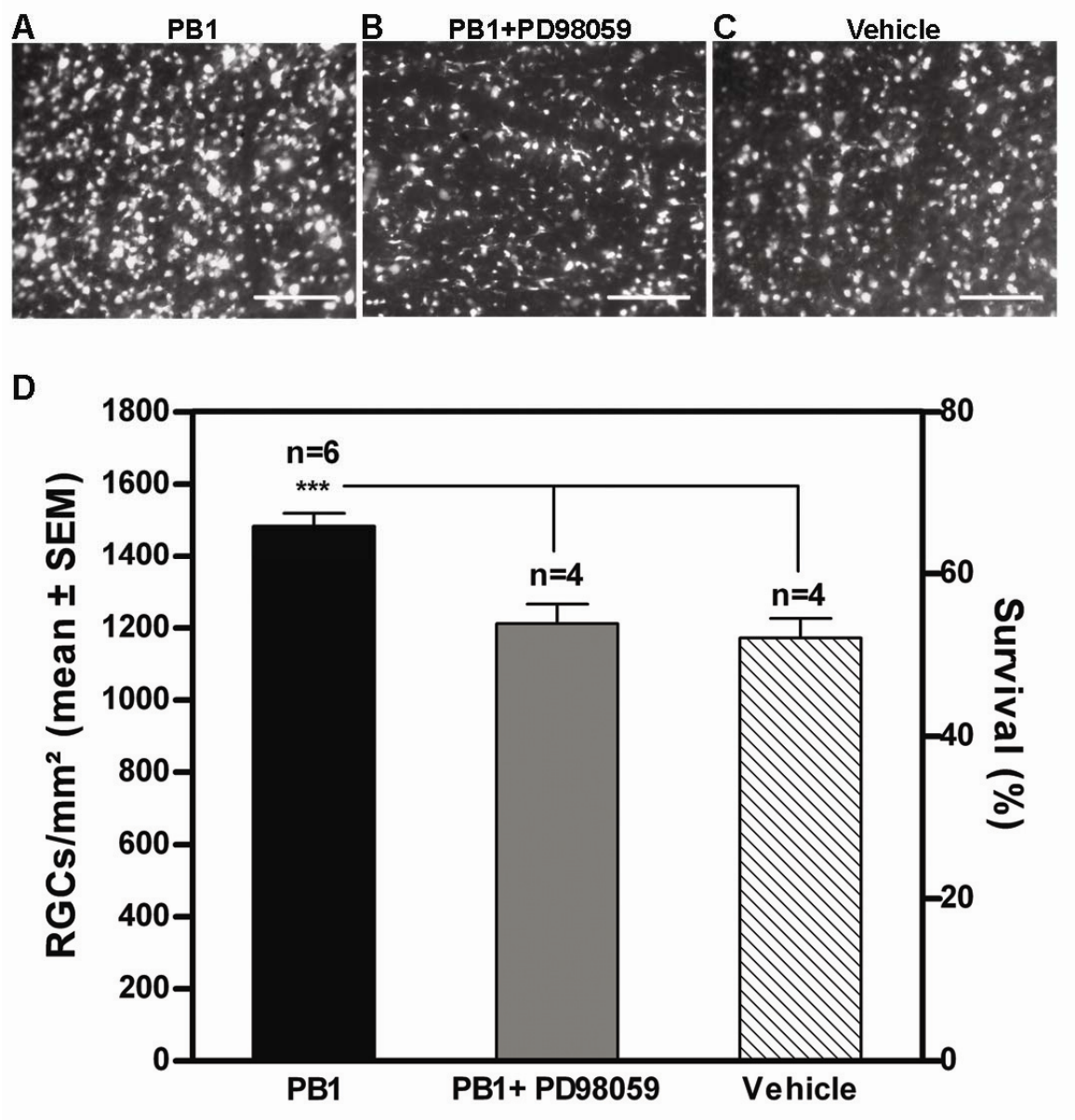
A
PB1
B
PB1+PD98059
C
Vehicle
D
RGCs/mm² (mean ± SEM)
Survival (%)
1800
1600
1400
1200
1000
800
600
400
200
0
80
60
40
20
0
n=6
***
n=4
n=4
PB1
PB1+ PD98059
Vehicle

CHAPTER 5

V. GENERAL DISCUSSION

V.1 STRUCTURAL PROTECTION IN GLAUCOMA

V.1.1 Galantamine, an acetylcholinesterase inhibitor, protects RGCs soma against IOP induced cell death.

In the first article presented in this thesis (Chapter 2), I explored the neuroprotective properties of galantamine in experimental glaucoma. For more than a decade, galantamine hydrobromide has been taken orally by Alzheimer's disease patient, resulting in optimum concentrations in the brain and providing significant improvements in their cognitive functions (Bores et al., 1996; Jann et al., 2002; Scott and Goa, 2000). Studies in human, dogs, mice and rats has shown that intraperitoneal, intravenous and oral administration of radioactively labeled galantamine is followed by rapid absorption and presence of galantamine in the plasma and brain tissues of the subjects (Mannens et al., 2002; Sweeney et al., 1989). Our data showed that systemic administration of galantamine significantly improves the survival of RGC somata. Systemic treatment with galantamine did not reduce the IOP in glaucomatous eyes and was able to significantly delay RGC death in an IOP-independent model of traumatic optic nerve damage (axotomy).

Unlike nicotinic or muscarinic agonists, galantamine has several advantages for the treatment of chronic neurodegenerative diseases like glaucoma. First, galantamine is a small molecule which easily crosses the blood-retinal-barrier. Second, the effect of galantamine is mediated by increasing the availability of ACh through inhibition of the AChE enzyme. Also, the allosteric potentiating properties of galantamine on nAChRs might enhance the sensitivity of these receptors and therefore improve the cholinergic signaling (Schrattenholz et al., 1996). We found that compared to other AChE inhibitors like donepezil, galantamine has a higher neuroprotective effect which this will translate into better long-term tolerability for galantamine. Unlike galantamine (a competitive AChE inhibitor), donepezil is a non-competitive AChE inhibitor and in the long-term can lead to downregulation of AChRs and development of resistance to the drug (Farlow, 2003; Wilkinson, 1999).

V.1.2. Phenylphosphine borane reducing complex 1 (PB1), promotes RGC survival in different paradigms of optic nerve injury.

In the third article presented here (Chapter 4), we described the neuroprotective properties of a small molecule free radical scavenger, PB1, in experimental glaucoma. The evidence gathered from glaucoma patients and experimental animals suggests that oxidative damage is a major contributor to the pathology of glaucoma (Izzotti et al., 2006; Tezel, 2006). Recent studies demonstrated that production of superoxide precedes RGC apoptosis and its levels increase dramatically at the single-cell level (Kanamori et al., 2010). Therefore, neutralizing excessive intracellular superoxide could provide neuroprotection.

To use a scavenging compound for therapeutic purposes, it must meet at least two requirements: high cellular permeability for easy delivery and high stability. PB1 is a phosphine based scavenger which contains a borane atom to protect the phosphine from oxidation and increase the chemical stability of the compound during storage and administration. In addition, having a non-polar phenyl group increases the ability of PB1 to cross the cell membranes. PB1 has been designed to inhibit oxidation of sulfhydryl groups on critical cellular molecules. Our data demonstrate that intravitreal delivery of PB1 in glaucomatous eyes, significantly promotes RGC survival. PB1 was also neuroprotective in the traumatic optic nerve injury (axotomy) and improved survival of RGCs. PB1 was injected intravitreally two weeks after OHT and RGC survival was examined at three or five weeks after OHT. PB1 extended the survival of damaged RGCs for weeks after initial delivery, a fact that highlights the importance of ROS neutralizing early in the development of the glaucoma.

Since labeling of RGCs with tracers like Fluorogold and DiI is one of the major techniques in our laboratory, we have established a protocol to identify the migratory phagocytic cells (that uptake the cell debris and the tracer) in order to exclude them from our RGC quantification. As showed in the Figure 2, E-F, Chapter 4, page 146; the phagocytic cells are detectable based on their intense Fluorogold content, thin and elongated cell body and their long processes. To reconfirm the identity of these cells, immunostaining with specific antibodies against the microglia and macrophage (isolectin-B4 and ED-1) has been used in our laboratory (Cheng et al., 2002). In general,

due to slower RGC death rate in glaucoma there are fewer phagocytic cells in the glaucomatous retinas at any given time compare to axotomy model. In the axotomy model, due to rapid rate and numerous concomitant RGCs death, the presence of phagocytic cells is more intense and demands trained eye to eliminate them from quantifications. However, an experienced researcher can easily distinguish phagocytic cells even in axotomy samples. We have recently adapted an immunostaining method for labeling RGCs that is based on detection of a protein called Brn3a, a transcription factor that is specifically expressed by RGCs; this technique allows easier and accurate quantification of RGCs in the retina (Nadal-Nicols et al., 2009).

V.1.3. Protection of RGC axons in glaucoma

One of the features of glaucomatous damage is the degenerative loss of RGC axons in the optic nerve. Loss of RGC axons becomes apparent as axonal bundles in the optic nerve develop irregularities and RGC axons become swollen and lose their myelin sheaths (Chauhan et al., 2002; Quigley et al., 1988). In our experimental glaucoma model, analysis of optic nerve cross-sections from glaucomatous eyes indicated a significant loss of axons at three and five weeks after induction of OHT. In the animals receiving daily treatment with galantamine, there was a significant increase in the number of healthy axons and integrity of the axonal bundles in the optic nerve. Therefore, RGC soma protection by galantamine is complemented by the RGC axonal protection.

Despite mediating significant RGC soma survival, PB1 was only able to protect RGC axons up to three weeks after induction of OHT. The difference in the protective potentials of PB1 at the axonal and cell soma levels could be explained using two arguments. First, the promotion of RGC soma survival and axonal regeneration are mediated by different pathways. For instance, while AAV-mediated increase of FGF-2 levels did not result in much RGC survival after axotomy, it significantly promoted regeneration of RGC axons (Sapieha et al., 2003). Conversely, Erk1/2 activation significantly improved RGCs survival after optic nerve injury but failed to induce RGC axon regeneration (Pernet et al., 2005). Galantamine, by activating different categories of ACh receptors, can simultaneously trigger several pathways and therefore mediate both RGC soma and axon protection. Since in our experiments PB1 treatment resulted in up-

regulation of BDNF and activation of ERK1/2 pathway, it is expected that PB1 mainly promotes RGC soma protection. Secondly, the delivery rout might be an important factor affecting the capacity of PB1 and galantamine to achieve axonal protection. Galantamine was delivered systemically for the entire experimental period, ensuring its availability and facilitating access to the optic nerve via the blood circulation. PB1 however, was only delivered once and intravitreally, which greatly limited its availability and access to the optic nerve. In a view of the current limitations of PB1 treatment, future studies should take into consideration a time-release nanoparticle-based delivery system or eye drops to maximize neuroprotective effects of PB1.

With regards to the timeline of the experiments, it might be argued that why our studies have not been extended beyond the 5 weeks after OHT surgery. In a previously published work in our laboratory, we have shown that RGC survival could be extended up to 7 weeks after OHT surgery (Zhou et al., 2005). However, in that case the neuroprotection was achieved by induction of a potent neuroprotective pathway through infecting the RGCs with a recombinant adeno-associated virus to transduce RGCs with genes encoding constitutively active MEK1. Compared to galantamine neuroprotection, the significant increase in the activation of Erk1/2 provides more robust protection of RGCs that could last for a longer period of time. I believe that galantamine represented significant neuroprotective ability in our experiments. However, as it is reflected in our functional experiments, rapid elevation of IOP and severity of the damage to the axons in this model, limits the prospects of the long term evaluation of galantamine neuroprotective profile. Therefore, to better evaluate the long-term neuroprotective potential of galantamine (beyond the 5 weeks), one might use an alternative glaucoma model like cauterization model with slower rate of IOP increase (Danias et al., 2006).

V.1.4. Protection of retinal microvessels in glaucoma

The findings presented in the second article of this thesis (Chapter 3) demonstrated that degenerative changes in glaucomatous retinas are not limited to RGCs but also affect retinal microvessels. Vascular atrophy and loss of microvasculature are characteristics of other neurodegenerative diseases like AD (Bailey et al., 2004; Weller et al., 2009). In AD, affected areas of the brain are marked by reduced capillary branching,

and loss of capillaries (Brown, 2010b; Challa et al., 2004). However, the current knowledge about the effect of glaucoma on the retinal microvasculature and their relation to RGCs death is limited. We initially detected a major capillary loss at five weeks after OHT; however, a more detailed analysis revealed that the loss of capillaries occurs as early as three days after OHT surgery. Our findings also indicated that galantamine administratation led to a higher density of retinal microvessels.

Not only the vasoprotective effects of galantamine expand the therapeutic use of this drug, but it also opens the possibility of preventive treatment in glaucoma regarding vascular risk factors. The idea of a preventive strategy to minimize vascular damage is not new. For instance, loss of retinal capillaries is a major characteristics of diabetic retinopathy caused by leukocyte adhesion to the endothelium and loss of pericytes (Hammes et al., 2002; Joussen et al., 2001). Inhibition of leukostasis by drugs like captopril and losartan or application of NGF to prevent pericytes death significantly reduces the number of degenerating capillaries in experimental diabetes (Hammes et al., 1995; Zhang et al., 2007b).

Unlike RGCs that are irreversibly lost, the retinal capillaries are dynamic and their capacity to regenerate can provide important support for long-term neuronal protection. Such a strategy has been proposed for the treatment of diabetic retinas. In another approach, intravitreally injected endothelial precursor cells were able to migrate into damaged or empty basement membrane of string capillaries in the diabetic retinas, and repaired the injured vessels (Bhatwadekar et al., 2009; Caballero et al., 2007). Here we showed the retinal capillaries are indeed part of initial insult to the retina in glaucoma and that galantamine provides a novel, drug-based therapy for neuroprotection and vasoprotection in glaucoma.

V.2. FUNCTIONAL PROTECTION IN GLAUCOMA

V.2.1. Galantamine treatment results in the recovery of visual evoked potentials

Visual information is converted to electrochemical signal by photoreceptors and relayed to the visual centers via RGC axons. The LGN is one of the main central targets of RGC axons in primates (Schiller and Malpeli, 1977). In the rodents, the majority of

RGC axons project to the superior colliculus (SC) and a smaller number to the dorsal lateral geniculate nucleus (dLGN) (Lund et al., 1976). Evidence shows that progression of glaucoma is often accompanied by visual deficits. Studies in primate glaucoma also indicate a significant reduction in light-stimulated responses in the visual cortex (Hare et al., 2001a). Cytochrome oxidase histochemistry also confirmed a significant reduction of functional inputs from RGCs to higher brain centers such as the LGN and visual cortex in primates with glaucoma (Crawford et al., 2001; Crawford et al., 2000).

Pathological changes in the optic disk and damage to RGC axons are proposed to be the main cause of visual deficits. We found significant damage and loss of axons in the optic nerves at five weeks after induction of OHT. Therefore, it was not surprising that we failed to record any signal at the SC following flash stimulation of glaucomatous eyes. Galantamine treatment failed to recover the VEP signal despite the significant protection of RGC axons and soma. We hypothesized that sustained high IOP impairs the physiological function of surviving RGCs and therefore results in visual defects. To evaluate this hypothesis, we combined galantamine treatment with an IOP lowering strategy. In this protocol, the IOP in the glaucomatous eye was controlled by topical (corneal) application of timolol, a commonly used ß-adrenergic receptor blocker. This treatment resulted in partial the recovery of VEP in galantamine-treated animals. The recovery of VEP was not due to a neuroprotective effect of timolol because there was no functional recovery in the PBS treated animals and RGC survival did not significantly increase following timolol application. In conclusion, our functional studies highlight the importance of a combined therapeutic strategy for the treatment of glaucoma, one that incorporates both control of IOP regulation and neuroprotection of RGCs.

With regards to an approach to have a better understanding about the health of RGCs at the end of experiments, two complementary methods could be used (besides VEP recordings). First, to use an immunostaining procedure like Brn3a, so we can exclusively label healthy and alive RGCs (Nadal-Nicols et al., 2009). Second, to apply the Fluorogold on the SC at the end of experiments instead of labeling the RGCs at the beginning; this method provides better information about the number of healthy RGCs that were able to pickup the fluorescent dye with their axonal terminals and transport it

back to their somata, therefore also represents the integrity of RGC connections to the brain centers.

V.2.2. Galantamine improves retinal blood flow in glaucomatous eyes

In the second article presented in this thesis (Chapter 3) we reported a significant recovery of retinal blood flow by galantamine. Neurovascular coupling is a well known activity-dependent phenomenon in the brain and retina. Stimulation of the retina by light flicker results in the dilation of retinal vessels leading to increase in retinal blood flow (Formaz et al., 1997; Ito et al., 2001; Scheiner et al., 1994).

Insufficient retinal blood flow can affect the neuronal activity and consequently translate into an abnormal VEP response in glaucomatous eyes. One of the steps in our VEP recording protocol was first to ensure the animals have an ERGs within the normal range. ERG recordings provided important information about the integrity of the intraretinal signaling as we found significant reduction of the b-wave in a number of animals with high IOP. Reducing the retinal blood flow by application of Et-1 have shown to significantly decrease the magnitude of VEP response (Hara et al., 2005). Elevation of IOP can similarly affect the retinal blood flow, resulting in functional deficits (Chen and Budenz, 1998; Yaoeda et al., 2003). In fact one of our findings following the application of timolol was significant improvement of the ERGs (data not shown). This data indicates that survival and health of RGCs is only one of the factors necessary for functional recovery in glaucoma.

The vasodilatory properties of galantamine, shown in our *ex vivo* experiments, is likely to lead the improved blood circulation *in vivo*. Nevertheless, the physical stress of high IOP in our experimental model demanded additional IOP lowering intervention for functional recovery. Visual deficits do not simply reflect IOP levels in glaucoma, as stepwise increases of IOP are better tolerated by healthy subjects than POAG patients (Pillunat et al., 1985). Therefore, it is likely that an underlying vasomodulatory problem in glaucomatous eyes plays a role in RGC death and disease progression in addition to a decline in normal retinal function.

V.3. MECHANISMS OF NEUROPROTECTION IN GLAUCOMA

V.3.1. Acetylcholine receptors and galantamine-mediated neuronal and vascular protection

Since galantamine is an allosteric potentiating ligand of nAChRs (Pereira et al., 2002; Samochocki et al., 2003), we initially hypothesized that its neuroprotective properties were mediated through nAChRs signaling. However, using both blockers of nAChRs and mAChRs, we found that mAChRs had a prominent role in galantamine-mediated neuroprotection. In our experiments with glaucoma model, the main method of drug delivery was daily i.p. injections of galantamine. However, intraocular application of galantamine was also used in the axotomy model. Intraocular injections of galantamine were in line with the intraocular injection of other drugs since systemic administration for a number of compounds (several muscarinic blockers) was not possible. Systemic application of muscarinic and nicotinic blockers used in our experiments had the risk of unwanted side effects (like Pirenzepine) or was uneconomical; some of them also did not cross the blood-retinal barrier. Scopolamine was the only muscarinic blocker capable of passing the blood-retinal barrier with minimum side effects and was used intraperitoneally along with galantamine in OHT experiments (Tang et al., 1997; Toide, 1989; Wilson, 2001).

Using subtype specific blockers of mAChRs, we found that M1 and M4 played a significant role in RGC survival, whereas galantamine-induced improvement of retinal blood flow and vascular protection depended on M1 and M3 subtypes. Studies on the retinal localization of mAChR subtypes in primate, rat and chick retinas showed that amacrine cells express M2 and M4 subtype, Müller cells express both M1 and M4 subtypes and bipolar cells and horizontal cells express M3 subtype (Da Silva et al., 2008; Fischer et al., 1998; Yamada et al., 2003). G-protein-coupled mAChR regulate Ca^{2+} entry that is linked to several signal transduction pathways that mediate cellular survival (Figure V.1). On the same note, although expression of mAChRs has not been detected on RGCs; muscarine increases the intracellular Ca^{2+} in rabbit RGCs (Baldridge, 1996). Future studies on intracellular calcium levels after application of galantamine might provide a better understanding of the role of mAChRs on RGC survival.

Galantamine-mediated signaling through neighboring Müller glia or neurons may also lead to production of pro-survival factors that protect injured RGCs. For instance, increasing the antioxidant capacity of the retina could significantly improve RGC survival in a non-cell-autonomous manner. Oxidative stress has been proposed to be a major contributor in glaucomatous neurodegeneration. Müller cells and horizontal cells synthesize and release glutathione which protects the retina against oxidative damage (Pow and Crook, 1995). There are reports of reduction in retinal antioxidant capacity in experimental glaucoma (Jann et al., 2002; Moreno et al., 2004). Muscarinic AChRs are involved in the activation of cellular antioxidant pathways, as shown in figure 1. Signaling through M1 subtype of mAChRs contributes to the regulation of Nrf2 activity (Espada et al., 2009). Nrf2 is a transcription factor that controls the expression of genes containing AREs (Kensler et al., 2007). HIF-1 is another transcription factor linked to the cellular response in hypoxic conditions and M1 mAChR has been shown to be involved in HIF-1 regulation (Hirota et al., 2004). Therefore, galantamine treatment via activation of mAChRs on Müller and horizontal cells may increase the antioxidant capacity of the retina and improve RGC survival. These data support a model in which non-cell-autonomous signaling events downstream of mAChR play a major role in galantamine-induced RGC neuroprotection. Unlike RGCs, retinal and brain endothelial cells express the M1 and M3 subtypes of mAChRs (Elhusseiny et al., 1999; Sastry, 1985b), therefore, galantamine-mediated signaling through this receptors can directly activate pro-survival pathways in endothelial cells.

Cholinergic signaling through mAChRs mediates vasodilation in the brain (Bény et al., 2008; Dauphin et al., 1994) and the presence of endothelial cells is necessary for this process (Schrattenholz et al., 1996). We similarly demonstrated that endothelial cells were necessary for galantamine-mediated relaxation of isolated retinal arterioles. Interestingly, endothelial cells are part of a non-neuronal cholinergic system due to expression of ChAT and possession of vesicular acetylcholine transporters (Kirkpatrick et al., 2001). This suggests that paracrine cholinergic signaling might contribute in endothelial cells vasodilatory functions. Muscarinic AChRs mediate release of Ca^{2+} from intracellular stores that triggers the production of endothelium-derived vasodilators like NO and prostacyclin (Fleming and Busse, 1999; Lückhoff et al., 1988).

FIGURE 1.

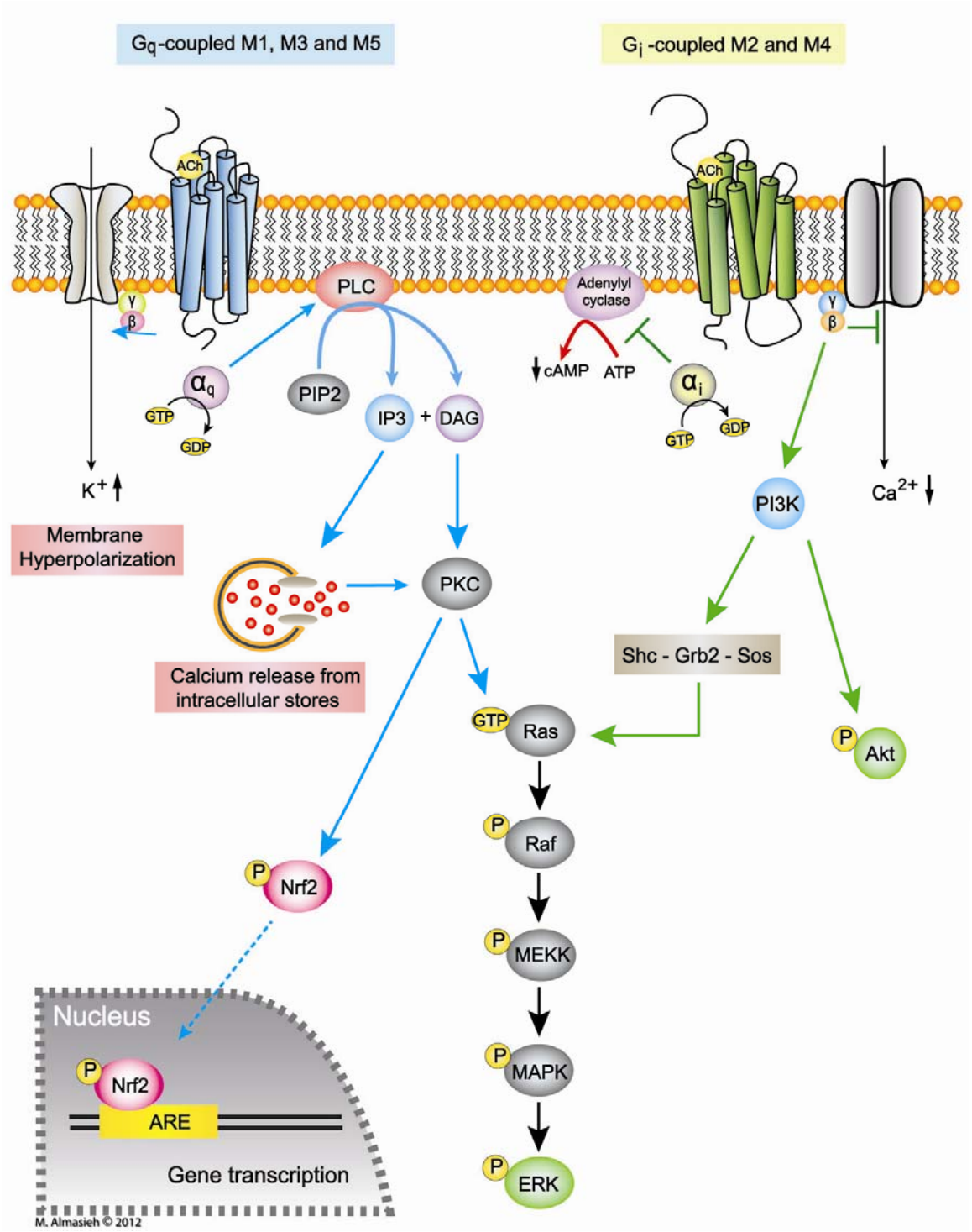
Gq-coupled M1, M3 and M5
Gi -coupled M2 and M4
ACh
ACh
PLC
Adenylyl cyclase
γ
β
γ
β
αq
GTP
GDP
PIP2
IP3 + DAG
cAMP
ATP
αi
GTP
GDP
K+
Membrane Hyperpolarization
PI3K
Ca2+
PKC
Calcium release from intracellular stores
Shc - Grb2 - Sos
GTP
Ras
P
Akt
P
Raf
P
Nrf2
P
MEKK
Nucleus
P
Nrf2
ARE
P
MAPK
Gene transcription
P
ERK
M. Almasieh © 2012

Figure 1. Muscarinic AChRs signaling and cell survival pathways. The M1, M3, and M5 mAChRs are selectively couple to the Gq/G11 type of G-proteins. Upon binding the ligand, these receptors undergo a conformational change exposing the binding site for the G-protein. The receptor then facilitates the exchange of G-protein-bound GDP for GTP that causes the dissociation of Gα from the Gβγ dimer. The GTP-bound Gα activates phospholipase C (PLC). Hydrolysis of phosphoinositol 4, 5-bisphosphate (PIP2) by PLC produces two intracellular messengers: 1,2-diacylglycerol (DAG) and inositol 1,4,5-trisphosphate (IP3). Membrane bound DAG promotes the translocation of PKC from the cytoplasm to the membrane and its subsequent activation. PKC then activates the Ras and consequently MAPK survival pathway. IP3 by binding to IP3 receptors located on cytoplasmic calcium stores results in the opening of their Ca^{2+} channels and release of Ca^{2+} into the cytosol. Increase of cytoplasmic Ca^{2+} levels activates PKC and consequently through MAPK pathway or activation of transcription factors like Nrf2 promotes cell survival. The Gβγ remains anchored to the membrane and by facilitating the K+ influx result in membrane hyperpolarization.

M2 and M4 receptors are coupled to $G_{i/o}$ type of G-proteins. Upon binding the ligand receptor facilitates exchange of GDP for GTP on Gα resulting in dissociation of the heterotrimer G-protein components. Gα then interacts with adenylcyclase that decreases in cAMP levels. The Gβγ activate the PI3K that promote cell survival via Akt or MAPK pathways. Interaction of Gβγ with calcium channel results in reduction of Ca^{2+} influx. Source of image: Mohammadali Almasieh.

Activation of M1/M3 receptors in the retina also results in the stimulation of nNOS activity and an increase in nNOS mRNA expression (Borda et al., 2005). Interestingly, in a eNOS deficient mice model, retinal expression of nNOS was significantly up-regulated resulting in normal retinal vasculature development (Al Shabrawey et al., 2003). Therefore, galantamine-mediated signaling through neuronal mAChRs could activate nNOS and participate in the improvement of retinal blood flow.

At the moment we are exploring several techniques to study the expression of muscarinic subtypes on RGCs and endothelial cells. Using the flow cytometry to separate RGCs and/or endothelial cells from retinal suspension and laser capture microdissection technique to separate RGCs from flat mounted retinas are currently in progress. Performing RT-PCR on this purified cell populations will help us to identify the specific muscarinic receptors expressed by these cells types. It is also important to remember allostric potentiating site of galantamine on nicotinic receptors is a different site from ligand binding site. Therefore it is not surprising if despite using nicotinic blockers, the allostric site still would be available for interaction with galantamine. The only way to study this interaction is to use an antibody called FK1, which selectively blocks the allosterically potentiating ligand site on nAChRs (Kihara et al., 2004). This antibody is not commercially available but we are in the process of a collaborative work to use this antibody in our future experiments.

V.3.2. Molecular mechanisms of PB1-mediated RGC neuroprotection

When the production of ROS overwhelms cellular antioxidant capacity, it results in disturbance of the redox system that in turn modifies activity of several cellular signaling pathways. The redox state of key cellular proteins and enzymes controls the pattern of gene expression, posttranslational protein modifications and ion channels properties. Pro-apoptotic pathways like SAPK are activated as their redox sensor member, ASK1, initiates a signaling cascade that leads to JNK and p38 stimulation and subsequent cell death (Kyriakis and Avruch, 2001; Sumbayev and Yasinska, 2005). Based on the molecular characteristics of borane-protected phosphines, we expected that PB1, via scavenging superoxide, would block pro-apoptotic pathways. However, PB1 treatment did not reduce the phosphorylated levels of ASK1 or p38 after axotomy.

Another possibility for PB1-induced RGC protection is through modification of survival pathways. The activity of a number of transcription factors like NF-κB, Nrf2 and HIF-1 is regulated by their redox state (Trachootham et al., 2008). Consequently, we found a significant increase of BDNF levels in the PB1-treated axotomized retinas. There are a number of studies suggesting that BDNF up-regulation is an early response in RGCs that undergo axonal injury. Retinal BDNF levels increase following both optic nerve axotomy (Gao et al., 1997) and experimental glaucoma (Guo et al., 2011; Rudzinski et al., 2004). A recent study used laser capture microdissection to produce RGC-enriched mRNA samples and was able to indicate a distinct increase in the BDNF mRNA levels early after ocular hypertension (Wang et al., 2011).

PB1 might induce the BDNF up-regulation at the transcriptional level. The cAMP response element binding protein (CREB) is a transcription factor regulating BDNF gene expression and its activity is also subjected to redox modulation (Bedogni et al., 2003; Tao et al., 1998). CREB is involved in the regulation of ROS detoxification (Herzig et al., 2001; Krönke et al., 2003; Lee et al., 2009) and in response to BDNF promotes transcription of pro-survival molecules such as Bcl-2 (Bonni et al., 1995; Finkbeiner et al., 1997; Wilson et al., 1996). CREB phosphorylation is triggered by Ca^{2+} influx through receptors like NMDA and requires translocation of calmodulin from the cytoplasm to the nucleus (Deisseroth et al., 1998). NMDA receptors contain a redox modulatory site and oxidation or reduction state of this site modifies Ca^{2+} current through these receptors (Lei et al., 1992; Levy et al., 1990). In our experiments, PB1 treatment did not result in CREB activation, however, since CREB activity might be brief and the transcriptional control of BDNF is complex, this issue requires further study.

The abundant expression of TrkB by RGCs translates BDNF stimulation into a strong pro-survival signaling through its downstream survival pathways ERK1/2 and Akt (Pérez and Caminos, 1995). In agreement with this hypothesis, we found significant increase in phospho-ERK1/2 levels in PB1 treated retinas. PB1 treatment did not induce Akt activation, consistent with previous studies showing that combined BDNF and TrkB upregulation promoted RGC survival via ERK1/2 pathway but not Akt (Cheng et al., 2002). Components of the ERK1/2 pathway are also regulated by their redox state. For instance, Ras, an upstream activator of ERK1/2 is under redox control (Lander et al.,

1996; Mallis et al., 2001). In addition, the thiol site on the TrkB receptor itself can be subject of a modification that results in autophosphorylation and activation of the tyrosine kinase receptors (Chen et al., 1998).

V.4. GENERAL CONCLUSIONS

The work presented in this thesis introduces new approaches in the treatment of glaucoma and provides insight into novel molecular mechanisms involved in this disease. We characterized the neuroprotective effects of galantamine and PB1 in experimental glaucoma with the goals to extend RGC survival and to improve functional outcome. Our study revealed the potent role of galantamine in the protection of RGC somata and axons. Galantamine, by protecting the retinal capillaries and improving retinal blood flow, also targets potential vascular defects in glaucoma. We found that the neuroprotective effect of galantamine is mediated through activity of mAChRs. G-protein-coupled M1 and M4 mAChR were involved in RGCs survival and axonal protection whereas vascular protection and blood flow improvement were mediated through M1 and M3 mAChRs. Galantamine has broad effect acting on other neurotransmitter systems, such as modulating the release of glutamate, serotonin and gamma-aminobutyric acid, thus expanding the possibility of RGC neuroprotection through other signaling pathways. The data from our functional studies suggest that an ideal therapy for glaucoma is to combine standard pressure controlling drugs and a neuroprotective treatment.

Oxidative stress contributes to glaucoma pathology and an imbalance in the redox regulation of critical proteins might lead to RGC death. We showed that treatment with PB1, a phosphane-borane reducing compound, significantly promoted RGCs survival. Significant improvement in the survival of axotomized RGCs was also achieved with PB1. Survival was mediated through up-regulation of BDNF by PB1and activation of the pro-survival ERK1/2 pathway. Redox balance plays an important role in the regulation of BDNF production and ERK1/2 pathway activity; therefore our study offers the interesting possibility that redox homeostasis in RGCs can influence neurotrophin-related pathways that promote RGC survival after axonal injury.

REFERENCES

Abramov, A., Jacobson, J., Wientjes, F., Hothersall, J., Canevari, L., Duchen, M., 2005. Expression and modulation of an NADPH oxidase in mammalian astrocytes. J Neurosci. 25, 9176-9184.

Ahmed, F.A., Chaudhary, P., Sharma, S.C., 2001. Effects of increased intraocular pressure on rat retinal ganglion cells. Int J Dev Neurosci. 19, 209-218.

Ahrlich, K., De Moraes, C.G.V., Teng, C., Prata, T., Tello, C., Ritch, R., Liebmann, J., 2010. Visual field progression differences between normal-tension and exfoliative high-tension glaucoma. Invest Ophthalmol Vis Sci. 51, 1458-1463.

Aihara, M., Lindsey, J., Weinreb, R., 2003. Experimental mouse ocular hypertension: establishment of the model. Invest Ophthalmol Vis Sci. 44, 4314-4320.

Al-Gayyar, M.M.H., Abdelsaid, M., Matragoon, S., Pillai, B., El Remessy, A., 2010. Neurovascular protective effect of FeTPPs in N-methyl-D-aspartate model: similarities to diabetes. Am J Pathol. 177, 1187-1197.

Al Shabrawey, M., El Remessy, A., Gu, X., Brooks, S., Hamed, M., Huang, P., Caldwell, R., 2003. Normal vascular development in mice deficient in endothelial NO synthase: possible role of neuronal NO synthase. Mol Vis. 9, 549-558.

Alderton, W.K., Cooper, C.E., Knowles, R.G., 2001. Nitric oxide synthases: structure, function and inhibition. Biochem J. 357, 593-615.

Andersen, J.K., 2004. Oxidative stress in neurodegeneration: cause or consequence? Nat Med. 5, S18-S25.

Anderson, D.R., Hendrickson, A., 1974. Effect of intraocular pressure on rapid axoplasmic transport in monkey optic nerve. Invest Ophthalmol. 13, 771-783.

Arias, E., Alés, E., Gabilan, N.H., Cano-Abad, M.F., Villarroya, M., García, A.G., López, M.G., 2004. Galantamine prevents apoptosis induced by [beta]-amyloid and thapsigargin: involvement of nicotinic acetylcholine receptors. Neuropharmacol. 46, 103-114.

Asomugha, C., Linn, D., Linn, C., 2010. ACh receptors link two signaling pathways to neuroprotection against glutamate-induced excitotoxicity in isolated RGCs. J Neurochem. 112, 214-226.

Aung, T., Husain, R., Gazzard, G., Chan, Y.-H., Devereux, J., Hoh, S.-T., Seah, S.K.L., 2004. Changes in retinal nerve fiber layer thickness after acute primary angle closure. Ophthalmology 111, 1475-1479.

Babizhayev, M.A., Bunin, A., 1989. Lipid peroxidation in open-angle glaucoma. Acta Ophthalmologica 67, 371-377.

Bachschmid, M., Schildknecht, S., Ullrich, V., 2005. Redox regulation of vascular prostanoid synthesis by the nitric oxide-superoxide system. Biochem. Biophys. Res. Commun. 338, 536-542.

Bailey, T., Rivara, C., Rocher, A., Hof, P., 2004. The nature and effects of cortical microvascular pathology in aging and Alzheimer's disease. Neurol Res. 26, 573-578.

Baldridge, W.H., 1996. Optical recordings of the effects of cholinergic ligands on neurons in the ganglion cell layer of mammalian retina. J Neurosci. 16, 5060-5072.

Bandopadhyay, R., Orte, C., Lawrenson, J.G., Reid, A.R., De Silva, S., Allt, G., 2001. Contractile proteins in pericytes at the blood-brain and blood-retinal barriers. J Neurocytol. 30, 35-44.

Beckman, J.S., 1996. Oxidative damage and tyrosine nitration from peroxynitrite. Chem Res Toxicol. 9, 836-844.

Beckman, J.S., Koppenol, W.H., 1996. Nitric oxide, superoxide, and peroxynitrite: the good, the bad, and ugly. Am J Physiol. 271, C1424-C1437.

Bedogni, B., Pani, G., Colavitti, R., Riccio, A., Borrello, S., Murphy, M., Smith, R., Eboli, M.L., Galeotti, T., 2003. Redox Regulation of cAMP-responsive Element-binding Protein and Induction of Manganous Superoxide Dismutase in Nerve Growth Factor-dependent Cell Survival. J. Biol. Chem. 278, 16510-16519.

Beelke, M., Sannita, W.G., 2002. Cholinergic function and dysfunction in the visual system. Methods Find Exp Clin Pharmacol. 24 Suppl D, 113-117.

Behndig, A., Svensson, B., Marklund, S.L., Karlsson, K., 1998. Superoxide dismutase isoenzymes in the human eye. Invest Ophthalmol Vis Sci. 39, 471-475.

Bény, J.-L., Nguyen, M., Marino, M., Matsui, M., 2008. Muscarinic receptor knockout mice confirm involvement of M3 receptor in endothelium-dependent vasodilatation in mouse arteries. J Cardiovasc Pharmacol. 51, 505-512.

Berkelaar, M., Clarke, D.B., Wang, Y.-C., Bray, G.M., Aguayo, A.J., 1994. Axotomy results in delayed death and apoptosis of retinal ganglion cells in adult rats. J. Neurosci. 14, 4368-4374.

Berkeley, J.L., Gomeza, J., Wess, J., Hamilton, S.E., Nathanson, N.M., Levey, A.I., 2001. M1 muscarinic acetylcholine receptors activate extracellular signal-regulated kinase in CA1 pyramidal neurons in mouse hippocampal slices. Mol Cell Neurosci. 18, 512-524.

Bertram, K.M., Bula, D.V., Pulido, J.S., Shippy, S.A., Gautam, S., Lu, M.J., Hatfield, R.M., Kim, J.H., Quirk, M.T., Arroyo, J.G., 2008. Amino-acid levels in subretinal and vitreous fluid of patients with retinal detachment. Eye 22, 582-589.

Bhatwadekar, A., Glenn, J., Curtis, T., Grant, M., Stitt, A., Gardiner, T., 2009. Retinal endothelial cell apoptosis stimulates recruitment of endothelial progenitor cells. Invest Ophthalmol Vis Sci. 50, 4967-4973.

Bigelow, D., Qian, W.-J., 2008. Quantitative proteome mapping of nitrotyrosines. Methods Enzymol 440, 191-205.

Birks, J., 2006. Cholinesterase inhibitors for Alzheimer's disease. Cochrane Database Syst Rev., CD005593.

Bjärnhall, G., Tomic, L., Mishima, H., Tsukamoto, H., Alm, A., 2007. Retinal mean transit time in patients with primary open-angle glaucoma and normal-tension glaucoma. Acta Ophthalmol Scand. 85, 67-72.

Boland, M., Zhang, L., Broman, A., Jampel, H., Quigley, H., 2008. Comparison of optic nerve head topography and visual field in eyes with open-angle and angle-closure glaucoma. Ophthalmology 115, 239-245.e232.

Bonni, A., Ginty, D.D., Dudek, H., Greenberg, M.E., 1995. Serine 133-Phosphorylated CREB Induces Transcription via a Cooperative Mechanism That May Confer Specificity to Neurotrophin Signals. Mol. Cell. Neurosci. 6, 168-183.

Bonovas, S., Peponis, V., Filioussi, K., 2004. Diabetes mellitus as a risk factor for primary open-angle glaucoma: a meta-analysis. Diabet Med. 21, 609-614.

Borda, E., Berra, A., Saravia, M., Ganzinelli, S., Sterin Borda, L., 2005. Correlations between neuronal nitric oxide synthase and muscarinic M3/M1 receptors in the rat retina. Exp Eye Res. 80, 391-399.

Bores, G.M., Huger, F.P., Petko, W., Mutlib, A.E., Camacho, F., Rush, D.K., Selk, D.E., Wolf, V., Kosley, R.W., Davis, L., Vargas, H.M., 1996. Pharmacological evaluation of novel Alzheimer's disease therapeutics: acetylcholinesterase inhibitors related to galanthamine. J Pharmacol Exp Ther. 277, 728-738.

Bovolenta, P., Frade, J.-M., Marti, E., Rodriguez-Peña, M.-A., Barde, Y.-A., Rodriguez-Tebar, A., 1996. Neurotrophin-3 Antibodies Disrupt the Normal Development of the Chick Retina. J Neurosci 16, 4402-4410.

Brecht, S., Kirchhof, R., Chromik, A., Willesen, M., Nicolaus, T., Raivich, G., Wessig, J., Waetzig, V., Goetz, M., Claussen, M., Pearse, D., Kuan, C.-Y., Vaudano, E., Behrens, A., Wagner, E., Flavell, R.A., Davis, R.J., Herdegen, T., 2005. Specific pathophysiological functions of JNK isoforms in the brain. Eur J Neurosci 21, 363-377.

Brooks, D., Garcia, G., Dreyer, E., Zurakowski, D., Franco-Bourland, R., 1997. Vitreous body glutamate concentration in dogs with glaucoma. Am J Vet Res 58, 864-867.

Brown, G.C., 1999. Nitric oxide and mitochondrial respiration. Biochim Biophys Acta. 1411, 351-369.

Brown, G.C., 2010a. Nitric oxide and neuronal death. Nitric Oxide 23, 153-165.

Brown, W., 2010b. A review of string vessels or collapsed, empty basement membrane tubes. J Alzheimers Dis. 21, 725-739.

Budinger, T., 2003. Progenitor endothelial cell involvement in Alzheimer's disease. Neurol Res. 25, 617-624.

Burgoyne, C., 2010. A biomechanical paradigm for axonal insult within the optic nerve head in aging and glaucoma. Exp Eye Res.

Caballero, S., Sengupta, N., Afzal, A., Chang, K.-H., Li Calzi, S., Guberski, D., Kern, T., Grant, M., 2007. Ischemic vascular damage can be repaired by healthy, but not diabetic, endothelial progenitor cells. Diabetes 56, 960-967.

Calabrese, V., Mancuso, C., Calvani, M., Rizzarelli, E., Butterfield, D.A., Stella, A.M.G., 2007. Nitric oxide in the central nervous system: neuroprotection versus neurotoxicity. Nat Rev Neurosci. 8, 766-775.

Caprioli, J., Munemasa, Y., Kwong, J.M.K., Piri, N., 2009. Overexpression of thioredoxins 1 and 2 increases retinal ganglion cell survival after pharmacologically induced oxidative stress, optic nerve transection, and in experimental glaucoma. Trans Am Ophthalmol Soc. 107, 161-165.

Cargnello, M., Roux, P.P., 2011. Activation and Function of the MAPKs and Their Substrates, the MAPK-Activated Protein Kinases. Microbiol. Mol. Biol. Rev. 75, 50-83.

Carter-Dawson, L., Crawford, M.L.J., Harwerth, R.S., Smith, E.L., Feldman, R., Shen, F.F., Mitchell, C.K., Whitetree, A., 2002. Vitreal Glutamate Concentration in Monkeys with Experimental Glaucoma. Investigative Ophthalmology & Visual Science 43, 2633-2637.

Carugo, O., Cemazar, M., Zahariev, S., Hudaky, I., Gaspari, Z., Perczel, A., Pongor, S., 2003. Vicinal disulfide turns. Protein Eng 16, 637-639.

Casson, R.J., 2006. Possible role of excitotoxicity in the pathogenesis of glaucoma. Clin. & Exp. Ophthalmol. 34, 54-63.

Castagne, V., Clarke, P.G., 1996. Axotomy-induced retinal ganglion cell death in development: its time- course and its diminution by antioxidants. Proc. Royal Soc. London B Biol. Sci. 263, 1193-1197.

Castagne, V., Lefevre, K., Natero, R., Clarke, P.G., Bedker, D.A., 1999. An optimal redox status for the survival of axotomized ganglion cells in the developing retina. Neurosci. 93, 313-320.

Caulfield, M.P., Birdsall, N.J., 1998. International Union of Pharmacology. XVII. Classification of muscarinic acetylcholine receptors. Pharmacol Rev. 50, 279-290.

Cellerino, A., Arango-Gonzlez, B., Pinzn-Duarte, G., Kohler, K., 2003. Brain-derived neurotrophic factor regulates expression of vasoactive intestinal polypeptide in retinal amacrine cells. J Comp Neurol. 467, 97-104.

Cellerino, A., Carroll, P., Thoenen, H., Barde, Y.A., 1997. Reduced size of retinal ganglion cell axons and hypomyelination in mice lacking brain-derived neurotrophic factor. Mol Cell Neurosci 9, 397-408.

Chakravarthy, U., Stitt, A.W., McNally, J., Bailie, J.R., Hoey, E.M., Duprex, P., 1995. Nitric oxide synthase activity and expression in retinal capillary endothelial cells and pericytes. Curr Eye Res. 14, 285-294.

Challa, V., Thore, C., Moody, D., Anstrom, J., Brown, W., 2004. Increase of white matter string vessels in Alzheimer's disease. J Alzheimers Dis. 6, 379-383.

Chandel, N.S., McClintock, D.S., Feliciano, C.E., Wood, T.M., Melendez, J.A., Rodriguez, A.M., Schumacker, P.T., 2000. Reactive oxygen species generated at mitochondrial complex III stabilize hypoxia-inducible factor-1alpha during hypoxia: a mechanism of O2 sensing. J Biol Chem. 275, 25130-25138.

Chao, M.V., 1994. The p75 neurotrophin receptor. J Neurobiol. 25, 1373-1385.

Charpie, J.R., Schreur, K.D., Papadopoulos, S.M., Webb, R.C., 1994. Endothelium dependency of contractile activity differs in infant and adult vertebral arteries. J Clin Invest 93, 1339-1343.

Chauhan, B., Pan, J., Archibald, M., LeVatte, T., Kelly, M.E.M., Tremblay, F., 2002. Effect of intraocular pressure on optic disc topography, electroretinography, and axonal loss in a chronic pressure-induced rat model of optic nerve damage. Invest Ophthalmol Vis Sci. 43, 2969-2976.

Chen, H., Weber, A.J., 2001. BDNF enhances retinal ganglion cell survival in cats with optic nerve damage. Invest. Ophthalmol. Vis. Sci. 42, 966-974.

Chen, H., Wei, X., Cho, K.-S., Chen, G., Sappington, R., Calkins, D., Chen, D., 2011. Optic neuropathy due to microbead-induced elevated intraocular pressure in the mouse. Invest Ophthalmol Vis Sci. 52, 36-44.

Chen, P.P., Budenz, D.L., 1998. The effects of cataract extraction on the visual field of eyes with chronic open-angle glaucoma. Am J Ophthalmol. 125, 325-333.

Chen, S., Diamond, J., 2002. Synaptically released glutamate activates extrasynaptic NMDA receptors on cells in the ganglion cell layer of rat retina. J Neurosci. 22, 2165-2173.

Chen, W., Martindale, J.L., Holbrook, N.J., Liu, Y., 1998 Tumor promoter arsenite activates extracellular signal-regulated kinase through a signaling pathway

mediated by epidermal growth factor receptor and Shc. Mol. Cell. Biol. 18, 5178-5188.

Cheng, L., Sapieha, P., Kittlerová, P., Hauswirth, W.W., Di Polo, A., 2002. TrkB gene transfer protects retinal ganglion cells from axotomy-induced death in vivo. J. Neurosci. 22, 3977-3986.

Chiou, G.C., 2001. Review: effects of nitric oxide on eye diseases and their treatment. J Ocul Pharmacol Ther. 17, 189-198.

Choi, D.W., Rothman, S.M., 1990. The role of glutamate neurotoxicity in hypoxic-ischemic neuronal death. Annu Rev Neurosci. 13, 171-182.

Choi, Y.B., Tenneti, L., Le, D.A., Ortiz, J., Bai, G., Chen, H.S., Lipton, S.A., 2000. Molecular basis of NMDA receptor-coupled ion channel modulation by S-nitrosylation. Nat Neurosci. 3, 15-21.

Chung, K.K., 2010. Modulation of pro-survival proteins by S-nitrosylation: implications for neurodegeneration. Apoptosis 15, 1364-1370.

Ciancaglini, M., Carpineto, P., Costagliola, C., Matropasqua, L., 2001. Perfusion of the optic nerve head and visual field damage in glaucomatous patients. Graefes Arch Clin Exp Ophthalmol. 239, 549-555.

CNTGSG, 1998. Comparison of glaucomatous progression between untreated patients with normal-tension glaucoma and patients with therapeutically reduced intraocular pressures. Am J Ophthalmol. 126, 487-497.

Cohen-Cory, S., Fraser, S.E., 1994. BDNF in the development of the visual system of *Xenopus*. Neuron 12, 747-761.

Colavitti, R., Pani, G., Bedogni, B., Anzevino, R., Borrello, S., Waltenberger, J., Galeotti, T., 2002. Reactive oxygen species as downstream mediators of angiogenic signaling by vascular endothelial growth factor receptor-2/KDR. J Biol Chem. 277, 3101-3108.

Coleman, A.L., Miglior, S., 2008. Risk Factors for Glaucoma Onset and Progression. Surv Ophthalmol. 53, S3-S10.

Collet, J.-F., Messens, J., 2010. Structure, Function, and Mechanism of Thioredoxin Proteins. Antioxidants & Redox Signaling 13, 1205-1216.

Congdon, N., O'Colmain, B., Klaver, C.C.W., Klein, R., Muoz, B., Friedman, D., Kempen, J., Taylor, H., Mitchell, P., 2004. Causes and prevalence of visual impairment among adults in the United States. Arch Ophthalmol. 122, 477-485.

Cordeiro, M., Guo, L., Maass, A., Luong, V., Moss, S.E., Fitzke, F.W., Salt, T.E., 2006. Beta amyloid and retinal ganglion cell apoptosis: implications and applications to glaucoma. Invest. Ophthalmol. Vis. Sci. 47, S2698.

Cox, B.C., Marritt, A.M., Perry, D.C., Kellar, K.J., 2008. Transport of multiple nicotinic acetylcholine receptors in the rat optic nerve: high densities of receptors containing alpha6 and beta3 subunits. J. Neurochem. 105, 1924-1938.

Crawford, M.L., Harwerth, R.S., Smith, E.L., Mills, S., Ewing, B., 2001. Experimental glaucoma in primates: changes in cytochrome oxidase blobs in V1 cortex. Invest Ophthalmol Vis Sci. 42, 358-364.

Crawford, M.L., Harwerth, R.S., Smith, E.L., Shen, F., Carter Dawson, L., 2000. Glaucoma in primates: cytochrome oxidase reactivity in parvo- and magnocellular pathways. Invest Ophthalmol Vis Sci. 41, 1791-1802.

Crespo, D., O'Leary, D.D.M., Maxwell Cowan, W., 1985. Changes in the numbers of optic nerve fibers during late prenatal and postnatal development in the albino rat. Dev Brain Res 19, 129-134.

Crish, S.D., Sappington, R.M., Inman, D.M., Horner, P.J., Calkins, D.J., 2010. Distal axonopathy with structural persistence in glaucomatous neurodegeneration. Proc Nat Acad Sci USA 107, 5196-5201.

Cronin Golomb, A., 1995. Vision in Alzheimer's disease. Gerontologist 35, 370-376.

Cronin Golomb, A., Corkin, S., Rizzo, J.F., Cohen, J., Growdon, J.H., Banks, K.S., 1991. Visual dysfunction in Alzheimer's disease: relation to normal aging. Annals of neurology 29, 41-52.

Cuadrado, A., Nebreda, A., 2010. Mechanisms and functions of p38 MAPK signalling. Biochem J. 429, 403-417.

Cueva Vargas, J.L., Osswald, I., Unsain, N., Barker, P.A., Bowie, D., Di Polo, A., 2011. Tumor necrosis factor-alpha and calcium permeable AMPA receptors mediate retinal ganglion cell death in experimental glaucoma. . Invest. Ophthalmol. Vis. Sci. (ARVO Supp.) 52, 3934.

Cui, Q., Tang, L.S., Hu, B., So, K.F., Yip, H.K., 2002. Expression of trkA, trkB, and trkC in injured and regenerating retinal ganglion cells of adult rats. Invest. Ophthalmol. Vis. Sci. 43, 1954-1964.

Curran, T., Franza, B.R., 1988. Fos and jun: The AP-1 connection. Cell 55, 395-397.

Da Silva, N., Herron, C., Stevens, K., Jollimore, C.A.B., Barnes, S., Kelly, M.E.M., 2008. Metabotropic receptor-activated calcium increases and store-operated calcium influx in mouse Müller cells. Investigative ophthalmology & visual science 49, 3065-3073.

Dalton, R., 2001. Private investigations. Nature 411, 129-130.

Danbolt, N.C., 2001. Glutamate uptake. Prog Neurobiol. 65, 1-105.

Danesh-Meyer, H.V., Levin, L.A., 2009. Neuroprotection: Extrapolating from Neurologic Diseases to the Eye. American Journal of Ophthalmology 148, 186-191.e182.

Danias, J., Shen, F., Kavalarakis, M., Chen, B., Goldblum, D., Lee, K., Zamora, M.-F., Su, Y., Brodie, S., Podos, S., Mittag, T., 2006. Characterization of retinal damage in the episcleral vein cauterization rat glaucoma model. Exp Eye Res. 82, 219-228.

Das, I., Hempstead, B.L., Macleish, P.R., Sparrow, J.R., 1997. Immunohistochemical analysis of the neurotrophins BDNF and NT-3 and their receptors trk B, trk C and p75 in the developing chick retina. Vis. Neurosci. 14, 835-842.

Dauphin, F., Linville, D.G., Hamel, E., 1994. Cholinergic dilatation and constriction of feline cerebral blood vessels are mediated by stimulation of phosphoinositide metabolism via two different muscarinic receptor subtypes. J Neurochem. 63, 544-551.

Davenport, A., 2002. International Union of Pharmacology. XXIX. Update on endothelin receptor nomenclature. Pharmacol Rev. 54, 219-226.

Daz, F., Villena, A., Vidal, L., Moreno, M., Garca-Campos, J., Pérez de Vargas, I., 2010. Experimental model of ocular hypertension in the rat: study of the optic nerve capillaries and action of hypotensive drugs. Invest Ophthalmol Vis Sci. 51, 946-951.

De La Paz, M.A., Epstein, D.L., 1996. Effect of age on superoxide dismutase activity of human trabecular meshwork. Invest Ophthalmol Vis Sci. 37, 1849-1853.

de Vries, H., Witte, M., Hondius, D., Rozemuller, A.J.M., Drukarch, B., Hoozemans, J., van Horssen, J., 2008. Nrf2-induced antioxidant protection: a promising target to counteract ROS-mediated damage in neurodegenerative disease? Free Radic Biol Med. 45, 1375-1383.

Deisseroth, K., Heist, E.K., Tsien, R.W., 1998. Translocation of calmodulin to the nucleus supports CREB phosphorylation in hippocampal neurons. Nature 392, 198-202.

Deokule, S., Weinreb, R., 2008. Relationships among systemic blood pressure, intraocular pressure, and open-angle glaucoma. Can J Ophthalmol. 43, 302-307.

Derouiche, A., Rauen, T., 1995. Coincidence of L-glutamate/L-aspartate transporter (GLAST) and glutamine synthetase (GS) immunoreactions in retinal glia: evidence for coupling of GLAST and GS in transmitter clearance. J. Neurosci. Res. 42, 131-143.

Di Polo, A., Aigner, L.J., Dunn, R.J., Bray, G.M., Aguayo, A.J., 1998. Prolonged delivery of brain-derived neurotrophic factor by adenovirus-infected Müller cells temporarily rescues injured retinal ganglion cells. Proc. Natl. Acad. Sci. USA 95, 3978-3983.

Diamond, J.S., 2001. Neuronal glutamate transporters limit activation of NMDA receptors by neurotransmitter spillover on CA1 pyramidal cells. J Neurosci. 21, 8328-8338.

Diederen, R.M.H., La Heij, E.C., Deutz, N.E.P., Kijlstra, A., Kessels, A.G.H., van Eijk, H.M.H., Liem, A.T.A., Dieudonné, S., Hendrikse, F., 2006. Increased glutamate levels in the vitreous of patients with retinal detachment. Exp Eye Res. 83, 45-50.

Dingledine, R., Borges, K., Bowie, D., Traynelis, S.F., 1999. The Glutamate Receptor Ion Channels. Pharmacol. Rev. 51, 7-62.

Donati, G., Pournaras, C.J., Munoz, J.L., Poitry, S., Poitry Yamate, C.L., Tsacopoulos, M., 1995. Nitric oxide controls arteriolar tone in the retina of the miniature pig. Invest Ophthalmol Vis Sci. 36, 2228-2237.

Dong, A., Shen, J., Zeng, M., Campochiaro, P., 2011. Vascular cell-adhesion molecule-1 plays a central role in the proangiogenic effects of oxidative stress. Proc Natl Acad Sci U S A. 108, 14614-14619.

Dong, A., Xie, B., Shen, J., Yoshida, T., Yokoi, K., Hackett, S., Campochiaro, P., 2009. Oxidative stress promotes ocular neovascularization. J Cell Physiol. 219, 544-552.

Dorner, G., Garhofer, G., Kiss, B., Polska, E., Polak, K., Riva, C., Schmetterer, L., 2003. Nitric oxide regulates retinal vascular tone in humans. Am J Physiol Heart Circ Physiol. 285, H631-H636.

Downs, J.C., Roberts, M., Burgoyne, C., 2008. Mechanical environment of the optic nerve head in glaucoma. Optom Vis Sci. 85, 425-435.

Dreyer, E.B., Zurakowski, D., Schumer, R.A., Podos, S.M., Lipton, S.A., 1996. Elevated glutamate levels in the vitreous body of humans and monkeys with glaucoma. Arch Ophthalmol 114, 299-305.

Dringen, R., Pawlowski, P., Hirrlinger, J., 2005. Peroxide detoxification by brain cells. J Neurosci Res. 79, 157-165.

Du, K., Montminy, M., 1998. CREB is a regulatory target for the protein kinase Akt/PKB. J Biol Chem. 273, 32377-32379.

Dugan, L.L., Creedon, D.J., Johnson, E.M., Holtzman, D.M., 1997. Rapid suppression of free radical formation by nerve growth factor involves the mitogen-activated protein kinase pathway. Proc Natl Acad Sci U S A. 94, 4086-4091.

Dugas, J., Mandemakers, W., Rogers, M., Ibrahim, A., Daneman, R., Barres, B., 2008. A novel purification method for CNS projection neurons leads to the identification of brain vascular cells as a source of trophic support for corticospinal motor neurons. J Neurosci. 28, 8294-8305.

Duranteau, J., Chandel, N.S., Kulisz, A., Shao, Z., Schumacker, P.T., 1998. Intracellular Signaling by Reactive Oxygen Species during Hypoxia in Cardiomyocytes. Journal of Biological Chemistry 273, 11619-11624.

El-Remessy, A., Bartoli, M., Platt, D., Fulton, D., Caldwell, R., 2005. Oxidative stress inactivates VEGF survival signaling in retinal endothelial cells via PI 3-kinase tyrosine nitration. J Cell Sci. 118, 243-252.

El Remessy, A.B., Al Shabrawey, M., Platt, D.H., Bartoli, M., Behzadian, M.A., Ghaly, N., Tsai, N., Motamed, K., Caldwell, R.B., 2007. Peroxynitrite mediates VEGF's angiogenic signal and function via a nitration-independent mechanism in endothelial cells. FASEB J. 21, 2528-2539.

Elhusseiny, A., Cohen, Z., Olivier, A., Stanimirović, D.B., Hamel, E., 1999. Functional acetylcholine muscarinic receptor subtypes in human brain microcirculation: identification and cellular localization. J Cereb Blood Flow Metab. 19, 794-802.

Emre, M., Orgl, S., Haufschild, T., Shaw, S.G., Flammer, J., 2005. Increased plasma endothelin-1 levels in patients with progressive open angle glaucoma. . British Journal of Ophthalmology. 89, 60-63.

Ergorul, C., Ray, A., Huang, W., Wang, D., Ben, Y., Cantuti Castelvetri, I., Grosskreutz, C., 2010. Hypoxia inducible factor-1α (HIF-1α) and some HIF-1 target genes are elevated in experimental glaucoma. Journal of molecular neuroscience 42, 183-191.

Espada, S., Rojo, A., Salinas, M., Cuadrado, A., 2009. The muscarinic M1 receptor activates Nrf2 through a signaling cascade that involves protein kinase C and inhibition of GSK-3beta: connecting neurotransmission with neuroprotection. J Neurochem. 110, 1107-1119.

Farlow, M., 2003. Clinical pharmacokinetics of galantamine. Clin Pharmacokinet. 42, 1383-1392.

Feher, J., Pescosolido, N., Tranquilli Leali, F., Cavallotti, C., 2005. Microvessels of the human optic nerve head: ultrastructural and radioreceptorial changes in eyes with increased IOP. Can J Ophthalmol. 40, 492-498.

Feilchenfeld, Z., Ycel, Y., Gupta, N., 2008. Oxidative injury to blood vessels and glia of the pre-laminar optic nerve head in human glaucoma. Exp Eye Res. 87, 409-414.

Felder, C.C., 1995. Muscarinic acetylcholine receptors: signal transduction through multiple effectors. FASEB J. 9, 619-625.

Feller, M.B., Wellis, D.P., Stellwagen, D., Werblin, F.S., Shatz, C.J., 1996. Requirement for cholinergic synaptic transmission in the propagation of spontaneous retinal waves. Science 272, 1182-1187.

Fernández-Durango, R., Rolln, R., Mediero, A., Roldn-Pallares, M., Garca-Feijo, J., Garca-Snchez, J., Fernndez-Cruz, A., Rpodas, A., 2003. Localization of endothelin-1 mRNA expression and immunoreactivity in the anterior segment of human eye: expression of ETA and ETB receptors. Mol Vis. 9, 103-109.

Fernndez-Durango, R., Fernndez-Martnez, A., Garca-Feijoo, J., Castillo, A., de la Casa, J.M., Garca-Bueno, B., Prez-Nievas, B., Fernndez-Cruz, A., Leza, J., 2008. Expression of nitrotyrosine and oxidative consequences in the trabecular meshwork of patients with primary open-angle glaucoma. Invest Ophthalmol Vis Sci. 49, 2506-2511.

Finkbeiner, S., Tavazoie, S.F., Maloratsky, A., Jacobs, K.M., Harris, K.M., Greenberg, M.E., 1997. CREB: A Major Mediator of Neuronal Neurotrophin Responses. Neuron 19, 1031-1047.

Fischer, A.J., McKinnon, L.A., Nathanson, N.M., Stell, W.K., 1998. Identification and localization of muscarinic acetylcholine receptors in the ocular tissues of the chick. J Comp Neurol. 392, 273-284.

Fiscus, R., 2002. Involvement of cyclic GMP and protein kinase G in the regulation of apoptosis and survival in neural cells. NeuroSignals 11, 175-190.

Flammer, J., Orgl, S., Costa, V., Orzalesi, N., Krieglstein, G., Serra, L., Renard, J.-P., Stefnsson, E., 2002. The impact of ocular blood flow in glaucoma. Prog Retin Eye Res. 21, 359-393.

Fleming, I., Busse, R., 1999. Signal transduction of eNOS activation. Cardiovasc Res. 43, 532-541.

Formaz, F., Riva, C.E., Geiser, M., 1997. Diffuse luminance flicker increases retinal vessel diameter in humans. Curr Eye Res. 16, 1252-1257.

Fournier, A.E., Beer, J., Arregui, C.O., Essagian, C., Aguayo, A.J., McKerracher, L., 1997. Brain-derived neurotrophic factor modulates GAP-43 but not Ta1 expression in injured retinal ganglion cells of adult rats. J. Neurosci. Res. 47, 561-572.

Frade, J.M., Bovolenta, P., Martinez-Morales, J.R., Arribas, A., Barbas, J.A., Rodriguez-Tebar, A., 1997. Control of early cell death by BDNF in the chick retina. Development 124, 3313-3320.

Frade, J.M., Bovolenta, P., Rodriguez-Tebar, A., 1999. Neurotrophins and other growth factors in the generation of retinal neurons. Microsc. Res. Tech. 45, 243-251.

Frade, J.M., Rodriguez-Tebar, A., Barde, Y.-A., 1996. Induction of cell death by endogenous nerve growth factor through its p75 receptor. Nature 383, 166-168.

Frank, R.N., Dutta, S., Mancini, M.A., 1987. Pericyte coverage is greater in the retinal than in the cerebral capillaries of the rat. Invest Ophthalmol Vis Sci. 28, 1086-1091.

Fridovich, I., 1995. Superoxide radical and superoxide dismutases. Annu Rev Biochem. 64, 97-112.

Fukuchi, T., Sawaguchi, S., Hara, H., Shirakashi, M., Iwata, K., 1992. Extracellular matrix changes of the optic nerve lamina cribrosa in monkey eyes with experimentally chronic glaucoma. Graefes Arch Clin Exp Ophthalmol. 230, 421-427.

Furukawa, M., Xiong, Y., 2005. BTB protein Keap1 targets antioxidant transcription factor Nrf2 for ubiquitination by the Cullin 3-Roc1 ligase. Mol Cell Biol. 25, 162-171.

Furukawa, Y., Okada, M., Akaike, N., Hayashi, T., Nabekura, J., 2000. Reduction of voltage-dependent magnesium block of N-methyl--aspartate receptor-mediated current by in vivo axonal injury. Neurosci 96, 385-392.

Gaasterland, D., Kupfer, C., 1974. Experimental glaucoma in the rhesus monkey. Invest Ophthalmol. 13, 455-457.

Gaasterland, D., Tanishima, T., Kuwabara, T., 1978. Axoplasmic flow during chronic experimental glaucoma. 1. Light and electron microscopic studies of the monkey optic nervehead during development of glaucomatous cupping. Invest Ophthalmol Vis Sci 17, 838-846.

Gabelt, B.A.T., Kaufman, P.L., 2005. Changes in aqueous humor dynamics with age and glaucoma. Prog Retin Eye Res. 24, 612-637.

Gallo, E., Iadecola, C., 2011. Neuronal nitric oxide contributes to neuroplasticity-associated protein expression through cGMP, protein kinase G, and extracellular signal-regulated kinase. J Neurosci. 31, 6947-6955.

Gao, H., Qiao, X., Hefti, F., Hollyfield, J.G., Knüsel, B., 1997. Elevated mRNA expression of brain-derived neurotrophic factor in retinal ganglion cell layer after optic nerve injury. Invest. Ophthalmol. Vis. Sci. 38, 1840-1847.

Garhöfer, G., Zawinka, C., Resch, H., Huemer, K.H., Dorner, G.T., Schmetterer, L., 2004. Diffuse luminance flicker increases blood flow in major retinal arteries and veins. Vision Res. 44, 833-838.

Garthwaite, J., 2008. Concepts of neural nitric oxide-mediated transmission. Eur J Neurosci. 27, 2783-2802.

Geiger, J.R.P., Melcher, T., Koh, D.S., Sakmann, B., Seeburg, P.H., Jonas, P., Monyer, H., 1995. Relative abundance of subunit mRNAs determines gating and Ca2+ permeability of AMPA receptors in principal neurons and interneurons in rat CNS. Neuron 15, 193-204.

Geiger, L.K., Kortuem, K.R., Alexejun, C., Levin, L.A., 2002. Reduced redox state allows prolonged survival of axotomized neonatal retinal ganglion cells. Neurosci. 109, 635-642.

Gelatt, K., MacKay, E., 2004. Prevalence of the breed-related glaucomas in pure-bred dogs in North America. Vet Ophthalmol. 7, 97-111.

Gerber, H.P., Condorelli, F., Park, J., Ferrara, N., 1997. Differential transcriptional regulation of the two vascular endothelial growth factor receptor genes. Flt-1, but not Flk-1/KDR, is up-regulated by hypoxia. J Biol Chem. 272, 23659-23667.

Gilbert, D., Lecchi, M., Arnaudeau, S., Bertrand, D., Demaurex, N., 2009. Local and global calcium signals associated with the opening of neuronal [alpha]7 nicotinic acetylcholine receptors. Cell calcium 45, 198-207.

Gilmore, G.C., Whitehouse, P.J., 1995. Contrast sensitivity in Alzheimer's disease: a 1-year longitudinal analysis. Optometry and vision science 72, 83-91.

Goel, M., Picciani, R., Lee, R., Bhattacharya, S., 2010. Aqueous humor dynamics: a review. Open Ophthalmol J. 4, 52-59.

Gonzalez-Hoyuela, M., Barbas, J.A., Rodriguez-Tebar, A., 2001. The autoregulation of retinal ganglion cell number. Development. 128, 117-124.

Gorter, J.A., Petrozzino, J.J., Aronica, E.M., Rosenbaum, D.M., Opitz, T., Bennett, M.V.L., Connor, J.A., Zukin, R.S., 1997. Global Ischemia Induces Downregulation of Glur2 mRNA and Increases AMPA Receptor-Mediated Ca2+ Influx in Hippocampal CA1 Neurons of Gerbil. J. Neurosci. 17, 6179-6188.

Gottanka, J., Kuhlmann, A., Scholz, M., Johnson, D., Ltjen-Drecoll, E., 2005. Pathophysiologic changes in the optic nerves of eyes with primary open angle and pseudoexfoliation glaucoma. Invest Ophthalmol Vis Sci. 46, 4170-4181.

Gotti, C., Fornasari, D., Clementi, F., 1997. Human neuronal nicotinic receptors. Prog Neurobiol. 53, 199-237.

Grooms, S.Y., Opitz, T., Bennett, M.V.L., Zukin, R.S., 2000. Status epilepticus decreases glutamate receptor 2 mRNA and protein expression in hippocampal pyramidal cells before neuronal death. Proc. Natl. Acad. Sci. U. S. A. 97, 3631-3636.

Gross, R., Ji, J., Chang, P., Pennesi, M., Yang, Z., Zhang, J., Wu, S., 2003. A mouse model of elevated intraocular pressure: retina and optic nerve findings. Trans Am Ophthalmol Soc. 101, 163-169.

Grozdanic, S., Kecova, H., Harper, M., Nilaweera, W., Kuehn, M., Kardon, R., 2010. Functional and structural changes in a canine model of hereditary primary angle-closure glaucoma. Invest Ophthalmol Vis Sci. 51, 255-263.

Gründer, T., Kohler, K., Kaletta, A., Guenther, E., 2000. The distribution and developmental regulation of NMDA receptor subunit proteins in the outer and inner retina of the rat. J Neurobiol. 44, 333-342.

Gunn, D., Gole, G., Barnett, N., 2011. Specific amacrine cell changes in an induced mouse model of glaucoma. Clin Experiment Ophthalmol. 39, 555-563.

Guo, L., Duggan, J., Cordeiro, M.F., 2010. Alzheimer's disease and retinal neurodegeneration. Current Alzheimer research 7, 3-14.

Guo, L., Moss, S., Alexander, R., Ali, R., Fitzke, F., Cordeiro, M.F., 2005. Retinal ganglion cell apoptosis in glaucoma is related to intraocular pressure and IOP-induced effects on extracellular matrix. Invest Ophthalmol Vis Sci. 46, 175-182.

Guo, L., Salt, T.E., Luong, V., Wood, N., Cheung, W., Maass, A., Ferrari, G., Russo-Marie, F., Sillito, A.M., Cheetham, M.E., Moss, S.E., Fitzke, F.W., Cordeiro, M.F., 2007. Targeting amyloid-beta in glaucoma treatment. Proc. Natl. Acad. Sci. U S A 104, 13444-13449.

Guo, S., Kim, W., Lok, J., Lee, S.-R., Besancon, E., Luo, B.-H., Stins, M., Wang, X., Dedhar, S., Lo, E., 2008. Neuroprotection via matrix-trophic coupling between cerebral endothelial cells and neurons. Proc Natl Acad Sci U S A. 105, 7582-7587.

Guo, Y., Johnson, E.C., Cepurna, W.O., Dyck, J.A., Doser, T., Morrison, J.C., 2011. Early Gene Expression Changes in the Retinal Ganglion Cell Layer of a Rat Glaucoma Model. Invest. Ophthalmol. Vis. Sci. 52, 1460-1473.

Gupta, N., Fong, J., Ang, L., Ycel, Y., 2008. Retinal tau pathology in human glaucomas. Canadian journal of ophthalmology 43, 53-60.

Hahm, J.O., Cramer, K.S., Sur, M., 1999. Pattern formation by retinal afferents in the ferret lateral geniculate nucleus: developmental segregation and the role of N-methyl-D-aspartate receptors. J Comp Neurol. 411, 327-345.

Hallbook, F., Backstrom, A., Kullander, K., Ebendal, T., Carri, N.G., 1996. Expression of neurotrophins and trk receptors in the avian retina. J Comp Neurol. 364, 664-676.

Halliwell, B., 2006. Oxidative stress and neurodegeneration: where are we now? Journal of Neurochemistry 97, 1634-1658.

Hammes, H.-P., Lin, J., Renner, O., Shani, M., Lundqvist, A., Betsholtz, C., Brownlee, M., Deutsch, U., 2002. Pericytes and the pathogenesis of diabetic retinopathy. Diabetes 51, 3107-3112.

Hammes, H.P., Federoff, H.J., Brownlee, M., 1995. Nerve growth factor prevents both neuroretinal programmed cell death and capillary pathology in experimental diabetes. Mol Med. 1, 527-534.

Hara, H., Ichikawa, M., Oku, H., Shimazawa, M., Araie, M., 2005. Bunazosin, a selective alpha1-adrenoceptor antagonist, as an anti-glaucoma drug: effects on ocular circulation and retinal neuronal damage. Cardiovasc Drug Rev. 23, 43-56.

Harada, C., Harada, T., Nakamura, K., Sakai, Y., Tanaka, K., Parada, L.F., 2006. Effect of p75NTR on the regulation of naturally occurring cell death and retinal ganglion cell number in the mouse eye. Dev. Biol. 290, 57-65.

Harada, T., Harada, C., Nakamura, K., Quah, H.-M., Okumura, A., Namekata, K., Saeki, T., Aihara, M., Yoshida, H., Mitani, A., Tanaka, K., 2007. The potential role of glutamate transporters in the pathogenesis of normal tension glaucoma. J Clin Invest. 117, 1763-1770.

Hare, W., WoldeMussie, E., Lai, R., Ton, H., Ruiz, G., Feldmann, B., Wijono, M., Chun, T., Wheeler, L., 2001a. Efficacy and safety of memantine, an NMDA-type open-channel blocker, for reduction of retinal injury associated with experimental glaucoma in rat and monkey. Surv Ophthalmol. 45 Suppl 3, S284-289.

Hare, W.A., Ton, H., Ruiz, G., Feldmann, B., Wijono, M., WoldeMussie, E., 2001b. Characterization of retinal injury using ERG measures obtained with both conventional and multifocal methods in chronic ocular hypertensive primates. Invest Ophthalmol Vis Sci. 42, 127-136.

Hare, W.A., WoldeMussie, E., Lai, R.K., Ton, H., Ruiz, G., Chun, T., Wheeler, L., 2004. Efficacy and Safety of Memantine Treatment for Reduction of Changes Associated with Experimental Glaucoma in Monkey, I: Functional Measures. Invest. Ophthalmol. Vis. Sci. 45, 2625-2639.

Hartwick, A.T.E., Hamilton, C.M., Baldridge, W.H., 2008. Glutamatergic calcium dynamics and deregulation of rat retinal ganglion cells. J Physiol 586, 3425-3446.

Hartwick, A.T.E., Zhang, X., Chauhan, B., Baldridge, W., 2005. Functional assessment of glutamate clearance mechanisms in a chronic rat glaucoma model using retinal ganglion cell calcium imaging. J Neurochem. 94, 794-807.

Hasegawa, J., Obara, T., Tanaka, K., Tachibana, M., 2006. High-density presynaptic transporters are required for glutamate removal from the first visual synapse. Neuron 50, 63-74.

Hashizume, K., Hirasawa, M., Imamura, Y., Noda, S., Shimizu, T., Shinoda, K., Kurihara, T., Noda, K., Ozawa, Y., Ishida, S., Miyake, Y., Shirasawa, T., Tsubota, K., 2008. Retinal dysfunction and progressive retinal cell death in SOD1-deficient mice. Am J Pathol. 172, 1325-1331.

Hatai, T., Matsuzawa, A., Inoshita, S., Mochida, Y., Kuroda, T., Sakamaki, K., Kuida, K., Yonehara, S., Ichijo, H., Takeda, K., 2000. Execution of apoptosis signal-regulating kinase 1 (ASK1)-induced apoptosis by the mitochondria-dependent caspase activation. J. Biol. Chem. 275, 26576-26581.

Hattori, K., Naguro, I., Runchel, C., Ichijo, H., 2009. The roles of ASK family proteins in stress responses and diseases. Cell Commun Signal 24, 7-9.

Hayes, J.D., McLellan, L.I., 1999. Glutathione and glutathione-dependent enzymes represent a co-ordinately regulated defence against oxidative stress. Free Radic Res. 31, 273-300.

Hayreh, S.S., March, W., Anderson, D.R., 1979. Pathogenesis of block of rapid orthograde axonal transport by elevated intraocular pressure. Exp Eye Res 28, 515-523.

Hellström, M., Harvey, A.R., 2011. Retinal ganglion cell gene therapy and visual system repair. Curr. Gene Ther. 11, 116-131.

Henry, E., Newby, D., Webb, D., Hadoke, P.W.F., O'Brien, C., 2006. Altered endothelin-1 vasoreactivity in patients with untreated normal-pressure glaucoma. Invest Ophthalmol Vis Sci. 47, 2528-2532.

Henry, E., Newby, D.E., Webb, D.J., O'Brien, C., 1999. Peripheral endothelial dysfunction in normal pressure glaucoma. Invest Ophthalmol Vis Sci. 40, 1710-1714.

Hernandez, M., Rodriguez, F.D., Sharma, S.C., Vecino, E., 2009. Immunohistochemical changes in rat retinas at various time periods of elevated intraocular pressure. Mol Vis. 15, 2696-2709.

Hernandez, M.R., Andrzejewska, W.M., Neufeld, A.H., 1990. Changes in the extracellular matrix of the human optic nerve head in primary open-angle glaucoma. Am J Ophthalmol. 109, 180-188.

Hernandez, M.R., Igoe, F., Neufeld, A.H., 1986. Extracellular matrix of the human optic nerve head. Am J Ophthalmol. 102, 139-148.

Hernandez, M.R., Miao, H., Lukas, T., 2008. Astrocytes in glaucomatous optic neuropathy. Prog Brain Res 173, 353-373.

Herzig, S., Long, F., Jhala, U.S., Hedrick, S., Quinn, R., Bauer, A., Rudolph, D., Schutz, G., Yoon, C., Puigserver, P., Spiegelman, B., Montminy, M., 2001. CREB regulates hepatic gluconeogenesis through the coactivator PGC-1. Nature 413, 179-183.

Herzog, K.-H., von Bartheld, C.S., 1998. Contributions of the optic tectum and the retina as sources of brain-derived neurotrophic factor for retinal ganglion cells in the chick embryo. J. Neurosci. 18, 2891-2906.

Hinton, D.R., Sadun, A.A., Blanks, J.C., Miller, C.A., 1986. Optic-nerve degeneration in Alzheimer's disease. The New England journal of medicine 315, 485-487.

Hirata, Y., Emori, T., Eguchi, S., Kanno, K., Imai, T., Ohta, K., Marumo, F., 1993. Endothelin receptor subtype B mediates synthesis of nitric oxide by cultured bovine endothelial cells. J Clin Invest. 91, 1367-1373.

Hirota, K., Fukuda, R., Takabuchi, S., Kizaka-Kondoh, S., Adachi, T., Fukuda, K., Semenza, G.L., 2004. Induction of hypoxia-inducible factor 1 activity by muscarinic acetylcholine receptor signaling. J. Biol. Chem. 279, 41521-41528.

Hofer, M., Pagliusi, S.R., Hohn, A., Leibrock, J., Barde, Y.A., 1990. Regional distribution of brain-derived neurotrophic factor mRNA in the adult mouse brain. EMBO J. 9, 2459-2464.

Hoh, S.-T., Aung, T., Chew, P.T.K., 2002. Medical management of angle closure glaucoma. Semin Ophthalmol. 17, 79-83.

Hollmann, M., Hartley, M., Heinemann, S., 1991. Ca2+ permeability of KA-AMPA--gated glutamate receptor channels depends on subunit composition. Science 252, 851-853.

Honkanen, R.A., Baruah, S., Zimmerman, M.B., Khanna, C.L., Weaver, Y.K., Narkiewicz, J., Waziri, R., Gehrs, K.M., Weingeist, T.A., Boldt, H.C., Folk, J.C., Russell, S.R., Kwon, Y.H., 2003. Vitreous amino acid concentrations in patients with glaucoma undergoing vitrectomy. Arch Ophthalmol 121, 183-188.

Hood, D.C., Frishman, L.J., Viswanathan, S., Robson, J.G., Ahmed, J., 1999. Evidence for a ganglion cell contribution to the primate electroretinogram (ERG): effects of TTX on the multifocal ERG in macaque. Vis Neurosci. 16, 411-416.

Hood, D.C., Kardon, R.H., 2007. A framework for comparing structural and functional measures of glaucomatous damage. Prog Retin Eye Res. 26, 688-710.

Hosur, V., Loring, R., 2011. α4β2 nicotinic receptors partially mediate anti-inflammatory effects through Janus kinase 2-signal transducer and activator of transcription 3 but not calcium or cAMP signaling. Mol Pharmacol. 79, 167-174.

Howell, G.R., Macalinao, D.G., Sousa, G.L., Walden, M., Soto, I., Kneeland, S.C., Barbay, J.M., King, B.L., Marchant, J.K., Hibbs, M., Stevens, B., Barres, B.A., Clark, A.F., Libby, R.T., John, S.W.M., 2011. Molecular clustering identifies complement and endothelin induction as early events in a mouse model of glaucoma. The Journal of Clinical Investigation 121, 1429-1444.

Hu, B., Yip, H.K., So, K.-F., 1998. Localization of p75 neurotrophin receptor in the retina of the adult SD rat: an immunocytochemical study at the light and electronmicroscopic levels. Glia 24, 187-197.

Hu, B., Yip, H.K., So, K.F., 1999. Expression of p75 neurotrophin receptor in the injured and regenerating retina. Neuroreport 10, 1293-1297.

Hu, Y., Cho, S., Goldberg, J.L., 2010. Neurotrophic effect of a novel TrkB agonist on retinal ganglion cells. Invest. Ophthalmol. Vis. Sci. 51, 1747-1754.

Huang, E.J., Reichardt, L.F., 2001. Neurotrophins: role in neuronal development and function. Annu. Rev. Neurosci. 24, 677-736.

Huang, E.J., Reichardt, L.F., 2003. Trk receptors: roles in neuronal signal transduction. Annu. Rev. Biochem. 72, 609-642. .

Ichijo, H., Nishida, E., Irie, K., Dijke, P.t., Saitoh, M., Moriguchi, T., Takagi, M., Matsumoto, K., Miyazono, K., Gotoh, Y., 1997. Induction of apoptosis by ASK1, a mammalian MAPKKK that activates SAPK/JNK and p38 signaling pathways. Science 275, 90-94.

Ikeda, K., Tanihara, H., Honda, Y., Tatsuno, T., Noguchi, H., Nakayama, C., 1999. BDNF attenuates retinal cell death caused by chemically induced hypoxia in rats. Invest Ophthalmol Vis Sci. 40, 2130-2140.

Ikonomovic, M.D., Mizukami, K., Davies, P., Hamilton, R., Sheffield, R., Armstrong, D.M., 1997. The loss of GluR2(3) immunoreactivity precedes neurofibrillary tangle formation in the entorhinal cortex and hippocampus of Alzheimer brains. J Neuropathol Exp Neurol. 56, 1018-1027.

Isenmann, S., Klöcker, N., Gravel, C., Bähr, M., 1998. Protection of axotomized retinal ganglion cells by adenovirally delivered BDNF in vivo. Eur. J. Neurosci. 10, 2751-2756.

Ishida, K., Yamamoto, T., Sugiyama, K., Kitazawa, Y., 2000. Disk hemorrhage is a significantly negative prognostic factor in normal-tension glaucoma. Am J Ophthalmol. 129, 707-714.

Ishikawa, K., Funayama, T., Ohtake, Y., Kimura, I., Ideta, H., Nakamoto, K., Yasuda, N., Fukuchi, T., Fujimaki, T., Murakami, A., Asaoka, R., Hotta, Y., Kanamoto, T., Tanihara, H., Miyaki, K., Mashima, Y., 2005. Association between glaucoma and gene polymorphism of endothelin type A receptor. Mol Vis. 11, 431-437.

Ishizaki, E., Fukumoto, M., Puro, D., 2009. Functional K(ATP) channels in the rat retinal microvasculature: topographical distribution, redox regulation, spermine modulation and diabetic alteration. J. Physiol. 587, 2233-2253.

Ito, H., Takahashi, K., Hatazawa, J., Kim, S.G., Kanno, I., 2001. Changes in human regional cerebral blood flow and cerebral blood volume during visual stimulation measured by positron emission tomography. J Cereb Blood Flow Metab. 21, 608-612.

Ito, Y., Shimazawa, M., Chen, Y.-N., Tsuruma, K., Yamashima, T., Araie, M., Hara, H., 2009. Morphological changes in the visual pathway induced by experimental glaucoma in Japanese monkeys. Exp Eye Res. 89, 246-255.

Izzotti, A., Bagnis, A., Sacc, S., 2006. The role of oxidative stress in glaucoma. Mutat Res. 612, 105-114.

Izzotti, A., Saccà, S.C., Cartiglia, C., De Flora, S., 2003. Oxidative deoxyribonucleic acid damage in the eyes of glaucoma patients. Am J Med. 114, 638-646.

Jackson, G., Owsley, C., 2003. Visual dysfunction, neurodegenerative diseases, and aging. Neurologic clinics 21, 709-728.

Jaffrey, S.R., Erdjument Bromage, H., Ferris, C.D., Tempst, P., Snyder, S.H., 2001a. Protein S-nitrosylation: a physiological signal for neuronal nitric oxide. Nat Cell Biol. 3, 193-197.

Jaffrey, S.R., Erdjument Bromage, H., Ferris, C.D., Tempst, P., Snyder, S.H., 2001b. Protein S-nitrosylation: a physiological signal for neuronal nitric oxide. Nat Cell Biol. 3, 193-197.

Jann, M., Shirley, K., Small, G., 2002. Clinical pharmacokinetics and pharmacodynamics of cholinesterase inhibitors. Clin Pharmacokinet. 41, 719-739.

Jelsma, T.N., Hyman Friedman, H., Berkelaar, M., Bray, G.M., Aguayo, A.J., 1993. Different forms of the neurotrophin receptor trkB mRNA predominate in rat retina and optic nerve. J. Neurobiol. 24, 1207-1214.

Ji, J., Chang, P., Pennesi, M., Yang, Z., Zhang, J., Li, D., Wu, S., Gross, R., 2005. Effects of elevated intraocular pressure on mouse retinal ganglion cells. Vision Res. 45, 169-179.

Jia, L., Cepurna, W.O., Johnson, E.C., Morrison, J.C., 2000. Patterns of intraocular pressure elevation after aqueous humor outflow obstruction in rats. Invest Ophthalmol Vis Sci. 41, 1380-1385.

Jiang, F., Li, C.G., Rand, M.J., 1998. Role of potassium channels in the nitrergic nerve stimulation-induced vasodilatation in the guinea-pig isolated basilar artery. Br. J. Pharmacol. 123, 106-112.

John, S.W., Smith, R.S., Savinova, O.V., Hawes, N.L., Chang, B., Turnbull, D., Davisson, M., Roderick, T.H., Heckenlively, J.R., 1998. Essential iris atrophy,

pigment dispersion, and glaucoma in DBA/2J mice. Invest Ophthalmol Vis Sci. 39, 951-962.

Johnson, C.A., Adams, A.J., Casson, E.J., Brandt, J.D., 1993. Blue-on-yellow perimetry can predict the development of glaucomatous visual field loss. Arch Ophthalmol. 111, 645-650.

Johnson, E., Jia, L., Cepurna, W., Doser, T., Morrison, J., 2007a. Global changes in optic nerve head gene expression after exposure to elevated intraocular pressure in a rat glaucoma model. Investigative ophthalmology & visual science 48, 3161-3177.

Johnson, E., Jia, L., Cepurna, W., Doser, T., Morrison, J., 2007b. Global changes in optic nerve head gene expression after exposure to elevated intraocular pressure in a rat glaucoma model. Invest Ophthalmol Vis Sci. 48, 3161-3177.

Johnson, E.C., Morrison, J.C., Farrell, S., Deppmeier, L., Moore, C.G., McGinty, M.R., 1996. The effect of chronically elevated intraocular pressure on the rat optic nerve head extracellular matrix. Exp Eye Res. 62, 663-674.

Johnson, J.E., Barde, Y.-A., Schwab, M., Thoenen, H., 1986. Brain-derived neurotrophic factor supports the survival of cultured rat retinal ganglion cells. J. Neurosci. 6, 3031-3038.

Johnstone, M., 2004. The aqueous outflow system as a mechanical pump: evidence from examination of tissue and aqueous movement in human and non-human primates. J Glaucoma. 13, 421-438.

Jonas, J.B., Budde, W.M., Panda Jonas, S., 1999. Ophthalmoscopic evaluation of the optic nerve head. Surv Ophthalmol. 43, 293-320.

Jonas, J.B., Gusek, G.C., Naumann, G.O., 1988. Optic disc, cup and neuroretinal rim size, configuration and correlations in normal eyes. Invest Ophthalmol Vis Sci. 29, 1151-1158.

Jonas, J.B., Mardin, C.Y., Schltzer-Schrehardt, U., Naumann, G.O., 1991. Morphometry of the human lamina cribrosa surface. Invest Ophthalmol Vis Sci. 32, 401-405.

Jonnala, R.R., Buccafusco, J.J., 2001. Relationship between the increased cell surface alpha7 nicotinic receptor expression and neuroprotection induced by several nicotinic receptor agonists. J Neurosci Res. 66, 565-572.

Joussen, A.M., Murata, T., Tsujikawa, A., Kirchhof, B., Bursell, S.E., Adamis, A.P., 2001. Leukocyte-mediated endothelial cell injury and death in the diabetic retina. Am J Pathol. 158, 147-152.

Just, A., Olson, A.J.M., Arendshorst, W., 2004. Dual constrictor and dilator actions of ET(B) receptors in the rat renal microcirculation: interactions with ET(A) receptors. Am J Physiol Renal Physiol. 286, F660-F668.

Just, A., Olson, A.J.M., Falck, J., Arendshorst, W., 2005. NO and NO-independent mechanisms mediate ETB receptor buffering of ET-1-induced renal vasoconstriction in the rat. Am J Physiol Regul Integr Comp Physiol. 288, R1168-R1177.

Kalia, L.V., Kalia, S.K., Salter, M.W., 2008. NMDA receptors in clinical neurology: excitatory times ahead. Lancet Neurol. 7, 742-755.

Kanamori, A., Catrinescu, M.-M., Kanamori, N., Mears, K.A., Beaubien, R., Levin, L.A., 2010. Superoxide is an associated signal for apoptosis in axonal injury. Brain 133, 2612-2625.

Kaplan, D.R., Hempstead, B.L., Martin-Zanca, D., Chao, M.V., Parada, L.F., 1991. The trk proto-oncogene product: A signal transducing receptor for nerve growth factor. Science 252, 554-558.

Katz, B., Rimmer, S., 1989. Ophthalmologic manifestations of Alzheimer's disease. Survey of ophthalmology 34, 31-43.

Kawahara, Y., Ito, K., Sun, H., Aizawa, H., Kanazawa, I., Kwak, S., 2004. Glutamate receptors: RNA editing and death of motor neurons. Nature 427, 801.

Kendell, K.R., Quigley, H.A., Kerrigan, L.A., Pease, M.E., Quigley, E.N., 1995. Primary open-angle glaucoma is not associated with photoreceptor loss. Invest. Ophthalmol. Vis. Sci. 36, 200-205.

Kensler, T., Wakabayashi, N., Biswal, S., 2007. Cell survival responses to environmental stresses via the Keap1-Nrf2-ARE pathway. Annu Rev Pharmacol Toxicol. 47, 89-116.

Kido, N., Tanihara, H., Honjo, M., Inatani, M., Tatsuno, T., Nakayama, C., Honda, Y., 2000. Neuroprotective effects of brain-derived neurotrophic factor in eyes with NMDA-induced neuronal death. Brain Res 884, 59-67.

Kihara, T., Sawada, H., Nakamizo, T., Kanki, R., Yamashita, H., Maelicke, A., Shimohama, S., 2004. Galantamine modulates nicotinic receptor and blocks A[beta]-enhanced glutamate toxicity. Biochem. Biophys. Res. Comm. 325, 976-982.

Kikuchi, M., Tenneti, L., Lipton, S.A., 2000. Role of p38 mitogen-activated protein kinase in axotomy-induced apoptosis of rat retinal ganglion cells. J Neurosci. 20, 5037-5044.

Kim, D.H., Kim, H.S., Ahn, M.D., Chun, M.H., 2004a. Ganglion cell death in rat retina by persistent intraocular pressure elevation. Korean J Ophthalmol 18, 15-22.

Kim, D.Y., Kim, S.H., Choi, H.B., Min, C.-k., Gwag, B.J., 2001. High Abundance of GluR1 mRNA and Reduced Q/R Editing of GluR2 mRNA in Individual NADPH-Diaphorase Neurons. Mol. Cell. Neurosci. 17, 1025-1033.

Kim, H., Li, Q., Hempstead, B., Madri, J., 2004b. Paracrine and autocrine functions of brain-derived neurotrophic factor (BDNF) and nerve growth factor (NGF) in brain-derived endothelial cells. J Biol Chem. 279, 33538-33546.

Kim, J., Kim, J., Park, J., Lee, S.-W., Kim, W., Yu, Y., Kim, K.-W., 2006a. Blood-neural barrier: intercellular communication at glio-vascular interface. J Biochem Mol Biol. 39, 339-345.

Kim, S., Kim, J., Kim, D., Ko, H., Kim, S., Yoo, T., Hwang, S., Park, S., 2006b. Investigations on the association between normal tension glaucoma and single nucleotide polymorphisms of the endothelin-1 and endothelin receptor genes. Mol Vis. 12, 1016-1021.

Kim, S., Won, S., Sohn, S., Kwon, H., Lee, J., Park, J., Gwag, B., 2002. Brain-derived neurotrophic factor can act as a pronecrotic factor through transcriptional and translational activation of NADPH oxidase. J Cell Biol. 159, 821-831.

Kim, Y.M., Bombeck, C.A., Billiar, T.R., 1999. Nitric oxide as a bifunctional regulator of apoptosis. Circ Res. 84, 253-256.

Kirby, E., Bandelow, S., Hogervorst, E., 2010. Visual Impairment in Alzheimer's Disease: A Critical Review. Journal of Alzheimer's Disease 21, 15-34.

Kirkpatrick, C.J., Bittinger, F., Unger, R.E., Kriegsmann, J., Kilbinger, H., Wessler, I., 2001. The non-neuronal cholinergic system in the endothelium: evidence and possible pathobiological significance. Jpn J Pharmacol. 85, 24-28.

Klcker, N., Cellerino, A., Bhr, M., 1998. Free radical scavenging and inhibition of nitric oxide synthase potentiates the neurotrophic effects of brain-derived neurotrophic factor on axotomized retinal ganglion cells In vivo. J Neurosci. 18, 1038-1046.

Klcker, N., Kermer, P., Gleichmann, M., Weller, M., Bhr, M., 1999. Both the neuronal and inducible isoforms contribute to upregulation of retinal nitric oxide synthase activity by brain-derived neurotrophic factor. J Neurosci. 19, 8517-8527.

Klein, B.E., Klein, R., Moss, S.E., 1984. Intraocular pressure in diabetic persons. Ophthalmology 91, 1356-1360.

Klein, B.E.K., Klein, R., Knudtson, M.D., 2005. Intraocular pressure and systemic blood pressure: longitudinal perspective: the Beaver Dam Eye Study. Br J Ophthalmol. 89, 284-287.

Klein, N., Nanduri, V., Jing, S., Lambelle, F., Tapley, P., Bryant, S., Cordon-Cardo, C., Jones, K.R., Reichardt, L.F., Barbacid, M., 1991. The trkB tyrosine kinase is a receptor for brain-derived neurotrophic factor and neurotrophin-3. Cell 66, 395-403.

Klöcker, N., Kermer, P., Weishaupt, J.H., Labes, M., Ankerhold, R., Bähr, M., 2000. Brain-derived neurotrophic factor-mediated neuroprotection of adult rat retinal ganglion cells in vivo does not exclusively depend on phosphatidyl-inositol-3'-kinase/protein kinase B signaling. J. Neurosci. 20, 6962-6967.

Kniesel, U., Wolburg, H., 2000. Tight junctions of the blood-brain barrier. Cell Mol Neurobiol. 20, 57-76.

Knox, D.L., Eagle, R.C., Jr., Green, W.R., 2007. Optic nerve hydropic axonal degeneration and blocked retrograde axoplasmic transport: histopathologic features in human high-pressure secondary Ggaucoma. Arch Ophthalmol 125, 347-353.

Ko, M.-L., Hu, D.-N., Ritch, R., Sharma, S.C., Chen, C.-F., 2001. Patterns of retinal ganglion cell survival after brain-derived neurotrophic factor administration in hypertensive eyes of rats. Neurosci Lett 305, 139-142.

Ko, M.-L., Peng, P.-H., Ma, M.-C., Ritch, R., Chen, C.-F., 2005. Dynamic changes in reactive oxygen species and antioxidant levels in retinas in experimental glaucoma. Free Radical Biology and Medicine 39, 365-373.

Kobayashi, M., Yamamoto, M., 2006. Nrf2-Keap1 regulation of cellular defense mechanisms against electrophiles and reactive oxygen species. Adv Enzyme Regul. 46, 113-140.

Koeberle, P.D., Ball, A.K., 1999. Nitric oxide synthase inhibition delays axonal degeneration and promotes the survival of axotomized retinal ganglion cells. Exp Neurol 158, 366 - 381.

Kong, G.Y., Van Bergen, N.J., Trounce, I.A., Crowston, J.G., 2009. Mitochondrial dysfunction and glaucoma. J Glaucoma 18, 93-100.

Koronyo-Hamaoui, M., Koronyo, Y., Ljubimov, A., Miller, C., Ko, M., Black, K., Schwartz, M., Farkas, D., 2011. Identification of amyloid plaques in retinas from Alzheimer's patients and noninvasive in vivo optical imaging of retinal plaques in a mouse model. Neuroimage 54 Suppl 1, S204-S217.

Krönke, G., Bochkov, V.N., Huber, J., Gruber, F., BlÃ¼ml, S., FÃ¼rnkranz, A., Kadl, A., Binder, B.R., Leitinger, N., 2003. Oxidized Phospholipids Induce Expression of Human Heme Oxygenase-1 Involving Activation of cAMP-responsive Element-binding Protein. J. Biol. Chem. 278, 51006-51014.

Krupin, T., Wax, M., Moolchandani, J., 1986. Aqueous production. Trans Ophthalmol Soc U K. 105, 156-161.

Kugler, P., Beyer, A., 2003. Expression of glutamate transporters in human and rat retina and rat optic nerve. Histochem Cell Biol. 120, 199-212.

Kumar, R., Baskaran, M., Chew, P.T.K., Friedman, D., Handa, S., Lavanya, R., Sakata, L., Wong, H.-T., Aung, T., 2008. Prevalence of plateau iris in primary angle closure suspects an ultrasound biomicroscopy study. Ophthalmology 115, 430-434.

Kwon, Y.H., Rickman, D.W., Baruah, S., Zimmerman, M.B., Kim, C.S., Boldt, H.C., Russell, S.R., Hayreh, S.S., 2004. Vitreous and retinal amino acid concentrations in experimental central retinal artery occlusion in the primate. Eye 19, 455-463.

Kyriakis, J.M., Avruch, J., 2001. Mammalian Mitogen-Activated Protein Kinase Signal Transduction Pathways Activated by Stress and Inflammation. Physiol. Rev. 81, 807-869.

Lagrèze, W.A., Darstein, M., Feuerstein, T.J., Otto, T., Landwehrmeyer, G.B., 2000. NMDA receptor subunit mRNA expression in human retinal ganglion cells. Graefes Arch Clin Exp Ophthalmol. 238, 486-490.

Lagrèze, W.A., Knorle, R., Bach, M., Feuerstein, T.J., 1998. Memantine is neuroprotective in a rat model of pressure-induced retinal ischemia. Invest. Ophthalmol. Vis. Sci. 39, 1063-1066.

Lam, D., Jim, J., To, E., Rasmussen, C., Kaufman, P., Matsubara, J., 2009. Astrocyte and microglial activation in the lateral geniculate nucleus and visual cortex of glaucomatous and optic nerve transected primates. Mol Vis. 15, 2217-2229.

Lam, D.S.C., Tham, C.C.Y., Lai, J.S.M., Leung, D.Y.L., 2007. Current approaches to the management of acute primary angle closure. Curr Opin Ophthalmol. 18, 146-151.

Lam, T.T., Abler, A.S., Kwong, J.M.K., Tso, M.O.M., 1999. N-Methyl-D-Aspartate (NMDA)-Induced Apoptosis in Rat Retina. Investigative Ophthalmology & Visual Science 40, 2391-2397.

Lamballe, F., Klein, R., Barbacid, M., 1991. trkC, a new member of the trk family of tyrosine protein kinases, is a receptor for neurotrophin-3. Cell 66, 967-979.

Lander, H.M., Milbank, A.J., Tauras, J.M., Hajjar, D.P., Hempstead, B.L., Schwartz, G.D., Kraemer, R.T., Mirza, U.A., Chait, B.T., Burk, S.C., Quilliam, L.A., 1996. Redox regulation of cell signalling. Nature 381, 380-381.

Laquis, S., Chaudhary, P., Sharma, S.C., 1998. The patterns of retinal ganglion cell death in hypertensive eyes. Brain Res. 784, 100-104.

Laties, A.M., 1967. Central retinal artery innervation. Absence of adrenergic innervation to the intraocular branches. Arch Ophthalmol. 77, 405-409.

Leaver, S.G., Cui, Q., Plant, G.W., Arulpragasam, A., Hisheh, S., Verhaagen, J., Harvey, A.R., 2006. AAV-mediated expression of CNTF promotes long-term survival and regeneration of adult rat retinal ganglion cells. Gene Ther 13, 1328-1341.

Lebrun-Julien, F., Duplan, L., Pernet, V., Osswald, I.K., Sapieha, P., Bourgeois, P., Dickson, K., Bowie, D., Barker, P.A., Di Polo, A., 2009a. Excitotoxic death of

retinal neurons in vivo occurs via a non-cell-autonomous mechanism. J. Neurosci. 29, 5536-5545.

Lebrun-Julien, F., Morquette, B., Douillette, A., Saragovi, H.U., Di Polo, A., 2009b. Inhibition of p75NTR in glia potentiates TrkA-mediated survival of injured retinal ganglion cells. Mol. Cell. Neurosci. 40, 410-420.

Lecht, S., Arien Zakay, H., Marcinkiewicz, C., Lelkes, P., Lazarovici, P., 2010. Nerve growth factor-induced protection of brain capillary endothelial cells exposed to oxygen-glucose deprivation involves attenuation of Erk phosphorylation. J Mol Neurosci. 41, 183-192.

Lee, A., Martin, C., 2004. Neuro-ophthalmic findings in the visual variant of Alzheimer's disease. Ophthalmology 111, 376-380.

Lee, B., Cao, R., Choi, Y.-S., Cho, H.-Y., Rhee, A.D., Hah, C.K., Hoyt, K.R., Obrietan, K., 2009. The CREB/CRE transcriptional pathway: protection against oxidative stress-mediated neuronal cell death. J. Neurochem. 108, 1251-1265.

Lee, V., Goedert, M., Trojanowski, J., 2001. Neurodegenerative tauopathies. Annu Rev Neurosci 24, 1121 - 1159.

Lei, S.Z., Pan, Z.H., Aggarwal, S.K., Chen, H.S., Hartman, J., Sucher, N.J., Lipton, S.A., 1992. Effect of nitric oxide production on the redox modulatory site of the NMDA receptor-channel complex. Neuron 8, 1087-1099.

Leske, M.C., 2007. Open-angle glaucoma -- an epidemiologic overview. Ophthalmic Epidemiol. 14, 166-172.

Leske, M.C., Heijl, A., Hussein, M., Bengtsson, B., Hyman, L., Komaroff, E., 2003. Factors for glaucoma progression and the effect of treatment: the early manifest glaucoma trial. Arch Ophthalmol. 121, 48-56.

Leventhal, C., Rafii, S., Rafii, D., Shahar, A., Goldman, S.A., 1999. Endothelial trophic support of neuronal production and recruitment from the adult mammalian subependyma. Mol Cell Neurosci. 13, 450-464.

Levkovitch-Verbin, H., Harris-Cerruti, C., Groner, Y., Wheeler, L.A., Schwartz, M., Yoles, E., 2000. RGC Death in Mice after Optic Nerve Crush Injury: Oxidative Stress and Neuroprotection. Invest. Ophthalmol. Vis. Sci. 41, 4169-4174.

Levkovitch-Verbin, H., Martin, K.R., Quigley, H.A., Baumrind, L.A., Pease, M.E., Valenta, D., 2002a. Measurement of amino acid levels in the vitreous humor of rats after chronic intraocular pressure elevation or optic nerve transection. J Glaucoma 11, 396-405.

Levkovitch-Verbin, H., Quigley, H., Martin, K.R.G., Valenta, D., Baumrind, L., Pease, M., 2002b. Translimbal laser photocoagulation to the trabecular meshwork as a model of glaucoma in rats. Invest. Ophthalmol. Vis. Sci. 43, 402-410.

Levy, A.P., Levy, N.S., Goldberg, M.A., 1996. Post-transcriptional regulation of vascular endothelial growth factor by hypoxia. J Biol Chem. 271, 2746-2753.

Levy, D.I., Sucher, N.J., Lipton, S.A., 1990. Redox modulation of NMDA receptor-mediated toxicity in mammalian central neurons. Neurosci Lett. 110, 291-296.

Lewin, A.S., Drenser, K.A., Hauswirth, W.W., Nishikawa, S., Yasumura, D., Flannery, J.G., LaVail, M.M., 1998. Ribozyme rescue of photoreceptor cells in a transgenic rat model of autosomal dominant retinitis pigmentosa. Nat. Med. 4, 967-971.

Li, Q., Puro, D.G., 2001. Adenosine activates ATP-sensitive K(+) currents in pericytes of rat retinal microvessels: role of A1 and A2a receptors. Brain Res. 907, 93-99.

Libby, R., Howell, G., Pang, I.-H., Savinova, O., Mehalow, A., Barter, J., Smith, R., Clark, A., John, S.W.M., 2007. Inducible nitric oxide synthase, Nos2, does not mediate optic neuropathy and retinopathy in the DBA/2J glaucoma model. BMC neuroscience 8, 108-108.

Lieven, C.J., Schlieve, C.R., Hoegger, M.J., Levin, L.A., 2006. Retinal ganglion cell axotomy induces an increase in intracellular superoxide anion. Invest. Ophthalmol. Vis. Sci. 47, 1477-1485.

Lillig, C.H., Holmgren, A., 2007. Thioredoxin and Related Molecules-From Biology to Health and Disease. Antioxid Redox Signal. 9, 25-47.

Lindqvist, N., Vidal-Sanz, M., Hallböök, F., 2002. Single cell RT-PCR analysis of tyrosine kinase receptor expression in adult rat retinal ganglion cells isolated by retinal sandwiching. Brain Res. Prot. 10, 75-83.

Lipton, S.A., 2004. Failures and successes of NMDA receptor antagonists: molecular basis for the use of open-channel blockers like memantine in the treatment of acute and chronic neurologic insults. NeuroRx 1, 101-110.

Liu, B., Neufeld, A.H., 2000. Expression of nitric oxide synthase-2 (NOS-2) in reactive astrocytes of the human glaucomatous optic nerve head. Glia 30, 178 - 186.

Liu, M., Duggan, J., Salt, T., Cordeiro, M.F., 2011. Dendritic changes in visual pathways in glaucoma and other neurodegenerative conditions. Experimental Eye Research 92, 244-250.

Loscalzo, J., Welch, G., 1995. Nitric oxide and its role in the cardiovascular system. Prog Cardiovasc Dis. 38, 87-104.

Lotery, A.J., 2005. Glutamate excitotoxicity in glaucoma: truth or fiction? . Eye 19, 369-370.

Loyo-Berros, N., Blustein, J., 2007. Primary-open glaucoma and myopia: a narrative review. WMJ 106, 85-89, 95.

Lückhoff, A., Pohl, U., Mlsch, A., Busse, R., 1988. Differential role of extra- and intracellular calcium in the release of EDRF and prostacyclin from cultured endothelial cells. Br J Pharmacol. 95, 189-196.

Lukasiewicz, P., 2005. Synaptic mechanisms that shape visual signaling at the inner retina. Prog Brain Res 147, 205-218.

Luksch, A., Polak, K., Beier, C., Polska, E., Wolzt, M., Dorner, G.T., Eichler, H.G., Schmetterer, L., 2000. Effects of systemic NO synthase inhibition on choroidal and optic nerve head blood flow in healthy subjects. Invest Ophthalmol Vis Sci. 41, 3080-3084.

Lund, J.S., Remington, F.L., Lund, R.D., 1976. Differential central distribution of optic nerve components in the rat. Brain Res. 116, 83-100.

Luthra, A., Gupta, N., Kaufman, P., Weinreb, R., Ycel, Y., 2005. Oxidative injury by peroxynitrite in neural and vascular tissue of the lateral geniculate nucleus in experimental glaucoma. Exp Eye Res. 80, 43-49.

Ma, Y.T., Hsieh, T., Forbes, M.E., Johnson, J.E., Frost, D.O., 1998. BDNF injected into the superior colliculus reduces developmental retinal ganglion cell death. J Neurosci 18, 2097-2107.

Mabuchi, F., Aihara, M., Mackey, M., Lindsey, J., Weinreb, R., 2003. Optic nerve damage in experimental mouse ocular hypertension. Invest Ophthalmol Vis Sci. 44, 4321-4330.

MacCumber, M.W., D'Anna, S.A., 1994. Endothelin receptor-binding subtypes in the human retina and choroid. Arch Ophthalmol. 112, 1231-1235.

Maelicke, A., 2000. Allosteric modulation of nicotinic receptors as a treatment strategy for Alzheimer's disease. Dement Geriatr Cogn Disord. 11 Suppl 1, 11-18.

Mallis, R.J., Buss, J.E., Thomas, J.A., 2001. Oxidative modification of H-ras: S-thiolation and S-nitrosylation of reactive cysteines. Biochem. J. 355, 145-153.

Manabe, S., Lipton, S.A., 2003. Divergent NMDA signals leading to proapoptotic and antiapoptotic pathways in the rat retina. Invest. Ophthalmol. Vis. Sci. 44, 385-392.

Mandell, J., Banker, G., 1996. Microtubule-associated proteins, phosphorylation gradients, and the establishment of neuronal polarity. Perspect Dev Neurobiol 4, 125 - 135.

Mannens, G.S.J., Snel, C.A.W., Hendrickx, J., Verhaeghe, T., Le Jeune, L., Bode, W., van Beijsterveldt, L., Lavrijsen, K., Leempoels, J., Van Osselaer, N., Van Peer, A., Meuldermans, W., 2002. The metabolism and excretion of galantamine in rats, dogs, and humans. Drug Metab Dispos. 30, 553-563.

Mansour-Robaey, S., Clarke, D.B., Wang, Y.-C., Bray, G.M., Aguayo, A.J., 1994. Effects of ocular injury and administration of brain-derived neurotrophic factor on survival and regrowth of axotomized retinal ganglion cells. Proc. Natl. Acad. Sci. USA 91, 1632-1636.

Martin, K.R., Levkovitch Verbin, H., Valenta, D., Baumrind, L., Pease, M., Quigley, H., 2002. Retinal glutamate transporter changes in experimental glaucoma and after optic nerve transection in the rat. Invest Ophthalmol Vis Sci. 43, 2236-2243.

Martin, K.R., Quigley, H., Valenta, D., Kielczewski, J., Pease, M., 2006. Optic nerve dynein motor protein distribution changes with intraocular pressure elevation in a rat model of glaucoma. Experimental Eye Research 83, 255-262.

Martin, K.R., Quigley, H.A., Zack, D.J., Levkovitch-Verbin, H., Kielczewski, J., Valenta, D., Baumrind, L., Pease, M.E., Klein, R.L., Hauswirth, W.W., 2003. Gene therapy with brain-derived neurotrophic factor as a protection: retinal ganglion cells in a rat glaucoma model. Invest Ophthalmol Vis Sci 44, 4357-4365.

Mastropasqua, L., Lobefalo, L., Mancini, A., Ciancaglini, M., Palma, S., 1992. Prevalence of myopia in open angle glaucoma. Eur J Ophthalmol. 2, 33-35.

Matsuo, J., Oku, H., Kanbara, Y., Kobayashi, T., Sugiyama, T., Ikeda, T., 2009. Involvement of NADPH oxidase and protein kinase C in endothelin-1-induced superoxide production in retinal microvessels. Exp. Eye. Res. 89, 693-699.

May, C., Lütjen-Drecoll, E., 2002. Morphology of the murine optic nerve. Invest Ophthalmol Vis Sci. 43, 2206-2212.

Mayer, M.L., Westbrook, G.L., Guthrie, P.B., 1984. Voltage-dependent block by Mg2+ of NMDA responses in spinal cord neurones. Nature 309, 261-263.

Mayr, B., Montminy, M., 2001. Transcriptional regulation by the phosphorylation-dependent factor CREB. Nat Rev Mol Cell Biol. 2, 599-609.

McKinnon, S., Lehman, D., Kerrigan Baumrind, L., Merges, C., Pease, M., Kerrigan, D., Ransom, N., Tahzib, N.G., Reitsamer, H., Levkovitch Verbin, H., Quigley, H., Zack, D., 2002. Caspase activation and amyloid precursor protein cleavage in rat ocular hypertension. Investigative ophthalmology & visual science 43, 1077-1087.

McKinnon, S.J., 2003. Glaucoma: ocular Alzheimer's disease? Front. Biosci. 8, 1140-1156.

McLeod, S.D., West, S.K., Quigley, H.A., Fozard, J.L., 1990. A longitudinal study of the relationship between intraocular and blood pressures. Invest Ophthalmol Vis Sci. 31, 2361-2366.

Medeiros, F., Sample, P., Zangwill, L., Bowd, C., Aihara, M., Weinreb, R., 2003. Corneal thickness as a risk factor for visual field loss in patients with preperimetric glaucomatous optic neuropathy. Am J Ophthalmol. 136, 805-813.

Mendez, M.F., Cherrier, M.M., Meadows, R.S., 1996. Depth perception in Alzheimer's disease. Perceptual and motor skills 83, 987-995.

Metea, M., Newman, E., 2007. Signalling within the neurovascular unit in the mammalian retina. Exp Physiol. 92, 635-640.

Meuchel, L., Thompson, M., Cassivi, S., Pabelick, C., Prakash, Y.S., 2011. Neurotrophins induce nitric oxide generation in human pulmonary artery endothelial cells. Cardiovasc Res. 91, 668-676.

Mey, J., Thanos, S., 1993. Intravitreal injections of neurotrophic factors support the survival of axotomized retinal ganglion cells in adult rats in vivo. Brain Res. 602, 304-317.

Mickley, E.J., Gray, G.A., Webb, D.J., 1997. Activation of endothelin ETA receptors masks the constrictor role of endothelin ETB receptors in rat isolated small mesenteric arteries. Br J Ophthalmol. 120, 1376-1382.

Migeon, J.C., Nathanson, N.M., 1994. Differential regulation of cAMP-mediated gene transcription by m1 and m4 muscarinic acetylcholine receptors. Preferential coupling of m4 receptors to Gi alpha-2. J. Biol. Chem. 269, 9767-9773.

Miller, F.D., Kaplan, D.R., 2001. Neurotrophin signalling pathways regulating neuronal apoptosis. Cell Mol Life Sci 58, 1045-1053.

Miller, K.M., Quigley, H.A., 1987. Comparison of optic disc features in low-tension and typical open-angle glaucoma. Ophthalmic Surg. 18, 882-889.

Min, W., Lin, Y., Tang, S., Yu, L., Zhang, H., Wan, T., Luhn, T., Fu, H., Chen, H., 2008. AIP1 Recruits Phosphatase PP2A to ASK1 in Tumor Necrosis Factor-Induced ASK1-JNK Activation. Circ Res 102, 840-848.

Minckler, D.S., Bunt, A.H., Johanson, G.W., 1977. Orthograde and retrograde axoplasmic transport during acute ocular hypertension in the monkey. Invest Ophthalmol Vis Sci 16 426-441.

Moon, J.-I., Kim, I.-B., Gwon, J.-S., Park, M.-H., Kang, T.-H., Lim, E.-J., Choi, K.-R., Chun, M.-H., 2005. Changes in retinal neuronal populations in the DBA/2J mouse. Cell Tissue Res. 320, 51-59.

Moore, C.G., Milne, S.T., Johnson, E.C., Morrison, J.C., 1993. A rat model of pressure-induced optic nerve damage (ARVO abstact). Invest Ophthalmol Vis Sci. , 1141.

Moreno, M., Campanelli, J., Sande, P., Snez, D., Keller-Sarmiento, M., Rosenstein, R., 2004. Retinal oxidative stress induced by high intraocular pressure. Free Radic Biol Med. 37, 803-812.

Morgan, J.E., Uchida, H., Caprioli, J., 2000. Retinal ganglion cell death in experimental glaucoma. Br J Ophthalmol. 84, 303-310.

Morrison, J.C., Dorman Pease, M.E., Dunkelberger, G.R., Quigley, H.A., 1990. Optic nerve head extracellular matrix in primary optic atrophy and experimental glaucoma. Arch Ophthalmol. 108, 1020-1024.

Morrison, J.C., Fraunfelder, F.W., Milne, S.T., Moore, C.G., 1995. Limbal microvasculature of the rat eye. Invest Ophthalmol Vis Sci. 36, 751-756.

Morrison, J.C., Moore, C.G., Deppmeier, L.M., Gold, B.G., Meshul, C.K., Johnson, E.C., 1997. A rat model of chronic pressure-induced optic nerve damage. Exp Eye Res. 64, 85-96.

Moser, K., Reindl, M., Blasig, I., Humpel, C., 2004. Brain capillary endothelial cells proliferate in response to NGF, express NGF receptors and secrete NGF after inflammation. Brain Res. 1017, 53-60.

Munemasa Y, A.J., Kwong JM, Caprioli J, Piri N., 2009. Redox proteins thioredoxin 1 and thioredoxin 2 support retinal ganglion cell survival in experimental glaucoma. Gene Ther. 16, 17-25.

Munemasa, Y., Kim, S.H., Ahn, J.H., Kwong, J.M.K., Caprioli, J., Piri, N., 2008. Protective Effect of Thioredoxins 1 and 2 in Retinal Ganglion Cells after Optic Nerve Transection and Oxidative Stress. Investigative Ophthalmology & Visual Science 49, 3535-3543.

Murphy, J., Archibald, M., Chauhan, B., 2010. The role of endothelin-1 and its receptors in optic nerve head astrocyte proliferation. Br J Ophthalmol. 94, 1233-1238.

Murphy, J.A., Clarke, D.B., 2006. Target-derived neurotrophins may influence the survival of adult retinal ganglion cells when local neurotrophic support is disrupted: Implications for glaucoma. Medical Hypotheses 67, 1208-1212.

Nadal-Nicols, F., Jimnez-Lpez, M., Sobrado Calvo, P., Nieto-Lpez, L., Cnovas-Martnez, I., Salinas Navarro, M., Vidal Sanz, M., Agudo, M., 2009. Brn3a as a marker of retinal ganglion cells: qualitative and quantitative time course studies in naive and optic nerve-injured retinas. Invest Ophthalmol Vis Sci. 50, 3860-3868.

Nagel, E., Vilser, W., Lanzl, I.M., Lanzi, I.M., 2001. Retinal vessel reaction to short-term IOP elevation in ocular hypertensive and glaucoma patients. Eur J Ophthalmol. 11, 338-344.

Nakaizumi, A., Puro, D., 2011. Vulnerability of the retinal microvasculature to hypoxia: role of polyamine-regulated K(ATP) channels. Invest. Ophthalmol. Vis. Sci. 52, 9345-9352.

Nakamura, K., Tan, F., Li, Z., Thiele, C., 2011. NGF activation of TrkA induces vascular endothelial growth factor expression via induction of hypoxia-inducible factor-1α. Mol Cell Neurosci. 46, 498-506.

Nakazawa, T., Tamai, M., Mori, N., 2002. Brain-derived neurotrophic factor prevents axotomized retinal ganglion cell death through MAPK and PI3K signaling pathways. Invest Ophthalmol Vis Sci 43, 3319-3326.

Nathanson, J.A., McKee, M., 1995. Alterations of ocular nitric oxide synthase in human glaucoma. Invest Ophthalmol Vis Sci. 36, 1774-1784.

Nemesure, B., Honkanen, R., Hennis, A., Wu, S.Y., Leske, M.C., 2007. Incident open-angle glaucoma and intraocular pressure. Ophthalmology 114, 1810-1815.

Neufeld, A., 2004. Pharmacologic neuroprotection with an inhibitor of nitric oxide synthase for the treatment of glaucoma. Brain Res Bull. 62, 455-459.

Neufeld, A.H., Hernandez, M.R., Gonzalez, M., 1997. Nitric oxide synthase in the human glaucomatous optic nerve head. Archives of ophthalmology 115, 497-503.

Neufeld, A.H., Shareef, S., Pena, J., 2000. Cellular localization of neuronal nitric oxide synthase (NOS-1) in the human and rat retina. J Comp Neurol. 416, 269-275.

Nguyen, S.M., Alexejun, C.N., Levin, L.A., 2003. Amplification of a Reactive Oxygen Species Signal in Axotomized Retinal Ganglion Cells. Antioxid. Redox. Sign. 5, 629-634.

Nguyen, T., Nioi, P., Pickett, C., 2009. The Nrf2-antioxidant response element signaling pathway and its activation by oxidative stress. J Biol Chem. 284, 13291-13295.

Nickells, R.W., 1999. Apoptosis of retinal ganglion cells in glaucoma: an update of the molecular pathways involved in cell death. Surv Ophthalmol. 43 Suppl 1, S151-S161.

Nicolela, M.T., Ferrier, S.N., Morrison, C.A., Archibald, M.L., LeVatte, T.L., Wallace, K., Chauhan, B.C., LeBlanc, R.P., 2003. Effects of Cold-Induced Vasospasm in Glaucoma: The Role of Endothelin-1. Investigative Ophthalmology & Visual Science 44, 2565-2572.

Nicolela, M.T., Hnik, P., Drance, S.M., 1996. Scanning laser Doppler flowmeter study of retinal and optic disk blood flow in glaucomatous patients. Am J Ophthalmol. 122, 775-783.

Nicotera, P., Brune, B., Bagetta, G., 1997. Nitric oxide: inducer or suppressor of apoptosis? Trends Pharmacol Sci. 18, 189-190.

Noske, W., Hensen, J., Wiederholt, M., 1997. Endothelin-like immunoreactivity in aqueous humor of patients with primary open-angle glaucoma and cataract,. Graefes Arch. Clin. Exp. Ophthalmol 235.

Nouri Mahdavi, K., Supawavej, C., Bitrian, E., Giaconi, J., Law, S., Coleman, A., Caprioli, J., 2011. Patterns of damage in chronic angle-closure glaucoma compared to primary open-angle glaucoma. Am J Ophthalmol. 152, 74-80.e72.

Nowak, L., Bregestovski, P., Ascher, P., Herbet, A., Prochiantz, A., 1984. Magnesium gates glutamate-activated channels in mouse central neurones. Nature 307, 462-465.

Osborne, N.N., 2008. Recent clinical findings with memantine should not mean that the idea of neuroprotection in glaucoma is abandoned. Acta Ophthalmol. 87, 450-454.

Osborne, N.N., Chidlow, G., Wood, J.P.M., 2006. Glutamate excitotoxicity in glaucoma: truth or fiction? By AJ Lotery. Eye 20, 1392-1394.

Osborne, N.N., Melena, J., Chidlow, G., Wood, J.P., 2001. A hypothesis to explain ganglion cell death caused by vascular insults at the optic nerve head: possible implication for the treatment of glaucoma. 85, 1252-1259.

Otori, Y., ., Shimada, S., Tanaka, K., Ishimoto, I., Tano, Y., Tohyama, M., 1994. Marked increase in glutamate-aspartate transporter (GLAST/GluT-1) mRNA following transient retinal ischemia. Brain Res. Mol. Brain Res. 27, 310-314.

Pacher, P., Beckman, J., Liaudet, L., 2007. Nitric oxide and peroxynitrite in health and disease. Physiol Rev. 87, 315-424.

Pang, I.-H., Johnson, E., Jia, L., Cepurna, W., Shepard, A., Hellberg, M., Clark, A., Morrison, J., 2005. Evaluation of inducible nitric oxide synthase in glaucomatous optic neuropathy and pressure-induced optic nerve damage. Investigative ophthalmology & visual science 46, 1313-1321.

Parisi, V., 2003. Correlation between morphological and functional retinal impairment in patients affected by ocular hypertension, glaucoma, demyelinating optic neuritis and Alzheimer's disease. Semin. Ophthalmol. 18, 50-57.

Park, C., Raines, R.T., 2001. Adjacent cysteine residues as a redox switch. Protein Eng 14, 939-942.

Park, J.B., Yiu, G., Kaneko, S., Wang, J., Chang, J., He, X.L., Garcia, K.C., He, Z., 2005. A TNF receptor family member, TROY, is a coreceptor with Nogo receptor in mediating the inhibitory activity of myelin inhibitors. Neuron 45, 345-351.

Parrilla-Reverter, G., Agudo, M., Sobrado-Calvo, P., Salinas-Navarro, M., Villegas-Pérez, M.P., Vidal-Sanz, M., 2009. Effects of different neurotrophic factors on the survival of retinal ganglion cells after a complete intraorbital nerve crush injury: A quantitative in vivo study. Exp. Eye Res. 89, 32-41.

Parsons, C.G., Danysz, W., Quack, G., 1999. Memantine is a clinically well tolerated N-methyl--aspartate (NMDA) receptor antagonist--a review of preclinical data. Neuropharmacology 38, 735-767.

Pearson, H.E., Stoffler, D.J., 1992. Retinal ganglion cell degeneration following loss of postsynaptic target neurons in the dorsal lateral geniculate nucleus of the adult cat. Experimental Neurology 116, 163-171.

Pearson, H.E., Thompson, T.P., 1993. Atrophy and degeneration of ganglion cells in central retina following loss of postsynaptic target neurons in the dorsal lateral geniculate nucleus of the adult cat. Exp. Neurol. 119, 113-119.

Pease, M.E., McKinnon, S.J., Quigley, H.A., Kerrigan-Baumrind, L.A., Zack, D.J., 2000. Obstructed axonal transport of BDNF and its receptor TrkB in experimental glaucoma. Invest Ophthalmol Vis Sci 41, 764-774.

Pederson, J.E., Anderson, D.R., 1980. The mode of progressive disc cupping in ocular hypertension and glaucoma. Arch Ophthalmol. 98, 490-495.

Peinado-Ramon, P., Salvador, M., Villegas-Perez, M.P., Vidal-Sanz, M., 1996. Effects of axotomy and intraocular administration of NT-4, NT-3, and brain-derived neurotrophic factor on the survival of adult rat retinal ganglion cells. A quantitative in vivo study. Invest. Ophthalmol. Vis. Sci. 37, 489-500.

Pellegrini-Giampietro, D.E., Zukin, R.S., Bennett, M.V., Cho, S., Pulsinelli, W.A., 1992. Switch in glutamate receptor subunit gene expression in CA1 subfield of hippocampus following global ischemia in rats. Proc. Natl. Acad. Sci. U. S. A. 89, 10499-10503.

Pena, J.D., Agapova, O., Gabelt, B.T., Levin, L.A., Lucarelli, M.J., Kaufman, P.L., Hernandez, M.R., 2001. Increased elastin expression in astrocytes of the lamina cribrosa in response to elevated intraocular pressure. Invest Ophthalmol Vis Sci. 42, 2303-2314.

Peng, Y.W., Blackstone, C.D., Huganir, R.L., Yau, K.W., 1995. Distribution of glutamate receptor subtypes in the vertebrate retina. Neuroscience 66, 483-497.

Pereira, E.F.R., Hilmas, C., Santos, M., Alkondon, M., Maelicke, A., Albuquerque, E., 2002. Unconventional ligands and modulators of nicotinic receptors. J Neurobiol. 53, 479-500.

Pérez, M.T.R., Caminos, E., 1995. Expression of brain-derived neurotrophic factor and its functional receptor in neonatal and adult rat retina. Neurosci. Lett. 183, 96-99.

Pérez, V., Lew, C., Cortez, L., Webb, C., Rodriguez, M., Liu, Y., Qi, W., Li, Y., Chaudhuri, A., Van Remmen, H., Richardson, A., Ikeno, Y., 2008. Thioredoxin 2 haploinsufficiency in mice results in impaired mitochondrial function and increased oxidative stress. Free Radic Biol Med. 44, 882-892.

Pernet, V., Bourgeois, P., Di Polo, A., 2007. A role for polyamines in retinal ganglion cell excitotoxic death. . J. Neurochem. 103, 1481-1490.

Pernet, V., Hauswirth, W., Di Polo, A., 2005. Extracellular signal-regulated kinase 1/2 mediates survival, but not axon regeneration, of adult injured central nervous system neurons in vivo. J Neurochem 93, 72-83.

Pierre, L.N., Davenport, A.P., 1998. Relative contribution of endothelin A and endothelin B receptors to vasoconstriction in small arteries from human heart and brain. J Cardiovasc Pharmacol. 31 Suppl 1, S74-S76.

Pillunat, L.E., Stodtmeister, R., Wilmanns, I., Christ, T., 1985. Autoregulation of ocular blood flow during changes in intraocular pressure. Preliminary results. Graefes Arch Clin Exp Ophthalmol. 223, 219-223.

Piltz-seymour, J.R., Grunwald, J.E., Hariprasad, S.M., Dupont, J., 2001. Optic nerve blood flow is diminished in eyes of primary open-angle glaucoma suspects. Am J Ophthalmol. 132, 63-69.

Plange, N., Kaup, M., Huber, K., Remky, A., Arend, O., 2006. Fluorescein filling defects of the optic nerve head in normal tension glaucoma, primary open-angle glaucoma, ocular hypertension and healthy controls. Ophthalmic Physiol Opt. 26, 26-32.

Platt, D., Bartoli, M., El Remessy, A., Al Shabrawey, M., Lemtalsi, T., Fulton, D., Caldwell, R., 2005. Peroxynitrite increases VEGF expression in vascular endothelial cells via STAT3. Free Radic Biol Med. 39, 1353-1361.

Polak, K., Luksch, A., Berisha, F., Fuchsjaeger Mayrl, G., Dallinger, S., Schmetterer, L., 2007. Altered nitric oxide system in patients with open-angle glaucoma. Arch Ophthalmol. 125, 494-498.

Pollock, G.S., Robichon, R., Boyd, K.A., Kerkel, K.A., Kramer, M., Lyles, J., Ambalavanar, R., Khan, A., Kaplan, D.R., Williams, R.W., Frost, D.O., 2003. TrkB receptor signaling regulates developmental death dynamics, but not final number, of retinal ganglion cells. J Neurosci 23, 10137-10145.

Pournaras, C.J., Rungger-Brändle, E., Riva, C.E., Hardarson, S.H., Stefansson, E., 2008. Regulation of retinal blood flow in health and disease. Prog Retin Eye Res. 27, 284-330.

Pow, D.V., Crook, D.K., 1995. Immunocytochemical evidence for the presence of high levels of reduced glutathione in radial glial cells and horizontal cells in the rabbit retina. Neuroscience Letters 193, 25-28.

Prasanna, G., Hulet, C., Desai, D., Krishnamoorthy, R.R., Narayan, S., Brun, A.-M., Suburo, A.M., Yorio, T., 2005. Effect of elevated intraocular pressure on endothelin-1 in a rat model of glaucoma. Pharmacological Research 51, 41-50.

Prasanna, G., Krishnamoorthy, R., Clark, A., Wordinger, R., Yorio, T., 2002. Human optic nerve head astrocytes as a target for endothelin-1. Invest Ophthalmol Vis Sci. 43, 2704-2713.

Quigley, H., Anderson, D.R., 1976. The dynamics and location of axonal transport blockade by acute intraocular pressure elevation in primate optic nerve. Invest Ophthalmol. 15, 606-616.

Quigley, H.A., 1999. Neuronal death in glaucoma. Prog. Retin. Eye Res. 18, 39-57.

Quigley, H.A., 2005. New paradigms in the mechanisms and management of glaucoma. Eye 19, 1241-1248.

Quigley, H.A., Addicks, E.M., 1980. Chronic experimental glaucoma in primates. II. Effect of extended intraocular pressure elevation on optic nerve head and axonal transport. Invest Ophthalmol Vis Sci 19, 137-152.

Quigley, H.A., Anderson, D.R., 1977. Distribution of axonal transport blockade by acute intraocular pressure elevation in the primate optic nerve head. Invest. Ophthalmol. Vis Sci. 16, 640-644.

Quigley, H.A., Broman, A.T., 2006. The number of people with glaucoma worldwide in 2010 and 2020. Br J Ophthalmol. 90, 262-267.

Quigley, H.A., Dunkelberger, G.R., Green, W.R., 1988. Chronic human glaucoma causing selectively greater loss of large optic nerve fibers. Ophthalmology 95, 357-363.

Quigley, H.A., Enger, C., Katz, J., Sommer, A., Scott, R., Gilbert, D., 1994. Risk factors for the development of glaucomatous visual field loss in ocular hypertension. Arch Ophthalmol. 112, 644-649.

Quigley, H.A., Hohman, R.M., Addicks, E.M., Green, W.R., 1984. Blood vessels of the glaucomatous optic disc in experimental primate and human eyes. Invest Ophthalmol Vis Sci. 25, 918-931.

Quigley, H.A., McKinnon, S.J., Zack, D.J., Pease, M.E., Kerrigan-Baumrind, L.A., Kerrigan, D.F., Mitchell, R.S., 2000. Retrograde axonal transport of BDNF in retinal ganglion cells is blocked by acute IOP elevation in rats. Invest Ophthalmol Vis Sci 41, 3460-3466.

Radius, R.L., Anderson, D.R., 1979. The histology of retinal nerve fiber layer bundles and bundle defects. Arch Ophthalmol. 97, 948-950.

Raff, M.C., Barres, B.A., Burne, J.F., Coles, H.S., Ishizaki, Y., Jacobson, M.D., 1993. Programmed cell death and the control of cell survival: lessons from the nervous system. Science 262, 695-700.

Rager, G.H., 1980. Development of the retinotectal projection in the chicken. Adv Anat Embryol Cell Biol 63, 1-90.

Rauen, T., Taylor, W.R., Kuhlbrodt, K., Wiessner, M., 1998. High-affinity glutamate transporters in the rat retina: a major role of the glial glutamate transporter GLAST-1 in transmitter clearance. Cell Tissue Res. 291, 19-31.

Rauen, T., Wiessner, M., Sullivan, R., Lee, A., Pow, D., 2004. A new GLT1 splice variant: cloning and immunolocalization of GLT1c in the mammalian retina and brain. Neurochem Int. 45, 1095-1106.

Razay, G., Wilcock, G.K., 2008. Galantamine in Alzheimer's disease. Exp. Rev. Neurother. 8, 9-17.

Reinstein, S., Rankin, A., Allbaugh, R., 2009. Canine glaucoma: pathophysiology and diagnosis. Compend Contin Educ Vet. 31, 450-453.

Reisberg, B., Doody, R., Stoffler, A., Schmitt, F., Ferris, S., Mobius, H.J., the Memantine Study, G., 2003. Memantine in Moderate-to-Severe Alzheimer's Disease. New Engl. J. Med. 348, 1333-1341.

Resnikoff, S., Pascolini, D., Etya'ale, D., Kocur, I., Pararajasegaram, R., Pokharel, G., Mariotti, S., 2004. Global data on visual impairment in the year 2002. Bull World Health Organ. 82, 844-851.

Rhee, K., Kim, Y.Y., Nam, D.H., Jung, H.R., 2001. Comparison of visual field defects between primary open-angle glaucoma and chronic primary angle-closure glaucoma in the early or moderate stage of the disease. Korean J Ophthalmol. 15, 27-31.

Riccio, A., Alvania, R., Lonze, B., Ramanan, N., Kim, T., Huang, Y., Dawson, T., Snyder, S., Ginty, D., 2006. A nitric oxide signaling pathway controls CREB-mediated gene expression in neurons. Mol Cell. 21, 283-294.

Rickman, D.W., Brecha, N.C., 1995. Expression of the proto-oncogene, trk, receptors in the developing rat retina. Vis. Neurosci. 12, 215-222.

Riva, C., Logean, E., Falsini, B., 2005. Visually evoked hemodynamical response and assessment of neurovascular coupling in the optic nerve and retina. Prog Retin Eye Res. 24, 183-215.

Rohrer, B., LaVail, M.M., Jones, K.R., Reichardt, L.F., 2001. Neurotrophin receptor TrkB activation is not required for the postnatal survival of retinal ganglion cells in vivo. Exp Neurol 172, 81-91.

Rosenblum, W.I., 1987. Hydroxyl radical mediates the endothelium-dependent relaxation produced by bradykinin in mouse cerebral arterioles. Circ. Res. 61, 601-603.

Rosenthal, R., Fromm, M., 2011. Endothelin antagonism as an active principle for glaucoma therapy. Br J Pharmacol. 162, 806-816.

Ross, C.D., Dunning, D.D., Juengel, L.I., Godfrey, D.A., 1985. Laminar distributions of choline acetyltransferase and acetylcholinesterase activities in the inner plexiform layer of rat retina. J Neurochem. 44, 1091-1099.

Rothe, T., Bähring, R., Carroll, P., Grantyn, R., 1999. Repetitive firing deficits and reduced sodium current density in retinal ganglion cells developing in the absence of BDNF. J Neurobiol 40, 407-419.

Rudzinski, M., Wong, T.P., Saragovi, H.U., 2004. Changes in retinal expression of neurotrophins and neurotrophin receptors induced by ocular hypertension. J. Neurobiol. 58, 341-354.

Russ, P.K., Davidson, M.K., Hoffman, L.H., Haselton, F.R., 1998. Partial characterization of the human retinal endothelial cell tight and adherens junction complexes. Invest Ophthalmol Vis Sci. 39, 2479-2485.

Sacc, S., Pascotto, A., Camicione, P., Capris, P., Izzotti, A., 2005. Oxidative DNA damage in the human trabecular meshwork: clinical correlation in patients with primary open-angle glaucoma. Arch Ophthalmol. 123, 458-463.

Saint Geniez, M., D'Amore, P., 2004. Development and pathology of the hyaloid, choroidal and retinal vasculature. Int J Dev Biol. 48, 1045-1058.

Saitoh, M., Nishitoh, H., Fujii, M., Takeda, K., Tobiume, K., Sawada, Y., Kawabata, M., Miyazono, K., Ichijo, H., 1998. Mammalian thioredoxin is a direct inhibitor of apoptosis signal-regulating kinase (ASK) 1. EMBO J 17, 2596-2606.

Sakata, L.M., DeLeón-Ortega, J., Girkin, C.A., 2007. Selective perimetry in glaucoma diagnosis. Curr Opin Ophthalmol. 18, 115-121

Salinas-Navarro, M., Alarcón-Martínez, L., Valiente-Soriano, F., Ortín-Martínez, A., Jiménez-López, M., Avilés-Trigueros, M., Villegas-Pérez, M., de la Villa, P., Vidal-Sanz, M., 2009. Functional and morphological effects of laser-induced ocular hypertension in retinas of adult albino Swiss mice. Mol Vis. 15, 2578-2598.

Salinas-Navarro, M., Alarcón-Martínez, L., Valiente-Soriano, F.J., Jiménez-López, M., Mayor-Torroglosa, S., Avilés-Trigueros, M., Villegas-Pérez, M.P., Vidal-Sanz, M., 2010. Ocular hypertension impairs optic nerve axonal transport leading to progressive retinal ganglion cell degeneration. Exp Eye Res 90, 168-183.

Samochocki, M., Hffle, A., Fehrenbacher, A., Jostock, R., Ludwig, J., Christner, C., Radina, M., Zerlin, M., Ullmer, C., Pereira, E.F.R., Lbbert, H., Albuquerque, E., Maelicke, A., 2003. Galantamine is an allosterically potentiating ligand of neuronal nicotinic but not of muscarinic acetylcholine receptors. J Pharmacol Exp Ther. 305, 1024-1036.

Sample, P.A., Bosworth, C.F., Blumenthal, E.Z., Girkin, C., Weinreb, R.N., 2000. Visual Function–Specific Perimetry for Indirect Comparison of Different Ganglion Cell Populations in Glaucoma. Invest Ophthalmol Vis Sci. 41, 1783-1790.

Sankar, P.S., Pasquale, L.R., Grosskreutz, C.L., 2001. Uveal effusion and secondary angle-closure glaucoma associated with topiramate use. Arch Ophthalmol. 119, 1210-1211.

Santhanam, A.V.R., Smith, L., Katusic, Z., 2010. Brain-derived neurotrophic factor stimulates production of prostacyclin in cerebral arteries. Stroke 41, 350-356.

Sapieha, P., Peltier, M., Rendahl, K., Manning, W., Di Polo, A., 2003. Fibroblast growth factor-2 gene delivery stimulates axon growth by adult retinal ganglion cells after acute optic nerve injury. Molecular and cellular neurosciences 24, 656-672.

Sappington, R., Carlson, B., Crish, S., Calkins, D., 2010. The microbead occlusion model: a paradigm for induced ocular hypertension in rats and mice. Invest Ophthalmol Vis Sci. 51, 207-216.

Sargent, P.B., 1993. The diversity of neuronal nicotinic acetylcholine receptors. Annu Rev Neurosci. 16, 403-443.

Sarma, B., Mugesh, G., 2008. Thiol cofactors for selenoenzymes and their synthetic mimics. Org Biomol Chem. 6, 965-974.

Sastry, B.V., 1985a. Cholinergic systems and multiple cholinergic receptors in ocular tissues. J Ocul Pharmacol. 1, 201-226.

Sastry, B.V., 1985b. Cholinergic systems and multiple cholinergic receptors in ocular tissues. Journal of ocular pharmacology 1, 201-226.

Sato, E., Ohtake, Y., Shinoda, K., Mashima, Y., Kimura, I., 2006. Decreased blood flow at neuroretinal rim of optic nerve head corresponds with visual field deficit in eyes with normal tension glaucoma. Graefes Arch Clin Exp Ophthalmol. 244, 795-801.

Satoh, T., Yamagata, T., Ishikawa, Y., Yamada, M., Uchiyama, Y., Hatanaka, H., 1999. Regulation of reactive oxygen species by nerve growth factor but not Bcl-2 as a novel mechanism of protection of PC12 cells from superoxide anion-induced death. J Biochem. 125, 952-959.

Scarisbrick, I.A., Jones, E.G., Isackson, P.J., 1993. Coexpression of mRNAs for NGF, BDNF, and NT-3 in the cardiovascular system of the pre- and postnatal rat. J Neurosci. 13, 875-893.

Scheiner, A.J., Riva, C.E., Kazahaya, K., Petrig, B.L., 1994. Effect of flicker on macular blood flow assessed by the blue field simulation technique. Invest Ophthalmol Vis Sci. 35, 3436-3441.

Schildknecht, S., Ullrich, V., 2009. Peroxynitrite as regulator of vascular prostanoid synthesis. Arch. Biochem. Biophys. 484, 183-189.

Schiller, P.H., Malpeli, J.G., 1977. Properties and tectal projections of monkey retinal ganglion cells. J Neurophysiol. 40, 428-445.

Schlieve, C.R., Tam, A., Nilsson, B.L., Lieven, C.J., Raines, R.T., Levin, L.A., 2006. Synthesis and characterization of a novel class of reducing agents that are highly neuroprotective for retinal ganglion cells. Exp. Eye Res. 83, 1252-1259.

Schmidt, M., Humphrey, M.F., Wssle, H., 1987. Action and localization of acetylcholine in the cat retina. J Neurophysiol. 58, 997-1015.

Schori, H., Kipnis, J., Yoles, E., WoldeMussie, E., Ruiz, G., Wheeler, L.A., Schwartz, M., 2001. Vaccination for protection of retinal ganglion cells against death from glutamate cytotoxicity and ocular hypertension: implications for glaucoma. Proc Natl Acad Sci U S A. 98, 3398-3403.

Schrattenholz, A., Godovac Zimmermann, J., Schfer, H.J., Albuquerque, E.X., Maelicke, A., 1993. Photoaffinity labeling of Torpedo acetylcholine receptor by physostigmine. Eur J Biochem. 216, 671-677.

Schrattenholz, A., Pereira, E.F., Roth, U., Weber, K.H., Albuquerque, E.X., Maelicke, A., 1996. Agonist responses of neuronal nicotinic acetylcholine receptors are potentiated by a novel class of allosterically acting ligands. Mol Pharmacol. 49, 1-6.

Schrder, B., Reinhardt Maelicke, S., Schrattenholz, A., McLane, K.E., Kretschmer, A., Conti Tronconi, B.M., Maelicke, A., 1994. Monoclonal antibodies FK1 and WF6 define two neighboring ligand binding sites on Torpedo acetylcholine receptor alpha-polypeptide. J Biol Chem. 269, 10407-10416.

Schtte, M., Werner, P., 1998. Redistribution of glutathione in the ischemic rat retina. Neurosci Lett. 246, 53-56.

Schuettauf, F., Thaler, S., Bolz, S., Fries, J., Kalbacher, H., Mankowska, A., Zurakowski, D., Zrenner, E., Rejdak, R., 2007. Alterations of amino acids and glutamate transport in the DBA/2J mouse retina; possible clues to degeneration. Graefes Arch Clin Exp Ophthalmol. 245, 1157-1168.

Scimemi, A., Tian, H., Diamond, J., 2009. Neuronal transporters regulate glutamate clearance, NMDA receptor activation, and synaptic plasticity in the hippocampus. J Neurosci. 29, 14581-14595.

Scott, L.J., Goa, K.L., 2000. Galantamine: a review of its use in Alzheimer's disease. Drugs 60, 1095-1122.

Sefton, A.J., Lam, K., 1984. Quantitative and morphological studies on developing optic axons in normal and enucleated albino rats. Exp Brain Res 57, 107-117.

Segal, R., Greenberg, M.E., 1996. Intracellular signaling pathway activated by neurotrophic factors. Ann. Rev. Neurosci. 19, 463-489.

Seki, M., Lipton, S., 2008. Targeting excitotoxic/free radical signaling pathways for therapeutic intervention in glaucoma. Prog Brain Res 173, 495-510.

Shao, Z., Browning, J.L., Lee, X., Scott, M.L., Shulga-Morskaya, S., Allaire, N., Thill, G., Levesque, M., Sah, D., McCoy, J.M., 2005. TAJ/TROY, an Orphan TNF Receptor Family Member, Binds Nogo-66 Receptor 1 and Regulates Axonal Regeneration. Neuron 45, 353-359.

Shareef, S., Sawada, A., Neufeld, A.H., 1999. Isoforms of nitric oxide synthase in the optic nerves of rat eyes with chronic moderately elevated intraocular pressure. Invest Ophthalmol Vis Sci. 40, 2884-2891.

Shareef, S.R., Garcia Valenzuela, E., Salierno, A., Walsh, J., Sharma, S.C., 1995. Chronic ocular hypertension following episcleral venous occlusion in rats. Exp Eye Res. 61, 379-382.

Sharma, P., Sample, P.A., Zangwill, L.M., Schuman, J.S., 2008. Diagnostic Tools for Glaucoma Detection and Management. Surv Ophthalmol. 53, S17-S32.

Shaywitz, A.J., Greenberg, M.E., 1999. CREB: a stimulus-induced transcription factor activated by a diverse array of extracellular signals. Annu Rev Biochem. 68, 821-861.

Sihota, R., 2011. Classification of primary angle closure disease. Curr Opin Ophthalmol. 22, 87-95.

Sit, A., Medeiros, F., Weinreb, R., 2004. Short-wavelength automated perimetry can predict glaucomatous standard visual field loss by ten years. Semin Ophthalmol. 19, 122-124.

Sloane, P.D., Zimmerman, S., Suchindran, C., Reed, P., Wang, L., Boustani, M., Sudha, S., 2002. The public health impact of Alzheimer's disease, 2000-2050: Potential Implication of Treatment Advances. Annual Review of Public Health 23, 213-231.

Snapyan, M., Lemasson, M., Brill, M., Blais, M., Massouh, M., Ninkovic, J., Gravel, C., Berthod, F., Gtz, M., Barker, P., Parent, A., Saghatelyan, A., 2009. Vasculature guides migrating neuronal precursors in the adult mammalian forebrain via brain-derived neurotrophic factor signaling. J Neurosci. 29, 4172-4188.

Sobey, C.G., Heistad, D.D., Faraci, F.M., 1997. Mechanisms of bradykinin-induced cerebral vasodilatation in rats. Evidence that reactive oxygen species activate K+ channels. Stroke. 28, 2290-2294.

Sommer, A., Tielsch, J.M., Katz, J., Quigley, H.A., Gottsch, J.D., Javitt, J.C., Martone, J.F., Royall, R.M., Witt, K.A., Ezrine, S., 1991. Racial differences in the cause-specific prevalence of blindness in east Baltimore. N Engl J Med. 325, 1412-1417.

Spector, R.H., 1990. Clinical Methods, The History, Physical, and Laboratory Examinations. Butterworth Publishers, Boston, 3rd edition, Visual Fields, Chapter 116.

Stewart, P.A., Tuor, U.I., 1994. Blood-eye barriers in the rat: correlation of ultrastructure with function. J Comp Neurol. 340, 566-576.

Stitt, A.W., Chakravarthy, U., Gardiner, T.A., Archer, D.B., 1996. Endothelin-like immunoreactivity and receptor binding in the choroid and retina. Curr Eye Res. 15, 111-117.

Strachan, F.E., Spratt, J.C., Wilkinson, I.B., Johnston, N.R., Gray, G.A., Webb, D.J., 1999. Systemic blockade of the endothelin-B receptor increases peripheral vascular resistance in healthy men. Hypertension 33, 581-585.

Sugiyama, T., Moriya, S., Oku, H., Azuma, I., 1995. Association of endothelin-1 with normal tension glaucoma: clinical and fundamental studies. . Survey of Ophthalmology. 39 S49-S56.

Sugiyama, T., Utsunomiya, K., Ota, H., Ogura, Y., Narabayashi, I., Ikeda, T., 2006. Comparative Study of Cerebral Blood Flow in Patients With Normal-tension Glaucoma and Control Subjects. Am. J. Ophthalmol. 141, 394-396.

Sullivan, R.K.P., Woldemussie, E., Macnab, L., Ruiz, G., Pow, D., 2006. Evoked expression of the glutamate transporter GLT-1c in retinal ganglion cells in human glaucoma and in a rat model. Invest Ophthalmol Vis Sci. 47, 3853-3859.

Sumbayev, V., Yasinska, I., 2005. Regulation of MAP kinase-dependent apoptotic pathway: implication of reactive oxygen and nitrogen species. Arch Biochem Biophys. 436, 406-412.

Sun, Z., Zhang, S., Chan, J., Zhang, D., 2007. Keap1 controls postinduction repression of the Nrf2-mediated antioxidant response by escorting nuclear export of Nrf2. Mol Cell Biol. 27, 6334-6349.

Swanson, K.I., Schlieve, C.R., Lieven, C.J., Levin, L.A., 2005. Neuroprotective effect of sulfhydryl reduction in a rat optic nerve crush model. Invest. Ophthalmol. Vis. Sci. 46, 3737-3741.

Sweeney, J.E., Puttfarcken, P.S., Coyle, J.T., 1989. Galanthamine, an acetylcholinesterase inhibitor: a time course of the effects on performance and neurochemical parameters in mice. Pharmacol Biochem Behav. 34, 129-137.

Takagi, C., King, G.L., Takagi, H., Lin, Y.W., Clermont, A.C., Bursell, S.E., 1996. Endothelin-1 action via endothelin receptors is a primary mechanism modulating retinal circulatory response to hyperoxia. Invest Ophthalmol Vis Sci. 37, 2099-2109.

Takahata, K., Katsuki, H., Kume, T., Nakata, D., Ito, K., Muraoka, S., Yoneda, F., Kashii, S., Honda, Y., Akaike, A., 2003. Retinal neuronal death induced by intraocular administration of a nitric oxide donor and its rescue by neurotrophic factors in rats. Invest Ophthalmol Vis Sci. 44, 1760-1766.

Takano, M., Horie, H., Iijima, Y., Dezawa, M., Sawada, H., Ishikawa, Y., 2002. Brain-derived Neurotrophic Factor Enhances Neurite Regeneration from Retinal Ganglion Cells in Aged Human Retina in vitro. Experimental Eye Research 74, 319-323.

Tamm, E., 2009. The trabecular meshwork outflow pathways: structural and functional aspects. Exp Eye Res. 88, 648-655.

Tamura, H., Kawakami, H., Kanamoto, T., Kato, T., Yokoyama, T., Sasaki, K., Izumi, Y., Matsumoto, M., Mishima, H.K., 2006. High frequency of open-angle glaucoma in Japanese patients with Alzheimer's disease. J. Neurol. Sci. 246, 79-83.

Tanaka, A., Wakita, U., Kambe, N., Iwasaki, T., Matsuda, H., 2004. An autocrine function of nerve growth factor for cell cycle regulation of vascular endothelial cells. Biochem Biophys Res Commun. 313, 1009-1014.

Tang, Y., Mishkin, M., Aigner, T.G., 1997. Effects of muscarinic blockade in perirhinal cortex during visual recognition. Proc Natl Acad Sci U S A. 94, 12667-12669.

Tao, X., Finkbeiner, S., Arnold, D.B., Shaywitz, A.J., Greenberg, M.E., 1998. Ca2+ influx regulates BDNF transcription by a CREB family transcription factor-dependent mechanism. Neuron 20, 709-726.

Tarongoy, P., Ho, C., Walton, D., 2009. Angle-closure glaucoma: the role of the lens in the pathogenesis, prevention, and treatment. Surv Ophthalmol. 54, 211-225.

Tay, D., So, K.F., Jen, L.S., Lau, K.C., 1986. The postnatal development of the optic nerve in hamsters: an electron microscopic study. Dev Brain Res 30, 268-273.

Teng, K.K., Hempstead, B.L., 2004. Neurotrophins and their receptors: signaling trios in complex biological systems. Cell. Mol. Life Sci. 61, 35-48.

Tezel, G., 2006. Oxidative stress in glaucomatous neurodegeneration: mechanisms and consequences. Prog Retin Eye Res. 25, 490-513.

Tezel, G., Kass, M.A., Kolker, A.E., Becker, B., Wax, M.B., 1997. Plasma and aqueous humor endothelin levels in primary open-angle glaucoma. Journal of glaucoma 6, 83-89.

Tezel, G., Kass, M.A., Kolker, A.E., Wax, M.B., 1996. Comparative optic disc analysis in normal pressure glaucoma, primary open-angle glaucoma, and ocular hypertension. Ophthalmology 103, 2105-2113.

Tezel, G., Wax, M., 2004. Hypoxia-inducible factor 1alpha in the glaucomatous retina and optic nerve head. Arch Ophthalmol. 122, 1348-1356.

Tezel, G.l.n., Yang, X., Cai, J., 2005. Proteomic Identification of Oxidatively Modified Retinal Proteins in a Chronic Pressure-Induced Rat Model of Glaucoma. Investigative Ophthalmology & Visual Science 46, 3177-3187.

Thaler, S., Fiedorowicz, M., Rejdak, R., Choragiewicz, T., Sulejczak, D., Stopa, P., Zarnowski, T., Zrenner, E., Grieb, P., Schuettauf, F., 2010. Neuroprotective effects of tempol on retinal ganglion cells in a partial optic nerve crush rat model with and without iron load. Exp Eye Res. 90, 254-260.

Thompson, S.A., Smith, O., Linn, D.M., Linn, C.L., 2006. Acetylcholine neuroprotection against glutamate-induced excitotoxicity in adult pig retinal ganglion cells is partially mediated through alpha4 nAChRs. Exp Eye Res. 83, 1135-1145.

Tielsch, J.M., Katz, J., Quigley, H.A., Javitt, J.C., Sommer, A., 1995. Diabetes, intraocular pressure, and primary open-angle glaucoma in the Baltimore Eye Survey. Ophthalmology 102, 48-53.

Toide, K., 1989. Effects of scopolamine on extracellular acetylcholine and choline levels and on spontaneous motor activity in freely moving rats measured by brain dialysis. Pharmacol Biochem Behav. 33, 109-113.

Trachootham, D., Lu, W., Ogasawara, M.A., Valle, N.R.-D., Huang, P., 2008. Redox Regulation of Cell Survival. Antioxid. Redox Sign. 10, 1343-1374.

Ueda, J., Sawaguchi, S., Hanyu, T., Yaoeda, K., Fukuchi, T., Abe, H., Ozawa, H., 1998. Experimental glaucoma model in the rat induced by laser trabecular photocoagulation after an intracameral injection of India ink. Jpn J Ophthalmol. 42, 337-344.

Ullian, E.M., Barkis, W.B., Chen, S., Diamond, J.S., Barres, B.A., 2004. Invulnerability of retinal ganglion cells to NMDA excitotoxicity. Molecular and Cellular Neuroscience 26, 544-557.

Urcola, J.H., Hernndez, M., Vecino, E., 2006. Three experimental glaucoma models in rats: comparison of the effects of intraocular pressure elevation on retinal ganglion cell size and death. Exp Eye Res. 83, 429-437.

Varma, R., Ying Lai, M., Francis, B., Nguyen, B., Deneen, J., Wilson, M.R., Azen, S., 2004. Prevalence of open-angle glaucoma and ocular hypertension in Latinos: the Los Angeles Latino Eye Study. Ophthalmology 111, 1439-1448.

Vecino, E., Caminos, E., Ugarte, M., Martín-Zanca, D., Osborne, N.N., 1998. Immunohistochemical distribution of neurotrophins and their receptors in the rat retina and the effects of ischemia and reperfusion. Gen. Pharmac. 30, 305-314.

Vendemiale, G., Grattagliano, I., Altomare, E., 1999. An update on the role of free radicals and antioxidant defense in human disease. International Journal of Clinical & Laboratory Research 29, 49-55.

Verdoorn, T.A., Burnashev, N., Monyer, H., Seeburg, P.H., Sakmann, B., 1991. Structural determinants of ion flow through recombinant glutamate receptor channels. Science 252, 1715-1718.

Vidal, L., Daz, F., Villena, A., Moreno, M., Campos, J., de-Vargas, I., 2006. Nitric oxide synthase in retina and optic nerve head of rat with increased intraocular pressure and effect of timolol. Brain Res Bull. 70, 406-413.

Wamsley, S., Gabelt, B.T., Dahl, D.B., Case, G.L., Sherwood, R.W., May, C.A., Hernandez, M.R., Kaufman, P.L., 2005. Vitreous glutamate concentration and axon loss in monkeys with experimental glaucoma. Arch Ophthalmol 123, 64-70.

Wang, D.Y., Ray, A., Rodgers, K., Ergorul, C., Hyman, B.T., Huang, W., Grosskreutz, C.L., 2011. Global Gene Expression Changes in Rat Retinal Ganglion Cells in Experimental Glaucoma. Invest. Ophthalmol. Vis. Sci. 51, 4084-4095.

Wang, L., Fortune, B., Cull, G., Dong, J., Cioffi, G.A., 2006. Endothelin B Receptor in Human Glaucoma and Experimentally Induced Optic Nerve Damage. Arch Ophthalmol 124, 717-724.

Wang, R.F., Schumer, R.A., Serle, J.B., Podos, S.M., 1998. A comparison of argon laser and diode laser photocoagulation of the trabecular meshwork to produce the glaucoma monkey model. J Glaucoma. 7, 45-49.

Wang, X., LeVatte, T.L., Archibald, M.L., Chauhan, B.C., 2009. Increase in endothelin B receptor expression in optic nerve astrocytes in endothelin-1 induced chronic experimental optic neuropathy. Experimental Eye Research 88, 378-385.

Watanabe, M., Fukuda, Y., 2002. Survival and axonal regeneration of retinal ganglion cells in adult cats. Progress in Retinal and Eye Research 21, 529-553.

Wax, M.B., Tezel, G., Saito, I., Gupta, R.S., Harley, J.B., Li, Z., Romano, C., 1998. Anti-Ro/SS-A positivity and heat shock protein antibodies in patients with normal-pressure glaucoma. Am J Ophthalmol. 125, 145-157.

Weber, A.J., Zelenak, D., 2001. Experimental glaucoma in the primate induced by latex microspheres. J Neurosci Methods. 111, 39-48.

Wei, E.P., Kontos, H.A., Beckman, J.S., 1996. Mechanisms of cerebral vasodilation by superoxide, hydrogen peroxide, and peroxynitrite. Am. J. Physiol. 271, H1262-H1266.

Weibel, D., Kreutzberg, G.W., Schwab, M.E., 1995. Brain-derived neurotrophic factor (BDNF) prevents lesion-induced axonal die-back in young rat optic nerve. Brain Res. 679, 249-254.

Weller, R., Boche, D., Nicoll, J.A.R., 2009. Microvasculature changes and cerebral amyloid angiopathy in Alzheimer's disease and their potential impact on therapy. Acta Neuropathol. 118, 87-102.

Wetmore, C., Ernfors, P., Persson, H., Olson, L., 1990. Localization of brain-derived neurotrophic factor mRNA to neurons in the brain by in situ hybridization. Exp Neurol. 109, 141-152.

Whitehouse, P.J., Price, D.L., Struble, R.G., Clark, A.W., Coyle, J.T., Delon, M.R., 1982. Alzheimer's disease and senile dementia: loss of neurons in the basal forebrain. Science 215, 1237-1239.

Wiggs, J., 2007. Genetic etiologies of glaucoma. Archives of ophthalmology 125, 30-37.

Wijono, M., WoldeMussie, E.R.G., Ruiz, G., 1999. Process of retinal ganglion damage by elevated intraocular pressure in rat eyes (ARVO Abstract). Invest Ophthalmol Vis Sci. 40, S672.

Wilkinson, D.G., 1999. The pharmacology of donepezil: a new treatment of Alzheimer's disease. Expert Opin. Pharmacother. 1, 121-135.

Willis, A.P., Leffler, C.W., 2001. Endothelial NO and prostanoid involvement in newborn and juvenile pig pial arteriolar vasomotor responses. Am J Physiol Heart Circ Physiol. 281, H2366-H2377.

Wilson, B.E., Mochon, E., Boxer, L.M., 1996. Induction of bcl-2 expression by phosphorylated CREB proteins during B- cell activation and rescue from apoptosis. Mol. Cell. Biol. 16, 5546-5556.

Wilson, D.A., 2001. Scopolamine enhances generalization between odor representations in rat olfactory cortex. Learn Mem. 8, 279-285.

Woldemussie, E., Wijono, M., Ruiz, G., 2004. Müller cell response to laser-induced increase in intraocular pressure in rats. GLIA 47, 109-119.

WoldeMussie, E.R.G., Feldman, B., 1997. Effect of chronically elevated intraocular pressure on loss of retinal ganglion cells in rats [ARVO Abstract]. Invest Ophthalmol Vis Sci. 38, S159.

Wong, R.O., 1999. Retinal waves and visual system development. Annu Rev Neurosci. 22, 29-47.

Wong, W.T., Myhr, K.L., Miller, E.D., Wong, R.O., 2000. Developmental changes in the neurotransmitter regulation of correlated spontaneous retinal activity. J Neurosci. 20, 351-360.

Wordinger, R.J., Clark, A.F., 1999. Effects of glucocorticoids on the trabecular meshwork: towards a better understanding of glaucoma. Prog Retin Eye Res. 18, 629-667.

Wostyn, P., 2006. Normal-tension glaucoma and Alzheimer's disease: hypothesis of a possible common underlying risk factor. Medical hypotheses 67, 1255-1256.

Wostyn, P., Audenaert, K., De Deyn, P.P., 2009. Alzheimer's disease and glaucoma: Is there a causal relationship? British Journal of Ophthalmology 93, 1557-1559.

Wu, E.H., Wong, Y.H., 2006. Activation of muscarinic M4 receptor augments NGF-induced pro-survival Akt signaling in PC12 cells. Cell Signal 18, 285-293.

Yamada, E., Dmitrieva, N., Keyser, K., Lindstrom, J., Hersh, L., Marshak, D., 2003. Synaptic connections of starburst amacrine cells and localization of acetylcholine receptors in primate retinas. J Comp Neurol. 461, 76-90.

Yamamoto, M., Sobue, G., Yamamoto, K., Terao, S., Mitsuma, T., 1996. Expression of mRNAs for neurotrophic factors (NGF, BDNF, NT-3, and GDNF) and their receptors (p75NGFR, trkA, trkB, and trkC) in the adult human peripheral nervous system and nonneural tissues. Neurochem Res. 21, 929-938.

Yanagisawa, M., Kurihara, H., Kimura, S., Tomobe, Y., Kobayashi, M., Mitsui, Y., Yazaki, Y., Goto, K., Masaki, T., 1988. A novel potent vasoconstrictor peptide produced by vascular endothelial cells. Nature 332, 411-415.

Yaoeda, K., Shirakashi, M., Fukushima, A., Funaki, S., Funaki, H., Abe, H., Tanabe, N., 2003. Relationship between optic nerve head microcirculation and visual field loss in glaucoma. Acta Ophthalmol Scand. 81, 253-259.

Yasumura, R., Meguro, A., Ota, M., Nomura, E., Uemoto, R., Kashiwagi, K., Mabuchi, F., Iijima, H., Kawase, K., Yamamoto, T., Nakamura, M., Negi, A., Sagara, T., Nishida, T., Inatani, M., Tanihara, H., Aihara, M., Araie, M., Fukuchi, T., Abe, H., Higashide, T., Sugiyama, K., Kanamoto, T., Kiuchi, Y., Iwase, A., Ohno, S., Inoko, H., Mizuki, N., 2011. Investigation of the association between SLC1A3 gene polymorphisms and normal tension glaucoma. Mol Vis. 17, 792-796.

Yochim, B., Mueller, A., Kane, K., Kahook, M., 2011. Prevalence of Cognitive Impairment, Depression, and Anxiety Symptoms Among Older Adults With Glaucoma. J Glaucoma In Press.

Yoneda, S., Hara, H., Hirata, A., Fukushima, M., Inomata, Y., Tanihara, H., 2005. Vitreous Fluid Levels of β-Amyloid (1–42) and Tau in Patients with Retinal Diseases. Japanese Journal of Ophthalmology 49, 106-108.

Yoshida, T., Oka, S.-i., Masutani, H., Nakamura, H., Yodoi, J., 2003. The role of thioredoxin in the aging process: involvement of oxidative stress. Antioxid Redox Signal. 5, 563-570.

Yücel, Y., Zhang, Q., Weinreb, R., Kaufman, P., Gupta, N., 2003. Effects of retinal ganglion cell loss on magno-, parvo-, koniocellular pathways in the lateral geniculate nucleus and visual cortex in glaucoma. Prog Retin Eye Res. 22, 465-481.

Yücel, Y.H., Zhang, Q., Gupta, N., Kaufman, P.L., Weinreb, R.N., 2000. Loss of neurons in magnocellular and parvocellular layers of the lateral geniculate nucleus in glaucoma. Arch Ophthalmol. 118, 378-384.

Yücel, Y.H., Zhang, Q., Weinreb, R.N., Kaufman, P.L., Gupta, N., 2001. Atrophy of relay neurons in magno- and parvocellular layers in the lateral geniculate nucleus in experimental glaucoma. Invest Ophthalmol Vis Sci. 42, 3216-3222.

Yuki, K., Ozawa, Y., Yoshida, T., Kurihara, T., Hirasawa, M., Ozeki, N., Shiba, D., Noda, K., Ishida, S., Tsubota, K., 2011. Retinal ganglion cell loss in superoxide dismutase 1 deficiency. Invest Ophthalmol Vis Sci. 52, 4143-4150.

Zhang, H., Zhang, R., Lin, Y., Li, J., Pober, J., Min, W., 2007a. RIP1-mediated AIP1 phosphorylation at a 14-3-3-binding site is critical for tumor necrosis factor-induced ASK1-JNK/p38 activation. J Biol Chem. 282, 14788-14796.

Zhang, J.-Z., Xi, X., Gao, L., Kern, T., 2007b. Captopril inhibits capillary degeneration in the early stages of diabetic retinopathy. Curr Eye Res. 32, 883-889.

Zhang, J., Diamond, J., 2006. Distinct perisynaptic and synaptic localization of NMDA and AMPA receptors on ganglion cells in rat retina. J Comp Neurol. 498, 810-820.

Zhou, Y., Pernet, V., Hauswirth, W.W., Di Polo, A., 2005. Activation of the extracellular signal-regulated kinase 1/2 pathway by AAV gene transfer protects retinal ganglion cells in glaucoma. Mol. Ther. 12, 402-412.

APPENDIX A

MAINTENANCE OF AXO-OLIGODENDROGLIAL PARANODAL JUNCTIONS REQUIRES DCC AND NETRIN-1

J Neurosci. 2008 Oct 22; 28(43):11003-14.

Andrew A. Jarjour[1,2], Sarah-Jane Bull[1,2], Mohammadali Almasieh[4], Sathyanath Rajasekharan[1,2], K. Adam Baker[1,2], Jeannie Mui[3], Jack P. Antel[1,2], Adriana Di Polo[4] and Timothy E. Kennedy[1,2,3]

[1]Montreal Neurological Institute, Departments of [2]Neurology and Neurosurgery and [3]Anatomy and Cell Biology, McGill University, Montreal, Quebec, Canada H3A 2B4, and [4]Department of Pathology and Cell Biology, Université de Montréal, Montreal, Quebec, Canada H3T 1J4

Correspondence: Timothy E. Kennedy, Centre for Neuronal Survival, Montreal Neurological Institute, McGill University, 3801 University Avenue, Montreal, Quebec, Canada H3A 2B4.

Running title: Netrin and DCC Regulate CNS Paranodal Myelin

ABSTRACT

Paranodal axoglial junctions are essential for the segregation of myelinated axons into distinct domains and efficient conduction of action potentials. Here, we show that netrin-1 and deleted in colorectal cancer (DCC) are enriched at the paranode in CNS myelin. We then address whether netrin-1 signaling influences paranodal adhesion between oligodendrocytes and axons. In the absence of netrin-1 or DCC function, oligodendroglial paranodes initially develop and mature normally but later become disorganized. Lack of DCC or netrin-1 resulted in detachment of paranodal loops from the axonal surface and the disappearance of transverse bands. Furthermore, the domain organization of myelin is compromised in the absence of netrin-1 signaling: K^+ channels inappropriately invade the paranodal region, and the normally restricted paranodal distribution of Caspr expands longitudinally along the axon. Our findings identify an essential role for netrin-1 and DCC regulating the maintenance of axoglial junctions.

Key words: myelin; axoglial junction; paranode; septate-like junctions; Caspr; neurofascin

INTRODUCTION

The functional division of myelinated axons into distinct domains is crucial for the establishment of saltatory conduction. Concentrated at nodes of Ranvier are high densities of voltage-gated sodium channels that depolarize the axonal membrane, generating and propagating the action potential (for review, see Poliak and Peles, 2003). Flanking the node are the paranodal axoglial junctions, where each layer of the myelin sheath terminates in a cytoplasm-filled membrane loop that tightly abuts the axon. The paranode separates the node from the juxtaparanodal domain, the outermost region of the internode (for review, see Poliak and Peles, 2003). Concentrated at the juxtaparanode are Shaker-type voltage-gated potassium channels, which maintain internodal resting potential by preventing hyperexcitation and action potential backpropagation after nodal Na+ influx (Wang et al., 1993; Chiu et al., 1999; Vabnick et al., 1999). The molecular mechanisms that regulate the formation and maintenance of paranodal junctions are not well understood.

The tight association between paranodal axonal and glial membranes is thought to act as a barrier between the node and the juxtaparanode, isolating electrical activity at the node of Ranvier from the internode and preventing the lateral diffusion of axonal proteins among domains (Poliak and Peles, 2003). Ultrastructurally, the points of contact between oligodendrocyte and axolemmal membranes are characterized by the presence of electron-dense ridges called transverse bands (Tao-Cheng and Rosenbluth, 1983). The axonal protein Caspr, also called paranodin, or ncp1, is concentrated at the paranode during myelination (Einheber et al., 1997). Caspr forms a complex in cis with the GPI (glycosylphosphatidylinositol)-linked protein contactin (Rios et al., 2000), and this association is required for the localization of Caspr to the axonal membrane (Faivre-Sarrailh et al., 2000). The recruitment of the Caspr–contactin complex to the paranodal domain is dependent on the presence of the 155 kDa isoform of neurofascin (nfc155). Nfc155 forms a complex with Caspr and contactin in trans, and all three are essential for the formation of normal paranodal axoglial junctions in both the CNS and PNS (Tait et al., 2000; Bhat et al., 2001; Boyle et al., 2001; Charles et al., 2002; Sherman et al., 2005; Bonnon et al., 2007). In the absence of either Caspr or contactin, transverse bands do not form, the close association between many paranodal loops and the axon is disrupted, and

potassium channels are mislocalized to the paranodal region (Bhat et al., 2001; Boyle et al., 2001). Similar phenotypes are generated by loss of either ceramide galactosyl transferase (CGT) or myelin and lymphocyte protein (MAL), which are required for the proper trafficking of nfc155 (Dupree et al., 1999; Schaeren-Wiemers et al., 2004; Schafer et al., 2004).

In the adult rat spinal cord, oligodendrocytes express netrin-1 and its receptor, deleted in colorectal cancer (DCC) (Manitt et al., 2001, 2004). Netrins are a small family of ~75 kDa proteins with homology to laminins. They are best known as secreted chemotropic guidance cues for migrating cells and axons. Signaling through DCC, they direct the reorganization of F-actin by regulating focal adhesion kinase (FAK), fyn, PI-3 kinase, and the Rho-GTPases Cdc42 and Rac1 (Moore et al., 2007). Additionally, they contribute to tissue morphogenesis by regulating cell–cell and cell–matrix adhesion; however, this is best understood outside the CNS (for review, see Baker et al., 2006). Subcellular fractionation of adult rat spinal cord white matter indicated that netrin-1 is enriched in fractions containing noncompact myelin membranes (Manitt et al., 2001). These membrane preparations typically contain proteins present at points of axoglial contact, including the paranodal junction (Menon et al., 2003). We demonstrate that DCC and netrin-1 are enriched at oligodendroglial paranodes and that, in the absence of netrin-1 or DCC function, CNS paranodes develop and mature normally, but this organization is subsequently lost. The essential contribution of netrin-1 and DCC to paranodal maintenance, but not formation, distinguishes the phenotypes reported here from those found previously in other mutants, and suggests that distinct mechanisms regulate the organization of the paranodal axoglial junction in the developing and mature CNS. In summary, our findings demonstrate that netrin-1 and its receptor DCC are required for the maintenance of paranodal axoglial contact and represent the first reported function for netrin-1 in the mature CNS.

MATERIALS AND METHODS

Animals

Adult male Sprague Dawley rats (180–200 g) and newborn CD1 mouse pups were obtained from Charles River Canada. Mice heterozygous for netrin-1 or DCC function

were obtained from Marc Tessier-Lavigne (Genentech, San Francisco, CA) and Robert Weinberg (Whitehead Institute for Biomedical Research, Cambridge, MA), respectively, and bred into a CD-1 genetic background. All procedures with animals were performed in accordance with the Canadian Council on Animal Care guidelines for the use of animals in research.

Antibodies

The following primary antibodies were used in this study: mouse monoclonal anti-Caspr (University of California Davis NeuroMab; catalog #75-001), guinea pig polyclonal anti-Caspr, rabbit polyclonal anti-Caspr (gift from Dr. David Colman, McGill University, Montreal, Quebec, Canada) (Svenningsen et al., 2003), mouse monoclonal anti-DCC intracellular domain (DCCIN) (BD Biosciences Pharmingen; catalog #554223), rabbit polyclonal anti-Kv1.2 (Alomone Labs; catalog #APC-010), mouse monoclonal anti-myelin basic protein (MBP) (Millipore Bioscience Research Reagents; catalog #MAB382), rabbit polyclonal anti-MBP (Millipore Bioscience Research Reagents; catalog #AB9046), rat monoclonal anti-MBP (Millipore Bioscience Research Reagents; catalog #MAB386), rabbit polyclonal anti-netrin PN2 (Manitt et al., 2001), rabbit polyclonal anti-neurofascin NFC2 (gift from Prof. Peter Brophy, University of Edinburgh, Edinburgh, UK; recognizes both 155 and 186 kDa isoforms of neurofascin) (Tait et al., 2000), mouse monoclonal anti-neurofilament 145 kDa (NFM) (Millipore Bioscience Research Reagents; catalog #MAB1621), chicken polyclonal anti-NFM (EnCor Biotechnology; catalog #CPCA-NF-M), chicken polyclonal anti-neurofilament 200 kDa (NFH) (EnCor; catalog #CPCA-NF-H), mouse anti-myelin proteolipid protein (PLP) (Millipore Bioscience Research Reagents; catalog #MAB388), mouse monoclonal anti-sodium channel (pan) (Na^+ch) (Sigma-Aldrich; catalog #S8809). Secondary antibodies used were Alexa 488-conjugated donkey anti-mouse (catalog #A21202) and goat anti-rabbit (catalog #A11008), Alexa 546-conjugated goat anti-mouse (catalog #A11030) and goat anti-rabbit (catalog #A11010), Alexa 633-conjugated goat anti-chicken (catalog #A21103) and goat anti-mouse (catalog #A21052), and Alexa 647-conjugated donkey anti-rabbit (catalog #A21244) from Invitrogen, and rhodamine-conjugated donkey anti-guinea pig (Jackson ImmunoResearch; catalog #706-295-148).

Immunocytochemistry and confocal analysis of adult rat spinal cord.

Adult rats were anesthetized with sodium pentobarbital (Somnotol; 65 mg/kg, i.p.; MTC Pharmaceuticals) and perfused transcardially with PBS, followed by 4% paraformaldehyde (PFA) in PBS at pH 7.4. Spinal cords were then equilibrated in 30% sucrose in PBS for 48 h at 4°C, embedded in optimal cutting temperature compound (Sakura Finetek), 18 μm longitudinal and coronal cryosections cut, and processed for immunohistochemistry. Images were captured using a Zeiss LSM 510 confocal microscope. In all cases, single confocal slices were collected.

Immunocytochemistry and confocal analysis of cerebellar slice cultures.

Cerebellar slice cultures were prepared based on previously published methods (Notterpek et al., 1993). Briefly, after decapitation, brains were dissected into ice-cold HBSS and 250 μm sagittal slices of cerebellum and attached brainstem were cut using a McIlwain tissue chopper. The tissue slices were placed on Millipore Millicell-CM organotypic culture inserts (Thermo Fisher Scientific) in medium containing 50% MEM with Earle's salts, 25% Earle's balanced salt solution, 25% heat-inactivated horse serum (HIHS), glutamax-II supplement with penicillin–streptomycin, amphotericin B (all purchased from Invitrogen), and 6.5 mg/ml glucose (Sigma-Aldrich). Membranes were transferred into fresh medium every 2 d. Slices processed after 25 d *in vitro* (DIV) are referred to in the text as "short-term cultures," and those processed at 7 weeks *in vitro* or later (49 DIV for netrin mutant litters processed for EM, 67 DIV for DCC mutant litters processed for EM, and 60 DIV for netrin-1 and DCC mutant litters processed for confocal analysis) are referred to as "long-term cultures."

Slices processed for immunolabeling were fixed while attached to membranes with 4% PFA in PBS for 1 h, rinsed in PBS for 10 min, and blocked with 3% HIHS, 2% BSA, 0.25% Triton X-100 in PBS for 2 h. Slices were then incubated in primary antibody 36–48 h, washed once for 10 min and then thrice for 1 h, incubated in secondary antibody overnight, washed, and mounted.

Confocal images were captured as described above. For analysis of sodium and potassium channel distribution, slices were labeled with mouse anti-Na^+ch and rabbit anti-Kv1.2 antibodies. The plane chosen for imaging was that at which nodal Na^+ch and

juxtaparanodal Kv1.2 immunoreactivity was closest. The distance between Na^+ch and Kv1.2 channel expression, and the length of the Na^+ch channel immunoreactivity were analyzed. For analysis of neurofascin localization, the distance between the outermost edges of the region of neurofascin immunoreactivity was measured. The plane chosen for imaging was that in which the node of Ranvier most evenly bisects the region of neurofascin immunolabeling. For analyses of Caspr immunoreactivity, the length of each Caspr expression domain was measured. For analyses of neurofascin and Caspr localization, slices were also labeled with chicken anti-NFH and mouse anti-MBP antibodies. Distances were measured using LSM 510 Image Browser software.

Electron microscopy

Slices and attached membrane were cut out from surrounding membrane and fixed overnight with 2.5% glutaraldehyde in 0.1 m sodium cacodylate buffer, osmicated with potassium ferrocyanide-reduced 1% osmium tetroxide solution for 1 h, and then dehydrated with successive 10 min rinses in 30, 50, 70, 80, 95, and 100% ethanol (three times). Tissue was then infiltrated with 1:1, 1:2, and 1:3 ethanol to Epon blends, and then in pure Epon, for 1 h each, and then embedded in Epon, tissue side down, in a plastic BEEM capsule (Structure Probe). The 70–100 nm sections were then cut onto 200 mesh copper grids and stained with 4% uranyl acetate for 5 min, followed by Reynolds's lead citrate for 3 min. Images were observed using a transmission electron microscope at 80 kV using a JEM-2000FX (JEOL; used for all analyses except for those of short-term netrin mutant cultures) or at 120 kV using a Tecnai 12 (FEI) Gatan Bioscan CCD camera. For each condition, at least two slices from each of two animals were analyzed. For analyses of compact myelin, the width of the periaxonal space at each axon was measured, and the periodicity of compact myelin was calculated. For analyses of paranodal myelin, because of technical limitations encountered during the embedding process, only single paranodes were analyzed at a time. Each paranode was examined for the presence of four “faults.” A paranode was credited with a fault if the majority of paranodal loops present lacked transverse bands; if neighboring paranodal glial membranes lacked electron density between apposed glial loops and these membranes were separated by two or more membrane widths (“interloop densities”); if at least one

paranodal loop had detached from the axonal surface by two or more membrane widths; or if at least one paranodal loop faced away from the axonal surface (depicted in Fig. 5A).

Oligodendrocyte precursor cell transplantation into retina and immunohisto-chemical analysis in vivo.

Oligodendrocyte precursor cells (OPCs) were purified by shake-off from a mixed glial culture derived from neonatal mouse cortices, as previously described (Jarjour et al., 2003). DCC−/− mice (CD-1 genetic background) were identified behaviorally and their cortices were cultured separately from their wild-type and heterozygote littermates. Genotypes were subsequently confirmed by PCR. Isolated OPCs were concentrated to a density of 15,000 cells/µl in OLDEM (oligodendrocyte defined medium) as described by us (Jarjour et al., 2003). The OPC suspension (2 µl) was injected into the vitreous chamber of the left eye of wild-type 2-month-old male CD-1 mice using a 10 µl Hamilton syringe with a 32 gauge glass microneedle. The needle tip was inserted into the superior (dorsal) hemisphere of the eye, at the level of the pars plana, at a 45° angle through the sclera into the vitreous body as described previously (Sapieha et al., 2005). This route of administration avoided retinal detachment or injury to eye structures, including the lens and the iris. The injection was performed within 1 min to slowly deposit the OPCs onto the retinal fiber layer. The needle was then gently removed, and surgical glue (Indermill; Tyco Health Care) was used to seal the injection site. Eight weeks after the transplantation, animals were perfused transcardially with 4% PFA. Eyes were then enucleated and the retinas were removed, fixed for an additional 30 min, and flat-mounted vitreal side up on a glass slide for examination of the ganglion cell layer. Retinal tissue was permeabilized in 2% Triton X-100, 0.5% DMSO in PBS for 4 d, and blocked for 2 h in 10% normal goat serum, 2% Triton X-100, and 0.5% DMSO in PBS. Retinas were then incubated in primary antibodies for 48 h and washed once for 5 min and thrice for 20 min. Secondary antibodies were applied for 2 h, and retinas were washed and mounted on slides. Images were collected and analyses performed as described for organotypic slices.

RESULTS

Long-term, myelinating cerebellar organotypic cultures

Netrin-1 and DCC are expressed by myelinating oligodendrocytes in the mature CNS (Manitt et al., 2001, 2004). To investigate possible roles of netrin-1 and DCC in myelination, we sought to examine CNS white matter in the absence of netrin-1 or dcc expression. However, mice lacking functional netrin-1 or DCC protein die within hours of birth (Serafini et al., 1996; Fazeli et al., 1997), weeks before the vast majority of CNS myelin forms in rodents. To circumvent this limitation, we established organotypic cerebellar slice cultures derived from either newborn [postnatal day 0 (P0)] netrin-1 or dcc knock-out mice and their wild-type littermates. In the developing rat cerebellum, MBP-positive oligodendroglia are first observed at P2 and increase in number throughout the white matter by P7. Myelinated axon segments are first observed at P7, and increase in abundance by P12, with extensive myelination seen by P20 (Reynolds and Wilkin, 1988). A similar time course is observed during cerebellar development in mice (Foran and Peterson, 1992). The time course of oligodendroglial development in cerebellar slice cultures derived from wild-type newborn mice was similar to that observed in vivo. MBP-positive oligodendrocytes were visible at 3 DIV and increased in number and process complexity between 3 and 7 DIV. Widespread MBP-positive myelin profiles were visible by 13 DIV, and myelination was extensive by 30 DIV (Fig. 1A–D). Using this method, we have maintained healthy myelinating cultures as long as 70 DIV.

Myelin develops normally in DCC- and netrin-1-deficient cerebellar slice cultures

To investigate whether netrin-1 and DCC are required for the proper organization of CNS myelin, cerebellar slice cultures were prepared from newborn netrin-1 and DCC mutant animals and their wild-type littermates and analyzed. Extensive MBP-positive myelin profiles were visible in long-term (>7 weeks of age) wild-type, $DCC^{-/-}$, and netrin-$1^{-/-}$ cultures (Fig. 1E–H). Compact myelin ultrastructure appeared normal in both $DCC^{-/-}$ and netrin-$1^{-/-}$ cerebellar slices and those collected from their wild-type littermates (Fig. 2; supplemental Table 1, available at www.jneurosci.org as supplemental material). Major dense lines, intraperiod lines, and periaxonal spaces were clearly evident in electron micrographs of $DCC^{-/-}$ and netrin-$1^{-/-}$ myelin cross sections, with the number

of myelin layers routinely exceeding 10, similar to wild-type myelin. The width of the periaxonal space (PS) was unaffected in both $DCC^{-/-}$ and netrin-$1^{-/-}$ slices (Fig. 2). Myelin periodicity was unaffected in netrin-1−/− slices, although a slight increase was observed in $DCC^{-/-}$ slices (10.83 ± 0.25 nm/wrap in $DCC^{+/+}$ internodes compared with 12.04 ± 0.35 nm/wrap in $DCC^{-/-}$ internodes; $p < 0.05$).

Netrin-1 and DCC are enriched at CNS paranodes

The lack of any obvious abnormalities in compact myelin is consistent with our previous subcellular fractionation of adult CNS white matter. These findings indicated that netrin-1 protein is not enriched in fractions containing compact myelin membranes, but that it is predominantly associated with fractions that include periaxonal and paranodal myelin membranes (Manitt et al., 2001). To further characterize the distribution of netrin-1 and its receptors in CNS white matter, we performed immunohistochemical analyses to determine whether these proteins were enriched in these regions. In 30 DIV wild-type cerebellar slice cultures, netrin-1 and DCC immunoreactivity overlapped with the distribution of Caspr, which is concentrated at paranodes (Fig. 3A–L). The distributions of netrin-1 and DCC protein were then examined immunohistochemically in adult rat spinal cord. Netrin-1 immunoreactivity colocalized with Caspr at the paranode in longitudinal sections, and DCC immunoreactivity was found in close proximity to the paranode (Fig. 3M–X). In axonal cross sections, netrin-1 immunoreactivity is closely associated with, and partially overlaps, that of Caspr (Fig. 3D–F,P–R), consistent with an enrichment of netrin-1 in regions in which the oligodendroglial paranodal loops closely appose the axonal surface. DCC immunoreactivity surrounded the axon at the paranode, but unlike netrin-1, it extended beyond the area delimited by Caspr (Fig. 3J–L,V–X). This is consistent with DCC localization to the oligodendroglial paranodal membrane loops, but not restricted to the region of axoglial contact.

Lack of DCC and netrin-1 leads to abnormalities in paranodal organization

The enrichment of netrin-1 and DCC protein at the paranodal region, as well as previous reports describing roles for netrins mediating short-range cell–cell and cell–matrix interactions (for review, see Baker et al., 2006), raises the possibility that netrin-1

may regulate axo-oligodendroglial interactions. To address this, paranodal regions in long-term cerebellar slice cultures derived from newborn netrin-1−/− and DCC−/− mice and their wild-type littermates were examined by transmission electron microscopy. The paranodal axoglial junction is composed of sequences of cytoplasm-containing loops of myelin membrane that tightly associate with each other and the axonal surface. In electron micrographs of myelinated axons, electron-dense transverse bands mark points of contact between paranodal myelin loops and the axolemma (for review, see Pedraza et al., 2001). In electron micrographs of wild-type cerebellar slice cultures, paranodal loops were regularly spaced, and transverse bands were present in which each loop of glial membrane contacted the axon (Fig. 4A,E), consistent with the appearance of these structures in vivo.

In long-term wild-type cerebellar slices, transverse bands and interloop densities were readily detected at the vast majority of paranodes (Fig. 4A,E). In contrast, paranodes in $DCC^{-/-}$ and netrin-$1^{-/-}$ slices were frequently disorganized (Fig. 4B–D,F–H). Transverse bands were often absent and, when present, were frequently diffuse (Fig. 4B,F, insets). Glial loops were abnormally separated from each other, resulting in a loss of interloop densities (Fig. 4B). Glial membranes without axonal contact were frequently observed (Fig. 4B,F), and everted glial loops, oriented away from the axon, were common (Fig. 4C,G). Occasionally, noncompact paranode-like myelin membranes were localized to internodal regions (Fig. 4D,H,I).

To quantify the differences between wild-type and DCC- or netrin-1-deficient paranodes in long-term cultures, paranodes were scored for the presence of each of four faults (Fig. 5A): (1) absence of transverse bands, (2) absence of interloop densities and abnormal separation between glial loops, (3) detachment of paranodal loops from the axolemma, and (4) presence of everted loops. In both DCC (Fig. 5B)- and netrin-1 (Fig. 5C)-deficient slices, all four faults were more frequent than in cultures obtained from wild-type littermates. On average, $DCC^{-/-}$ paranodes scored 1.78 ± 0.13 faults per paranode compared with 0.18 ± 0.05 for wild-type paranodes ($p < 0.005$), whereas netrin-$1^{-/-}$ paranodes were more severely disorganized, scoring a mean of 2.43 ± 0.09 faults per paranode compared with 0.27 ± 0.05 for wild-type paranodes ($p < 0.005$) (Fig. 5D; supplemental Table 2, available at www.jneurosci.org as supplemental material). When

paranodes were binned according to the number of faults, >50% of netrin$^{-/-}$ paranodes and ~30% of DCC$^{-/-}$ paranodes, were classified as "severely abnormal," having three to four faults per paranode (Fig. 5E,F; supplemental Table 3, available at www.jneurosci.org as supplemental material). Consistent with these trends, quantification of the number of aberrant paranodal loops revealed a fourfold to sevenfold increase in everted loops and a 6- to 10-fold increase in detached loops in DCC$^{-/-}$ and netrin-1$^{-/-}$ compared with wild type (supplemental Table 4, available at www.jneurosci.org as supplemental material).

The organization of paranodal and juxtaparanodal domains requires netrin-1 and DCC

The paranodal axoglial apparatus has been described to act as a barrier, preventing the diffusion of potassium channels from the juxtaparanode into the paranode (for review, see Poliak and Peles, 2003). To investigate whether the ultrastructural abnormalities present in the netrin-1- or DCC-deficient slices result in a failure of the paranode to properly segregate nodal sodium channels (Na^+ch) and juxtaparanodal potassium channels (Kv1.2), we measured the distance between the Na^+ch and Kv1.2-immunoreactive domains and the length of the Na^+ch-immunoreactive band (Fig. 6; supplemental Table 5, available at www.jneurosci.org as supplemental material). In wild-type cultures, a clear gap was visible between nodal Na+ch and juxtaparanodal Kv1.2 immunoreactivity (Fig. 6A,B). In netrin-1$^{-/-}$ and DCC$^{-/-}$ cultures, however, Kv1.2 immunoreactivity was often inappropriately localized to the paranode (Fig. 6C,D, arrowheads), and the mean distance between Na^+ch and Kv1.2 immunoreactivity was reduced in netrin-1$^{-/-}$ and DCC$^{-/-}$ cultures relative to wild-type cultures (Fig. 6E). In addition, the Na^+ch-immunoreactive domain was lengthened by ~1.5-fold in netrin-1$^{-/-}$ nodes relative to netrin-1$^{+/+}$ nodes (Fig. 6A,C, arrow;F), but no such increase was observed in DCC$^{-/-}$ nodes (Fig. 6B,D,F). These data indicate that the paranodal axoglial junction fails to appropriately constrain the localization of ion channels at nodes of Ranvier lacking netrin-1$^{-/-}$ or DCC$^{-/-}$. Furthermore, as suggested by the increased severity of the netrin-1$^{-/-}$ ultrastructural phenotype, the failure of the paranodal barrier

appears to be more severe in the absence of netrin-1, because Na^+ch localization is also affected.

Localization of Caspr and neurofascin in DCC$^{-/-}$ and netrin-1$^{-/-}$ paranodes

Nfc155 and Caspr are concentrated at paranodal oligodendroglial and neuronal membranes, respectively, and are essential components of a protein complex required for paranodal organization (Tait et al., 2000; Bhat et al., 2001; Charles et al., 2002; Sherman et al., 2005). In previous studies of mutant animals with disruption of paranodal organization, the distribution of nfc155 and Caspr is aberrantly diffuse along myelinated axons instead of concentrated at paranodes (Marcus et al., 2002). Using antibodies that recognize either neurofascin, both 155 and 186 kDa isoforms, or Caspr, we investigated whether loss of netrin-1 or DCC function affects the expression or localization of these proteins (Figs. 7, 8; supplemental Table 5, available at www.jneurosci.org as supplemental material). Neurofascin localization is not altered in DCC$^{-/-}$ (Fig. 7A–D) or netrin-1$^{-/-}$ slices (Fig. 8A–D), and the length of the neurofascin-immunoreactive domain is not affected in paranodal regions lacking DCC or netrin-1 (supplemental Table 5, available at www.jneurosci.org as supplemental material). In contrast, the region of Caspr immunoreactivity flanking DCC$^{-/-}$ and netrin-1$^{-/-}$ nodes of Ranvier is markedly lengthened relative to that observed in cultures derived from their wild-type littermates (supplemental Table 5, available at www.jneurosci.org as supplemental material). Specifically, the Caspr-immunopositive domain expands from 2.84 ± 0.14 μm in DCC$^{+/+}$ paranodes to 4.99 ± 0.28 μm in DCC$^{-/-}$ paranodes ($p < 0.05$), and from 3.76 ± 0.16 μm to 5.47 ± 0.29 μm in netrin-1$^{+/+}$ and netrin-1$^{-/-}$ paranodes ($p < 0.005$), respectively.

Netrin-1 and DCC are required for the maintenance of CNS paranodal junctions

Descriptions of aberrant paranodal organization in mutant mouse strains have reported junctions that form normally, but later become disorganized (Marcus et al., 2002; Schaeren-Wiemers et al., 2004; Rasband et al., 2005). To determine whether paranode formation occurs normally in netrin-1 and DCC mutants, we examined the organization of paranodal myelin in short-term (25 DIV) cerebellar slice cultures. In wild-type cultures at 25 DIV, paranodal loops were regularly spaced and transverse bands were present, confirming that paranodal junctions had formed and matured fully by this

stage (Fig. 9A,F). In contrast to what we observed in long-term cultures, 25 DIV netrin-$1^{-/-}$ and $DCC^{-/-}$ paranodes were indistinguishable from $netrin^{+/+}$ and $DCC^{+/+}$ paranodes (Fig. 9B,G), indicating that netrin-1 and DCC are not required for the development of paranodal axoglial contacts. Quantification of the faults observed in long-term cultures, revealed no significant increase in any one fault in the absence of either netrin-1 or DCC at 25 DIV (Fig. 9C,H; supplemental Table 2, available at www.jneurosci.org as supplemental material), and the mean number of faults per paranode did not significantly differ between netrin-$1^{-/-}$ or $DCC^{-/-}$ and wild-type cultures (Fig. 9D,I; supplemental Table 2, available at www.jneurosci.org as supplemental material). When the paranodes were binned as described above, the vast majority of both wild-type and mutant paranodes were classified as normal (Fig. 9E,J; supplemental Table 3, available at www.jneurosci.org as supplemental material).

Consistent with the lack of an abnormal ultrastructural phenotype, sodium and potassium channels were appropriately segregated at wild-type and netrin-1 or DCC-null nodes of Ranvier in 25 DIV cultures (supplemental Fig. S1A–D, available at www.jneurosci.org as supplemental material). The distance separating Na^+ch and Kv1.2-immunoreactive domains was unaltered in netrin-$1^{-/-}$ or $DCC^{-/-}$ slices, and no increase in the length of the Na^+ch-immunoreactive band was observed (supplemental Fig. S1E–H, supplemental Table 5, available at www.jneurosci.org as supplemental material). Neurofascin was present in both 25 DIV wild-type and mutant cultures, and its distribution was unaltered in the absence of netrin-1 or DCC (supplemental Figs. S2, S3A–D,I; supplemental Table 5, available at www.jneurosci.org as supplemental material). The distribution of Caspr at netrin-$1^{-/-}$ or $DCC^{-/-}$ paranodes in short-term cultures was indistinguishable from that observed in wild-type cultures (supplemental Figs. S2, S3E–H,J; supplemental Table 5, available at www.jneurosci.org as supplemental material), consistent with normal initial development of the paranodal region in the absence of netrin-1 or DCC. The normal organization of paranodal axoglial junctions in short-term cultures and the disruption of the ultrastructure and domain organization in long-term cultures indicate that the defects observed in older netrin-$1^{-/-}$ and $DCC^{-/-}$ cultures are not a consequence of aberrant myelin formation, but of maintenance of the axoglial junction.

Disruption of paranodal domains formed by DCC$^{-/-}$ oligodendrocytes in vivo

To determine whether netrin signaling is similarly required for the maintenance of oligodendroglial paranodal junctions in vivo, we assessed the capacity of OPCs derived from DCC$^{-/-}$ mice to myelinate retinal ganglion cell axons when transplanted into the eyes of wild-type mice. The axons of retinal ganglion cells are myelinated in the optic nerve; however, OPCs do not invade the retina during development and the proximal segment of the axon within the retina remains unmyelinated (Berliner, 1931). Thus, the intraretinal segment of the ganglion cell axons provides a unique opportunity to assess the capacity of OPCs transplanted into the retina to myelinate, in the absence of competition from endogenous OPCs (Laeng et al., 1996). OPCs were isolated from mixed glial cultures derived from newborn DCC$^{-/-}$ pups and their wild-type and heterozygote littermates. OPCs were then transplanted into the retina by intravitreal injection into the eyes of adult mice (Fig. 10A), and the retinas were isolated and analyzed 8 weeks later. None of the host retinas exhibited any signs of an immune response. Abundant MBP-immunopositive myelin segments were observed along retinal ganglion cell axons in eyes that received OPCs of all genotypes (Fig. 10B). Paranodal specializations, visualized using the paranodal marker Caspr, were readily detected in newly myelinated axons (Fig. 10C–H). Quantitative analysis revealed a significant extension of the Caspr-immunoreactive domain, characteristic of a disrupted paranode structure, along retinal ganglion cell axons myelinated by DCC$^{-/-}$ oligodendrocytes compared with control retinas myelinated by oligodendrocytes expressing DCC (Fig. 10E–H). Specifically, the Caspr-immunopositive domain expanded from 2.47 ± 0.19 μm ($n = 28$) in paranodes expressing DCC to 3.14 ± 0.15 μm in DCC$^{-/-}$ paranodes ($n = 40$; $p < 0.01$). Consistent with the phenotype found in cerebellar slice cultures lacking DCC or netrin-1, these findings indicate that netrin signaling through DCC regulates paranodal organization in the mature CNS in vivo. Importantly, these findings also indicate that the paranodal deficiencies detected result from the loss of a cell-autonomous function of DCC in oligodendrocytes.

DISCUSSION

Netrins function as long-range guidance cues that direct cell and axon migration, and also at short-range, regulating cell–cell and cell–matrix adhesion (Baker et al., 2006). Signaling through its receptor DCC, netrin-1 directs the reorganization of F-actin by regulating FAK, fyn, PI3-kinse, and the Rho-GTPases Cdc42 and Rac1 (Moore et al., 2007). In the adult CNS, expression of netrin-1 and its receptors is widespread in neuronal and glial cells including oligodendrocytes (Manitt et al., 2001, 2004). Using subcellular fractionation of CNS white matter, we previously demonstrated an enrichment of netrin-1 protein in noncompact myelin membranes implicated in axoglial contact (Manitt et al., 2001). Here, we show that netrin-1 and DCC are enriched in the paranodal region both in the adult CNS in vivo and in organotypic cerebellar cultures. Paranodal myelin developed normally in the absence of netrin-1 or DCC function, but became disorganized in mature myelin. Furthermore, our transplantation studies demonstrate a cell-autonomous requirement for DCC signaling in oligodendrocytes in vivo. We conclude that netrin-1 and DCC are required for the maintenance, but not the development, of CNS paranodal axoglial junctions.

The demonstration that paranodal loops form and mature normally but later became disordered in the absence of netrin-1 and DCC is consistent with a role for these proteins in the maintenance of axoglial junctions. Reports documenting CNS paranodal phenotypes in mice lacking CGT (Dupree et al., 1998, 1999; Marcus et al., 2002; Rasband et al., 2003), ceramide sulfotransferase ($CST^{-/-}$) (Ishibashi et al., 2002), MAL (Schaeren-Wiemers et al., 2004), 2′,3′-cyclic nucleotide 3′-phosphodiesterase ($CNP^{-/-}$) (Rasband et al., 2005), or CGT–myelin-associated glycoprotein (MAG) double mutants ($CGT^{-/-}$:$MAG^{-/-}$) (Marcus et al., 2002), have described these gene products as being either directly or indirectly required for the maintenance of the paranodal region. In each case, the paranodes begin to develop normally and then become progressively disordered, but the age of onset and severity of disorganization of the paranodal region vary considerably among them. Significant differences exist, however, between previously reported maintenance phenotypes and those described here. Unlike in the absence of Caspr, contactin, neurofascin, CGT, or MAL, paranodes appear to mature completely in the absence of either netrin-1 or DCC. Caspr and neurofascin cluster, and well ordered

transverse bands appear in a manner indistinguishable from cultures derived from wild-type cerebella. It is only after the paranodes have matured that the axoglial junction destabilizes. In all previous reports of paranodal maintenance phenotypes, transverse bands either do not form at all or develop abnormally. A second key distinction between the netrin-$1^{-/-}$ and $DCC^{-/-}$ phenotypes reported here and previous studies is that neurofascin remains localized to the paranodal region at longer time points, despite the ultrastructural defects and loss of domain segregation observed.

Nfc155 present on the glial membrane is required for the recruitment of the axonal Caspr–contactin complex to the paranode (Sherman et al., 2005) and associates in trans with contactin in this complex (Bonnon et al., 2007). A plausible hypothesis is that, in the absence of netrin-1 or DCC, the disengagement of the oligodendroglial membrane from the axonal surface disrupts the interactions between nfc155 and the Caspr–contactin complex, freeing a proportion of these molecules to diffuse laterally along the axon and away from the paranode. This interpretation implies that, although the nfc155–Caspr–contactin complex is necessary, it is not sufficient for the maintenance of paranodal organization. Alternatively, the absence of netrin-1 or DCC may influence the localization of nfc155 to the paranodal plasma membrane, resulting in decreased availability of nfc155 to bind the Caspr–contactin complex. In this case, netrin–DCC signaling would be required to maintain the integrity of the nfc155–Caspr–contactin complex at the paranode. A third possibility is that nfc155 and DCC may signal cooperatively through common downstream signaling effectors; however, because little is known regarding the intracellular signaling downstream of either DCC or nfc155 in oligodendrocytes, additional studies are necessary to elucidate the underlying mechanisms involved.

Although the phenotypes observed in netrin-$1^{-/-}$ and $DCC^{-/-}$ cerebellar slice cultures are similar, they are not identical. Minor increases in the periodicity of compact myelin (Fig. 2; supplemental Table 1, available at www.jneurosci.org as supplemental material) are observed in $DCC^{-/-}$, but not netrin-$1^{-/-}$, slices. Meanwhile, the ultrastructural abnormalities observed in the netrin-1 mutant paranodes are more severe than those found in the DCC mutants, as evidenced by the significantly larger mean number of faults per paranode (Fig. 5D) and the greater number of paranodes scored to be

severely abnormal (Fig. 5, compare E, F). In addition, whereas potassium channel localization is aberrant in both DCC$^{-/-}$ and netrin-1$^{-/-}$ paranodes, the sodium channel domain is also lengthened in the absence of netrin-1 (Fig. 6, compare A, C with B, D). Spreading of the domain occupied by the sodium channels has been reported at CNS paranodes in Caspr$^{-/-}$ (Bhat et al., 2001) and CGT$^{-/-}$ (Dupree et al., 1999) mutant mice but not, for example, in MAL mutants (Schaeren-Wiemers et al., 2004). The increased severity of the netrin-1$^{-/-}$ phenotype suggests that netrin-1 function at the paranode may be mediated in part by a DCC-independent mechanism. Oligodendrocytes express UNC5 netrin receptors in the mature CNS (Manitt et al., 2004), and it remains to be determined how they may additionally contribute to netrin-1 function at the paranode.

How, then, do netrin-1 and DCC contribute to the maintenance of paranodal axoglial junctions? Netrin-1 is a secreted protein; however, consistent with the restricted distribution of netrin-1 found at paranodes, most netrin-1 in the CNS is not freely soluble but membrane-associated (Manitt et al., 2001). Furthermore, disrupting DCC function blocks cellular adherence to immobilized substrate-bound netrin-1, supporting roles for netrin-1 and DCC mediating cell–cell or cell–matrix adhesion (Shekarabi et al., 2005). These findings suggest that netrin-1 and DCC may directly contribute to adhesion between oligodendroglial paranodal loops and the axonal plasma membrane. Netrin-1 binds heparin with high affinity, and heparin sulfate proteoglycans have been hypothesized to localize netrin-1 on cell surfaces (Serafini et al., 1994; Kappler et al., 2000; Suzuki et al., 2006). Consistent with a potential role mediating adhesion at paranodes, recent findings have identified short-range roles for netrin-1 influencing tissue morphogenesis outside the CNS by regulating cell–cell interactions (for review, see Baker et al., 2006).

In neurons, DCC influences cytoskeletal organization and axon guidance by regulating the src family kinase fyn and the Rho-GTPases Cdc42 and Rac1 (Shekarabi and Kennedy, 2002; Li et al., 2004; Meriane et al., 2004; Shekarabi et al., 2005). Interestingly, loss of Cdc42 or Rac1 in oligodendroctyes results in disorganization of both compact and noncompact myelin membranes (Thurnherr et al., 2006). Fyn is also required for myelination in vivo (Sperber et al., 2001) and fyn-null oligodendrocytes do not form myelin-like membrane sheets in vitro (Osterhout et al., 1999). A similar defect

in membrane sheet formation is detected when netrin-1 or DCC-null oligodendrocytes are allowed to mature in vitro, without neurons (S. Rajasekharan and T. E. Kennedy, unpublished data); however, the possibility that the regulation of Rho-GTPases and fyn by DCC and netrin-1 contributes to paranode maintenance remains to be investigated.

In summary, we conclude that netrin-1 and DCC are required to maintain the appropriate organization of axoglial membranes at CNS paranodal junctions. Our data identify an essential cell-autonomous role for netrin-1 signaling through DCC during oligodendrocyte maturation and myelination, and support the hypothesis that DCC influences paranodal organization by regulating the local organization of the actin cytoskeleton and promoting axo-oligodendroglial adhesion. The novel phenotypes identified reveal a previously unknown mechanism required for axoglial adhesion and is the first identified function for netrin-1 and DCC in the mature CNS.

This work was supported by grants from the Multiple Sclerosis Society of Canada and Canadian Institutes of Health Research. A.A.J., S.-J.B., and S.R. were supported by Multiple Sclerosis Society of Canada studentships, and K.A.B. was supported by a Jeanne Timmins Costello Fellowship from the Montreal Neurological Institute. T.E.K. is a Killam Foundation Scholar and holds a Chercheur Nationaux Award from Fonds de la Recherche en Santé du Québec. We thank Liliana Pedraza, Alejandro Roth, David Colman, Nina Bauer, and Anna Williams for comments on this manuscript and Hojatollah Vali for expert guidance regarding electron microscopy.

References

Baker KA, Moore SW, Jarjour AA, Kennedy TE (2006) When a diffusible axon guidance cue stops diffusing: roles for netrins in adhesion and morphogenesis. Curr Opin Neurobiol 16:529 –534.

BerlinerML (1931) Cytologic studies on the retina. I. Normal coexistence of oligodendroglia and myelinated nerve fibers. Arch Ophthalmol 6:740 –751.

Bhat MA, Rios JC, Lu Y, Garcia-Fresco GP, Ching W, St Martin M, Li J, Einheber S, Chesler M, Rosenbluth J, Salzer JL, Bellen HJ (2001) Axonglia interactions and the domain organization of myelinated axons requires neurexin IV/Caspr/Paranodin. Neuron 30:369 –383.

Bonnon C, Bel C, Goutebroze L, Maigret B, Girault JA, Faivre-Sarrailh C (2007) PGY repeats and N-glycans govern the trafficking of paranodin and its selective association with contactin and neurofascin-155. Mol Biol Cell 18:229 –241.

Boyle ME, Berglund EO, Murai KK, Weber L, Peles E, Ranscht B (2001) Contactin orchestrates assembly of the septate-like junctions at the paranode in myelinated peripheral nerve. Neuron 30:385–397.

Charles P, Tait S, Faivre-Sarrailh C, Barbin G, Gunn-Moore F, Denisenko- Nehrbass N, Guennoc AM, Girault JA, Brophy PJ, Lubetzki C (2002) Neurofascin is a glial receptor for the paranodin/Caspr-contactin axonal complex at the axoglial junction. Curr Biol 12:217–220.

Chiu SY, Zhou L, Zhang CL, Messing A (1999) Analysis of potassium channel functions in mammalian axons by gene knockouts. J Neurocytol 28:349 –364.

Dupree JL, Coetzee T, Blight A, Suzuki K, Popko B (1998) Myelin galactolipids are essential for proper node of Ranvier formation in the CNS. J Neurosci 18:1642–1649.

Dupree JL, Girault JA, Popko B (1999) Axo-glial interactions regulate the localization of axonal paranodal proteins. J Cell Biol 147:1145–1152.

Einheber S, Zanazzi G, Ching W, Scherer S, Milner TA, Peles E, Salzer JL (1997) The axonal membrane protein Caspr, a homologue of neurexin IV, is a component of the septate-like paranodal junctions that assemble during myelination. J Cell Biol 139:1495–1506.

Faivre-Sarrailh C, Gauthier F, Denisenko-Nehrbass N, Le Bivic A, Rougon G, Girault JA (2000) The glycosylphosphatidyl inositol-anchored adhesion molecule F3/contactin is required for surface transport of paranodin/ contactin-associated protein (caspr). J Cell Biol 149:491–502.

Fazeli A, Dickinson SL, Hermiston ML, Tighe RV, Steen RG, Small CG, Stoeckli ET, Keino-Masu K, Masu M, Rayburn H, Simons J, Bronson RT, Gordon JI, Tessier-Lavigne M, Weinberg RA (1997) Phenotype of mice lacking functional Deleted in colorectal cancer (Dcc) gene. Nature 386:796–804.

Foran DR, Peterson AC (1992) Myelin acquisition in the central nervous system of the mouse revealed by an MBP-Lac Z transgene. J Neurosci 12:4890–4897.

Ishibashi T, Dupree JL, Ikenaka K, Hirahara Y, Honke K, Peles E, Popko B, Suzuki K, Nishino H, Baba H (2002) A myelin galactolipid, sulfatide, is essential for maintenance of ion channels on myelinated axon but not essential for initial cluster formation. J Neurosci 22:6507– 6514.

Jarjour AA, Manitt C, Moore SW, Thompson KM, Yuh SJ, Kennedy TE (2003) Netrin-1 is a chemorepellent for oligodendrocyte precursor cells in the embryonic spinal cord. J Neurosci 23:3735–3744.

Kappler J, Franken S, Junghans U, Hoffmann R, Linke T, Mu¨ller HW, Koch KW (2000) Glycosaminoglycan-binding properties and secondary structure of the C-terminus of netrin-1. Biochem Biophys Res Commun 271:287–291.

Laeng P, Molthagen M, Yu EG, Bartsch U (1996) Transplantation of oligodendrocyte progenitor cells into the rat retina: extensive myelination of retinal ganglion cell axons. Glia 18:200 –210.

Li W, Lee J, Vikis HG, Lee SH, Liu G, Aurandt J, Shen TL, Fearon ER, Guan JL, Han M, Rao Y, Hong K, Guan KL (2004) Activation of FAK and Src are receptor-proximal events required for netrin signaling. Nat Neurosci 7:1213–1221.

Manitt C, Colicos MA, Thompson KM, Rousselle E, Peterson AC, Kennedy TE (2001) Widespread expression of netrin-1 by neurons and oligodendrocytes in the adult mammalian spinal cord. J Neurosci 21:3911–3922.

Manitt C, Thompson KM, Kennedy TE (2004) Developmental shift in expression of netrin receptors in the rat spinal cord: predominance of UNC-5 homologues in adulthood. J Neurosci Res 77:690 –700.

Marcus J, Dupree JL, Popko B (2002) Myelin-associated glycoprotein and myelin galactolipids stabilize developing axo-glial interactions. J Cell Biol 156:567–577.

Menon K, Rasband MN, Taylor CM, Brophy P, Bansal R, Pfeiffer SE (2003) The myelin-axolemmal complex: biochemical dissection and the role of galactosphingolipids. J Neurochem 87:995–1009.

Meriane M, Tcherkezian J, Webber CA, Danek EI, Triki I, McFarlane S, Bloch-Gallego E, Lamarche-VaneN (2004) Phosphorylation of DCC by Fyn mediates Netrin-1 signaling in growth cone guidance. J Cell Biol 167:687– 698.

Moore SW, Tessier-Lavigne M, Kennedy TE (2007) Netrins and their receptors. Adv Exp Med Biol 621:17–31.

Notterpek LM, Bullock PN, Malek-Hedayat S, Fisher R, Rome LH (1993) Myelination in cerebellar slice cultures: development of a system amenable to biochemical analysis. J Neurosci Res 36:621– 634.

Osterhout DJ, Wolven A, Wolf RM, Resh MD, Chao MV (1999) Morphological differentiation of oligodendrocytes requires activation of Fyn tyrosine kinase. J Cell Biol 145:1209 –1218.

Pedraza L, Huang JK, Colman DR (2001) Organizing principles of the axoglial apparatus. Neuron 30:335–344.

Poliak S, Peles E (2003) The local differentiation of myelinated axons at nodes of Ranvier. Nat Rev Neurosci 4:968 –980.

Rasband MN, Taylor CM, Bansal R (2003) Paranodal transverse bands are required for maintenance but not initiation of Nav1.6 sodium channel clustering in CNS optic nerve axons. Glia 44:173–182.

Rasband MN, Tayler J, Kaga Y, Yang Y, Lappe-Siefke C, Nave KA, Bansal R (2005) CNP is required for maintenance of axon-glia interactions at nodes of Ranvier in the CNS. Glia 50:86 –90.

Reynolds R, Wilkin GP (1988) Development of macroglial cells in rat cerebellum. II. An in situ immunohistochemical study of oligodendroglial lineage from precursor to mature myelinating cell. Development 102:409–425.

Rios JC, Melendez-Vasquez CV, Einheber S, Lustig M, Grumet M, Hemperly J, Peles E, Salzer JL (2000) Contactin-associated protein (Caspr) and contactin form a complex that is targeted to the paranodal junctions during myelination. J Neurosci 20:8354–8364.

Sapieha PS, Duplan L, Uetani N, Joly S, Tremblay ML, Kennedy TE, Di Polo A (2005) Receptor protein tyrosine phosphatase sigma inhibits axon regrowth in the adult injured CNS. Mol Cell Neurosci 28:625– 635.

Schaeren-Wiemers N, Bonnet A, Erb M, Erne B, Bartsch U, Kern F, Mantei N, Sherman D, SuterU (2004) The raft-associated protein MAL is required for maintenance of proper axon-glia interactions in the central nervous system. J Cell Biol 166:731–742.

Schafer DP, Bansal R, Hedstrom KL, Pfeiffer SE, Rasband MN (2004) Does paranode formation and maintenance require partitioning of neurofascin 155 into lipid rafts? J Neurosci 24:3176 –3185.

Serafini T, Kennedy TE, Galko MJ, Mirzayan C, Jessell TM, Tessier-Lavigne M (1994) The netrins define a family of axon outgrowth-promoting proteins homologous to C. elegans UNC-6. Cell 78:409–424.

Serafini T, Colamarino SA, Leonardo ED, Wang H, Beddington R, Skarnes WC, Tessier-Lavigne M (1996) Netrin-1 is required for commissural axon guidance in the developing vertebrate nervous system. Cell 87:1001–1014.

Shekarabi M, Kennedy TE (2002) The netrin-1 receptor DCC promotes filopodia formation and cell spreading by activating Cdc42 and Rac1. Mol Cell Neurosci 19:1–17.

Shekarabi M, Moore SW, Tritsch NX, Morris SJ, Bouchard JF, Kennedy TE (2005) Deleted in colorectal cancer binding netrin-1 mediates cell substrate adhesion and recruits Cdc42, Rac1, Pak1, and N-WASP into an intracellular signaling complex that promotes growth cone expansion. J Neurosci 25:3132–3141.

Sherman DL, Tait S, Melrose S, Johnson R, Zonta B, Court FA, Macklin WB, Meek S, Smith AJ, Cottrell DF, Brophy PJ (2005) Neurofascins are required to establish axonal domains for saltatory conduction. Neuron 48:737–742.

Sperber BR, Boyle-Walsh EA, Engleka MJ, Gadue P, Peterson AC, Stein PL, Scherer SS, McMorris FA (2001) A unique role for Fyn in CNS myelination. J Neurosci 21:2039 –2047.

Suzuki N, Toyoda H, Sano M, Nishiwaki K (2006) Chondroitin acts in the guidance of gonadal distal tip cells in C. elegans. Dev Biol 300:635– 646.

Svenningsen AF, Shan WS, Colman DR, Pedraza L (2003) Rapid method for culturing embryonic neuron-glial cell cocultures. J Neurosci Res 72:565–573.

Tait S, Gunn-Moore F, Collinson JM, Huang J, Lubetzki C, Pedraza L, Sherman DL, Colman DR, Brophy PJ (2000) An oligodendrocyte cell adhesion molecule at the site of assembly of the paranodal axo-glial junction. J Cell Biol 150:657– 666.

Tao-Cheng JH, Rosenbluth J (1983) Axolemmal differentiation in myelinated fibers of rat peripheral nerves. Brain Res 285:251–263.

Thurnherr T, Benninger Y,WuX, Chrostek A, Krause SM, Nave KA, Franklin RJ, Brakebusch C, Suter U, Relvas JB (2006) Cdc42 and Rac1 signaling are both required for and act synergistically in the correct formation of myelin sheaths in the CNS. J Neurosci 26:10110 –10119.

Vabnick I, Trimmer JS, Schwarz TL, Levinson SR, Risal D, Shrager P (1999) Dynamic potassium channel distributions during axonal development prevent aberrant firing patterns. J Neurosci 19:747–758.

Wang H, Kunkel DD, Martin TM, Schwartzkroin PA, Tempel BL (1993) Heteromultimeric K^+ channels in terminal and juxtaparanodal regions of neurons. Nature 365:75–79.

Figure 1. Normal myelin formation in wild-type and netrin-1 and DCC mutant cerebellar organotypic cultures.

Oligodendrocyte maturation and myelination in slices of newborn mouse cerebellum follows a similar time course to that in vivo and occurs normally in the absence of netrin and DCC. After 3 DIV, oligodendrocytes, immunolabeled with an antibody against MBP and visualized using Alexa 488-conjugated secondary antibodies (green), can be readily detected (A). They increase in number and complexity between 3 and 7 DIV (B). By 14 DIV, many myelinated axons are visible (C), and by 30 DIV, extensive myelination is observed throughout the white matter (D). Abundant myelination is observed in long-term slice cultures derived from both $DCC^{-/-}$ and netrin-$1^{-/-}$ mutant animals (F, H) and their wild-type littermates (E, G). Magnification: 20× objective. Scale bar, 100 μm.

Figure 2. Compact myelin ultrastructure is normal in long-term netrin-1 and DCC mutant cerebellar slice cultures.

Spacing between layers of the myelin sheath was analyzed by transmission electron microscopy in cross sections cut from cerebellar slice cultures derived from $DCC^{-/-}$ or netrin-$1^{-/-}$ animals (B, D, respectively) and their wild-type littermates (A, C, respectively). The width of the periaxonal space was unaffected in the mutant slices. Although the periodicity of netrin-$1^{+/+}$ and netrin-$1^{-/-}$ myelin wraps was not significantly different, the absence of DCC expression resulted in a small (~11%), but significant, increase in the spacing between layers of compact myelin (supplemental Table 1, available at www.jneurosci.org as supplemental material). Electron micrographs were imaged at 410,000×. Ax, Axon; PS, periaxonal space. Scale bar, 50 nm.

Figure 3. Distribution of netrin-1 and DCC in myelinated cerebellar organotypic slice cultures and adult rat spinal cord.

Triple-label immunohistochemical analysis of longitudinal (A–C, G–I, M–O, S–U) and cross-sectional (D–F, J–L, P–R, V–X) images of the paranode in mature (30 DIV) cerebellar slice cultures (A–L) and adult rat spinal cord (M–X). Caspr immunoreactivity was visualized using Alexa 546-conjugated secondary antibodies (red). PLP (C), MBP (I), and NFH (O, R, U, X) immunoreactivity was visualized using Alexa 633-conjugated secondary antibodies (blue). Netrin-1 and DCC proteins were visualized using Alexa 488-conjugated secondary antibodies (green). Netrin-1 protein (A–F, M–R) is localized to the paranodal axoglial junction, where it is closely associated, and partially overlaps with Caspr. DCC protein (G–L, S–X) surrounds the axon at the paranode but does not colocalize with Caspr to the same extent as netrin-1. Magnification: A–C, G–I, M–O, S–U, 100× objective; digital zoom, 4; D–F, J–L, P–R, V–X, 100× objective; digital zoom, 10. Scale bars: A–C, G–I, M–O, S–U, 2 μm; D–F, J–L, P–R, V–X, 500 nm.

Figure 4. Abnormal paranodal myelin in long-term DCC- and netrin-1-deficient organotypic slice cultures.

The organization of both paranodal and internodal myelin was examined using transmission electron microscopy in long-term (A–D, 67 DIV; E–H, 49 DIV) organotypic slice cultures derived from newborn DCC or netrin-1 mutant mouse cerebellum (B–D, F–H) or that of their wild-type littermates (A, E). In slices collected from wild-type animals, paranodal myelin was well organized, and electron-dense transverse bands between the axonal and oligodendrocyte membranes (A, E, black arrowheads) and interloop densities between paranodal loops (A, white arrowhead) were present. In contrast, in slices lacking DCC or netrin-1, transverse bands are frequently disordered (B, F, insets, black arrowheads) or absent (B, F, insets, white arrowheads), and paranodal loops were often disorganized. Myelin membranes were frequently separated from the axolemma (B, F, black arrows) and from each other (B, white arrow). Paranodal loops oriented away from the axon were also frequently observed in the mutants (C, G, arrows). Regions of myelin decompaction resembling paranodal loops were also present in mutant internodal myelin (D, H, I). Magnification: A–H, 68,000×; I, 25,000×. Scale bars: A–H, 200 nm; I, 500 nm; A, B, E, F, insets, 100 nm.

Figure 5. Quantification of paranodal defects in the absence of netrin-1 or DCC.
The integrity of paranodal myelin was analyzed in electron micrographs of transverse sections of long-term cerebellar slice cultures derived from $DCC^{-/-}$ (67 DIV) or netrin-$1^{-/-}$ (49 DIV) mice and their wild-type littermates. A, Myelin paranodes were examined for four defects: lack of transverse bands (1), lack of interloop densities (2), separation of paranodal myelin loops from the axonal surface (3), and everted paranodal loops (4). Each observation was counted as one fault. B, C, In both netrin and DCC mutants, the incidence of each of the four defects was increased, as was the mean number of faults per paranode (D). DCC (E) and netrin-1 (F) wild-type and mutant paranodes were classified as normal (0 faults), mildly abnormal (1 fault), moderately abnormal (2 faults), and severely abnormal (3–4 faults). Notably, whereas 97% of $DCC^{+/+}$ paranodes and 97% of netrin-$1^{+/+}$ paranodes examined were classified as normal or mildly abnormal, not a single wild-type paranode was severely abnormal. OL, Oligodendroglial membrane; AX, axolemma; TB, transverse bands; ID, interloop densities. **$p < 0.005$. Error bars indicate SEM.

Figure 6. Disruption of the domain organization of the node of Ranvier in long-term netrin-1- and DCC-deficient slice cultures.

Long-term (60 DIV) cerebellar slice cultures were double-labeled with antibodies against Na^+ch and Kv1.2 (A–D). Kv1.2 protein was visualized using Alexa 488-conjugated secondary antibodies (green), and Na^+ch proteins were visualized using Alexa 546-conjugated secondary antibodies (red). In cultures lacking netrin-1 (C) or DCC (D), a reduced distance between Na^+ channels localized within the node of Ranvier and K^+ channels normally localized to the juxtaparanodal region was detected. This decrease was primarily attributable to the apparent "leaking" of K^+ channels into the paranode, and occasionally the node itself (C, D, arrowheads; E). In netrin-$1^{-/-}$, but not $DCC^{-/-}$ slices, the length of the Na^+ch-positive domain was increased relative to control (C, arrow; F). Magnification: 100× objective; digital zoom, 4. Scale bar, 2 μm. *$p < 0.05$, **$p < 0.005$. Error bars indicate SEM.

Figure 7. Caspr, but not neurofascin, distribution is altered in long-term DCC-deficient cultures.

Long-term (60 DIV) cerebellar slice cultures were triple-labeled with antibodies against NFH, MBP, and either nfc (A–D) or Caspr (E–H). MBP was visualized using Alexa 488-conjugated secondary antibodies (green), NFH was visualized using Alexa 633-conjugated secondary antibodies (blue), and nfc or Caspr were visualized using Alexa 546-conjugated secondary antibodies (red). The length of nfc-immunoreactive bands were unchanged between $DCC^{-/-}$ and $DCC^{+/+}$ nodal regions, whereas Caspr-immunoreactive domains were lengthened at $DCC^{-/-}$ paranodes relative to wild-type slices (supplemental Table 5, available at www.jneurosci.org as supplemental material). Magnification: 100× objective; digital zoom, 4. Scale bar, 2 μm.

Figure 8. Caspr, but not neurofascin, distribution is altered in long-term netrin-1-deficient cultures.

Long-term (60 DIV) cerebellar slice cultures were triple-labeled with antibodies against NFH, MBP, and either nfc (A–D) or Caspr (E–H). MBP was visualized using Alexa 488-conjugated secondary antibodies (green), NFH was visualized using Alexa 633-conjugated secondary antibodies (blue), and nfc or Caspr were visualized using Alexa 546-conjugated secondary antibodies (red). The length of nfc-immunoreactive bands were unchanged between netrin-$1^{-/-}$ and netrin-$1^{+/+}$ nodal regions, whereas Caspr-immunoreactive domains were lengthened at netrin-$1^{-/-}$ paranodes relative to wild-type slices (supplemental Table 5, available at www.jneurosci.org as supplemental material). Magnification: 100× objective; digital zoom, 4. Scale bar, 2 μm.

Figure 9. Normal ultrastructure of paranodal myelin in short-term netrin-1- and DCC-deficient cerebellar slice cultures.

The organization of paranodal myelin was studied by transmission electron microscopy in short-term organotypic slice cultures derived from newborn netrin-$1^{-/-}$ or $DCC^{-/-}$ animals and their wild-type littermates (A, B; F, G, respectively). At this age, paranodal myelin was well organized in both wild-type and mutant cultures. In almost every paranode studied at this age, transverse bands linked the axonal and oligodendrocyte membranes, and paranodal loops were closely apposed to each other. Detached and everted loops were rarely observed in short-term cultures (C–E, H–J). Magnification: 25,000×. Scale bars, 500 nm. Error bars indicate SEM.

Figure 10. Altered paranodal Caspr distribution in retinal ganglion cell axons myelinated by DCC$^{-/-}$ oligodendrocytes in vivo.

Injection of OPCs into the eyes of adult mice results in myelination (A). Flat-mounted retina (B) was double-labeled with antibodies against MBP to visualize myelin and Caspr to visualize paranodes (C–H). MBP was visualized using Alexa 488-conjugated antibodies (green). Caspr was visualized using Alexa 546-conjugated antibodies (red). The Caspr-immunoreactive domains were lengthened in the DCC$^{-/-}$ myelin group (G, H) compared with oligodendrocytes expressing DCC (E, F). The white arrowheads (H) illustrate the edges of the Caspr-immunoreactive domain measured. Magnification: B, 10× objective; C, 100× objective; D, 100× objective; digital zoom, 2; E–H, 100× objective; digital zoom, 4. Scale bars: C, D, 5 μm; E–H, 2 μm.

FIGURES

FIGURE 1

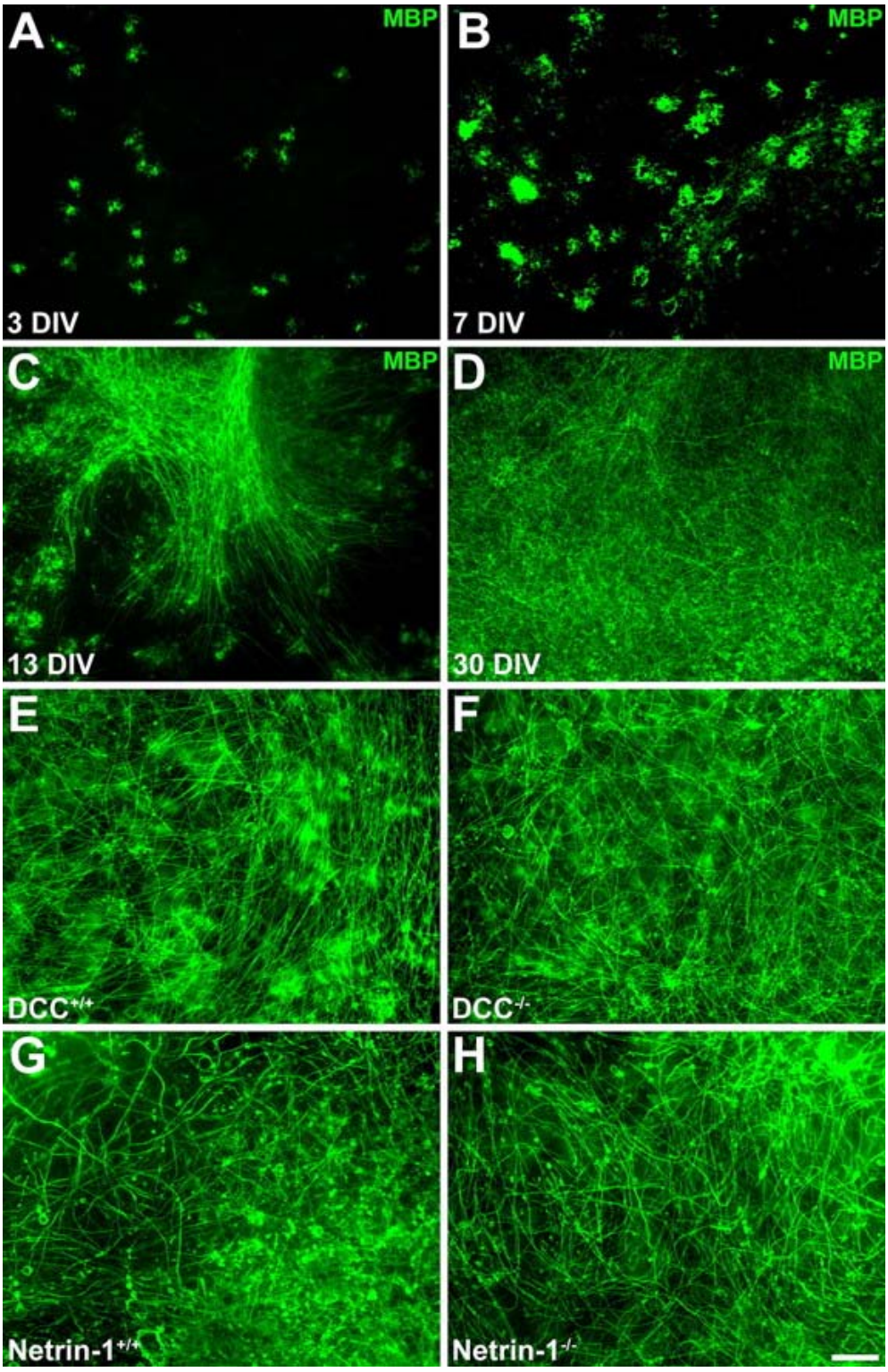

FIGURE 2

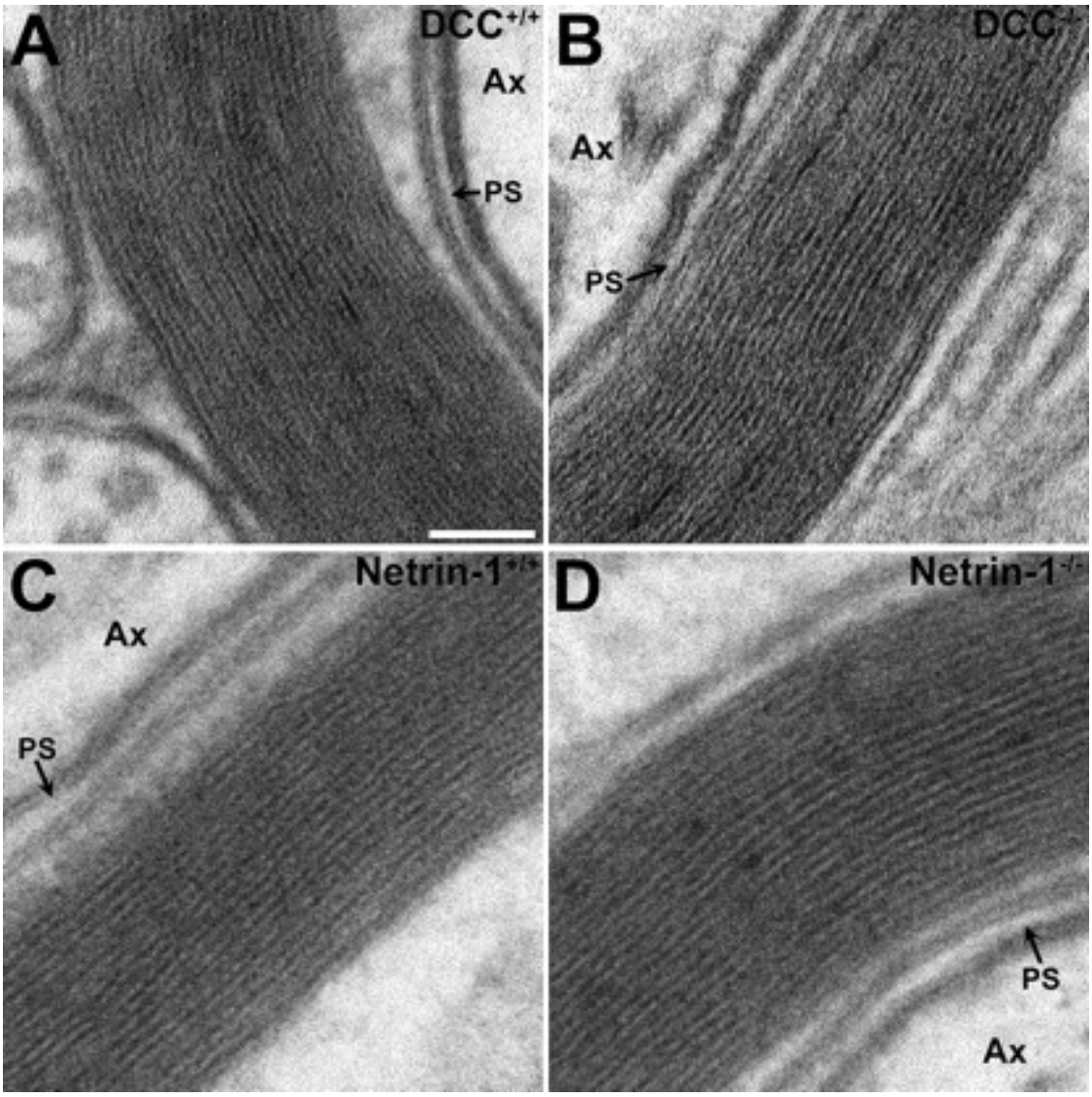

FIGURE 3

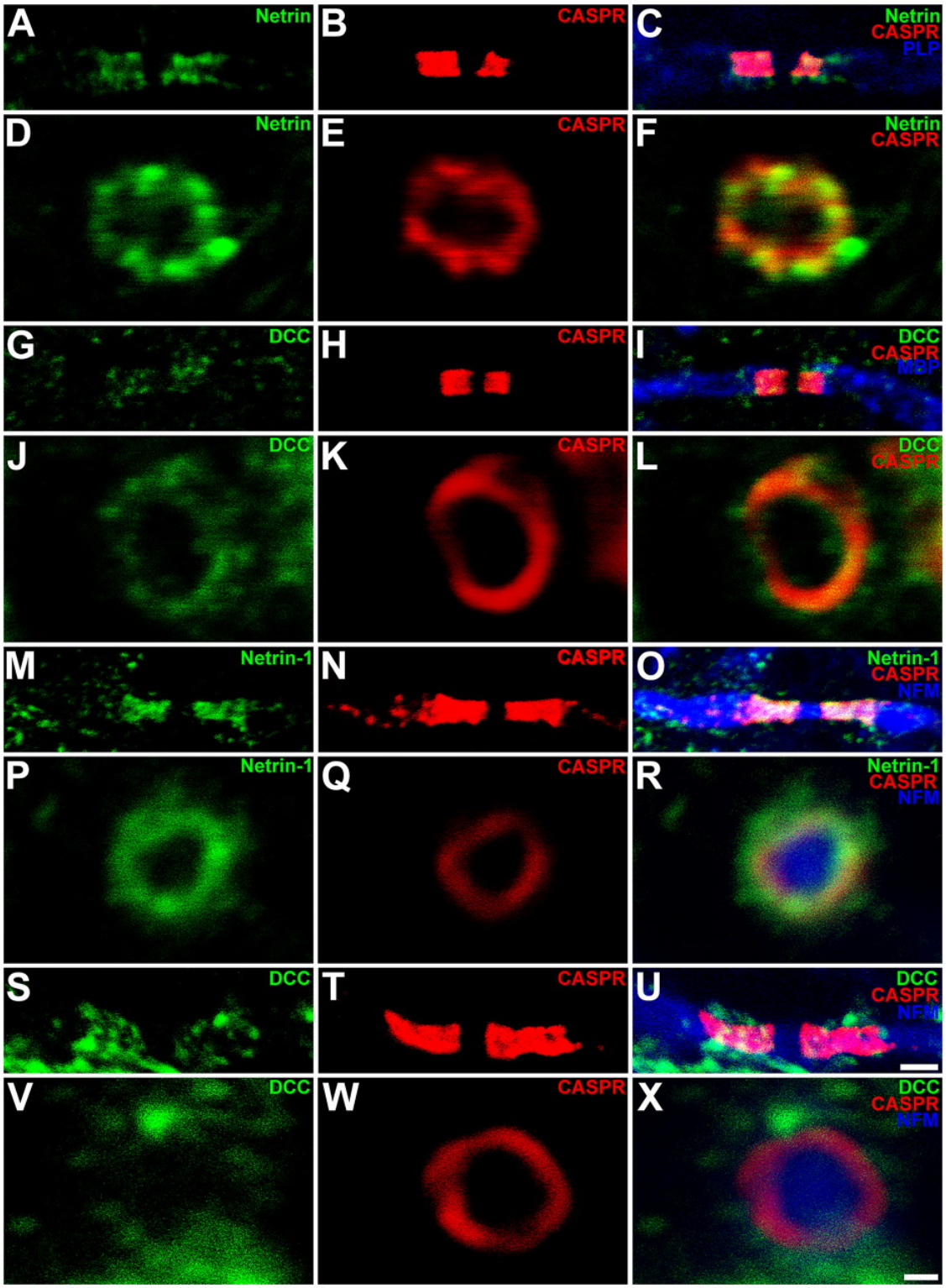
A
Netrin
B
CASPR
C
Netrin
CASPR
PLP
D
Netrin
E
CASPR
F
Netrin
CASPR
G
DCC
H
CASPR
I
DCC
CASPR
MBP
J
DCC
K
CASPR
L
DCC
CASPR
M
Netrin-1
N
CASPR
O
Netrin-1
CASPR
NFM
P
Netrin-1
Q
CASPR
R
Netrin-1
CASPR
NFM
S
DCC
T
CASPR
U
DCC
CASPR
NFM
V
DCC
W
CASPR
X
DCC
CASPR
NFM

FIGURE 4

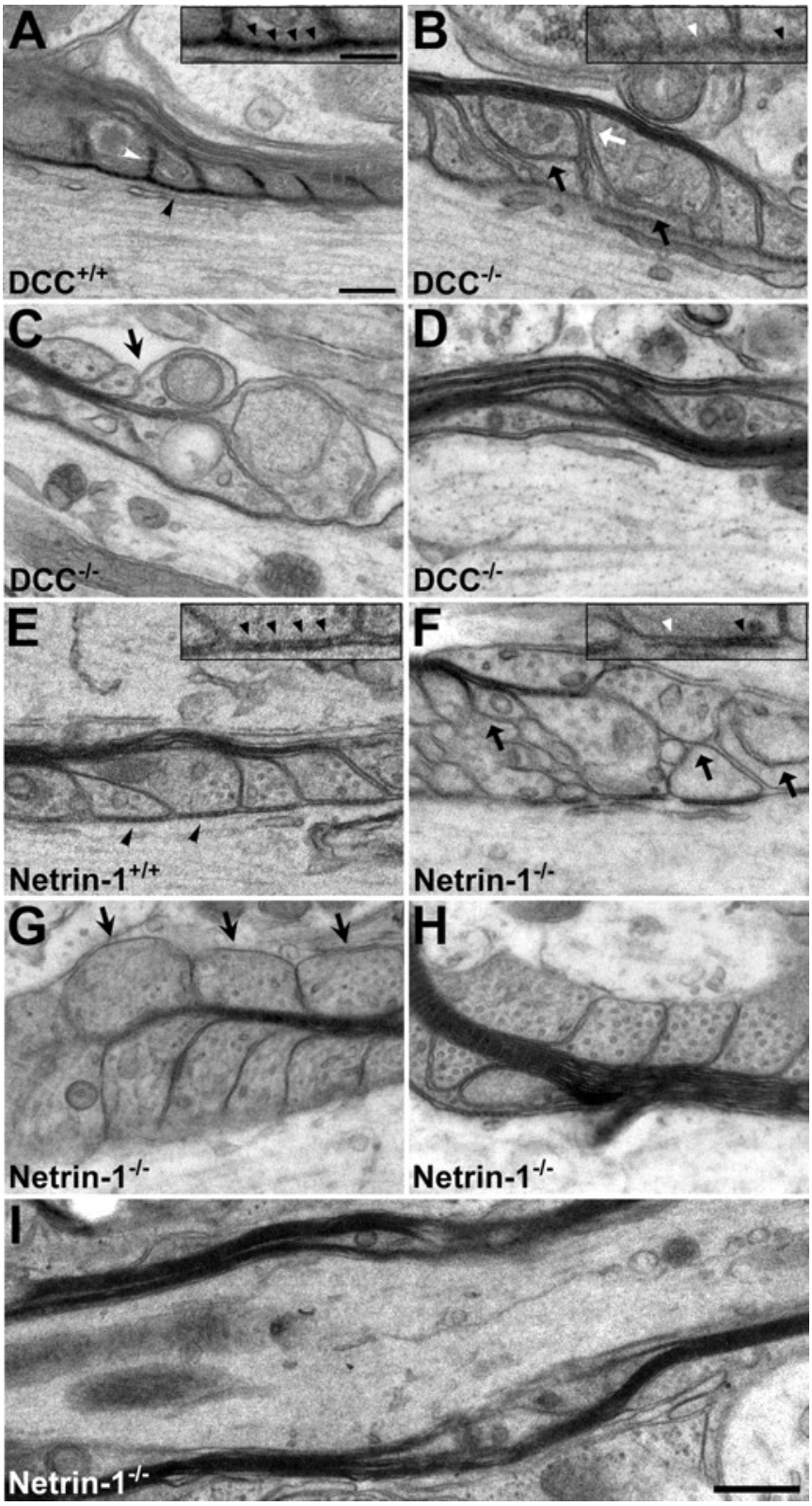
A
DCC+/+
B
DCC-/-
C
DCC-/-
D
DCC-/-
E
Netrin-1+/+
F
Netrin-1-/-
G
Netrin-1-/-
H
Netrin-1-/-
I
Netrin-1-/-

FIGURE 5

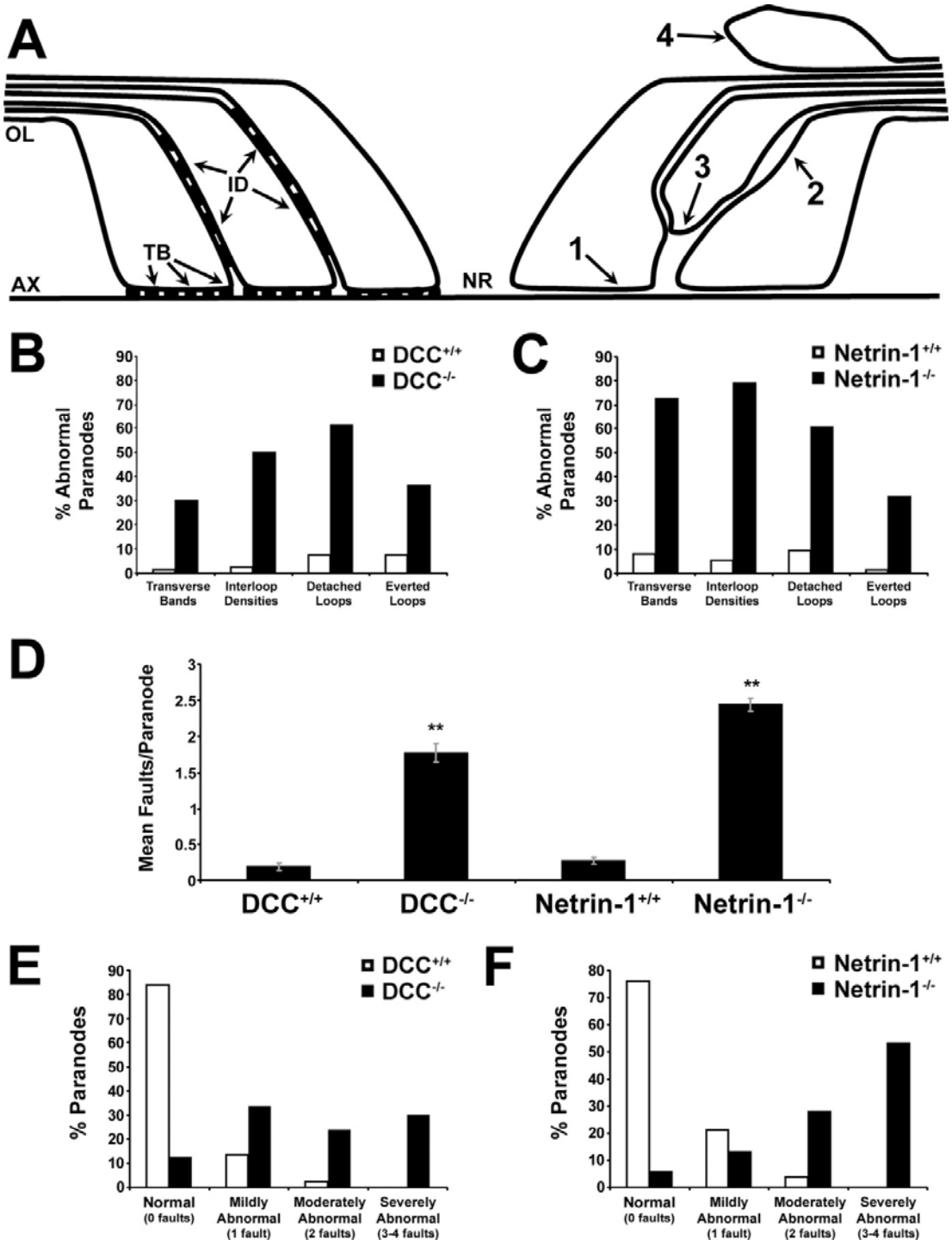
A
OL
AX
TB
ID
NR
1
2
3
4
B
% Abnormal Paranodes
DCC+/+
DCC-/-
Transverse Bands
Interloop Densities
Detached Loops
Everted Loops
C
% Abnormal Paranodes
Netrin-1+/+
Netrin-1-/-
Transverse Bands
Interloop Densities
Detached Loops
Everted Loops
D
Mean Faults/Paranode
**
**
DCC+/+
DCC-/-
Netrin-1+/+
Netrin-1-/-
E
% Paranodes
DCC+/+
DCC-/-
Normal (0 faults)
Mildly Abnormal (1 fault)
Moderately Abnormal (2 faults)
Severely Abnormal (3-4 faults)
F
% Paranodes
Netrin-1+/+
Netrin-1-/-
Normal (0 faults)
Mildly Abnormal (1 fault)
Moderately Abnormal (2 faults)
Severely Abnormal (3-4 faults)

FIGURE 6

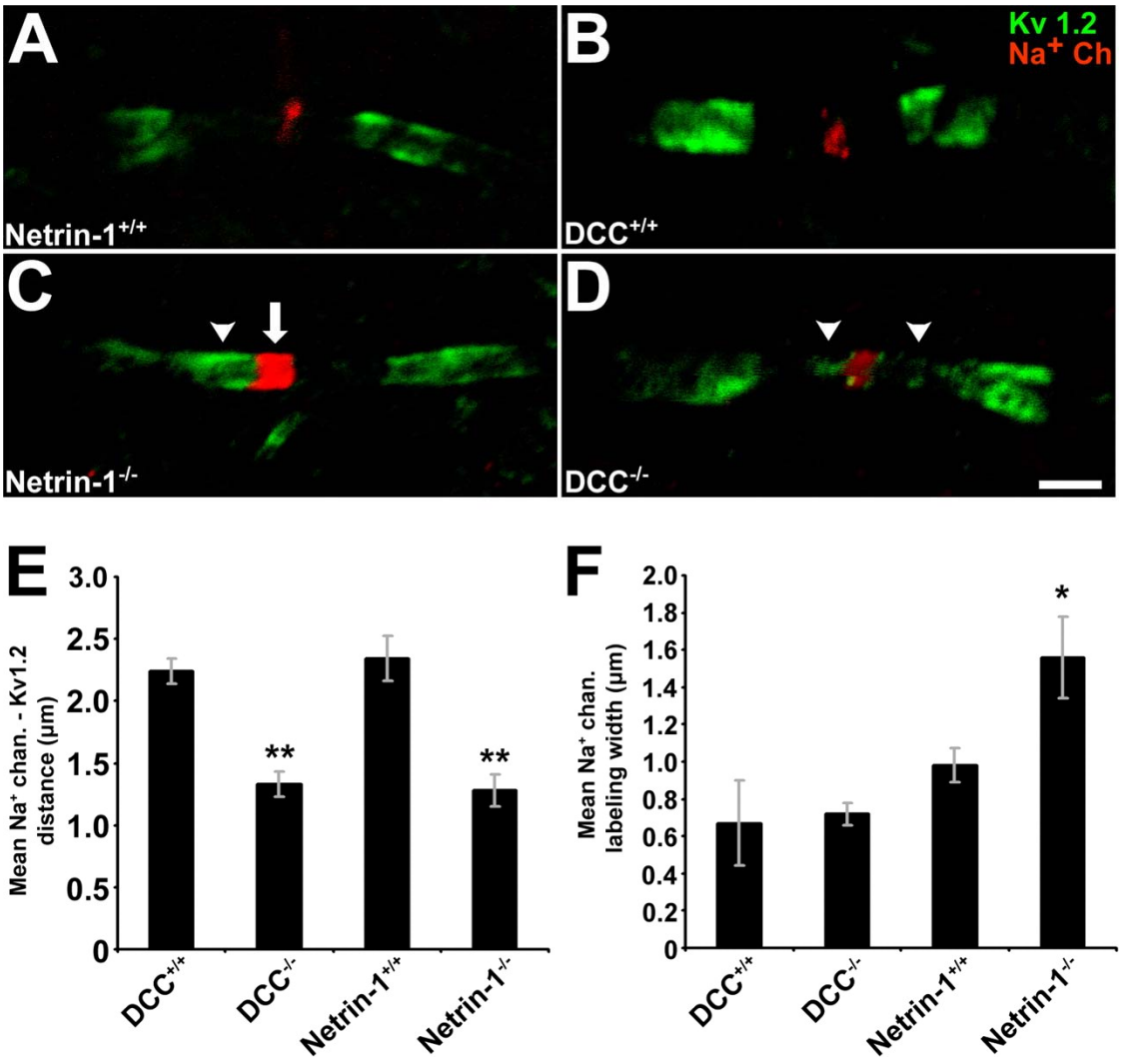
A
Netrin-1+/+
B
Kv 1.2
Na+ Ch
DCC+/+
C
Netrin-1-/-
D
DCC-/-
E
Mean Na+ chan. - Kv1.2 distance (µm)
3.0
2.5
2.0
1.5
1.0
0.5
0
**
**
DCC+/+
DCC-/-
Netrin-1+/+
Netrin-1-/-
F
Mean Na+ chan. labeling width (µm)
2.0
1.8
1.6
1.4
1.2
1.0
0.8
0.6
0.4
0.2
0
*
DCC+/+
DCC-/-
Netrin-1+/+
Netrin-1-/-

FIGURE 7

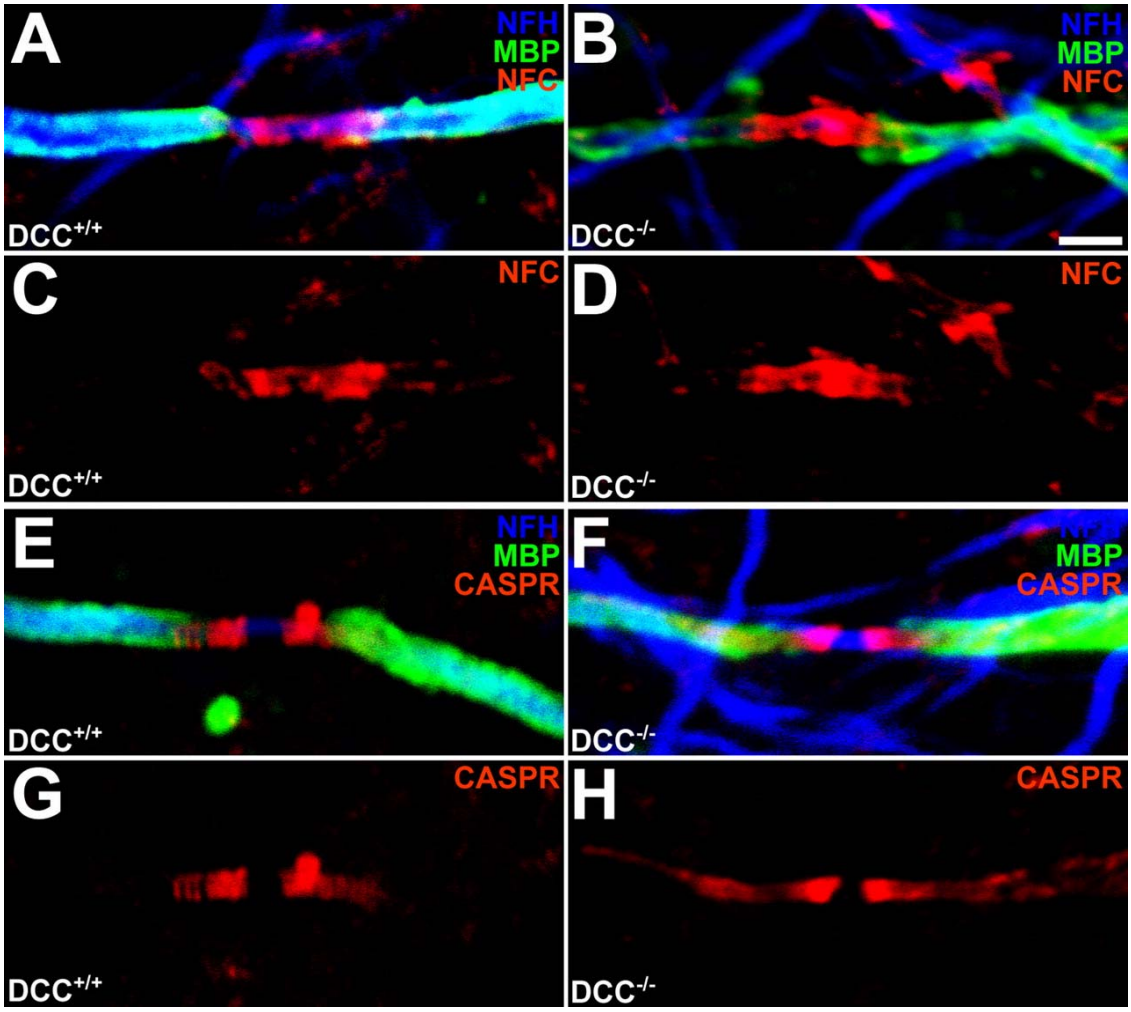
A
NFH
MBP
NFC
DCC+/+
B
NFH
MBP
NFC
DCC-/-
C
NFC
DCC+/+
D
NFC
DCC-/-
E
NFH
MBP
CASPR
DCC+/+
F
MBP
CASPR
DCC-/-
G
CASPR
DCC+/+
H
CASPR
DCC-/-

FIGURE 8

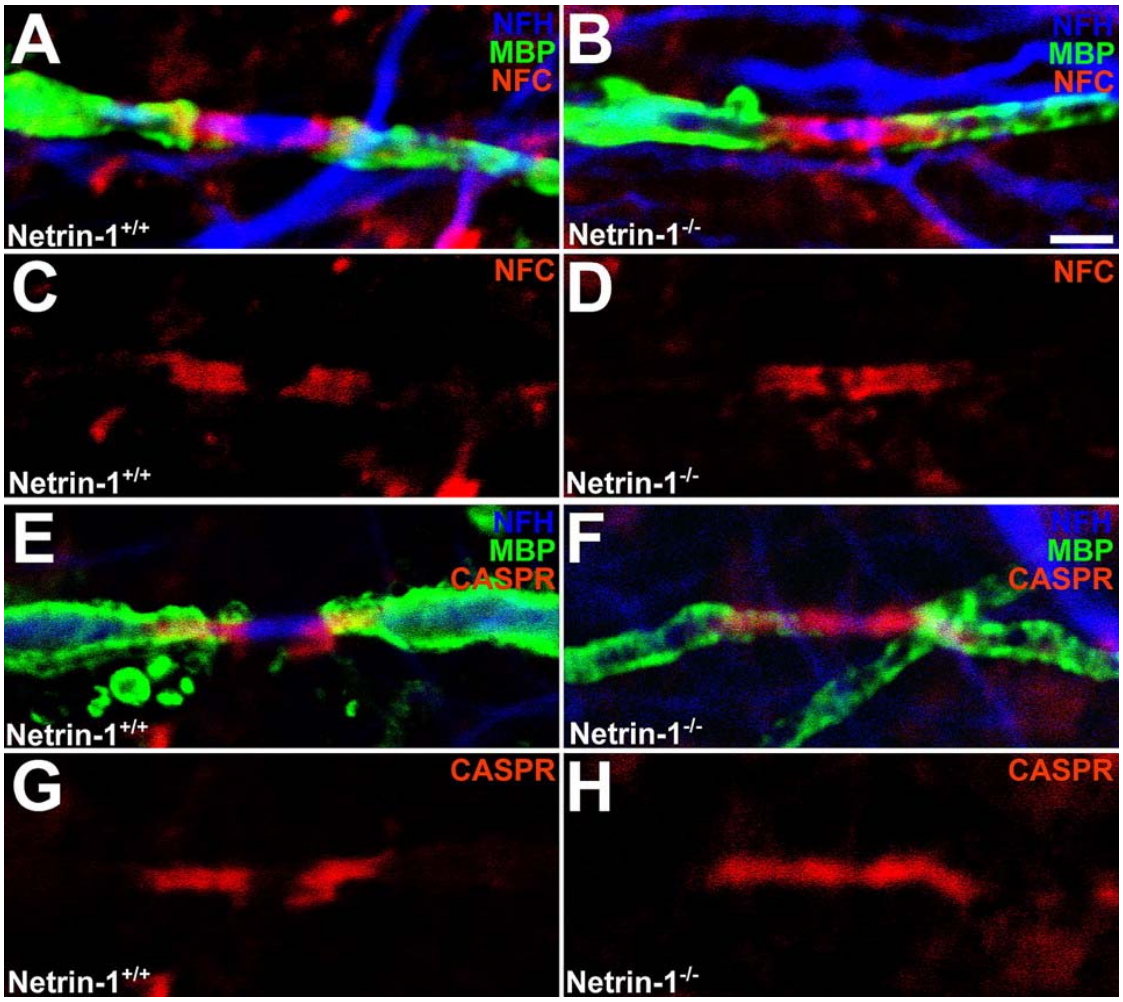
A
NFH
MBP
NFC
Netrin-1+/+
B
NFH
MBP
NFC
Netrin-1-/-
C
NFC
Netrin-1+/+
D
NFC
Netrin-1-/-
E
NFH
MBP
CASPR
Netrin-1+/+
F
NFH
MBP
CASPR
Netrin-1-/-
G
CASPR
Netrin-1+/+
H
CASPR
Netrin-1-/-

FIGURE 9

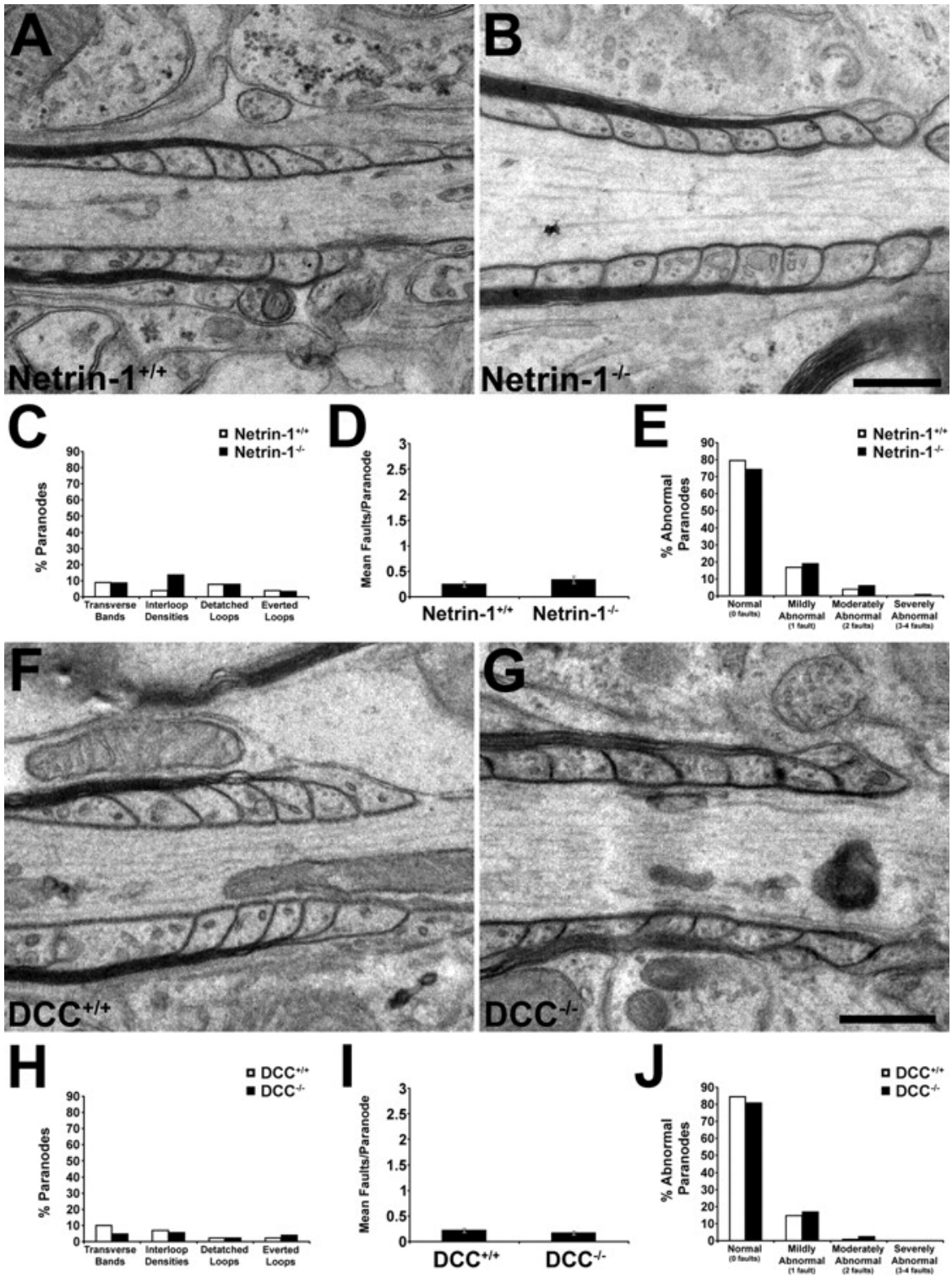
A
Netrin-1+/+
B
Netrin-1-/-
C
Netrin-1+/+
Netrin-1-/-
% Paranodes
Transverse Bands
Interloop Densities
Detatched Loops
Everted Loops
D
Mean Faults/Paranode
Netrin-1+/+
Netrin-1-/-
E
Netrin-1+/+
Netrin-1-/-
% Abnormal Paranodes
Normal (0 faults)
Mildly Abnormal (1 fault)
Moderately Abnormal (2 faults)
Severely Abnormal (3-4 faults)
F
DCC+/+
G
DCC-/-
H
DCC+/+
DCC-/-
% Paranodes
Transverse Bands
Interloop Densities
Detatched Loops
Everted Loops
I
Mean Faults/Paranode
DCC+/+
DCC-/-
J
DCC+/+
DCC-/-
% Abnormal Paranodes
Normal (0 faults)
Mildly Abnormal (1 fault)
Moderately Abnormal (2 faults)
Severely Abnormal (3-4 faults)

FIGURE 10

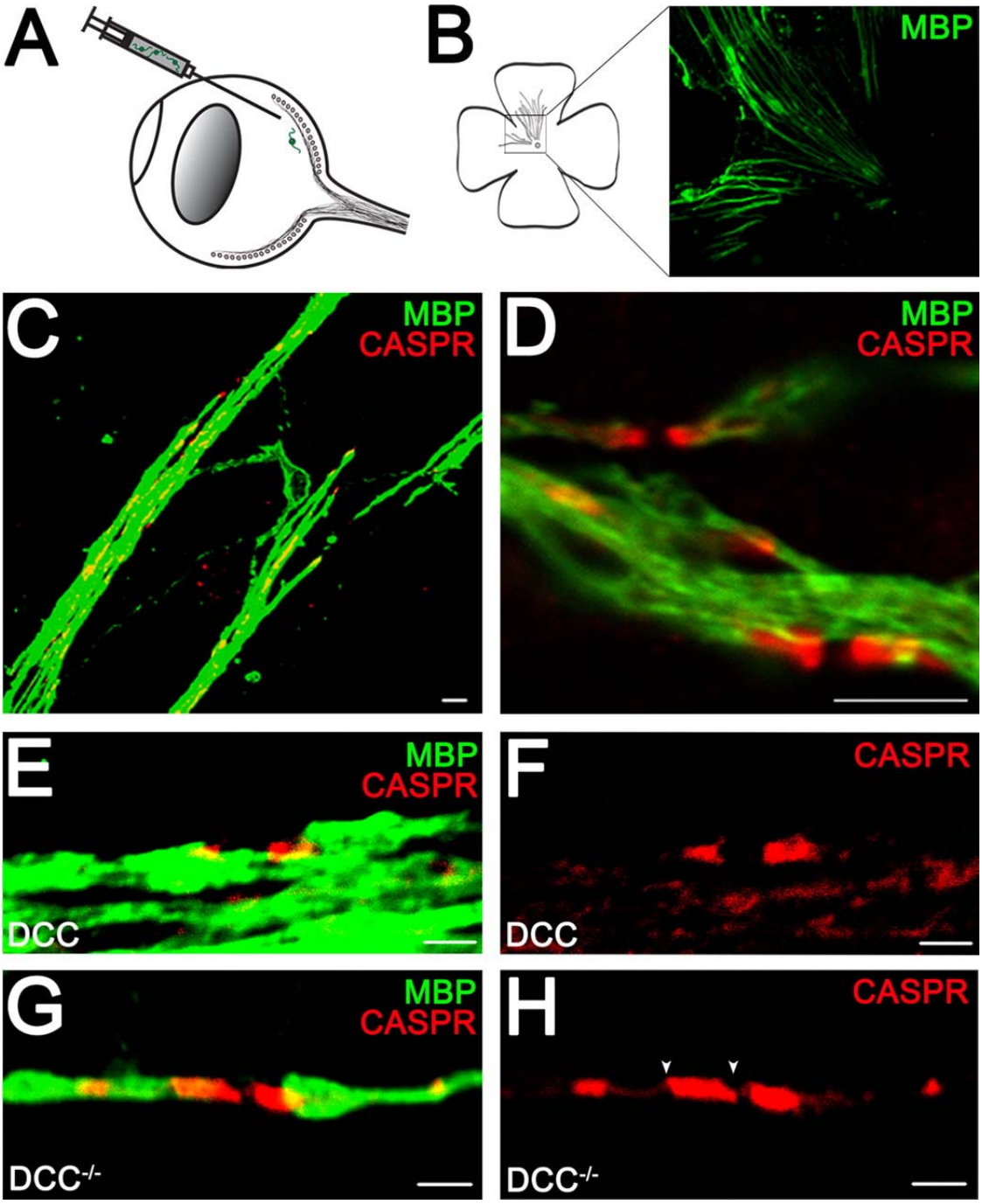
A
B
MBP
C
MBP
CASPR
D
MBP
CASPR
E
MBP
CASPR
DCC
F
CASPR
DCC
G
MBP
CASPR
DCC-/-
H
CASPR
DCC-/-

APPENDIX B

CONTRIBUTION TO THE ARTICLES

For the article **"Structural and functional neuroprotection in glaucoma: role of galantamine-mediated activation of muscarinic acetylcholine receptors"** (Chapter 2 in the thesis), I performed all of the experiments in this paper and Dr. Yu Zhou contributed in production of preliminary data. I have formulated the initial draft and figures of this manuscript for publication, which was then revised with assistance from my supervisors.

For the article **"Retinal microvasculature protection correlates with retinal ganglion cell survival and blood flow restoration in experimental glaucoma"** (Chapter 3 in the thesis), I performed all the *in vivo* experiments. Alex Dong worked on the isolated arterioles and Mylène Pouliot helped me in retinal blood flow measurements. I have prepared the draft and figures of this manuscript, with assistance from my supervisor.

For the article **"A cell-permeable phosphine-borane complex delays retinal ganglion cell death after axonal injury through activation of the pro-survival extracellular signal-regulated kinases 1/2 pathway"** (Chapter 4 in the thesis), I performed all of the experiments and generated all of the data presented in this paper. Christopher J. Lieven helped with synthesis of the PB1 compound. I have prepared the initial draft and figures of this manuscript for publication, which was then revised with assistance from my supervisors.

For the article **"Maintenance of axo-oligodendroglial paranodal junctions requires DCC and netrin-1"** (Appendix A in the thesis), I performed the oligodendrocyte precursor cell transplantation into the retina of newborn mouse pups via intravitreal injections and also helped in perfusion of experimental animals. The result of my contribution is reflected in figure 10 of this article.